



---

Universidad de Valladolid



**PROGRAMA DE DOCTORADO EN  
INVESTIGACIÓN BIOMÉDICA**

TESIS DOCTORAL:

**EFFECTS OF INTERFERONS AND THEIR  
INTERACTIONS WITH OTHER LIGANDS IN  
HUMAN AORTIC VALVE CELLS**

Presentada por Iván Parra Izquierdo para optar al grado  
de doctor por la Universidad de Valladolid

Dirigida por:

Dra. María del Carmen García Rodríguez





**DEFENCE AUTHORIZATION BY THE PhD THESIS SUPERVISOR**

*(As required by section 7.2. of the Regulation concerning doctoral thesis defense at UVa)*

TO THE CHAIRMAN OF THE PhD BOARD OF THE UNIVERSIDAD DE VALLADOLID

Full name: M<sup>a</sup> del Carmen García Rodríguez

ID: 12323936F

Department: Instituto de Biología y Genética Molecular

University or Research Institution: Instituto de Biología y Genética Molecular

Postal address: (IBGM, C/ Sanz y Forés 3, laboratorio E10, 47003 Valladolid

E-mail: cgarcia@ibgm.uva.es

I hereby authorize the defense of the PhD thesis entitled “EFFECTS OF INTERFERONS AND THEIR INTERACTIONS WITH OTHER LIGANDS IN HUMAN AORTIC VALVE CELLS”

Written by Mr. Iván Parra Izquierdo

under my supervision, within the PhD program in Investigación Biomédica de la Universidad de Valladolid.

After taking into account the following considerations, the thesis includes novel contributions to the field and meets the requirements for the Degree of Doctor of Philosophy.

Thesis supervisor,

Place and date: Valladolid, June 28<sup>th</sup>, 2019

Signature:



# **INDEX**



# INDEX

---

<b>ABBREVIATIONS</b> .....	<b>1</b>
<b>ABSTRACT</b> .....	<b>7</b>
<b>INTRODUCTION</b> .....	<b>11</b>
<b>I.1-Mammalian heart valves</b> .....	<b>11</b>
I.1.1-Heart valve physiology.....	13
I.1.2-Valvular heart diseases .....	15
<b>I.2-Calcific aortic valve disease</b> .....	<b>19</b>
I.2.1-CAVD risk factors .....	19
I.2.2-CAVD diagnosis.....	21
I.2.3-CAVD management and treatment .....	22
<b>I.3-Molecular mechanisms of CAVD</b> .....	<b>24</b>
I.3.1-Initial triggers of CAVD: haemodynamic and genetic factors.....	24
I.3.2-Initiation phase: endothelial dysfunction and inflammation .....	26
I.3.3-Propagation phase: fibrosis, angiogenesis, and osteogenesis .....	32
I.3.4-Last phase .....	35
<b>I.4-Interferons and JAK/STAT pathways</b> .....	<b>37</b>
I.4.1-IFN types and their receptors .....	37
I.4.2-JAK/STAT pathways .....	39
I.4.3-JAK/STAT pathways, IFN and cardiovascular disease .....	43
<b>I.5-Toll-like receptors</b> .....	<b>45</b>
I.5.1-TLR types and ligands.....	46
I.5.2-TLR signalling.....	48
I.5.3-TLR and cardiovascular disease .....	51
<b>HYPOTHESIS AND OBJECTIVES</b> .....	<b>57</b>
<b>MATERIALS AND METHODS</b> .....	<b>61</b>
<b>M.1-Human valve samples</b> .....	<b>61</b>
<b>M.2-Human VIC and VEC isolation and culture</b> .....	<b>62</b>
M.2.1-Cell isolation .....	62
M.2.2-Cell culture .....	62
M.2.3-Human valve endothelial cell purification by cell sorting .....	63
<b>M.3-Valve cell characterization by immunofluorescence</b> .....	<b>63</b>

M.3.1- $\alpha$ -SMA detection in VIC .....	63
M.3.2-CD31 and VWF detection in VEC .....	64
<b>M.4-Protocol for cell activation .....</b>	<b>65</b>
<b>M.5-Quantitative reverse transcription polymerase chain reaction (RT-qPCR) .....</b>	<b>67</b>
M.5.1-RNA purification.....	67
M.5.2-Retrotranscriptase reaction .....	68
M.5.3-Quantitative PCR .....	68
<b>M.6-Protein analysis by immunoblot (Western Blot) .....</b>	<b>70</b>
M.6.1-Protein extraction and quantitation by the bicinchoninic acid (BCA) assay.....	70
M.6.2-Western blot procedure: SDS-PAGE and transfer .....	71
M.6.3-Protein immunodetection and visualization by chemiluminescence .....	71
<b>M.7-Enzyme-linked immunosorbent assay (ELISA) .....</b>	<b>73</b>
<b>M.8-Proliferation assay.....</b>	<b>74</b>
<b>M.9-<i>In vitro</i> calcification assays .....</b>	<b>74</b>
M.9.1-Staining of calcium-phosphate crystals with Alizarin Red dye .....	74
M.9.2-Calcium deposits quantification .....	75
<b>M.10-Apoptosis/necrosis assay by flow cytometry .....</b>	<b>75</b>
<b>M.11-Ectopic phosphatase activity .....</b>	<b>76</b>
<b>M.12-HIF-1<math>\alpha</math> detection by immunofluorescence .....</b>	<b>76</b>
<b>M.13-Dynamic adhesion assays in side-specific VEC .....</b>	<b>76</b>
<b>M.14-Migration (wound healing) assay in side-specific VEC .....</b>	<b>77</b>
<b>M.15-RNA interference assays.....</b>	<b>78</b>
<b>M.16-Conditioned medium experiments.....</b>	<b>78</b>
<b>M.17-Statistical analysis .....</b>	<b>79</b>
<b>RESULTS .....</b>	<b>83</b>
<b>R.1-Common effects of type I and II IFN in human VIC.....</b>	<b>84</b>
R.1.1-Human aortic valve tissue and explanted cells express IFN receptors .....	85
R.1.2-IFN activate several signalling pathways in control VIC .....	85
R.1.3-IFN cooperate with LPS to induce a pro-inflammatory phenotype in VIC .....	90
R.1.4-IFN drive VIC differentiation towards a pro-osteogenic phenotype .....	96
R.1.5-IFN and LPS induce VIC calcification to a higher extent in male cells .....	98
<b>R.2-Specific mechanisms of IFN-<math>\alpha</math> in VIC .....</b>	<b>106</b>
R.2.1-IFN- $\alpha$ and TLR cooperation is specific for TLR2-4 ligands .....	107

R.2.2-IFN- $\alpha$ drives VIC differentiation towards an osteoblast-like phenotype.....	107
R.2.3-BMP-2 signalling plays a role on male preferential calcification.....	110
R.2.4-Female-specific Akt activation is a protective mechanism for calcification .....	113
<b>R.3-Specific mechanisms of IFN-<math>\gamma</math> in VIC .....</b>	<b>115</b>
R.3.1-IFN- $\gamma$ and LPS interplay promotes HIF-1 $\alpha$ induction in VIC .....	116
R.3.2-IFN- $\gamma$ treatment induces a pro-angiogenic phenotype in male VIC .....	122
R.3.3-Chemical stabilization of HIF-1 $\alpha$ increases VIC calcification .....	123
R.3.4-Signalling pathways involved in sex-differences upon IFN- $\gamma$ +LPS treatment.....	124
R.3.5-Mechanistic differences of IFN in osteogenic differentiation.....	126
<b>R.4-Correlation of IFN findings in intact valve tissue .....</b>	<b>129</b>
R.4.1-Expression of IFN receptors, HIF-1 $\alpha$ and related molecules in control and calcified valves from males .....	130
R.4.2-Intrinsic sex-differences in calcified valve tissue .....	131
<b>R.5-Type I IFN signalling mediates Poly(I:C) effects in VIC .....</b>	<b>134</b>
R.5.1-dsRNA treatment activates IFN signalling in VIC .....	135
R.5.2-JAK/STAT signalling blockade reduced Poly(I:C)-induced effects.....	138
<b>R.6-Relevance of IFN-<math>\gamma</math>+LPS effects in the AV context and VEC side-specific effects .....</b>	<b>143</b>
R.6.1-Effects of secreted factors by VIC activated with IFN- $\gamma$ +LPS in VEC.....	143
R.6.2-Effects of IFN- $\gamma$ and TNF- $\alpha$ in side-specific VEC .....	146
<b>DISCUSSION .....</b>	<b>157</b>
<b>D.1-IFN as pro-inflammatory and osteogenic cytokines in VIC.....</b>	<b>157</b>
D.1.1-IFN- $\alpha$ effects in VIC .....	157
D.1.2-IFN- $\gamma$ effects in VIC .....	161
D.1.3-Mechanistic differences between type I and II IFN.....	163
<b>D.2-Novel insights into TLR4/3 ligands in VIC.....</b>	<b>164</b>
D.2.1-Novel insights into LPS effects in VIC .....	164
D.2.2-Type I IFN signalling mediates Poly(I:C) effects in VIC.....	165
<b>D.3-JAK/STAT and TLR interplay in VIC .....</b>	<b>167</b>
D.3.1-IFN- $\alpha$ and LPS interplay on inflammation and osteogenesis .....	168
D.3.2-IFN- $\gamma$ and LPS interplay on inflammation, angiogenesis and osteogenesis.....	169
<b>D.4-Sex-differences in VIC responses .....</b>	<b>171</b>
<b>D.5-VIC-VEC communication and its potential role for CAVD .....</b>	<b>175</b>
<b>D.6-IFN-<math>\gamma</math> and TNF-<math>\alpha</math> effects in VEC.....</b>	<b>176</b>
<b>D.7-JAK/STAT as potential therapeutic targets for CAVD .....</b>	<b>179</b>

D.7.1-Type I IFN and CAVD .....	179
D.7.2-Type II interferons and CAVD .....	180
<b>D.8-Limitations of the study .....</b>	<b>182</b>
<b>CONCLUSIONS .....</b>	<b>187</b>
<b>BIBLIOGRAPHY .....</b>	<b>191</b>
<b>ANNEXS .....</b>	<b>207</b>
<b>ANNEX 1-MATERIALS .....</b>	<b>207</b>
<b>ANNEX 2-PEER-REVIEWED RESEARCH PAPERS .....</b>	<b>213</b>

## **ABBREVIATIONS**



# ABBREVIATIONS

---

Akt: Protein kinase B  
ARS: Alizarin red staining  
AS: Aortic valve stenosis  
AV: Aortic valve  
aVEC: Aortic-side valvular endothelial cells  
aVIC: Activated valvular interstitial cells  
BCA: Bicinchoninic acid assay  
BCL2: B-cell lymphoma-2  
BMP-2: Bone morphogenetic protein-2  
BSA: Bovine serum albumin  
CAVD: Calcific aortic valve disease  
CM: Conditioned medium  
CNMD: Chondromodulin-1  
DAMP: Damage-associated molecular patterns  
DAPI: 4', 6-diamidino-2-phenylindole  
dsRNA: Double-stranded RNA  
EDTA: Ethylenediaminetetraacetic acid  
EGM-2: Endothelial growth medium-2  
ELISA: Enzyme linked immunosorbent assay  
EndMT: Endothelial-to-mesenchymal transition  
eNOS: Endothelial nitric oxide synthetase  
ERK: Extracellular signal-regulated kinase  
FITC: Fluorescein isothiocyanate  
FBSi: Inactivated fetal bovine serum  
HIF-1 $\alpha$ : Hypoxia inducible factor 1 $\alpha$   
ICAM-1: Intercellular adhesion molecule 1  
IFN: Interferons  
IFNAR: Interferon  $\alpha/\beta$  receptor  
IFNGR: Interferon  $\gamma$  receptor  
IL: Interleukin  
IRF: Interferon regulatory factor

JAK: Janus kinases  
JNK: c-Jun N terminal kinases  
LDL: Low density lipoprotein  
Lp(a): Lipoprotein A  
LPS: Lipopolysaccharide  
MAPK: Mitogen-activated protein kinases  
MGP: Matrix-Gla protein  
MyD88: Myeloid differentiation primary response protein 88  
MMP: Matrix metalloproteinase  
MSX2: Homeobox protein MSX-2  
MTT: 3-(4,5-dimethylthiazol-2-yl)-2,5-diphenyltetrazolium bromide  
NF- $\kappa$ B: Nuclear factor kappa-light-chain-enhancer of activated B cells  
OM: Osteogenic medium  
OPG: Osteoprotegerin  
OSX: Osterix  
PAMP: Pathogen-associated molecular patterns  
PGE<sub>2</sub>: Prostaglandin E<sub>2</sub>  
Pi: Inorganic phosphate  
PIAS: Protein inhibitor of activated STAT  
PI3K: Phosphatidylinositol 3 kinase  
Poly (I:C): Polyinosinic:polycytidylic acid  
PRR: Pattern recognition receptor  
qPCR: Quantitative polymerase chain reaction  
qVIC: Quiescent valvular interstitial cells  
RUNX2: Runt-related transcription factor-2  
SD: Standard deviation  
SDS: Sodium dodecyl sulphate  
 $\alpha$ -SMA:  $\alpha$ -Smooth muscle actin  
RANK: Receptor activator of nuclear factor  $\kappa$ B  
RANKL: Receptor activator of nuclear factor  $\kappa$ B ligand  
siRNA: Small interference RNAs  
SOCS: Suppressors of cytokine signalling  
SOST: Sclerostin  
STAT: Signal transducers and activators of transcription

TLR: Toll-like receptors

TGF- $\beta$ : Transforming growth factor- $\beta$

TNAP: Tissue non-specific alkaline phosphatase

TNF- $\alpha$ : Tumor necrosis factor- $\alpha$

TRAF: Tumor necrosis factor receptor (TNF-R)-associated factor

TRIF: TIR-domain-containing adapter-inducing interferon- $\beta$

Ut: Untreated conditions

VCAM-1: Vascular cell adhesion molecule

VEC: Valvular endothelial cells

VEGF-A: Vascular endothelial growth factor A

VIC: Aortic valve interstitial cells

VSMC: Vascular smooth muscle cells

vVEC: Ventricular-side aortic valve endothelial cells

VWF: Von Willebrand factor



# **ABSTRACT**



# ABSTRACT

---

Introduction: Calcific aortic valve disease (CAVD) is the most common aetiology of acquired aortic valve disease. Initially considered a passive and degenerative process, the current view has redefined CAVD as an athero-inflammatory process in early stages that then progresses into a more complex condition. Supporting the role of inflammation-induced valve calcification are growing evidences on the induction of inflammation and subsequent pro-calcifying responses in valve interstitial (VIC) and endothelial cells (VEC) by immune mediators such as Toll-like receptor (TLR) ligands and tumor necrosis factor- $\alpha$  (TNF- $\alpha$ ).

Objectives: Prompted by evidences of a constitutive interferon (IFN) activity associated to ectopic calcification in a rare disease, the Singleton-Merten syndrome, and the infiltration of immune cells secreting IFN in diseased valves, we aimed to explore the role of these cytokines and Janus kinases (JAK)/Signal transducers and activators of transcription (STAT) pathways on CAVD pathogenesis.

Materials and methods: Human aortic valve cells explanted from patients with no valve disease were used as a model for studying CAVD underlying processes. Cells were exposed to recombinant IFN- $\alpha$  or IFN- $\gamma$  combined or not with TLR ligands (in VIC) or TNF- $\alpha$  (in VEC). Inflammation, calcification and angiogenic responses as well as cell proliferation and apoptosis were studied using different cellular and molecular biology techniques such as Western Blot, ELISA, qPCR, flow cytometry, immunofluorescence and calcification assays. In addition, total protein and RNA were extracted from both non-mineralized and calcified valves for gene and protein expression analysis.

Results: IFN activate several signalling pathways and promote inflammatory responses in VIC, characterized by adhesion molecule expression and nuclear factor- $\kappa$ B activation. In addition, IFN trigger VIC differentiation towards a pro-osteogenic phenotype and promote calcific nodule formation in high-phosphate conditions. Strikingly, we found an IFN-Lipopolysaccharide (a TLR4 ligand) interplay that further potentiates the pro-inflammatory, pro-angiogenic and pro-osteogenic responses. Significant findings include the blockade of the responses JAK inhibitors currently used in clinics named Jakinibs. Additionally, this study provides several new insights about sex-differences in CAVD, with unexpected greater responses to IFN and LPS in male cells and identified some of the underlying molecular mechanisms such as larger protein kinase B/Akt activation in cells

from females, and larger osteogenic signalling, hypoxia-inducible factor (HIF)-1 $\alpha$  and extracellular signal-regulated kinases activation in male cells. We also found sex-differences in gene expression profile in calcified valve tissue that correlate with lower valve calcification in female patients. Furthermore, our work demonstrates a novel role for type I IFN signalling on TLR3-mediated effects in VIC. Finally, data unveiled IFN- $\gamma$  as a pro-inflammatory cytokine in VEC as well as differences on monocyte adhesion to side-specific VEC monolayers in response to IFN- $\gamma$  and TNF- $\alpha$  with potential relevance in CAVD pathogenesis.

Conclusions: Our findings highlight that IFN act as pro-inflammatory and pro-osteogenic cytokines in valve cells and support the model of inflammation-induced calcification, the concept of additional pro-angiogenic mechanisms beyond valve thickening and hypoxia, and the notion of CAVD as a sex-divergent disease from the early inflammatory stages. Clinically relevant findings include the blockade of IFN-induced responses by Jakinibs, and by a HIF-1 $\alpha$  inhibitor. JAK/STAT and HIF-1 $\alpha$  pathways emerge as potential therapeutic targets for CAVD.

# **INTRODUCTION**



# INTRODUCTION

---

## I.1-Mammalian heart valves

In animals, the heart is composed of red muscle and a variable number of chambers. Mammalian hearts are composed of four different cavities, two atria and two ventricles (**Figure I**) that function as a pump to simultaneously deliver blood to the lungs and the rest of the body as follows:

- a) The deoxygenated blood from the different tissues is delivered to the right atrium through the superior and inferior vena cava. This blood is then transferred to the right ventricle, which pumps it to the lungs through the pulmonary artery.
- b) The oxygenated blood returns to the left atrium of the heart through the pulmonary veins. After reaching the left ventricle, it gets pumped through the aorta artery to the rest of the body. During this process, the oxygen is delivered to the different tissues and the unoxygenated blood finally returns to the right atrium, starting a new cycle.

The human heart has different valves whose function is to regulate blood flow direction: the semilunar valves, aortic (AV) and pulmonary, and the atrioventricular valves, mitral and tricuspid. The pulmonary valve regulates the flow from the right ventricle to the pulmonary artery, whereas the AV regulates the flow from the left ventricle to the aorta. The mitral valve separates the left ventricle and atrium, whereas the tricuspid valve separates the right ventricle and atrium (**Figure I**).

The cardiac valves open and close over  $3 \times 10^9$  times in a lifespan of 70 years. The left-side valves, mitral and aortic, regulate the highest-pressure process, which reaches a transvalvular pressure of about 120 and 80 mmHg respectively (systemic circulation). In contrast, the transvalvular pressure on the right-side valves, tricuspid and pulmonary, is approximately of 25 and 10 mmHg, respectively (pulmonary circulation).<sup>1</sup> To note, the AV, which is the main focus of this thesis, is exposed to an unique mechanical environment within the cardiovascular system, with the opposing sides of the valve experiencing markedly different hemodynamic shear stresses from the surrounding blood flow.

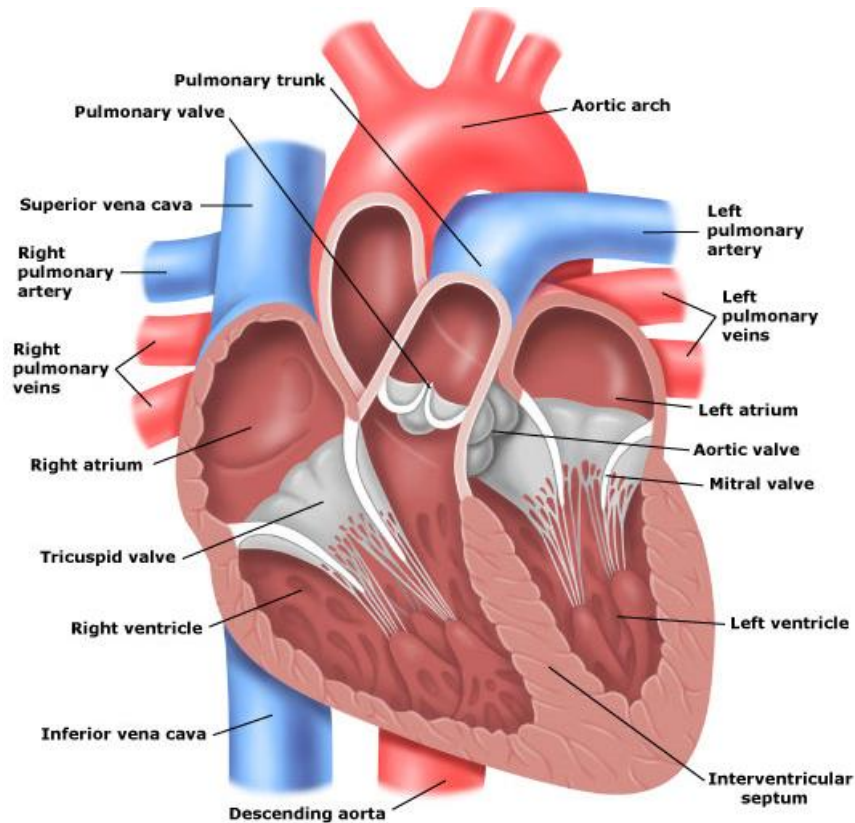


**Figure I. Representation of the human heart anatomy.** Taken from: <http://nursingmedic.blogspot.com/2010/11/anatomy-of-heart.html>.

The cardiac cycle is characterized by a mixture of electric and mechanical events. In the most simplified model, the cardiac cycle can be divided into two phases named diastole and systole. During the former one, the atrioventricular valves are open and allow the blood to flow into the heart and to reach the ventricles, which are in a relaxed state. When the ventricles are full of blood, the atrioventricular valves close and the semilunar valves open. At the same time, the electrical stimulation triggers the contraction of the ventricles, which subsequently pumps the blood outside the heart through the pulmonary and aorta arteries. It is therefore crucial for the correct performance of the heart that the four valves preserve their physiology and function. However, some conditions such as infections, degeneration and congenital disorders can lead to valve malfunctioning, which in general affects the whole cardiac operation.<sup>1</sup>

## **I.1.1-Heart valve physiology**

### *I.1.1.1-Structure of the valves*

The physiology of the heart valves differs mainly in their structure. The atrioventricular valves are composed of two (mitral valve) or three leaflets (tricuspid valve) that have the same structure. These valves, but not the semilunar valves, also have a specialized supportive structure connecting the valve to the ventricles, which is composed of three chordae tendineae that insert into two papillary muscles.<sup>2</sup> In contrast, the semilunar valves are normally composed of three cusps attached to a cylindrical structure named root that connect the ventricles to the major arteries. The importance of the AV is remarked by its connection to the right and left coronary arteries; in fact, the AV cusps are classified as the right, left, and non-coronary.<sup>3</sup>

The functionality of the heart valves is accomplished by a complex and specialized organization of cells and extracellular matrix layers. In general, the same composition and cell types can be found in the four heart valves. The outer surfaces of the valves are covered by a continuous endothelium and the valve interstice is arranged in three main layers named fibrosa, spongiosa and ventricularis, each of them showing specific structures and functions. The fibrosa layer is oriented to the major arteries or to the atrium depending on the valve. It is composed of a dense connective tissue containing collagen fibres oriented circumferentially that supports most of the haemodynamic challenges of the valves. The spongiosa is the middle layer and contains mainly glycosaminoglycans whose major function is to support and facilitate the movements of the valve cups. Finally, the ventricularis layer is oriented to the ventricle and composed of elastin fibres oriented radially, thereby allowing valve flexibility in each cycle.

In humans, the AV is an avascular and usually tricuspid structure of  $\leq 1$  mm in thickness that is attached to the aorta via a fibrous annulus named aortic root. A schematic representation of the AV structure is shown in **Figure II**.

### *I.1.1.2-Cellular components of the valves*

Under normal conditions, the resident valve cells can be grouped in valvular endothelial cells (VEC) and valvular interstitial cells (VIC) (**Figure II**).

VEC: These cells populate the outer layers of the valve, the endothelium. VEC are specialized cells with homeostatic functions such as the regulation of nutrient transmission, extracellular matrix synthesis, inflammation and VIC phenotype, and also have anti-thrombotic

functions.<sup>4</sup> Phenotypically, VEC share common functions with vascular endothelial cells such as Von Willebrand factor (VWF) expression, nitric oxide synthesis, prostacyclin and extracellular matrix proteins production, and also have typical endothelial cellular junctions.<sup>5</sup> However, there are growing evidences of intrinsic differences among vascular and valvular endothelial cells. Remarkably, a major difference is that vascular endothelial cells align parallel to the direction of the blood flow, whereas VEC do it perpendicularly to the blood flow and circumferentially within the valve cusps.<sup>6</sup> Furthermore, the transcriptional profile of vascular and valvular endothelial cells revealed phenotypic differences regarding inflammatory and osteogenic genes and the marked influence of shear stress.<sup>7</sup> Therefore, the unique haemodynamic pattern and the specialization of VEC might have an important role in both AV homeostasis and disease. Importantly, VEC lining the aortic (aVEC) or the ventricular (vVEC) sides of the valve are under different shear stress conditions and exhibit pathophysiological differences.

VIC: These cells, which are crucial to valve function, are arranged in subpopulations within the different layers and secrete extracellular matrix molecules, providing strength and elasticity to the valve. The term VIC encompasses a heterogeneous population composed of fibroblasts, myofibroblasts and smooth muscle cells.<sup>8,9</sup> In homeostatic conditions, most cells exhibit a fibroblastic phenotype recently termed quiescent VIC (qVIC), characterized by neither active matrix remodelling activity nor contractility. Intriguingly, there are also a small percentage of myofibroblast-like cells named activated VIC (aVIC), characterized by proliferative and contractile properties and whose main function is to maintain extracellular matrix homeostasis. Moreover, these cells express the marker  $\alpha$ -smooth muscle actin ( $\alpha$ -SMA) and secrete different growth factors, cytokines and molecules related with extracellular matrix remodelling such as matrix metalloproteinases (MMP) and their counterparts tissue inhibitor of metalloproteinases (TIMP). The normal functionality of the AV depends on the reversible transition and delicate balance of VIC phenotypes, a process whose disruption has been pointed to trigger valve disease.<sup>10,11,12</sup> Importantly, and as detailed later, many evidences support the hypothesis of qVIC becoming activated and undergoing a phenotype transition to osteoblast-like bone forming cells as a mechanism of valve calcification.<sup>13</sup>

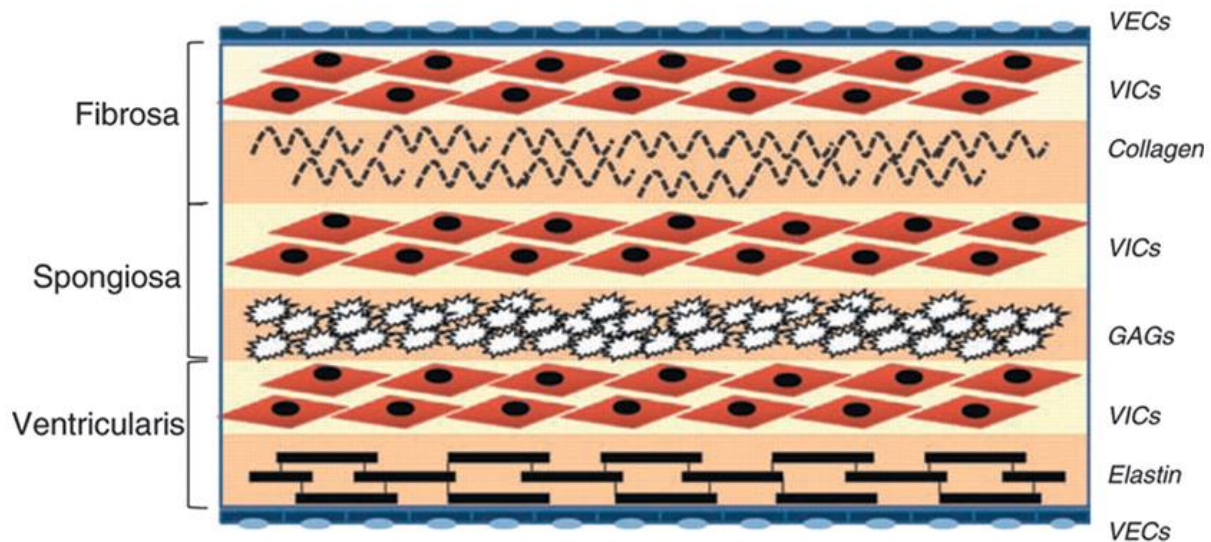


**Figure II. Aortic valve layers structure and cellular components.** GAGs indicates glycosaminoglycans. Reproduced with permission from<sup>13</sup>.

The normal cellular and matrix architecture of the valves may be disrupted by the exposure to biochemical or mechanical stress that results in endothelium dysfunction and the presence of immune cell infiltrates. This creates an inflammatory milieu that, together with an extensive matrix remodelling of the cusps, can lead to the development of different pathological states affecting valve and heart function.

### I.1.2-Valvular heart diseases

The global burden of the valvular heart diseases is still poorly known given the socio-economic differences between countries and the high rate of asymptomatic cases. Their most known cause is rheumatic fever due to the exposure to different strains of *Streptococcus*, which promotes a relatively fast development of valvular heart disease.<sup>14</sup> However, the prevalence of degenerative valve diseases is increasing in developed countries, due to the higher life expectancy as well as the changes in the lifestyle. A recent large-scale community echocardiographic screening, the OxVALVE population cohort study, revealed that half of the population over 65 years suffer from different types and grades of valvular diseases.<sup>15</sup> Therefore, valvular heart diseases emerge as high prevalence conditions with global socio-economic impact, which supports the necessity of a better understanding of their mechanisms and the development of novel and effective treatments.

The four heart valves may suffer from different disease states triggered by a wide variety of risk factors and conditions. In general, the two main outcomes of valvular heart diseases are stenosis and regurgitation. In the case of stenosis, the heart valve loses its homeostasis and the exacerbated

remodelling as well as the generation of calcific nodules within the valve leads to its thickening and incomplete opening. The four heart valves can suffer stenosis. In contrast, regurgitation happens when the valve is not completely closed during diastole, allowing a limited amount of pumped blood to return. In both cases, the maintenance of the cardiac function implies an additional demand on heart performance that can trigger cardiac events such as ventricle hypertrophy or even stroke or sudden death. In the next paragraph, the most important valvular diseases and their characteristics are described.

#### *1.1.2.1-Mitral valve diseases*

Mitral valve stenosis, characterized by leaflet thickening and fusion that impairs the valve performance, is a low-prevalence valvular disease affecting only 0.2% of the population over 75 years.<sup>14</sup> Its main cause is rheumatic heart disease, which is thought to be related to an exaggerated immune reaction and subsequent inflammation in response to *Streptococcus* antigens. For the symptomatic cases, percutaneous transluminal mitral valvuloplasty is the recommended treatment, and, when not possible, valve replacement is the only available therapy.<sup>16</sup>

Mitral valve regurgitation is one of the most common types of valvular heart disease, affecting approximately 9.3% of the population over 75 years.<sup>14</sup> It is a complex disease, also called mitral insufficiency or mitral incompetence, characterized by the reverse blood flow to the left atrium that subsequently promotes cardiac muscle hypertrophy. Two types of mitral regurgitation can be distinguished: (i) Primary, which is caused by structural defects triggered by either congenital or acquired causes. The most important primary mitral regurgitation type is mitral valve prolapse, which is triggered by diverse syndromes whose common outcome is an abnormal extracellular matrix deposition and reorganization of the connective tissue. (ii) Secondary, caused indirectly by the dilatation of the left ventricle, whose enlargement affects valve function. The damage leading to mitral regurgitation is usually triggered by rheumatic fever, infective endocarditis or valve damage after an ischemic disease. Its treatment varies depending on each case, encompassing from drug-based therapies for symptoms release to valve replacement in the worst cases.<sup>16</sup>

#### *1.1.2.2-Tricuspid valve diseases*

Very little is known about the stenosis of the tricuspid valve, which is a rare disease often linked to tricuspid regurgitation and mitral stenosis. Depending on leaflet condition, surgery for valve repair or replacement are the only available options. Current guidelines suggest the early intervention prior to the development of irreversible damage within the right ventricle.<sup>16</sup>

Tricuspid valve regurgitation has a prevalence of approximately 10% of the global population and it is frequently linked to mitral regurgitation.<sup>16</sup> It is in most cases secondary to a wide variety of conditions such as infective endocarditis, rheumatic heart disease, carcinoid syndrome, myxomatous disease, endomyocardial fibrosis, drug-induced valve diseases, and thoracic trauma. These diseases alter the cardiac function causing right ventricle dysfunction that affects the tricuspid valve. The current guidelines recommend heart surgery for valve repair or replacement, even if there are still not symptoms.<sup>16</sup>

#### *1.1.2.3-Pulmonary valve diseases*

This valve rarely undergoes acquired valve disease, being the most cases caused by congenital conditions. Pulmonary valve diseases are often associated to other cardiac malformations, such as tetralogy of Fallot, Williams syndrome, or transposition of the great arteries. Pulmonary stenosis accounts for approximately 8% of all the heart congenital defects. The systemic increase in pressure overload can trigger a subsequent tricuspid regurgitation. Valve replacement is the most common therapy in this case. Pulmonary regurgitation is thought to be present in a high percentage of the population in a low degree, although rarely progresses to heart failure.<sup>17</sup>

#### *1.1.2.4-Aortic valve diseases*

The AV shows a similar structure than the pulmonary valve, although in contrast to the latter it frequently suffers from acquired valve disease. In fact, AV regurgitation is present in 2.0% of population over 75 years in developed countries.<sup>14</sup> The aetiology of the disease can be infective, due to rheumatic fever, degenerative, or congenital in the case of bicuspid valves. The current guidelines indicate valve replacement only in symptomatic cases or when the left ventricle hypertrophy occurs.<sup>16</sup>

In developed countries, aortic valve stenosis (AS) is the most common valve disease requiring surgery and a growing health burden. First described by J.G. Mönckeberg in 1904, AS is a common finding in elderly subjects from developed countries, affecting approximately 3% of the population over 75 years.<sup>14</sup> Moreover, it has been estimated that approximately 34% of the population over 65 years suffer from early and asymptomatic AV lesions named AV sclerosis, characterized by valve thickening and the generation of small calcification foci. Despite the limited valve damage, AV sclerosis has been associated to an increase of 50% in the possibilities of suffering myocardial infarction and cardiovascular death.<sup>18</sup> Over time, close to 16% of AV sclerosis patients progress into AS, a symptomatic state characterized by the presence of calcification nodules

and valve thickening that obstruct the left ventricular outflow and impair the haemodynamic performance of the valve.<sup>19</sup> This condition affects not only the valve but also the myocardium, since increased left ventricular diastolic pressure is a typical secondary outcome of AS. The spectrum of AV disease ranges from aortic sclerosis to severe symptomatic AS, with an onset of symptoms that occurs late in the disease (**Figure III**).<sup>19</sup>

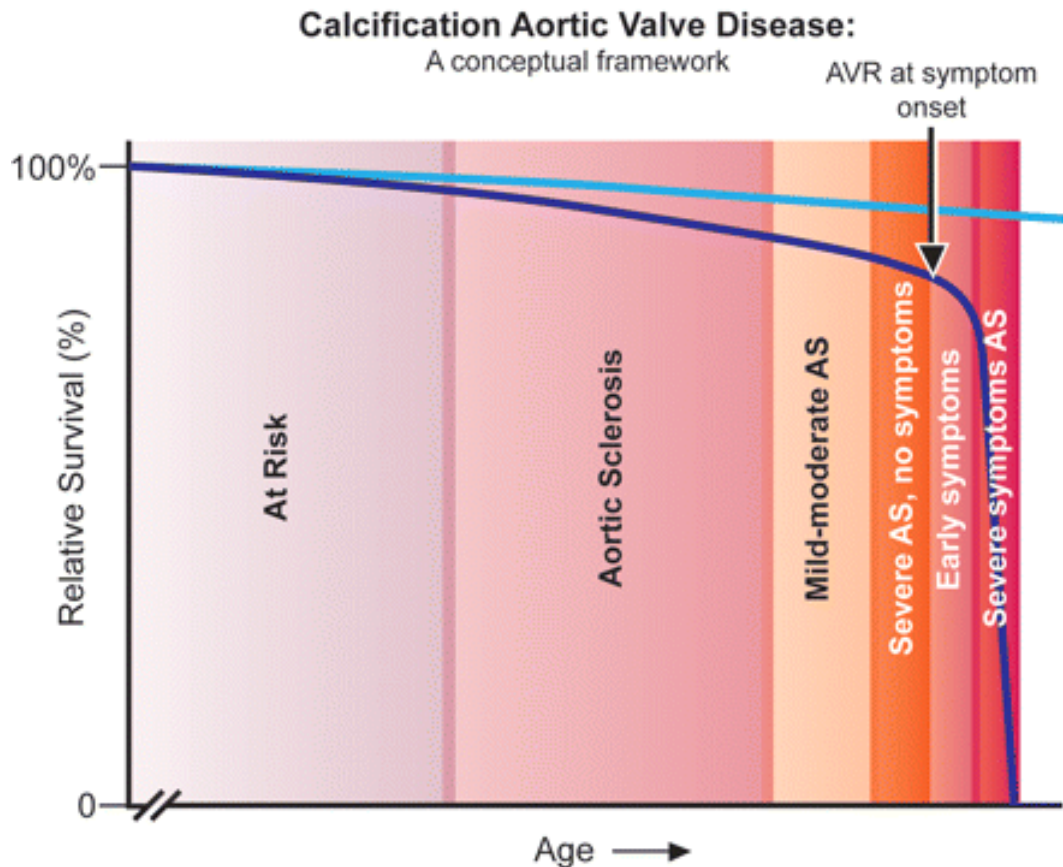


**Figure III. Aortic valve disease development diagram.** Purple line indicates the deviation of the survival curve from the expected event-free survival (light blue line). AVR indicates aortic valve replacement. Reproduced with permission from<sup>19</sup>.

Nowadays, we lack any pharmacological treatment for AS, being valve replacement by surgery or transcatheter aortic valve implantation the only available options for patients. Therefore, it is of extreme importance to understand the molecular processes leading to the progression of AV sclerosis to AS to develop novel and safe therapeutic targets for the early intervention of the disease. In this line, the underlying mechanisms leading to ectopic calcification in AV tissue arise as the more feasible therapeutic targets for the treatment of AS. The AV is the most diseased and replaced valve, and the severe form of AV disease is the focus of the current thesis.

## **I.2- Calcific aortic valve disease**

Calcific aortic valve disease (CAVD), the most prevalent form of AV sclerosis and AS in developed countries, was at first glance thought as a passive process consequence of valve tissue degeneration, although the current view is that it is the result of an active process. During the last decades, a series of evidences have shown active and cell-mediated processes as the main mechanisms driving its onset and progression. The initial stages of CAVD are thought to be similar than an atherosclerotic process sharing common risk factors such as hypertension, age and low-density lipoprotein among others, as shown in the Cardiovascular Health Study.<sup>20</sup> However, the mechanisms lately diverge in CAVD through a more complex disease.<sup>21</sup>

### **I.2.1-CAVD risk factors**

Age: It is a risk factor for degenerative CAVD, with a two-fold increase for each 10 years of age, as reported in the largest study performed in a cohort of more than 5,000 patients.<sup>20</sup>

Smoking: It is a risk factor for general morbidity and mortality, reducing the life expectancy in 10 years. In addition, smokers have a 50% of chances to die for smoking-associated conditions, specially cardiovascular events, and smoking increases a 35% the chances of suffering CAVD relative to non-smokers.<sup>20</sup>

Hypertension: This condition occurs when the systolic blood pressure is  $\geq 140$  mmHg and/or the diastolic blood pressure is  $\geq 90$  mmHg, which has been associated to a higher predisposition for cardiovascular events, and specifically to an increase in the risk of CAVD in approximately 20%.<sup>20</sup>

Male sex: Epidemiologic studies have shown that male sex presents a two-fold increase of risk for AS compared to females.<sup>20</sup> In addition, emerging evidences point to different or divergent mechanisms leading to CAVD in males and females, since the former ones present significant higher levels of calcification as demonstrated by different clinical studies in Caucasian population.<sup>22,23</sup> At the *in vitro* level, an initial report demonstrated intrinsic differences in gene expression and cellular processes such as proliferation when comparing porcine male and female valve cells,<sup>24</sup> whereas a more recent report showed sex-differences in response to osteogenic medium (OM).<sup>25</sup> Altogether, these findings prompted the researchers to ask whether CAVD is a sex-specific disease since the early stages or whether it shares the same onset with different types of progression in male and female patients, a question that merits further investigation to better understand CAVD.<sup>26</sup>

Diabetes mellitus: This epidemic disease exhibits a high rate of prevalence and strong correlation with the development of cardiovascular diseases. The association of diabetes with CAVD has been demonstrated by numerous reports, including the Multi-Ethnic Study of Atherosclerosis, which demonstrated an increase in AV calcium content in patients with diabetes mellitus.<sup>27</sup> However, little is known about the effects of this disease on the progression of AS.

Obesity and renal failure: The correlation of obesity with CAVD progression is still not clear, although some studies support obesity as a risk factor for the disease, indicating that an elevated body mass index ( $\geq 30 \text{ kg/m}^2$ ) correlates with CAVD development.<sup>28</sup> Regarding renal failure, chronic kidney disease has been shown to have a powerful impact on the presence and severity of AS.<sup>29</sup>

Lipids and oxidized phospholipid transporters: Dyslipidaemia is a central and very-well known contributor to the development of atherosclerosis, in which low density lipoprotein (LDL)-cholesterol levels play a major role. In fact, a meta-analysis of 27 different clinical trials revealed that lowering LDL-cholesterol levels with statins reduced up to 25% the risk for cardiovascular mortality and non-fatal myocardial infarction.<sup>30</sup> LDL-cholesterol levels have also been associated with a greater prevalence of CAVD.<sup>14</sup> The similarities between atherosclerosis and CAVD early stages, as well as the promising *in vitro* effects of statins in VIC, prompted to develop a series of randomized clinical trials using different statins for the treatment of AV sclerosis or AS, i.e. the Scottish Aortic Stenosis and Lipid Lowering Trial, Impact on Regression (SALTIRE),<sup>31</sup> the Simvastatin and Ezetimibe in Aortic Stenosis (SEAS),<sup>32</sup> and the Aortic Stenosis Progression Observation: Measuring Effects of Rosuvastatin (ASTRONOMER).<sup>33</sup> Unfortunately, all these trials failed to show any relationship between statin treatment and a significant reduction in the progression of CAVD. A potential reason of this failure could be a late intervention when the disease has progressed and exhibit more complex mechanisms in which lipids may not play a key role.

Lipoprotein A (Lp(a)), a transporter of oxidized phospholipids considered a well-studied risk factor for cardiovascular disease, has been pointed as an important predictor of AV disease.<sup>34</sup> Increasing evidences indicate its potential role as a therapeutic target for the disease. A recent multimodality imaging analysis of a clinically representative cohort of patients with AS revealed the association of Lp(a) and oxidized phospholipids-apoB levels with increased AV calcification and faster disease progression, suggesting that lowering Lp(a) or inactivating oxidized phospholipids may slow AS progression.<sup>35</sup>

Bicuspid aortic valve: Bicuspid AV is the most common congenital cardiac abnormality and has been associated with mutations in the *NOTCH1* gene.<sup>36</sup> The different physiology of the valve strongly affects the haemodynamic regulation and the wall shear stress supported by the tissue, which promotes a more frequent and accelerated development of CAVD as compared to tricuspid AV.<sup>37</sup>

### **I.2.2-CAVD diagnosis**

The detection of cardiac calcifications is an emerging predictive value for future cardiovascular events. A recent review outlined the importance of the early detection by innovative techniques of both atherosclerosis and cardiac calcifications in order to improve the current prediction based on classical cardiovascular risk factors and the use of validated algorithms, i.e., the Framingham Risk Score, the Pooled Cohort Equations, and the European SCORE Risk Charts.<sup>38</sup> Therefore, it is mandatory to develop more accurate techniques allowing the clinicians not only to detect the presence of cardiac calcifications, but also their severity. The conventional technique for the diagnosis of CAVD is two-dimensional echocardiogram, however the limitations of this technique to distinguish the degree of stenosis are prompting clinicians to develop novel and complementary techniques such as computed tomography calcium scoring, and positron emission tomography.

Doppler-Echocardiography: This relatively inexpensive and harmless technique is based on the use of sound waves to produce video images of the heart (**Figure IVA**). The echocardiogram is a key diagnostic tool providing information about the condition of the AV and its causes and severity, and it can also be used to detect other valvular diseases, such as aortic regurgitation, mitral stenosis and mitral regurgitation. The main parameter indicating AS is the valve area, although since it shows some limitations, additional measurements such as flow rate, mean pressure gradient, ventricular function, size and wall thickness, degree of valve calcification, and blood pressure help to define more accurately the condition of the valve.<sup>16</sup>

Depending on the indicated parameters, four different grades of severity of AS can be defined:<sup>16</sup> (i) High-gradient aortic stenosis: valve area  $\leq 1 \text{ cm}^2$  and mean gradient  $> 40 \text{ mmHg}$ . (ii) Low-flow, low-gradient aortic stenosis with reduced ejection fraction: valve area  $\leq 1 \text{ cm}^2$ , mean gradient  $< 40 \text{ mmHg}$ , ejection fraction  $< 50\%$ , and stroke volume index (SVi)  $\leq 35 \text{ mL/m}^2$ . In this case, further investigation with low dose of dobutamin stress during echocardiography is necessary to truly distinguish AS from other conditions generating similar cardiovascular outcomes. (iii) Low-

flow, low-gradient aortic stenosis with preserved ejection fraction: valve area  $\leq 1 \text{ cm}^2$  and mean gradient  $< 40 \text{ mmHg}$ , ejection fraction  $\geq 50\%$  and  $\text{SVi} \leq 35 \text{ mL/m}^2$ . (iv) Normal-flow, low-gradient aortic stenosis with preserved ejection fraction: valve area  $\leq 1 \text{ cm}^2$  and mean gradient  $< 40 \text{ mmHg}$ , ejection fraction  $\geq 50\%$  and  $\text{SVi} > 35 \text{ mL/m}^2$ .

Computed tomography (CT) calcium Scoring: This technique, based on the use of X-rays, can provide a more detailed, reproducible, and accurate assessment of the calcification burden in the AV than echocardiography, demonstrating a strong association and diagnostic value for severe AS (**Figure IVB**), and it could be a future clinical routine technique.<sup>39</sup>

Positron emission tomography (PET): It is a non-invasive technique that allows to monitor the activity of specific biological processes within tissues, including the AV, by the use of different radiotracers binding to regions where a biological process is occurring. In the case of the AV, PET allows not only the detection of calcifications but also the evaluation of the extent of inflammation. The positron-emitting radiotracer  $^{18}\text{F}$ -fluoride binds to regions of newly developing microcalcification with a good predictive value as demonstrated in a recent study.<sup>40</sup> Therefore, optimized  $^{18}\text{F}$ -fluoride PET-CT holds a promise as a powerful research technique that could improve our understanding of the disease and be used as a biomarker of calcification activity in clinical trials of novel therapies.<sup>40</sup> A comparison of calcification imaging obtained with different techniques is shown in **Figure IV**.

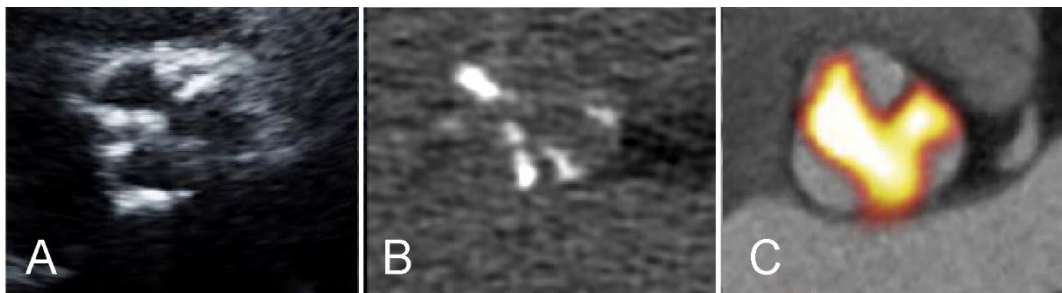


**Figure IV. Comparison of different methods for imaging calcification in the same patient with AS.** (A) 2-dimensional echocardiography. (B) CT calcium scoring. (C)  $^{18}\text{F}$ -fluoride PET-CT. Reproduced with permission from<sup>41</sup>.

---

### I.2.3-CAVD management and treatment

The disease is usually detected by echocardiography performed for routine examinations or after the presence of systolic murmurs. Its management depends on a wide variety of factors, especially the severity of the disease and whether this is worsening in subsequent follow-up

appointments. Initial symptoms of AS usually include fatigue, easy tiring, loss of energy, swelling of the ankles, palpitations, shortness of breath, chest pain, and dizziness or loss of consciousness.

If AV sclerosis is detected, the intervention is usually preventive, with changes in the lifestyle whose main objective is to reduce the influence of risk factors on the progression of the disease. If the disease progresses to moderate AS, the patient requires treatment by a cardiologist as well as a follow-up annual echocardiogram. These recommendations are sometimes accompanied by preventive treatments, such as angiotensin-converting enzyme inhibitors,  $\beta$ -blockers, and/or diuretics. However, no medical treatment has been approved or recommended for directly addressing CAVD,<sup>16</sup> and when severe AS is detected, even if there are no symptoms, surgery is the only recommended option. Four main surgical options arise for CAVD patients:<sup>16</sup>

Aortic valve repair: It is a common procedure for the case of leaking bicuspid aortic valves consisting on reshaping the aortic valve cusps, thus allowing the valve to open and close more completely. It has some advantages as compared to valve replacement, such as a lower tendency towards clot formation, and the lower probability of infection.

Balloon valvuloplasty: It is not a commonly used procedure. The technique consists in the introduction of a flexible and thin tube tipped with a deflated balloon that is directed to the valve, where it is inflated to stretch the narrowed valve. Then the balloon deflates and is removed. This method is used for either children or adults who cannot undergo open-heart surgery.

Aortic valve replacement: This procedure consists in the replacement of the dysfunctional heart valve for either a biological or a synthetic valve in an open-heart surgery. Mechanical valves are commonly composed of carbon, metal, or plastic. Their main advantage is the improved durability compared to biological valves, however, they present higher chances of blood clot formation. Biological valves from animal tissue, mostly porcine, although sometimes human donors, show less durability but lower chances towards blot clot formation. A third option is called “The Ross Procedure”, which consists in the substitution of the damaged aortic valve for a pulmonary allograft. A valve taken from a cadaver is then used to replace the pulmonary valve of the patient. The Ross procedure is used in patients younger than 40 to 50 years to avoid the long-term use of anticoagulant medications after surgery.<sup>16</sup>

Transcatheter aortic valve replacement: Also called transcatheter aortic valve implantation or TAVI, it is a newly developed technique that has improved the surgery conditions and lowered the chances for an open-heart intervention. Transcatheter AV replacement is the equivalent process of an arterial

stent in the AV context and provides a functional replacement to the valve site through a catheter. The new valve is expanded pushing the old cusps out of the way and manages the regulation of the blood flow.<sup>16</sup>

The election of the adequate procedure depends on the disease severity as well as the physical condition and age of the patient. Over the last years, the development of these less invasive techniques has improved the quality of life after the procedure. However, the risk of surgery in elderly patients and the problems that sometimes arise after valve surgery reinforce the necessity of the identification of novel drug targets to delay or reverse the disease without a surgical intervention. The understanding of the molecular mechanisms leading to valve leaflet thickening and calcification is a matter of urgency for the scientific community regarding the increasing prevalence of aortic valvular disease in developed and undeveloped countries.

### **I.3-Molecular mechanisms of CAVD**

CAVD is currently considered an active and multifaceted pathobiological process. Its molecular mechanisms are not fully elucidated although several processes are known to be relevant to CAVD pathogenesis, i.e. endothelial dysfunction, inflammation, fibrosis, angiogenesis, and calcification.<sup>41</sup>

The causes involved in the initiation of AV sclerosis are still unknown, but emerging evidences point to endothelial damage and dysfunction as the first step of the disease.<sup>41</sup> Once the endothelium is disrupted, it is essential for the maintenance of the valve performance that the homeostatic mechanisms repair the damage so the valve can return to its normal function. However, in some cases this process does not work properly, thus initiating the development of CAVD. The disease progression can be divided into three main stages.<sup>42</sup> The first stage is an atherosclerosis-like process in which immune cell infiltration and lipid deposition play a key role on the activation of resident valve cells. During this phase, the initial microcalcifications are also developed within the valve cusps. The second and third phases are characterized by the development of macrocalcifications as well as other pathological processes such as neoangiogenesis. In this section we summarize the current knowledge on CAVD initiation and progression.

#### **I.3.1-Initial triggers of CAVD: haemodynamic and genetic factors**

The aetiology of the disease can be infective, degenerative, or only congenital. Rheumatic CAVD seems to be caused by an unresolved throat infection with *Streptococcus* that triggers the

development of rheumatic heart disease, which is a chronic condition resulting from acute rheumatic fever after the infection with the former pathogen. Both rheumatic fever and rheumatic heart disease may cause damage to the heart valves that can result in stenosis and regurgitation.<sup>43</sup>

For non-rheumatic tricuspid CAVD, the focus of the current study, the initial causes of the disease remain still unidentified, although a wide amount of evidences points to a role of the hostile haemodynamic environment to which the AV is exposed. The interplay between fluid haemodynamic and different challenges including present risk factors, infections, or increased serum levels of inflammatory mediators, is thought to play a key role on CAVD initiation. As noted earlier, the fluid dynamic context of the AV differs from the rest of the valves, and the mechanical environment has been related to the preferential disease progression as compared to another semilunar valve with physiologically similarities, the pulmonary valve.<sup>44</sup> The high peripheral resistance developed during each cardiac cycle causes a substantial diastolic back pressure on the valve in the closed position, which affects the endothelial layer. This pressure creates an oscillatory shear stress that has been commonly linked to atheroprone regions,<sup>45</sup> only in the aortic side of the valve (**Figure V**). Therefore, as mentioned earlier, aVEC are exposed to a different haemodynamic environment than vVEC and vascular endothelial cells,<sup>46</sup> the latter exposed to a laminar blood flow with high and constant pressure in the straight regions ( $> 15$  dynes/cm<sup>2</sup>), and a disturbed and much lower flow in curved regions ( $< 4$  dynes/cm<sup>2</sup>).<sup>45</sup>

Hostile shear stress affects not only to the outside layer and aVEC, but also influences the behaviour of VIC from the fibrosa layer, which suffer from high mechanical stress especially during diastole (**Figure V**). The physiological relevance of the complex haemodynamic environment in the AV could trigger different outcomes not only by its own effects, but also by potentiating the responsiveness of VEC and VIC to different insults, i.e., inflammatory stimuli.

The notion of a key role for the fluid dynamics in CAVD development is further supported by the higher rate of disease found in bicuspid aortic valves, which are exposed to an even more hostile environment than tricuspid valves, characterized by a strong eccentric jet coming out of the valve and the associated vortex formation. In bicuspid AV, the most common congenital cardiac abnormality, the presence of only two abnormal cusps drastically alters the vortex evolution both temporally and spatially,<sup>44</sup> consequently most bicuspid AV patients suffer cardiac events and need surgery for valve replacement at earlier ages.

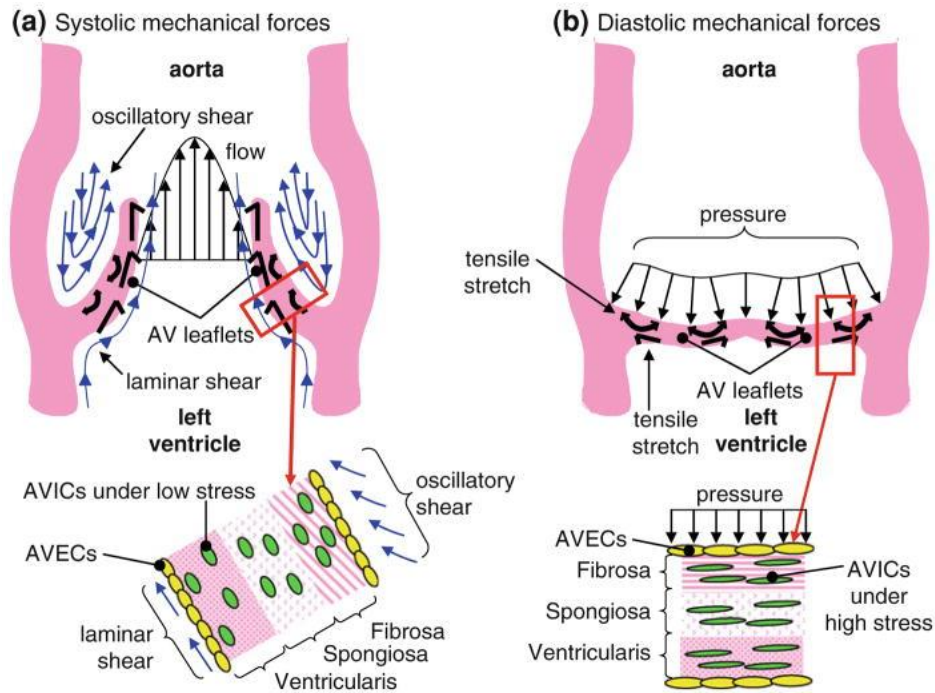


**Figure V. Representation of the different wall shear stress under the aortic and the ventricular side of the valve during a cardiac cycle.** (A) Under systolic mechanical forces, the ventricularis VEC experience straight shear while the VIC feel bending forces. (B) Diastolic mechanical forces include compression of the fibrosa VEC (AVEC) and high stress tensile strain on the aortic VIC (AVIC). Reproduced with permission from<sup>44</sup>.

The complex environment within the AV is thought to be accurately regulated, and the disruption of valve homeostasis by external factors or conditions is actively controlled to maintain valve function. However, when the endothelial damage is not properly repaired, homeostasis is disrupted, and the diseased state can progress to the first stage of CAVD.

Three stages for CAVD pathogenesis have been proposed based on clinical data and innovative optical molecular imaging techniques; the initiation and propagation phases, which are asymptomatic stages, and a late-stage phase with clinical manifestations. A scheme describing the three phases of CAVD is shown in **Figure VI**.

### **I.3.2-Initiation phase: endothelial dysfunction and inflammation**

The first stage of the disease seems to be initiated after an unresolved endothelial damage. During this phase, inflammation has been pointed as the driving mechanism, with a good amount of evidences suggesting that CAVD is an athero-inflammatory disease at least in its initial phases.<sup>21</sup> At the later stages of this phase, the first microcalcification nodules are formed, as disclosed by innovative optical molecular imaging that allowed the detection of early calcifications.<sup>47,41</sup>

### *1.3.2.1-Endothelial dysfunction*

The pathologic environment created by disturbed blood flow can in turn activate resident valve cells (both VIC and VEC). The contribution of these cells to the progression of the first stages of the disease gained attention over the last decades by the demonstration of their active roles in the complex regulation of valve mineralization. The first report showing a role for the endothelium in CAVD, published in 2003, demonstrated the association between AV sclerosis and systemic endothelial dysfunction.<sup>48</sup> In this line, an early event in CAVD is the production of reactive oxidative stress that co-localizes with calcified regions, as demonstrated in explanted human calcified AV.<sup>49</sup> Additionally, the treatment with the endothelial nitric oxide synthetase (eNOS) inhibitor L-NAME, reduced the oxidative stress in calcified valves, pointing to the endothelium as the major source of oxidative stress within the valve.<sup>49</sup> In addition, endothelial dysfunction and oxidative stress can be further promoted by pro-inflammatory cytokines, mainly tumor necrosis factor- $\alpha$  (TNF- $\alpha$ ), which are secreted by infiltrated immune cells in the early stages of the disease.<sup>50</sup> The relevance of the endothelium in CAVD initiation is also supported by the differential transcriptional profile of porcine aVEC and vVEC, the former showing lower expression levels of protective and anti-calcifying genes such as osteoprotegerin (OPG),<sup>51</sup> which correlates with the fibrosa layer-preferential calcification. Finally, pro-inflammatory cytokines<sup>52</sup> and the altered extracellular matrix<sup>53</sup> can trigger endothelial-to-mesenchymal transition (EndMT), a source of osteogenic cells within the valve. Collectively, these evidences stress out the importance of the endothelium in maintaining AV homeostasis, and demonstrate that the potential disruption of VEC homeostasis further contributes to CAVD initiation.

### *1.3.2.2-Inflammation: Immune cell infiltration, lipid deposition, and NF- $\kappa$ B activation*

Inflammation is a well-known inductor of vascular calcification<sup>54</sup> and also plays a role on CAVD initial stages (**Figure VI**). The inflammatory response is a demonstrated hallmark of CAVD, supported by increasing evidences in both clinical and cellular studies as described in the next paragraphs.<sup>55,56,57</sup>

Immune cell infiltration: After endothelial dysfunction occurs, the expression of adhesion molecules, i.e., intercellular adhesion molecule-1 (ICAM-1) and vascular cell adhesion molecule-1 (VCAM-1), facilitates the infiltration of immune cells such as monocytes, mast cells and T lymphocytes.<sup>58</sup> Infiltrated monocytes are then differentiated into macrophages, which secrete a wide range of inflammatory cytokines such as TNF- $\alpha$  and extracellular matrix remodelling molecules such as

MMP. Additionally, not only macrophages but also T lymphocytes secrete active cytokines that affect resident valve cells behaviour, i.e., interleukin (IL)-6 and IL-8. Strikingly, high serum levels of IL-6 have been linked to the development of cardiovascular events, and this cytokine is overexpressed in CAVD and is strong inducer of *in vitro* calcification of VIC.<sup>59</sup> Furthermore, another important cytokine with a reported role in CAVD is IL-1 $\beta$ , which is known to induce a pro-inflammatory phenotype<sup>60</sup> and the secretion of matrix remodelling molecules in VIC.<sup>61</sup> Finally, the activation of innate immunity also leads to the expression of several factors involved in tissue remodelling such as MMP and transforming growth factor- $\beta$ 1 (TGF- $\beta$ 1), which is overexpressed in CAVD and promotes VIC calcification mainly via apoptosis-related mechanisms.<sup>62</sup> In general, the signalling triggered by all these cytokines converges on the activation of the transcription factor nuclear factor kappa-light-chain-enhancer of activated B cells (NF- $\kappa$ B), whose chronic activation promotes VIC calcification (reviewed in<sup>56</sup>). Collectively, these evidences point to VIC as the master and most important sensors of the inflammatory milieu during early CAVD and as the major promoters of calcification in the context of the AV.

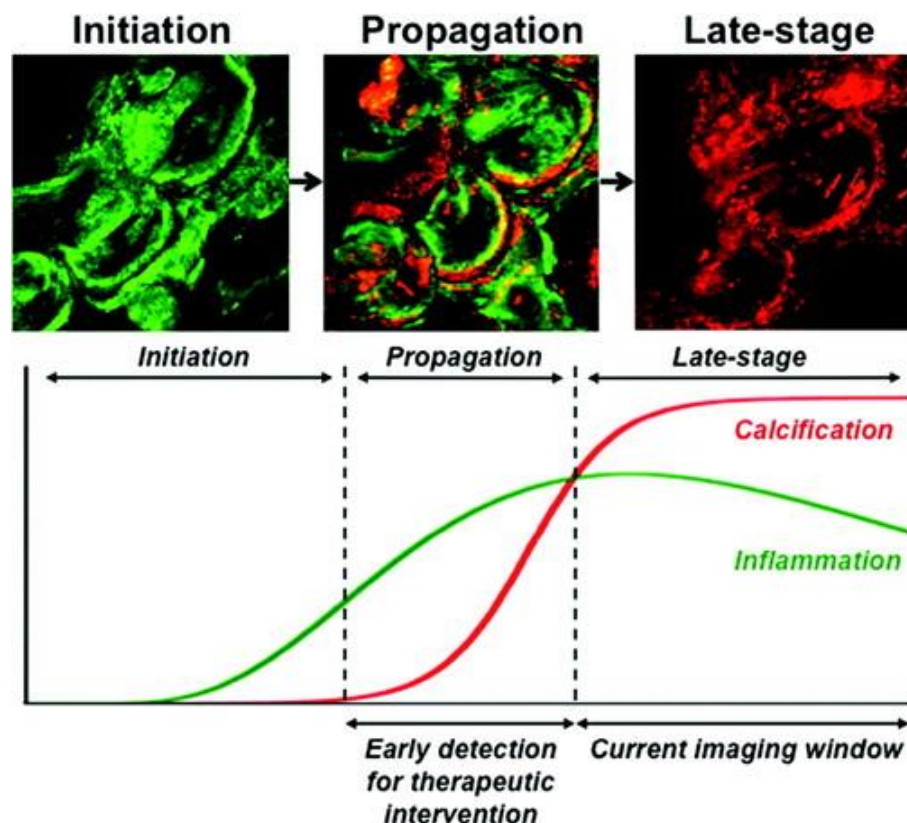


**Figure VI. Inflammation as a key mechanism of CAVD.** Molecular imaging detects 3 stages of calcification in CAVD: initiation, propagation, and late-stage calcification, in mice co-injected with nanoparticles to visualize macrophages (green) and near-infrared fluorescence imaging agent to detect calcification (red). Reproduced with permission from<sup>42</sup>.

Lipoprotein deposition and lipids metabolism: In addition to immune cell infiltration, the initiation of the inflammatory process in the AV might be driven by lipid accumulation within the valve cusps. Circulating Lp(a) and LDL are also deposited within the valve, the latter being oxidized during the process (oxLDL). Strikingly, oxLDL, inflammatory cell infiltrates and the expression of TNF- $\alpha$  co-localize in calcified valves.<sup>63</sup> Other important mediator of the initial stages of CAVD is Lp(a), which carries a high content in lysophosphatidylcholine. The enzyme autotaxin, which is transported to the valve by Lp(a) and secreted by VIC, can transform lysophosphatidylcholine into lysophosphatidic acid that subsequently promotes inflammation and mineralization of the AV.<sup>64</sup> Supporting this notion, recent reports revealed that Lp(a) and oxidized phospholipids promote valve calcification in patients with AS,<sup>35</sup> and the treatment of VIC with Lp(a) strongly promotes cell mineralization.<sup>65</sup> Another important pathway in the regulation of inflammation is the arachidonic acid route, the precursor of lipid mediators like leukotrienes and prostaglandins. The first enzyme of this route with a reported role in CAVD is 5-lipoxygenase, which is overexpressed in CAVD and triggers leukotriene synthesis and the subsequent inflammation of VIC.<sup>66</sup> Regarding prostaglandins, the inducible enzyme cyclooxygenase-2 is expressed by VIC isolated from AS valves and it has been shown to mediate calcification in a mouse *Klotho* model of CAVD.<sup>67</sup>

Pathogen-derived molecules: Other subsets of immunostimulatory molecules can be derived from pathogens such as virus and bacteria. In fact, a significant pathogen cargo has been found together with immune cells in inflamed areas of calcified valves, as demonstrated in a study detecting *Chlamydia pneumoniae*, *Helicobacter pylori*, *Cytomegalovirus*, *Epstein-Barr virus*, and *Herpes simplex* virus in the fibrosa layer of stenotic valves.<sup>68</sup> Moreover, bacteria associated with chronic periodontal infection have also been detected in the fibrosa layer of the AV,<sup>69</sup> and inoculation of oral bacteria is reported to cause CAVD in a rabbit model of low-grade endocarditis.<sup>70</sup> Moreover, pathogen-associated molecular patterns (PAMP) can be sensed by innate immune receptors, including Toll-like receptors (TLR). These receptors, known to mediate inflammation and to play a crucial role in the control of infection and the maintenance of tissue homeostasis, have been associated to CAVD pathogenesis,<sup>71</sup> as explained at length below.

Renin-angiotensin system activation: The pro-pathogenic milieu of the initial stages of CAVD is not restricted to cytokines and lipid mediators; in fact, angiotensin converting enzyme and its product angiotensin II are expressed and colocalize with LDL in calcified aortic valves.<sup>72</sup> Moreover, angiotensin II type I receptor is expressed by fibroblasts only in valve lesions.<sup>72</sup> Furthermore, data from a genetically hyperlipidaemic animal model associated angiotensin II to leaflet thickening and endothelial derangements, a phenomena linked to the early phase of AS. In ApoE-deficient and

atherosclerosis-prone mice, angiotensin II promoted AV injury by a mechanism involving its type I receptor.<sup>73</sup>

### *1.3.2.3-Valve cell differentiation and microcalcification*

Accumulating evidences point to AV calcification as an active cellular-mediated process involving a phenotypic switch of resident valve cells toward bone-forming cells:

VIC: The pro-inflammatory environment described above can be sensed by the inner resident VIC. As noted earlier, in normal conditions, most cells are in a quiescent state and approximately only 5% of VIC are in an activated myofibroblast state. However, upon tissue damage, the balance seems to be disrupted and a higher number of cells undergo the phenotypic change to a myofibroblast phenotype, a condition that when turns chronic, promotes CAVD development.<sup>13</sup> Myofibroblast or aVIC, are considered the key regulators of the ensuing valve calcification, by mechanisms involving apoptosis (dystrophic calcification) and osteogenic-like calcification, although it is still not clear whether qVIC can directly differentiate to osteoblast-like cells or transition to aVIC is a necessary step.

(i) Dystrophic calcification is the most prevalent form of calcification found in calcified valves, rather than true bone formation.<sup>74</sup> Emerging evidences indicate that the formation of calcific nodules by VIC is mediated by matrix vesicles containing a wide variety of enzymes and ions. In dystrophic calcification, cellular necrosis, as a passive process, and apoptosis, as an active process mediated by caspase activation, are the mechanisms leading to the formation and expansion of amorphous calcium phosphate nodules. In this context, damaged VIC generate apoptotic bodies containing calcium and inorganic phosphate (Pi) ions, thus facilitating the formation of crystals of hydroxyapatite.<sup>75</sup> Nano-analytical electron microscopy studies revealed that this crystalline hydroxyapatite formed after cellular damage differs from bone mineral both crystallographically and structurally, and suggested that mineralized spherical particles may play a fundamental role in calcific lesion formation.<sup>76</sup>

(ii) Osteogenic calcification is also mediated by VIC and characterized by the formation of true mature lamellar bone structures. Some valve cusps from CAVD patients present evidence of bone matrix, including osteoid cells, highly organized collagen scaffolds, multi-nucleated osteoclast-like cells, and fatty marrow pockets.<sup>74</sup>

Controversially, a potential third mechanism of calcification has been proposed based on the discordance between the low rate of true bone formation in calcified valves (only 13%)<sup>77</sup> and the high prevalence of osteogenic marker expression in most of calcified AV.<sup>78,79</sup> This may be explained by the presence of a subset of VIC that present a osteogenic-like activity that is different from a true bone formation.<sup>43</sup> Whether the different mechanisms of calcification can co-exist and/or synergize remains to be further explored.

The role of VIC as the major regulators of valve calcification has been extensively demonstrated.<sup>80,81</sup> VIC can sense a wide variety of stimuli present in the AV environment at the early stages of CAVD, and express several cytokine and immune receptors including TLR, which are pathogen and danger-derived sensors reported to promote inflammation and subsequent calcification in the valve context.<sup>71</sup> Collectively, evidences point to VIC as the master and most important sensors of the inflammatory milieu during early CAVD as well as the major promoters of calcification in the context of the AV and could be responsible for valve lesion formation.

VEC: Endothelial valve cells may suffer differentiation and are also a known source of osteogenic cells in the context of the AV via EndMT, a process reported to be triggered by inflammatory cytokines<sup>52</sup> and the altered extracellular matrix.<sup>53</sup>

Additional sources of myofibroblasts and osteoblasts in CAVD may include mesenchymal progenitor-like cells and circulating progenitor cells.<sup>79</sup>

At the clinical level, several studies support the notion of an inflammation-dependent initiation of calcification in CAVD. In fact, the first evidences of active bone activity in the AV that correlated with the presence of an inflammatory environment were reported several years ago.<sup>77</sup> New insights based on novel imaging approaches further support the notion of and inflammation-dependent calcification in the context of the aortic valve.<sup>82</sup> Together, the evidences point to a strong involvement of inflammation in the initiation phase of the disease, a role that loses relevance in the propagation and late-stage phases of the disease, where calcification and fibrosis-related signalling pathways play a major role (**Figure VI**). Therefore, it seems likely that the therapeutic intervention during the initial stage could be the best strategy to avoid the contribution of more complex and challenging processes to the disease progression. In this line, the early detection of the disease using novel biomarkers and/or developed imaging techniques emerges as an essential necessity step for the therapeutic intervention in the initiation phase.

To summarize, the first stage of CAVD is characterized by an atherosclerotic remodelling of the valve that includes early endothelial damage and the subsequent immune cell infiltration and lipid deposition. The disease progresses with the activation of qVIC and the formation of microcalcification by both osteogenic and dystrophic processes. When microcalcifications have been formed, the disease progresses toward a new stage.

### **I.3.3-Propagation phase: fibrosis, angiogenesis, and osteogenesis**

During this phase of the disease inflammation loses its predominance as a pathogenic process, whereas new pathological mechanisms start to account for CAVD progression.

#### *I.3.3.1-Abnormal extracellular matrix remodelling and progressive fibrosis*

A crucial process to maintain valve homeostasis and to ensure valve longevity and function is extracellular matrix remodelling, which is tightly regulated in normal conditions by the balance between MMP and their antagonists TIMP. This balance is altered in CAVD tissue, where some MMP family members such as MMP-1,2,3 are overexpressed and others such as MMP-9 are newly expressed.<sup>83</sup> The disruption of MMP/TIMP balance and the increased and defective deposition of extracellular proteins promote the development of fibrosis within the valve. This abnormal matrix remodelling also leads to increased stiffness, which promotes VIC activation and calcification, as demonstrated by an *in vitro* study based on the use of collagen hydrogels simulating different matrix compositions and conditions.<sup>84</sup> In addition, the development of hydroxyapatite crystals itself further activates VIC, thus promoting increased osteogenic responses. Supporting this theory, valve cell culture in 3D platforms containing embedded hydroxyapatite crystals, like those of diseased valves, promoted VIC and VEC activation and differentiation, and also inhibited VEC protection against VIC calcification.<sup>85</sup> Additional studies supporting the positive feedback loop on calcification also outlined the induction of apoptotic processes in VEC as well as the myofibroblastic activation of VIC upon exposure to crystalline calcified particles from human aortae.<sup>86</sup>

#### *I.3.3.2-Osteogenic molecular mechanisms*

Human calcified AV exhibit overexpression of several osteogenic genes as compared to healthy valves.<sup>87</sup> The osteogenic phenotype induced in VIC during the propagation phase includes a wide variety of bone-related pathways and a complex regulation of their interactions. In the next paragraphs the different osteogenic pathways and transcription factors associated to CAVD progression will be described.

Transcription factors: Gene profiling analysis have demonstrated increased valvular expression of several osteoblast-specific proteins, including the *Runt-related transcription factor 2* (*CBFA1/RUNX2*) gene,<sup>79</sup> a transcription factor known to be essential for the regulation of osteoblast differentiation.<sup>88</sup> RUNX2 seems to be the most important transcription factor in the regulation of osteogenesis in VIC, by acting as the downstream mediator of several osteogenic signalling pathways as explained below. Additionally, another osteoblastic transcription factors reported to be overexpressed in CAVD are osterix (*OSX*)<sup>89</sup> and homeobox protein *MSX-2* (*MSX2*),<sup>90</sup> although their role in the disease pathogenesis remains to be further explored.

Morphogens: One of the most important osteogenic signalling morphogens is bone morphogenetic protein-2 (*BMP-2*), a potent osteogenic differentiation factor that belongs to the TGF- $\beta$  superfamily that is overexpressed in calcified valves.<sup>79</sup> Remarkably, recombinant *BMP-2* promotes VIC mineralization, and also plays an essential role as a downstream mediator of TLR-induced osteogenesis by triggering the expression of the *RUNX2* as well as osteoblastic proteins like osteopontin.<sup>91</sup> More recently, *BMP-2* has been pointed as a necessary osteogenic signalling molecule to promote AV calcification both *in vitro* and *in vivo*.<sup>92</sup> Collectively, evidences indicate that *BMP-2* is a master osteogenic signalling molecule with implications in the differentiation of VIC to an osteoblast-like phenotype and the ensuing calcification.

Bone remodelling factors of the TNF superfamily: Another pathway involved in the regulation of ossification in the AV is the receptor activator of NF- $\kappa$ B (*RANK*), a member of the TNF superfamily, and its ligand (*RANKL*).<sup>41</sup> The regulation of this pathway is complex and depends on the balance between *RANKL* and *OPG*, a soluble decoy receptor that acts as a competitive inhibitor of *RANKL-RANK* binding. Remarkably, during CAVD, *RANKL* is overexpressed, whereas *OPG* downregulated, which might have an important role in AV pathogenesis as secreted *RANKL* has been reported to promote extracellular matrix proteins production as well as pro-osteogenic gene expression in VIC.<sup>93</sup> One important finding regarding the *RANKL/RANK/OPG* axis is its potential controversial implication in bone remodelling and ectopic calcification. Whereas in bone the binding of *RANKL* to *RANK* promotes osteoclast activity and osteoporosis,<sup>94</sup> in vascular and valvular cells it produces the contrary effects,<sup>95</sup> a paradox in which inflammation seems to play an essential role.

Regulators of osteoblast differentiation and maturation: The wingless-related integration site (*Wnt*)/ $\beta$ -catenin pathways are regulators of osteoblast differentiation that have been implicated in a wide range of cellular processes including the myofibroblastic and osteogenic differentiation of VIC. Indeed, this pathway seems to be the key regulator of the TGF- $\beta$ 1-mediated activation of VIC by

inducing the accumulation and a rapid nuclear translocation of  $\beta$ -catenin and increasing Wnt signalling.<sup>96</sup>

Phosphate metabolism: The activation of these pro-osteogenic pathways usually leads to the expression of mineralization-regulating proteins, such as tissue non-specific alkaline phosphatase (TNAP), osteopontin, osteocalcin, osteonectin, collagen type I and II, and bone sialoproteins, some of them being upregulated in calcified valves compared to healthy ones.<sup>97</sup> The expression of TNAP was reported to be essential for the production of osteogenic extracellular matrix by VIC,<sup>98</sup> data that directly link VIC calcification to the regulation of phosphate and its metabolism. Indeed, ectopic mineralization is known to be dependent on the nucleation of Pi with calcium ions. Remarkably, the analysis of mineral metabolism in the Cardiovascular Health Study pointed to Pi as a potential risk factor for CAVD. The study revealed that higher serum Pi levels within the normal range were associated with AV calcification in a community-based cohort of older adults.<sup>99</sup> At the molecular level, Husseini and colleagues identified that the type III sodium-dependent Pi cotransporter is overexpressed in stenotic valves and contributes to the Pi-induced calcification of VIC. Moreover, Pi promotes the dysregulation of mitochondrial membrane potential and the release of cytochrome c within the cytosol that subsequently lead to cell apoptosis.<sup>100</sup>

Phosphate metabolism is dependent on the action of enzymes named ectonucleotidases. Two main steps regulate Pi production from adenosine tri-phosphate. The first one implies the action of ectonucleotide pyrophosphatase/phosphodiesterase 1, an enzyme that converts adenosine tri-phosphate to inorganic adenosine monophosphate and pyrophosphate, which acts as a calcification inhibitor by its binding to Pi and calcium crystals.<sup>101</sup> In the second step, TNAP converts adenosine monophosphate and pyrophosphate into Pi. An increased activity of TNAP can result in the imbalanced ratio of Pi and calcification inhibitors, thus triggering VIC calcification.<sup>98</sup> The role of ectonucleotidases and its potential as therapeutic targets for CAVD remains to be further explored.

Osteo-inhibitory mechanisms: Not only pro-osteogenic but also osteo-inhibitory mechanisms regulate valve calcification. In this regard, the blood vessels and the AV produce matrix Gla protein (MGP), which is reported to prevent VIC mineralization when carboxylated through a vitamin K-dependent process.<sup>102</sup> Another abovementioned inhibitor of calcification is OPG, which impedes the binding of RANKL to its receptor RANK. Also, a key repressor of osteogenesis in the context of the aortic valve is NOTCH1,<sup>103</sup> which is known to regulate cell fate and differentiation, as well as cardiac valve formation. NOTCH1 belongs to a family of cell surface receptors whose expression is increased in the aortic valve. Individuals with loss-of-function mutations in NOTCH1 exhibit larger

rates of calcification and AS.<sup>36</sup> Regarding its repression mechanism, it appears to inhibit the BMP-2-mediated osteoblast-like calcification.<sup>103</sup>

### *1.3.3.3-Angiogenesis*

Another main feature of the propagation phase of CAVD is neoangiogenesis. Mature healthy valves are known to be avascular structures, however, a pathological formation of new vascular vessels within calcified valves was reported several years ago in studies pointing to a potential role for angiogenesis on CAVD progression.<sup>77,104</sup> Pro-angiogenic and angio-inhibitory factors are balanced in the homeostatic AV. In those conditions, the action of protective factors such as chondromodulin (CNMD)<sup>105</sup> prevents the development of neovessels in the valve. When valve homeostasis is disrupted, the effect of pro-angiogenic factors overtake the inhibitory factors, therefore triggering the formation of new vascular vessels.<sup>106</sup> Regarding the molecular mechanisms and pathways leading to neoangiogenesis in the AV, it has been recently reported that the master transcription factor for angiogenesis, hypoxia inducible factor-1 $\alpha$  (HIF-1 $\alpha$ ), is present in areas containing increased expression of vascular endothelial growth factor-A (VEGF-A), calcification, and new vessels in stenotic valves.<sup>107</sup> Another member of the HIF family, HIF-2 $\alpha$ , has also been found in calcified regions of stenotic valves, where the authors also detected an increased expression of VEGF-A and collagen X.<sup>108</sup> These evidences lead to think that the axis HIF/VEGF-A may be controlling the development of neovessels within the valve. Besides, the main inducers of HIF-1 $\alpha$  expression in VIC are thought to be at first glance a consequence of valve leaflet thickening and reduction in O<sub>2</sub> availability in valve cusps, however, additional active mechanisms could also account for HIF-1/2 $\alpha$  expression in calcified valves. Therefore, it is essential to understand the mechanisms for neovessels generation in CAVD, which could be even a potential novel therapeutic target for the disease.

To summarize, during the propagation phase abnormal matrix remodelling, neoangiogenesis and calcification co-exist as the major mechanisms inducing the progression of CAVD, and VIC are considered the main regulators of the calcification progression. Several matrix remodelling molecules and osteogenic pathways are up-regulated in calcified valves as compared to control valves, thus highlighting the complexity of CAVD progression.

### **1.3.4-Last phase**

At the beginning of the last stage of CAVD, the valve cusps are already thickened and vascularized, microcalcifications are widespread, and macrocalcifications start to be developed. The

initial atherosclerotic process has lost importance as the main mechanism in favour of a positive feedback loop of abnormal extracellular matrix and calcific nodules effects in VIC.<sup>42</sup> With time, the degeneration of the valve can trigger additional cardiac problems such as left ventricular hypertrophy. When CAVD reaches its final stages, valve area is significantly reduced, and aortic regurgitation occurs, and when this is severe, surgical intervention is usually the selected therapy for patients.

Altogether, current knowledge from clinical and experimental evidences points to CAVD as a complex and active disease, with a wide variety of pathologic processes implicated and the participation of several cytokines and cellular types (**Figure VII**).

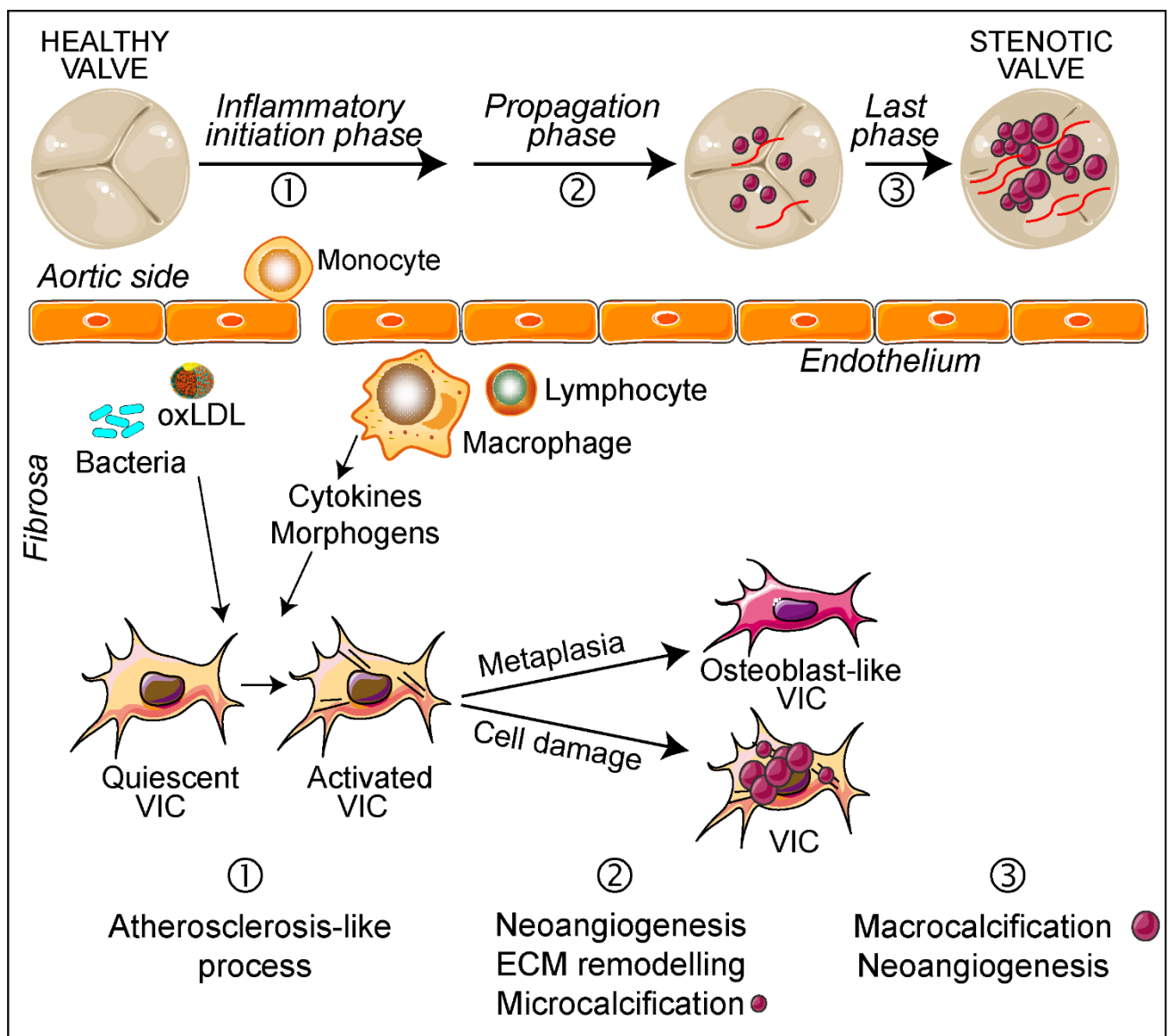


**Figure VII.** Simplified scheme of the three stages of the disease, indicating the different cellular types and processes taking part. ECM indicates extracellular matrix. Modified with permission from<sup>71</sup>.

## **I.4-Interferons and JAK/STAT pathways**

Cytokines such as interferons (IFN) and their signalling pathways have been associated to cardiovascular diseases such as atherogenesis.<sup>109</sup> Here, we summarize the current knowledge on IFN function, signalling routes and their reported role on cardiovascular diseases.

### **I.4.1-IFN types and their receptors**

In 1957, Alick Isaacs and Jean Lindenmann reported the phenomenon of “virus interference”, setting the basis for the discovery of the IFN, which are a group of soluble glycoproteins involved in a wide variety of cellular responses, especially the response to viral infections.<sup>110</sup> IFN allow for communication between cells by triggering the protective defences of the immune system to eradicate pathogens or tumours. There are 3 different families of IFN, named type I, II and III IFN. Whereas type I IFN are predominantly expressed by innate immune cells and activated fibroblasts, the functionally similar type III IFN, (IFN- $\lambda$ 1-4), are more restricted and primarily act on epithelial surfaces.<sup>111</sup> Finally, type II IFN (IFN- $\gamma$ ), is synthesized by natural killer and T cells and exerts antiviral functions mainly by the activation of macrophages.<sup>112</sup>

#### *I.4.1.1-Type I IFN*

Members of type I IFN include IFN- $\alpha$ ,  $\beta$ ,  $\kappa$ ,  $\delta$ ,  $\epsilon$ ,  $\tau$ ,  $\omega$ , and  $\zeta$ . These pleiotropic cytokines are associated not only to the response to viral, but also to bacterial infection. Most cell types secrete type I IFN in response to a viral challenge. All subtypes can signal through a receptor composed of the IFN- $\alpha/\beta$  receptor subunits 1 (IFNAR1) and 2 (IFNAR2).<sup>113</sup> Type I IFN binding to IFNAR1/2 complex triggers the activation of Janus kinases (JAK)/Signal transducers and activators of transcription (STAT) signalling pathways and IFN-sensitive response elements that regulate the expression of several genes (**Figure VIII**). The genes activated by type I IFN regulate a large number of cellular functions such as: interferon regulatory factor 3 (IRF3) and IRF7 expression, dendritic cell activation, T cell survival, NK cell activation, chemokine expression, lymphatic node retention, as well as antiproliferative and antiviral effects.<sup>111,114</sup> Remarkably, classical and important antiviral actions of type I IFN include the induction of the double-stranded RNA (dsRNA)-activated protein kinase R, which inhibits the cellular translational machinery, and 2'-5'-oligoadenylate synthetase/RNaseL, which degrades foreign RNA.<sup>115</sup>

### *1.4.1.2-Type II IFN*

The only member of type II IFN family is IFN- $\gamma$ . This cytokine is sensed by a heterodimeric receptor composed of the IFN- $\gamma$  receptor subunits 1 (IFNGR1) and 2 (IFNGR2) (**Figure VIII**). IFN- $\gamma$  activates the so-called gamma-activated sequences (GAS), which have important roles in tissue homeostasis, immune and inflammatory responses, and tumour immunosurveillance.<sup>112</sup> Specific immune functions of GAS genes are related to IRF1 expression, upregulation of MHC pathways, chemokine expression, Treg cell inhibition, Th1 cell differentiation and antiproliferative actions. IFN- $\gamma$  also mediates the polarization of macrophages to an ‘M1-like’ state, which is characterized by increased pro-inflammatory activity and macrophage resistance to tolerogenic and anti-inflammatory factors.<sup>114</sup> Moreover it should be noted that, in some cases, type I IFN induce a cross-signalling that activates the canonical IFN- $\gamma$ -mediated formation of STAT1 dimers and the activation of GAS (**Figure VIII**).<sup>111</sup>

The importance of type I and II IFN relies not only on the effects triggered by their signalling, but also on their role as master cross-regulators of other immune pathways. In this regard, a substantial cooperation between the signalling pathways induced by type I IFN and the TNF- $\alpha$  pathway has been described.<sup>111</sup> The role of IFN- $\gamma$  as a master regulator of inflammatory pathways is widely known. Remarkably, the regulation of TLR responses by IFN- $\gamma$  and STAT1 has been reported in different systems, thus reinforcing the role of this cytokine as a key connector of the innate and adaptive immunity responses.<sup>116</sup>

### *1.4.1.3-Type III IFN*

IFN- $\lambda$  1–4 proteins, also termed IL-28 and IL-29, are structurally more closely related to the IL-10 family.<sup>117</sup> This subtype is poorly understood, although is known to share some functionalities with type I IFN by also activating JAK signalling pathways and inducing the expression of IFN-stimulated genes. Recent information demonstrates its importance in some types of virus or fungal infections by exhibiting antiviral effects at barrier surfaces, i.e. respiratory and gastrointestinal tracts, as well as the blood-brain barrier.<sup>118</sup>

### *1.4.1.4-Interferon regulatory factors*

The expression of IFN is closely related to the IRF transcription factors. In mammals, nine different IRF family members have been described.<sup>119</sup> Their structure comprises a conserved amino-terminal DNA binding domain with a helix-loop-helix shape and a motif containing five tryptophan

residues. The IRF-association domains 1 and 2 are located in the carboxyterminal region and mediate homodimeric and heterodimeric interactions with other IRF family members, transcription factors, and co-factors.<sup>119</sup> IRF are important molecules mediating the activation of immune cells, and their functions include virus-mediated activation of IFN, and modulation of cell growth, differentiation, apoptosis, and immune system activity.<sup>120</sup>

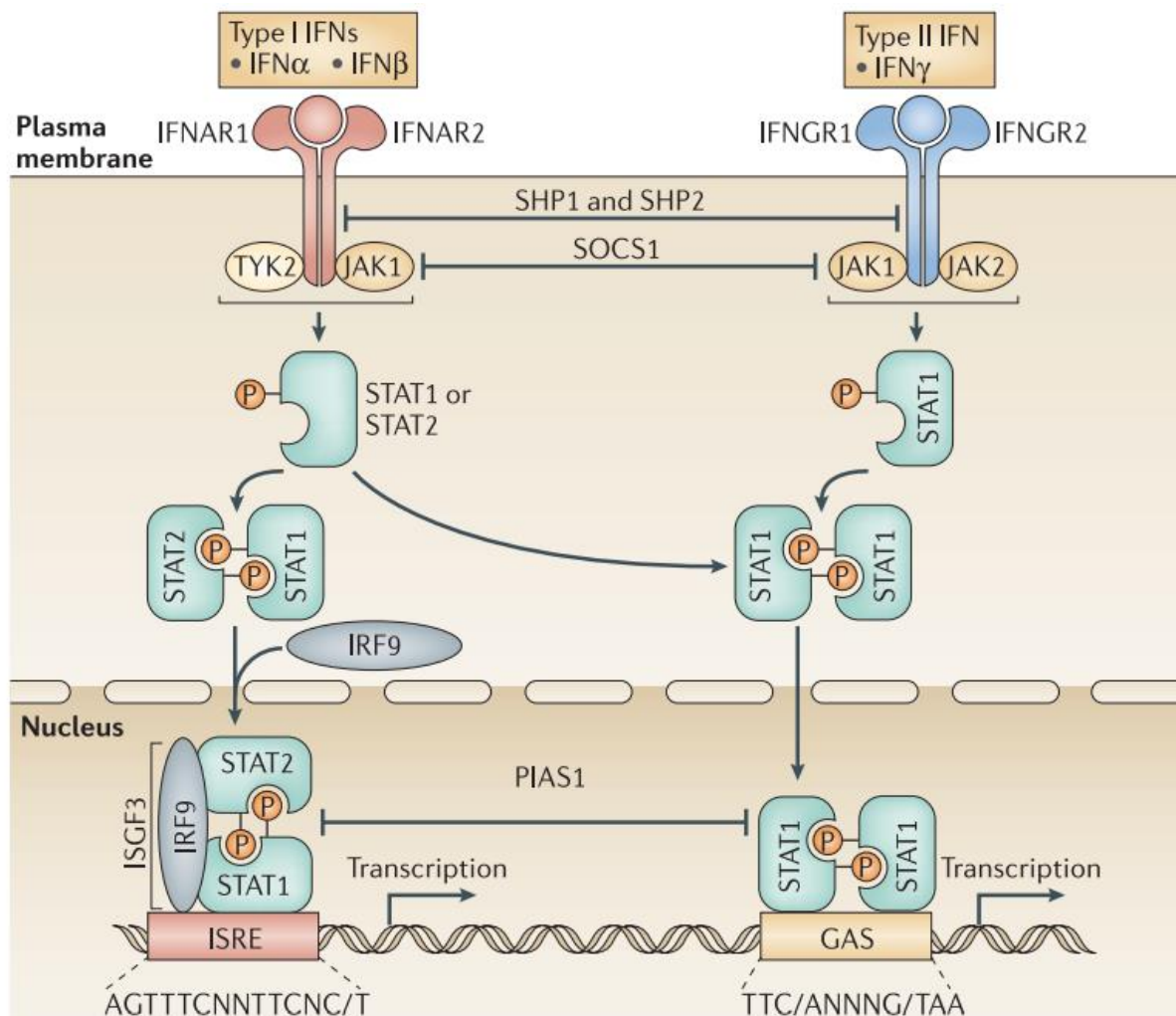


**Figure VIII. Type I and II IFN signalling.** Schematic representation of canonical type I and II IFN signalling. ISRE indicates IFN-sensitive response elements; PIAS, protein inhibitor of activated STAT; SHP, short heterodimer partners; SOCS, suppressors of cytokine signalling. Taken with permission from<sup>114</sup>.

### I.4.2-JAK/STAT pathways

The JAK/STAT pathways are pleiotropic cascades used to transduce a multitude of signals for development and homeostasis in animals, from human to flies. JAK/STAT are master regulatory routes involved in the sensing of more than 50 different cytokines and growth factors<sup>121</sup> that coordinate the innate and adaptive immunity as well as the regulation of cell fate, including

proliferation, differentiation, migration, apoptosis, and cell survival. The JAK/STAT response strongly depends on the signal, tissue, and cellular context.<sup>122,123</sup>

Three major groups of proteins participate in JAK/STAT signalling upon ligand binding: (i) the receptors, which sense a large range of different cytokines and growth factors; (ii) the JAK tyrosine kinases, which initiate the cascade upon ligand-receptor binding; (iii) the STAT transcription factors, which dimerize and translocate to the nucleus to activate the transcription of target genes.

The cytokine receptors, including IFN receptors, consist of two or more transmembrane polypeptide chains, and are associated with one or more JAK.<sup>115,124</sup> Ligand binding causes the dimerization of the receptors that brings the associated JAK close in proximity, thus promoting its autoactivation through trans-phosphorylation of tyrosine residues. The activated JAK then phosphorylate signature tyrosine residues in the cytoplasmic region of the receptors, thus creating docking sites for the binding of the Src-homology2 (SH2) domains of STAT transcription factors. Upon recruitment to the receptor complex, STAT proteins are phosphorylated by JAK at tyrosine residues from the SH2 and transactivation domains, causing its separation from the receptor and the formation of STAT homo or heterodimers, which is followed by translocation to the nucleus, where they function as transcription factors by binding to conserved DNA recognition sites.<sup>115,124</sup>

#### *1.4.2.1-Janus kinases or JAK*

The JAK were first named “just another kinases”. However, upon the discovery of their key implication on the sensing of IFN and other cytokines, they were called Janus kinases in honour to the two-faced roman god Janus, because they contain two similar phosphate-transferring domains. In mammals, the JAK family comprises four members: JAK1, JAK2, JAK3, and the tyrosine kinase TYK2. They are typically located in the endosomes and the plasma membrane, along with their cognate receptors. These proteins are large size kinases (120-140 kDa) that contain a tyrosine kinase domain, which is essential for the enzymatic activity of JAK and contains conserved tyrosine residues necessary for JAK activation, and a catalytically inactive pseudo-kinase domain. Both regions bind the receptors through amino-terminal band-4.1, ezrin, radixin, moesin domains. JAK1, JAK2 and TYK2 are ubiquitously expressed, whereas the expression of JAK3 seems to be restricted to cells of the hematopoietic lineage and vascular smooth muscle cells (VSMC).<sup>125,123,124</sup>

JAK1 is involved in the response to many cytokines such as type I and II IFN and several IL (2, 4, 7, 9, 10, 13, 15, 20, 21, 22, 28). JAK2 mediates the response to hormone-like cytokines such as

the growth hormone, prolactin, erythropoietin and thrombopoietin, and to cytokines involved in hematopoietic cell development, such as IL-3 and granulocyte macrophage colony-stimulating factor and IFN- $\gamma$ . JAK3 exclusively mediates signals through cytokines that use the common  $\gamma$  chain, which are IL-2, 4, 7, 9, 15, 21. TYK2 associates with cytokine receptors that signal through JAK1 or JAK2, but not with JAK3, and plays an essential role on the transduction of several cytokines such as type I IFN, IL-6, IL-10, and IL-12/IL-23. The function of TYK2 also seems to be associated with the cellular response to lipopolysaccharide (LPS), although it is not clear whether this is a direct or indirect mechanism.<sup>125,124</sup>

#### *1.4.2.2-STAT*

The activation of JAK triggers signalling through STAT transcription factors. Mammalians have 7 types of STAT transcription factors: STAT1, 2, 3, 4, 5a, 5b, and 6. They are composed of 750 to 900 amino acids and each STAT consists of seven conserved functional domains: The N-terminal domain, a coiled-coil domain, a central DNA-binding domain, a linker region, a SH2 domain followed by a single conserved tyrosine residue, and a C-terminal transcriptional activation domain. As noted earlier, upon ligand binding, STAT are recruited to the receptor and activated by tyrosine phosphorylation by JAK, which in turn promotes their dissociation and the formation of STAT dimers. Then, STAT dimers migrate to the nucleus through the nuclear pore complex by a mechanism dependent on importin  $\alpha$ -5, where they activate different subset of genes. STAT1, 3, 4, 5, and 6 form homodimer complexes and some of them form heterodimeric or heterotrimeric complexes, an aspect that will be detailed below. In addition, all the STAT proteins, except STAT2, can be phosphorylated on at least one serine residue by various serine kinases such as p38, c-Jun N terminal kinases (JNK), and phosphatidylinositol 3 kinase (PI3K), which further enhances the STAT-mediated gene transcription.<sup>124,122</sup> STAT family members include:

**STAT1:** The founding member of the STAT family is widely expressed, reaching high levels of expression in heart, thymus and spleen. It is involved in type I and II IFN signalling (**Figure VIII**). Upon type I IFN binding, the receptor forms a complex composed of STAT1, STAT2 and IRF9. Then, this complex undergoes nuclear translocation and subsequent binding to IFN-sensitive response elements in target genes. Upon IFN- $\gamma$  binding to its receptor, STAT1 forms homodimers that translocate to the nucleus and bind GAS involved in the response to viral and bacterial infections (**Figure VIII**). In general, STAT1 signalling is pro-inflammatory and anti-proliferative, although some other context-dependent effects have been reported.<sup>124</sup> In addition, the regulation of STAT1 responses is tightly linked to the regulation of STAT3. In fact, STAT3 is usually related with an

enhanced proliferation and anti-inflammatory activity. Thus, the balance between the activation of both STAT proteins could determine the extent of the inflammation as well as the cell fate. In addition to IFN, other cytokines such as IL (2, 3, 6, 10, 11, 12, 15, 17, 22) and growth factors such as fibroblast growth factor-1, granulocyte macrophage colony-stimulating factor or VEGF amongst others signal through STAT1.<sup>121</sup>

STAT2: It is expressed in most tissues. Initially described as a component of the complex formed upon type I IFN challenge, it is known to be critically involved in the regulation of type I IFN autocrine loop. It is also involved in the responses to IL-17 epithelial growth factors, angiotensin, and urokinase-type plasminogen activator.<sup>121</sup>

STAT3: It has been classically related to IL-6 signalling, promoting acute phase gene expression and being expressed in most tissues. In addition, it transduces signals from a wide range of cytokines, i.e, IFN, IL (6, 11, 10, 11, 19, 20, 21, 22, 24, 26, 27, 31), granulocyte colony-stimulating factor, and leptin, among others, as well as from several growth factors and oncogenes. In this regard, the JAK/STAT3 axis has been proposed as a potential therapeutic target for the treatment of solid tumours since it is constitutively activated in many cancers and promote cell proliferation.<sup>126</sup> Moreover, it plays an essential role on Th17 differentiation in mice and humans. Strikingly, regarding the inflammatory response, STAT3 paradoxically promotes inflammation in some settings while inhibits it in others.<sup>122</sup>

STAT4: Its expression is restricted to myeloid cells, thymus and testis. Its main activator is IL-12, being therefore critical for the Th1 differentiation process as well as for the IL-12-dependent activation of NK cells. Other cytokines or growth factors that activate STAT4 are IFN, IL-13, IL-17, IL-23, and urokinase-type plasminogen activator.<sup>124,127</sup>

STAT5: It consists of two isoforms, STAT5a and STAT5b, which exhibit differential expression in muscle, brain, mammary gland, and secretory organs. Together with STAT3, they exhibit the highest degree of homology to invertebrate STAT and are functionally pleiotropic. They play a role in the biological response to IFN, IL (2, 3, 5, 7, 9, 15), and granulocyte macrophage colony-stimulating factor among others.<sup>121,127</sup> They play an essential role in erythropoiesis and lymphopoiesis.<sup>124</sup>

STAT6: It plays a critical role for the IL-4/IL-13-dependent polarization of naïve CD4<sup>+</sup> lymphocytes into Th2 effectors, as well as on the proliferation and maturation of B cells. Intriguingly, STAT6 also mediates IFN responses and its homodimers recognize GAS elements.<sup>124,127</sup>

### *1.4.2.3-Mechanisms of JAK/STAT regulation*

JAK/STAT signalling has a wide variety of positive and negative regulators that control and prevent inappropriate cytokine responses. Within minutes after ligand binding, the STAT are already activated and located in the nucleus, whereas after some hours, they are exported back to the cytoplasm. The most important negative feedback loops regulating STAT activation include the dephosphorylation by protein tyrosine phosphatases, the direct inhibition by protein inhibitors of activated STAT (PIAS) and suppressor of cytokine signalling (SOCS), and the nuclear export of STAT.<sup>124,111</sup>

Several phosphatases have been related to the attenuation of JAK/STAT signalling, such as short heterodimer partners 1 and 2 or protein tyrosine phosphatases1B. These phosphatases target either the receptor complex at the cell membrane or the phosphorylated STAT molecules in the nucleus. Only short heterodimer partners-2 and TC-protein tyrosine phosphatase have been implicated in nuclear STAT dephosphorylation, which is critical for STAT nuclear export. Regarding STAT translocation, several evidences point to a continuous balance between nuclear import and export processes even under inactivated conditions. The underlying mechanisms are still poorly understood, but translocation seems to be regulated by multiple nuclear export and nuclear localization sequence elements. The PIAS family of proteins (PIAS1, PIAS3, PIASx and PIASy) negatively regulate STAT signalling by mechanisms dependent either on their binding to STAT or by acting as E3 SUMO-protein ligases. The SOCS proteins antagonize STAT activation in a classically known feedback loop and play an essential role in the inhibition of both IFN- $\gamma$  and IL-6 responses. Mechanisms of SOCS-induced STAT downregulation include the physical obstruction of STAT recruitment to the receptor complex, as well as the blockade of JAK kinase activity. In addition, SOCS proteins facilitate the ubiquitination of JAK, thus targeting them for proteasomal degradation. Additional mechanisms for the regulation of STAT include covalent modifications, such as serine phosphorylation, acetylation, and *O*-glycosylation.<sup>124,128</sup>

### **1.4.3-JAK/STAT pathways, IFN and cardiovascular disease**

JAK/STAT signalling plays a role on several disorders, including cardiovascular diseases. Human JAK mutations have been related to numerous diseases, including severe combined immune deficiency, certain leukemias, polycythaemia vera, and other myeloproliferative disorders. In this base, JAK have become attractive targets for the development of therapeutics for a variety of hematopoietic and immune system disorders, and there are several JAK inhibitors approved for the

treatment of autoimmune diseases. For example, tofacitinib is used for the treatment of rheumatoid arthritis,<sup>129</sup> and the JAK1/2 inhibitor ruxolitinib for polycythemia vera<sup>130</sup> and myelofibrosis.<sup>131</sup>

Dysregulation of JAK/STAT signalling is also associated with various cardiovascular diseases, exhibiting a complex and diverse signalling with differential effects depending on the context. Indeed, STAT3 has been shown as a protective transcription factor for compensatory hypertrophy by promoting a reduction in apoptosis.<sup>132</sup> Besides, STAT1 activation in the heart has been associated with cell death and ischemic disease progression.<sup>133</sup>

Regarding plaque formation, IFN are thought to be pro-atherogenic cytokines, since they exacerbate the inflammatory response and are master regulators of VSMC fate and apoptosis.<sup>109</sup> In addition, the JAK/STAT pathways can also regulate another inflammatory routes. In this line, IFN- $\alpha$  acts as an inflammatory amplifier by increasing TLR4 expression and cytokine production, which turns into plaque destabilization.<sup>134</sup> In addition, STAT1 acts as the key regulator of the interplay between TLR4 ligands and IFN- $\gamma$ , which potentiates a pro-atherogenic state in human atherosclerosis.<sup>135</sup>

In CAVD, not straightforward associations of IFN with the disease have been reported to date, although other cytokines like IL-6, which activates JAK/STAT among other pathways,<sup>136</sup> have been reported to promote VIC mineralization.<sup>59</sup> Interestingly, gene profiling analysis of severe calcified stenotic human AV identified the overexpression of IFN-related cytokines, i.e., monokine induced by IFN- $\gamma$ , now renamed to CXCL9.<sup>137</sup> Importantly, IFN- $\gamma$  is secreted by T lymphocytes in calcified valves in an active form, and impairs the calcium resorption potential of osteoclasts.<sup>138</sup>

The most intriguing evidence associating enhanced type I IFN activity and ectopic calcification in non-skeletal tissues, i.e aorta and AV, derives from a rare autosomal dominant disease named Singleton-Merten syndrome (SMS), first reported in 1973.<sup>139</sup> These patients showed abnormalities in dentition and hands, as well as severe calcification and intimal weakening of the aortic arch and valve.<sup>139</sup> In some cases of SMS, the early onset of calcification in the aorta and AV can be observed in children or young adults.<sup>140</sup> The causes of this rare condition are still not completely understood, but emerging evidences point to mutations on genes encoding to cytosolic nucleic acid sensors as the potential cause. Strikingly, this disease is currently considered a type I interferonopathy whose pathobiology links calcification with constitutive type I IFN activity.<sup>141,142</sup> Particularly, mutations affecting two retinoic acid-inducible gene I (RIG-I)-like receptors family members<sup>143,142</sup> named melanoma differentiation-associated gene 5<sup>144</sup> and RIG-I<sup>140</sup> have been identified as the plausible cause of the disease. DDX58 mutations cause the constitutive activation of

RIG-I, which in turn triggers type I interferon production.<sup>140</sup> Collectively, these evidences directly link a constitutive type I IFN activity with ectopic calcification in non-skeletal tissues, including aorta and heart valves.

In the cardiovascular system, as mentioned earlier, some effects of IFN-JAK/STAT on atherogenesis are potentiated by cooperation with TLR signalling pathways,<sup>134,135</sup> which has been associated to inflammation and CAVD. A putative interplay of IFN and TLR signalling in the context of CAVD, which shares some pathobiological similarities with atherogenesis, has not been explored.

## **I.5-Toll-like receptors**

The TLR are part of a family of germline-encoded innate immunity receptors called pattern recognition receptors (PRR). In addition to TLR, the PRR family also includes the RIG-I, retinoic acid-inducible gene-I like receptors or RLR, the Nod-like receptors or NLR, and C-type lectin receptors.<sup>145</sup> The PRR are located in cellular membranes and cytosolic compartments of a wide range of cellular types within the human body. Furthermore, in addition to their role on the regulation of innate immunity, PRR are also important for the activation of the acquired immunity. These receptors are sensors not only of PAMP from a myriad of microorganisms, but also of damage-associated molecular patterns (DAMP) released upon tissue injury. First, PAMP are usually very conserved pathogen motifs with low mutation rates that are not present in mammals.<sup>145</sup> Second, DAMP are molecules derived from damaged tissue, blood vessels or necrotic cells, i.e., nucleic acids, which activate TLR receptors in the absence of pathogens, a process known as sterile inflammation.<sup>146</sup>

The role of TLR in the immune response was first described in 1996 when Hoffman and colleagues demonstrated a role for these receptors in the host response to pathogens, specifically upon challenge with *Aspergillus fumigatus*.<sup>147</sup> One important hit regarding the TLR family was the discovery of TLR4 as the sensor of the Gram-negative bacteria pattern LPS.<sup>148</sup> These evidences, among others, were a major step forward in the innate immunity field, in which it was previously thought that the pathogens were not recognized by specific receptors. Regarding their structure, these receptors are type I transmembrane glycoproteins containing an extracellular leucine-rich repeat domain, a transmembrane domain, and an intracellular Toll-IL-1 receptor (TIR) domain.<sup>146</sup> The extracellular domains possess segments of 24-29 amino acids containing the conserved sequence LXXLXLXX, being L leucine and X any other amino acid. The intracellular domains are homologs

to the receptor for IL-1, with a so-called TIR domain exhibiting 3 areas highly specialized in binding to intracellular signalling proteins. Importantly, the complete sensing of ligands requires TLR dimerization and the participation of a series of co-receptors that will be described later. Despite the dissimilarities in ligand interaction and co-receptors, the extracellular domains of TLR all have a horse-shaped structure. Additionally, TLR-ligand complexes adopt a M-shape in which the C-termini of the extracellular domains converge in the middle.<sup>146</sup>

The TLR family plays an important role in the detection of virus and bacteria, acting as the first defence line of the innate immunity system. The binding of these patterns to the corresponding TLR triggers a series of responses whose major outcome is the rapid initiation of the inflammatory response.<sup>146</sup> In fact, inflammation is essential for host protection by the elimination of invading pathogens and by the initiation of repair mechanisms ultimately designed to restore homeostasis.

### **I.5.1-TLR types and ligands**

So far, 13 TLR types have been identified. The first nine are conserved in both humans and mice, while TLR10 is expressed only in humans and TLR11 to TLR13 are present only in mice.<sup>146</sup> Bacterial cell wall components are broadly recognized by TLR expressed on plasmatic cell membranes (TLR1, 2, 4, 5, 6, 10), though nucleic acid sensors (TLR3, 7, 8 and 9) are located almost exclusively in endosomal compartments. To note, TLR4 can be present in both cellular locations.

TLR have a highly-conserved structure in the evolution, although each receptor recognizes specific patterns and triggers the expression of a different subset of genes.<sup>149</sup>

TLR1: It is found on the surface of macrophages and neutrophils. There is not known ligand for TLR1 alone, however, in association with TLR2, this receptor recognizes triacetylated lipoproteins. The TLR1-TLR2 dimer supposedly exhibits a high specificity given that currently there are not evidences of their involvement in diacetylated lipoproteins detection.<sup>149</sup>

TLR2: This receptor recognizes components from a variety of microbial pathogens, including lipoproteins from Gram-negative bacteria, peptidoglycan and lipoteichoic acid from Gram-positive bacteria, or zymosan from fungi. This receptor also dimerizes with both TLR1 and TLR6. As mentioned earlier, the TLR2/1 complex recognizes tryacylated proteins, whereas TLR2/6 senses lipoteichoic acid and diacylated polypeptides.<sup>146</sup> In addition, several endogenous molecules are recognized by TLR2 such as high mobility group box 1, and components of the extracellular matrix such as biglycan, and heat shock proteins.<sup>150</sup> A widely used synthetic TLR2/1 ligand is Pam<sub>3</sub>CSK<sub>4</sub>, a

tripalmitoylated lipopeptide mimicking the acetylated amino terminus of bacterial lipoproteins, and as TLR2/6 synthetic ligand, the diacylated lipopeptide Pam<sub>2</sub>CSK<sub>4</sub>. Also, a cell wall preparation of *Saccharomyces cerevisiae*, composed primarily of glucans, mannans, mannoproteins and chitin, activates TLR2 in synergistic collaboration with dectin-1, a C-type lectin receptor.

TLR3: It is an endosomal receptor involved in the recognition of dsRNA, whose source can be either viruses or eukaryotic cells, which can be the result of replication of positive-strand RNA viruses, dsRNA viruses, and DNA virus or released from injured and necrotic cells.<sup>151</sup> This receptor, broadly expressed and well conserved among vertebrates, uses alternative signalling routes than other TLR, as will be described later. The most commonly used synthetic ligand for TLR3 is Polyinosinic:polycytidylic acid (Poly(I:C)), which simulates viral dsRNA.

TLR4: It was the first TLR to be identified and it recognizes the bacterial LPS, a major component of the outer membrane of Gram-negative bacteria exhibiting potent immuno-stimulatory activity. It should be noted that intracellular LPS recognition may also take place endogenously by inflammasome/caspase-11 routes. The complex LPS structure and TLR4 signalling requires the association with some co-receptors for an optimal binding. LPS is comprised of an oligosaccharide nucleus, a specific O chain composed of repeated sequences of hydrophilic polysaccharides, and a hydrophobic domain named lipid A, which is responsible of its biological activity. LPS binds to LPS-binding protein in serum, and this complex is later associated with the cluster of differentiation (CD)-14, which is critically involved in the recognition of LPS by TLR4. Other important co-receptor in some systems is MD-2, a secreted protein binding to the extracellular portion of TLR4. In addition to LPS, TLR4 can also sense a wide range of ligands, such as taxol and endogenous molecules like heat shock proteins and components of the extracellular matrix, i.e., fibronectin, oligosaccharides of hyaluronic acid.<sup>149,146</sup>

TLR5: It recognizes flagellin, a monomeric constituent of bacterial flagella. This pattern is highly conserved amongst both Gram-positive and Gram-negative bacteria. This receptor is not widely expressed and seems to be specific of cells from mucosal surfaces including lung and intestines.<sup>149</sup>

TLR6: As TLR1, there are not known ligands reported to activate TLR6 alone. However, as mentioned earlier, it is functionally associated with TLR2 forming heterodimers that are essential for the recognition of mycoplasma-derived diacyl lipopeptides.<sup>149</sup>

TLR7: It is an endosomal receptor for the recognition of unmethylated single stranded RNA derived from viruses, although it was first shown by its implication in the recognition of synthetic

compounds that are approved for viral-related diseases. It should be noted that, due to its spatial location, it is not able to recognize single stranded RNA from the host.<sup>149</sup> Imiquimod, a drug used in dermatologic treatments, signals via TLR7 and is widely used in research as a TLR7 ligand.

TLR8: It is a less-studied receptor that shows a similar structure and function than TLR7 and it is involved in the recognition of single-stranded RNA and imidazoquinolines. This receptor is present in regulatory T lymphocytes and its activation negatively regulates T cell activity. A synthetic TLR8-sensed compound is the imidazoquinoline Resiquimod.<sup>149</sup>

TLR9: It is an endosome/lysosome-located receptor recognizing both unmethylated deoxycytosine-deoxyguanosine sites from bacteria and virus that rarely infect humans, and DNA derived from damaged cells. A short single-stranded synthetic DNA molecule, deoxycytosine-deoxyguanosine ODN, is the common ligand used to mimic TLR9 activation.

TLR10: It is closely related to TLR1 and TLR6 and it has been proposed to act as a co-receptor for TLR1/6.<sup>149</sup> It is the only TLR without a clearly defined ligand although *Listeria monocytogenes* and influenza virus ligands have been reported to be recognized by TLR10. It has been identified in mucosal sites that are highly affected during acute viral infections.

## **I.5.2-TLR signalling**

Stimulation of TLR by PAMP or DAMP triggers signalling routes subsequently leading to the expression of several genes involved in the regulation of immune responses and cell fate. After ligand recognition, TLR undergo oligomerization and the recruitment of a series of signalling adaptors that regulate the signalling downstream the receptor. So far, five different adaptors have been identified,<sup>145</sup> which are: myeloid differentiation primary response protein 88 (MyD88), TIR domain-containing adaptor inducing IFN- $\beta$  (TRIF), TIR domain-containing adaptor protein, TRIF-related adaptor molecule, and sterile  $\alpha$  and heat-armorillo motifs containing protein. Since MyD88 is the most common TLR adaptor, the TLR-mediated signalling is commonly classified as MyD88-dependent pathway and the TRIF-dependent/MyD88-independent pathways (**Figure IX**).<sup>149</sup>

MyD88-dependent routes: All the TLR, except TLR3, can signal through the MyD88-dependent pathway.<sup>149</sup> In the first step, the binding of the ligands either promotes the direct activation of MyD88 (for TLR1,5,6,7,8,9) or the recruitment of TIR domain-containing adaptor protein that subsequently activates MyD88 (for TLR2 and 4). MyD88 harbours a TIR domain in the C-terminal and a death domain in the N-terminal portion that, upon stimulation, establishes an interaction with

another homologous death region located in an IL-1 receptor-associated kinase (IRAK) protein. MyD88 initially recruits IRAK-4 that subsequently phosphorylates IRAK-1. The complex composed of MyD88, IRAK-4 and IRAK-1 initiates the recruitment of TNF receptor associated factor (TRAF)-6, a factor associated with a wide variety of proteins that diverge the signalling into different downstream pathways. TRAF6 recruits TGF- $\beta$ -activated kinase 1 and TGF- $\beta$ -activated kinase 1 binding protein 1, 2 and 3 to constitute a ubiquitin-conjugated enzyme complex. At this point, the signalling cascade bifurcates promoting the activation of two different pathways: (i) The formed complex phosphorylates I $\kappa$ B kinase (IKK)- $\beta$ , which forms part of a heterodimer together with IKK- $\alpha$  and NF- $\kappa$ B essential modulator. This IKK complex then phosphorylates I $\kappa$ B $\alpha$ , which is an NF- $\kappa$ B inhibitory protein. Phosphorylated I $\kappa$ B undergoes degradation by the ubiquitin-proteasome system, which exposes the nuclear location sequence of NF- $\kappa$ B, thereby promoting its translocation and activation of the inflammatory response (**Figure IX**); (ii) TGF- $\beta$ -activated kinase 1 also activates the mitogen-activated protein kinases (MAPK) cascade, which is responsible for the nuclear translocation of different transcription factors that subsequently activate target genes related with cytokine expression, cell survival, and proliferation.<sup>145,149,146</sup>

Additionally, two less common MyD88-dependent pathways lead to the induction of type I IFN responses. First, a specific pathway for TLR7 and 9 has been described. It consists on the induction of IRF3 and type I IFN after a viral infection via MyD88/TRAF6 and the subsequent activation of IRF5 and IRF7. Second, TLR2 and TLR5 also display a MyD88/TRAF6-mediated activation of IRF5.<sup>146</sup>

TRIF-dependent routes: In response to stimulation with dsRNA, TLR3 recruits another adaptor protein, TRIF. Additionally, TLR4 triggers TRIF-dependent signalling although, in contrast to TLR3, it requires another adaptor, TRIF-related adaptor molecule, as well as the receptor internalization. TRIF signalling involves the activation of two different cascades: (i) TRIF interacts with receptor-interacting protein 1, thus leading to TRIF-dependent-NF- $\kappa$ B and MAPK activation via similar mechanisms than the MyD88-dependent route. (ii) TRIF also interacts with TRAF3 that bridges to TBK1 and IKKi/IKK $\epsilon$  thus directly activating IRF3, which dimerizes and later translocates to the nucleus (**Figure IX**). In humans, the last reported TLR adaptor protein is sterile  $\alpha$  and heat-armorillo motifs containing protein, which functions as an inhibitor of TRIF-dependent signalling.<sup>146</sup>

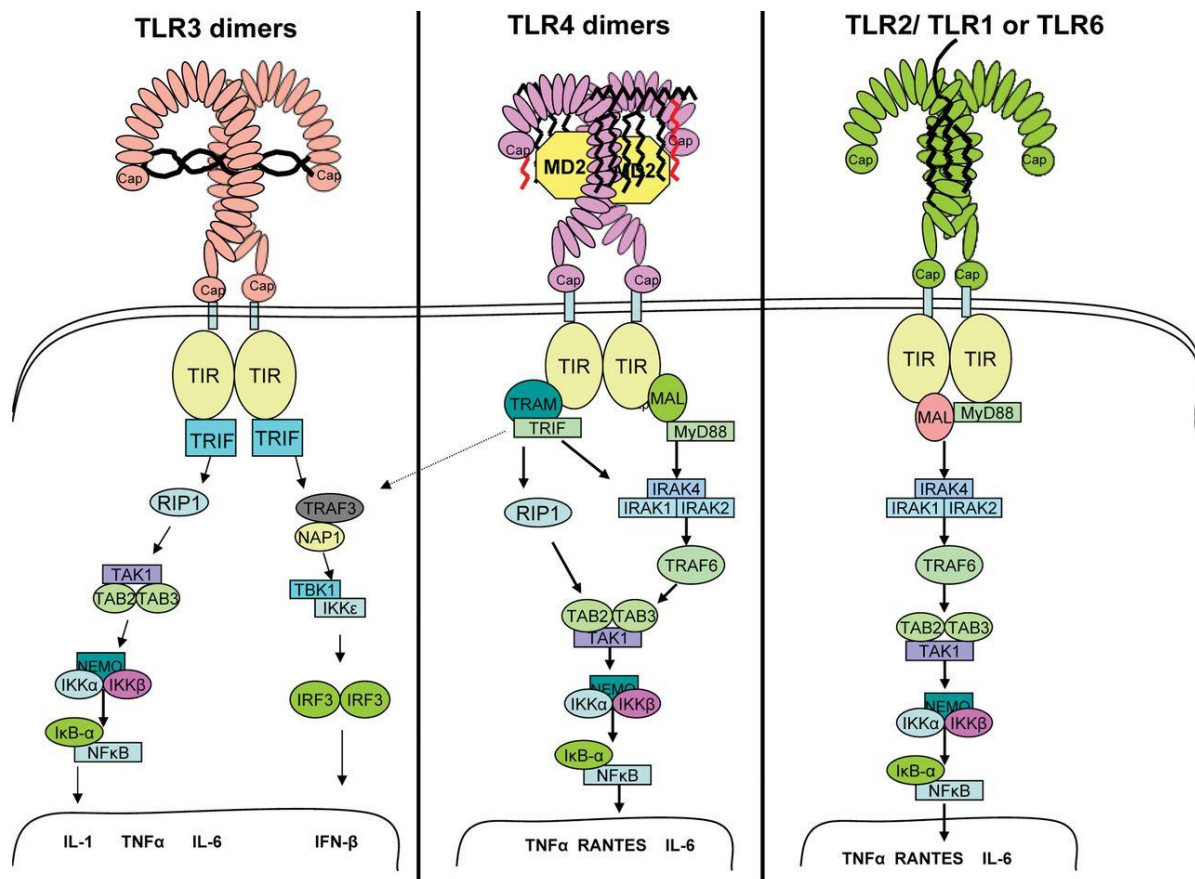


**Figure IX. Scheme of canonical TLR dimerization and signalling.** NEMO indicates NF-κB essential modulator; TAB, TGF-β-activated kinase 1 binding protein; TAK1, TGF-β-activated kinase 1; TRAM, TRIF-related adaptor molecule. Reproduced with permission from<sup>152</sup>.

The transcription factor NF-κB plays an essential role in the TLR-mediated responses by regulating the expression of the pro-inflammatory genes such as TNF-α, IL-1, ICAM-1, VCAM-1, cyclooxygenase-2 amongst others, and genes related to cell survival, differentiation and proliferation.<sup>153</sup> In mammals, there are five NF-κB family members: p65 or RelA, p50 or NF-κB1, p52, NF-κB2, RelB, and c-Rel.<sup>154</sup> The members of the NF-κB family form dimers that bind to consensus sequences in their regulated genes. The most common dimer is p50-p65. The activation of NF-κB dimers is tightly regulated not only by the IKK up-stream signalling, but also by other chemical modifications including ubiquitination, acetylation, methylation or isomerization.<sup>153</sup>

The MAPK are a family of serine-threonine specific protein kinases widely expressed in all cell types whose main function is to connect cell-surface receptors to regulatory targets within the cell. A three-step process regulates MAPK activation. MAPK are phosphorylated and activated by MAPK kinases, which in turn are phosphorylated and activated by MAPKK kinases. In response to TLR, three MAPK are activated via TAK1 signalling, namely extracellular signal-regulated kinase (ERK), p38 and JNK. Several transcription factors are activated by the MAPK with a complex and

context-dependent regulation. Among them, the most important transcription factors are AP-1, composed of Jun and Fos family members, CCAT/enhancer-binding protein  $\beta$  and activating transcription factors, and cAMP response element binding protein. These pathways are involved in the regulation of numerous cellular events associated with inflammation, cell proliferation and survival in response to a variety of external stimuli such as cytokines and mitogens, PAMP and DAMP.<sup>146,155</sup>

IRF are the key players of the TLR-induced production of type I IFN. In this regard, IRF1, IRF3, IRF5, and IRF7, which are expressed in most cell types and organs, can be activated by TLR signalling to induce IFN expression. IRF1 and IRF5 interact with and are activated by MyD88-dependent signalling. In addition, the transcriptional activation of the IFN- $\beta$  promoter by TRIF-dependent pathways via IRF3 and IRF7 has been extensively studied. IRF3 shows a more restricted capacity of DNA binding. However, IRF7, which is activated by TLR7 and TLR9, exhibits wider DNA binding specificity, which accounts for its capacity to induce several IFN- $\alpha$  subtypes.<sup>156,157</sup>

IRF2 and IRF4 regulate the extent of the response thus controlling the production of type I IFN. First, IRF2 is widely expressed in various cells and organs and it functions as a competitive inhibitor of the IRF1-mediated transcriptional activation of type I IFN and also acts as a transcriptional activator of histone H4. Second, IRF4 is constitutively expressed in cardiomyocytes, neurons, macrophages and dendritic cells and it is also abundant in lymphocytes. It retards the interactions of IRF5 with MyD88, thus reducing the TLR-dependent inflammatory responses. IRF6 is a less studied member expressed only in the skin, where is required for keratinocyte differentiation. IRF8 is expressed in cardiomyocytes, neurons, and lymphocytes and its main function is to regulate the differentiation and activation of immune cells. Finally, IRF9, which is widely expressed, is necessary for the formation of IFN-stimulated gene factor 3 to promote type I IFN-inducible genes.<sup>157,119</sup>

### **I.5.3-TLR and cardiovascular disease**

The rapid signalling triggered by TLR induces an acute inflammatory response to pathogen and/or damage-derived molecules that later resolves to restore homeostasis. However, in some cases, chronic exposure to harmful stimuli and/or exacerbated TLR signalling contributes to the development of chronic inflammation and subsequent diseases. In this line, the exacerbated TLR response has been related with systemic lupus erythematosus, cardiovascular diseases, asthma, type I diabetes, multiple sclerosis, bowel inflammation, and rheumatoid arthritis.<sup>158,159</sup>

In the context of cardiovascular diseases, TLR have been described to be involved in the pathogenesis of atherosclerosis, acute coronary syndromes, stroke, viral myocarditis, sepsis, ischemia/reperfusion injury, and heart failure.<sup>159</sup> Several lines of evidence implicate TLR signalling in the inflammatory process underlying atherosclerosis. For example, TLR 1, 2, 4 and 5 are expressed in atherosclerotic plaques by both resident vascular cells and leukocytes. Moreover, TLR4 is up-regulated in atheroprone areas of vascular vessels. Finally, TLR engagement triggers the expression of adhesion molecules, inflammatory cytokines, and matrix remodelling molecules in vascular endothelial and smooth muscle cells.<sup>159</sup>

The role of TLR in CAVD has been addressed by our group and others.<sup>71</sup> Although there is not a straightforward association of increased TLR signalling with CAVD development in *in vivo* model, increasing evidences demonstrate that these pathways are up-regulated in calcified valves.<sup>160</sup> *In vitro* evidences also support a role for TLR in the initiation of CAVD. In this regard, VIC, which are candidates to suffer calcification, express high levels of TLR2 and TLR4, and respond to its ligands by triggering inflammation and subsequent osteogenic responses (**Figure X**).<sup>71</sup> Emerging work from our group and others stressed out the importance of these receptors as master sensors of a wide variety of molecules in the AV context,<sup>71</sup> demonstrating that TLR activation leads to osteogenesis and calcification of VIC.<sup>71</sup> In addition, *in vivo* administration of LPS in C57BL/6 mice induced AV lesions and thickening.<sup>161</sup>

As previously indicated, bacterial and viral cargo has been detected in calcified valves.<sup>68</sup> Meng and colleagues first showed that the Gram-negative bacteria motif LPS promoted an inflammatory and osteogenic phenotype in VIC.<sup>162</sup> A further study revealed that TLR2 and TLR4 were the most expressed TLR in VIC, and demonstrated a link between its increased expression/signalling and the induction of responses relevant to CAVD pathogenesis.<sup>163</sup> Work from our group further disclosed that the nucleic acid sensor TLR3 also triggered inflammatory and osteogenic responses in VIC, suggesting a role of viral patterns in CAVD initiation.<sup>164</sup> Extensive work has been performed since then to identify potential TLR ligands, PAMP and DAMP, in the context of the AV (**Figure X**).

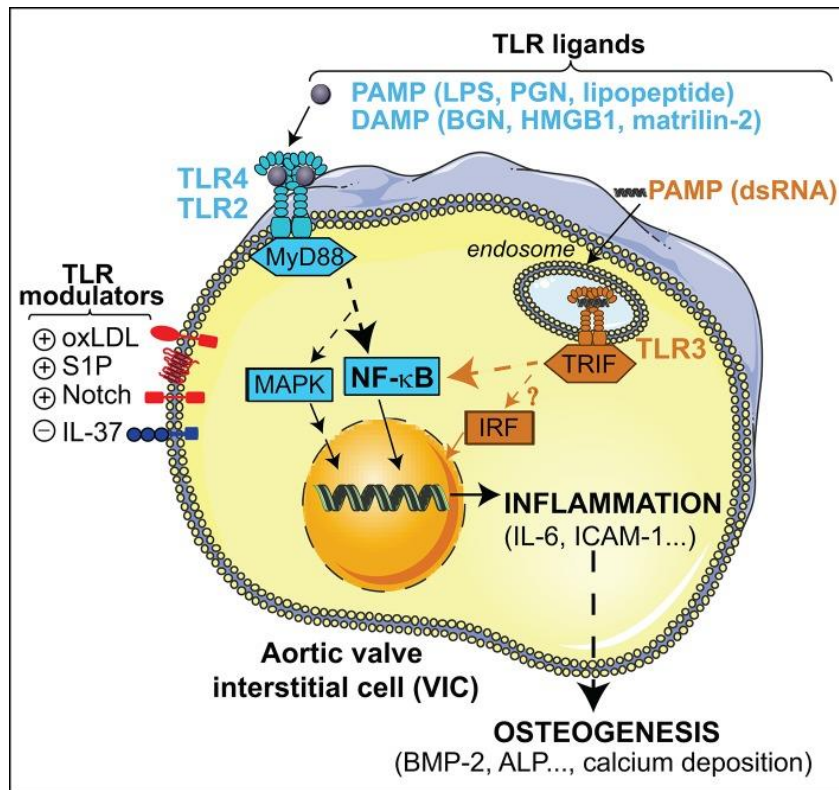


**Figure X. TLR ligands and its effects in VIC.** TLR engagement by several PAMP and DAMP triggers inflammatory and osteogenic responses in VIC. BGN indicates, biglycan; HMGB1, high-mobility group box-1; PGN, peptidoglycan; S1P, sphingosine 1-phosphate. Reproduced with permission from<sup>71</sup>.

In addition to sensing PAMP, TLR activation can also occur in the AV via sensing different extracellular matrix proteins and molecules that are up-regulated in the disease. In this line, soluble biglycan, a small proteoglycan that is overexpressed in CAVD,<sup>165</sup> activates TLR signalling in VIC promoting inflammation and osteogenesis.<sup>166</sup> Matrilin-2 is another extracellular matrix accumulated in calcified human nodules that induces inflammation and calcification of VIC via TLR2 and TLR4 signaling.<sup>167</sup> Other example of PAMP is high mobility group box 1, a nuclear regulatory protein that is secreted under certain conditions, and act as a pro-inflammatory cytokine. It has been detected overexpressed in tissue and plasma levels of CAVD patients,<sup>168</sup> and it has also been demonstrated that, once secreted, high mobility group box 1 induces pro-osteogenic responses in VIC via activation of TLR4.<sup>169</sup> Finally, other important molecules with marked implications in CAVD progression are oxLDL, which have been shown as modulators of the LPS-induced TLR responses by promoting a synergistic increase of osteogenic markers expression in human VIC.<sup>170</sup> More importantly, a later study focused on the protective effects of IL-37 showed that TLR2 and TLR4 blockade with neutralizing antibodies prevented the oxLDL-induced activation of NF-κB and ERK in VIC.<sup>161</sup> Additional research is needed to elucidate the role of TLR *in vivo* and to evaluate whether TLR signalling could be a potential therapeutic target for CAVD.



## **HYPOTHESIS AND OBJECTIVES**



# HYPOTHESIS AND OBJECTIVES

---

Based on recent findings linking type I IFN activity with the early onset of calcification in the atypical SMS,<sup>142</sup> the presence of T lymphocytes in aortic valves,<sup>171</sup> and the release of type IFN upon TLR activation of VIC,<sup>164</sup> we hypothesized that IFN could play a role on CAVD pathogenesis via activation of inflammation and the subsequent osteogenesis in aortic valve cells. The specific objectives of the study were:

- 1-To identify the different signalling pathways activated by recombinant IFN- $\alpha$  and IFN- $\gamma$  in human VIC and to check a potential cooperation with the TLR4 ligand LPS.
- 2-To determine whether recombinant IFN- $\alpha$  and IFN- $\gamma$ , alone or combined with LPS, upregulate CAVD underlying processes such as inflammation, osteoblastic differentiation, calcific nodule formation, and angiogenesis, in human VIC.
- 3-To elucidate the molecular mechanisms regulating IFN responses, as well as to analyse potential differences between IFN- $\alpha$  and IFN- $\gamma$  in VIC.
- 4-To confirm the in vitro findings of VIC with the gene and protein expression profile of valve tissue obtained from control and calcified human aortic valves.
- 5-To analyse whether IFN secretion accounts for the TLR3 ligand Poly(I:C)-induced effects in VIC.
- 6-To check potential valve-side effects of IFN- $\gamma$  on inflammation and monocyte adhesion in VEC isolated from the aortic and the ventricular side of the valve.



## **MATERIALS AND METHODS**



# MATERIALS AND METHODS

---

The composition of buffers, the references and source of reagents, kits, and materials used in the study are listed on the supplementary **Annex 1**.

## **M.1-Human valve samples**

Human tricuspid valve samples were obtained from patients who underwent surgery in the Hospital Clínico Universitario of Valladolid. Diagnosis protocols and surgical procedures for heart transplantation and valve replacement followed the current European guidelines. Research complies with good scientific practice and with the Helsinki Declaration. The study design had been approved by the local ethical committee of the Hospital Clínico Universitario of Valladolid (IRB protocol number PI 15-263). All the patients were previously informed of the procedure and signed the consent for valve donation.

Control non-mineralized valves were from recipients of heart transplantation with valve disease excluded by echocardiography. Calcified valves included explanted valves from patients who underwent valve replacement after non-rheumatic CAVD diagnosis. The criteria for the inclusion of the calcified valves in the study were an aortic valve area of  $0.7 \pm 0.2 \text{ cm}^2$ , a haemodynamic peak gradient of  $88 \pm 22 \text{ mmHg}$ , and a mean gradient of  $56 \pm 15 \text{ mmHg}$ . Representative pictures of control and calcified valves are shown in **Figure XI**. Collected specimens were kept on ice until they were either frozen or processed as indicated below. The patient demographics are shown at the beginning of each part in the Results section.

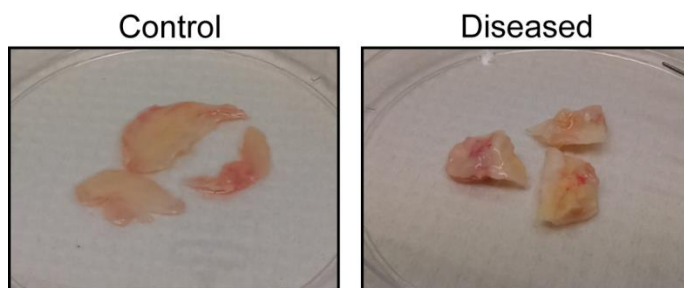


**Figure XI. Photographs of a control (left) and a calcified (right) aortic valve included in the study.**

---

## **M.2-Human VIC and VEC isolation and culture**

### **M.2.1-Cell isolation**

VIC and VEC were isolated from human tricuspid aortic valve cusps following a modification of a previously described method that is based on tissue digestion with type II collagenase.<sup>163,164</sup> First, valve cusps were rinsed with Earle's balanced salt solution and then digested in 2.5 mg/mL of collagenase in M199 medium for 15 min at 37 °C under shaking conditions. After vortexing, VEC were isolated by centrifugation at 200 x g for 5 min, plated on cell culture dishes and purified as indicated below. VIC were obtained after a further digestion of valve tissue with a 0.8 mg/mL collagenase solution for 3 h at 37 °C. After vortexing, the cell suspension was centrifuged at 500 x g for 2 min to remove tissue, and the supernatant was spun again at 1100 x g for 8 min at 4 °C. Cells were then plated onto 75 cm<sup>2</sup> flasks and cultured as indicated below.

Side-specific VEC, from either the aortic or the ventricular side of the valve, were isolated in The Magdi Yacoub Institute (Harefield, UK) under the supervision of Dr. Adrian H. Chester and Professor Sir Magdi Yacoub during a short-term stay held from September to December 2018. A custom-made device that allowed single-side exposition to collagenase was used. Briefly, the device was placed on a P10 dish filled with a 2.5 mg/mL collagenase solution. Then, the aortic side of the valve was orientated down and placed over the device, allowing the digestion for 15 min without agitation in an incubator at 37 °C. aVEC were then collected by centrifugation of the collagenase solution. Then, the valve was turned around and the ventricular side of the valve was placed in a different dish with other device coupled, and the isolation protocol was repeated.

### **M.2.2-Cell culture**

VIC were cultured in growth medium: M199 medium supplemented with 1% antibiotic-antimycotic solution (100 units penicillin, 100 µg/mL streptomycin, and 0.25 µg/mL amphotericin B) and 10% of heat-inactivated fetal bovine serum (FBSi) as previously described.<sup>163,164</sup> VEC were cultured in Endothelial Growth Medium-2 (EGM-2) supplemented with 10% FBSi, 1% Antibiotic-antimycotic solution, 1% L-glutamine and 4% EGM-2 supplement. For VEC, culture plates were pre-coated with 1% gelatin in phosphate saline buffer (PBS) for at least 30 min at 37 °C.

Both VIC and VEC were cultured in an incubator at 37 °C and 5% CO<sub>2</sub>, under humid atmosphere. Medium was replaced twice a week. Cells were grown to approximately 85-90% of

confluence and then subcultured to the ratio 1:3 or 1:4. For that, cells previously washed with PBS were detached using trypsin-ethylenediaminetetraacetic acid (EDTA). Cells from passages 3 to 8 were used for the experiments.

For long-term storage, cells were frozen in FBSi supplemented with 10% of dimethyl sulfoxide. Cells were initially frozen in cryotubes in a -80 °C freezer and then transferred to liquid nitrogen containers. Cells were quickly thawed in warmed growth medium.

### **M.2.3-Human valve endothelial cell purification by cell sorting**

To increase VEC population purity, cell sorting for platelet-endothelial cell adhesion molecule 1 (PECAM-1/CD31), an endothelial cell marker, was performed. Briefly, cells were detached with trypsin-EDTA and centrifuged at 453 x g for 5 min. Cells were then incubated with blocking buffer (human serum and 0.5 mM EDTA) for 10 min at 4 °C in a wheel. Then, cells were spun and incubated with a CD31-Fluorescein isothiocyanate (FITC) conjugated antibody (1:1000) in staining buffer (PBS supplemented with 5% of human serum and 0.5 mM EDTA) for 30 min at 4 °C in the dark. Cells were washed twice with staining buffer and filtered using a Falcon® 12x75 mm tube with cell strainer cap (35 µm nylon mesh). Finally, stained cells were sorted in a BD FACSAria™ flow cytometer (BD Biosciences, San Jose, CA). The CD31-positive cells were collected in EGM-2 and cultured in gelatin-coated dishes.

## **M.3-Valve cell characterization by immunofluorescence**

Cell phenotype was confirmed by immunofluorescence analysis for myofibroblast and endothelial markers as indicated below. Most VIC were positive for  $\alpha$ -SMA, consistent with a myofibroblast phenotype. Most VEC were positive for CD31 and VWF (**Figure XII**), consistent with an endothelial phenotype.

### **M.3.1- $\alpha$ -SMA detection in VIC**

A total of 10,000 VIC were seeded on uncoated coverslips overnight. The following day, cells were activated with the corresponding stimuli for 48 h or left untreated. Cells were then fixed and permeabilized with methanol for 6 min at -20 °C. Non-specific epitope binding was avoided by incubation with 5% of bovine serum albumin (BSA) in PBS for 30 min at room temperature. Next, immunostaining was performed by incubating cells with the primary antibody, mouse anti-human  $\alpha$ -smooth muscle actin (1:100 in PBS-1% BSA), for 1 h at room temperature. This step was followed

by 5 washes with PBS, and a final incubation with the corresponding fluorescent-labelled secondary antibody, a rat anti-mouse IgG (H+L) (FITC) polyclonal antibody (1:1000 in PBS-1% BSA), for 1 h in the dark. Before mounting the coverslip, cell nuclei were stained with DAPI (4', 6-diamidino-2-phenylindole; 1:1000 dilution in PBS-1% BSA) for 10 min at room temperature. Coverslips were mounted using a gelvatol solution composed of 10% gelvatol (polyvinyl alcohol, w/v), 24% glycerol (v/v), 50% Tris 0.1 M pH 8.5 (v/v) and 2.5% DABCO (1-4, diazabicyclo octane; v/v). Results were visualized under a fluorescence microscope coupled to a digital camera (Nikon Eclipse 80i) using FITC filter settings (490 nm excitation and 525 emission wavelength) (**Figure XII**).

The total corrected cellular fluorescence (TCCF) was calculated using the ImageJ software (U.S., NIH) as follows: integrated density – (area of selected cell x mean fluorescence of background readings). The fluorescence of at least 8 independent cells was used to calculate the mean of each condition.

### **M.3.2-CD31 and VWF detection in VEC**

VEC were seeded on 1% gelatin-coated coverslips. The following day the cells were washed twice in PBS, fixed and permeabilized with 4% formaldehyde solution for 10 min at room temperature. Cells were then washed 3 times with PBS and permeabilized with Triton-x-100 (0.5% v/v in PBS) for 3 min and blocked for 30 min with 3% BSA in PBS. Immunostaining with the corresponding primary and secondary antibodies and DAPI staining were performed as indicated above. Permafluor aqueous mounting fluid was used as the mounting solution and the fluorescence was analysed by Ziess LSM 510 confocal microscope (**Figure XII**).

Primary antibodies used were a mouse anti-human CD31 (1:200 in PBS-1% BSA) and a rabbit anti-human VWF (1:500 in PBS-1% BSA). Secondary antibodies included an Alexa Fluor 488 goat anti-mouse IgG (H+L) antibody (1:1000 in PBS-1% BSA) and an Alexa Fluor 594 goat anti-rabbit IgG (H+L) antibody (1:1000 in PBS-1% BSA).

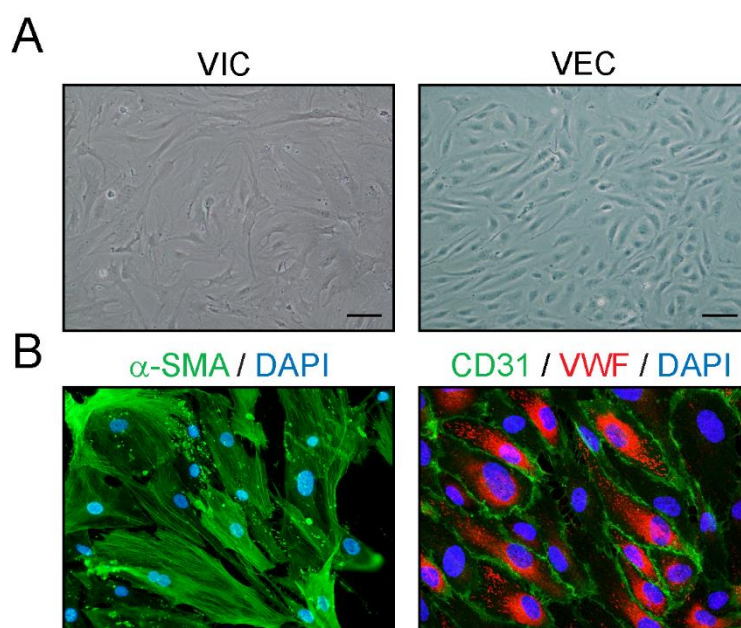


**Figure XII. Characterization of aortic valve interstitial and endothelial cells.** (A) Bright field microphotographs of VIC (left) and VEC (right). Black line indicates 50  $\mu$ m. (B) Merged immunofluorescence images for either a myofibroblast marker of VIC ( $\alpha$ -SMA; left) or specific endothelial markers of VEC (CD31 and VWF; right) and DAPI nuclear staining.

---

## **M.4-Protocol for cell activation**

Before activation, VIC were cultured for at least 6 h in cell activation medium (M199 supplemented with 2% FBSi and 1% of antibiotic-antimycotic solution). Then, the corresponding stimuli or pharmacological drugs were added, and cells were incubated for the indicated times. Medium volumes were 1.0 mL for 6-well plates and 0.5 mL for 12-well plates, unless otherwise indicated.

For Western Blot experiments in side-specific VEC, approximately 150,000 side-specific VEC were seeded in 6-well plates coated with 1% gelatin. The following day, 1.9 mL of EGM-2 were added and cells were sheared for 72 total h, as previously reported<sup>172</sup> (after 48 h of shearing the corresponding stimuli were added without changing media).

A list of recombinant stimuli and TLR ligands, including their working concentrations and diluent is shown in **Table 1**. To note, the water used as a solvent was endotoxin-free. References and vendors are indicated in **Annex 1**.

**Table 1: Stimuli used in this study.**

STIMULUS	TARGET RECEPTOR	WORKING CONCENTRATION	DILUENT
<b>Flagellin</b>	TLR5	1 µg/mL	Endotoxin-free water
<b>Human recombinant IFN-<math>\alpha</math></b> (s.a. $\geq 1.8 \times 10^8$ IU/mg)	IFNAR1/2	0.1-100 ng/mL	Endotoxin-free water, M199 2% FBSi
<b>Human recombinant IFN-<math>\gamma</math></b> (s.a. $\geq 2 \times 10^7$ IU/mg)	IFNGR1/2	0.1-100 ng/mL	Endotoxin-free water, M199 2% FBSi
<b>Human recombinant TNF-<math>\alpha</math></b>	TNFR	5 ng/mL	Endotoxin-free water, M199 2% FBSi
<b>Imiquimod</b>	TLR7	5 µg/mL	Endotoxin-free water
<b>LPS from <i>Escherichia coli</i> O111B4</b>	TLR4	1 µg/mL	Endotoxin-free water *Boiled at 120 °C for 3 h
<b>Pam<sub>2</sub>CSK<sub>4</sub></b>	TLR2/TLR6	100 ng/mL	Endotoxin-free water
<b>Poly (I:C)</b>	TLR3 and others	1 µg/mL	Endotoxin-free water
<b>Human recombinant TGF-<math>\beta</math>1</b>	TGFR- $\beta$	10 ng/mL	Endotoxin-free water

s.a. indicates specific activity

In experiments designed to inhibit receptors and signalling routes, cells were pre-treated with the corresponding compound (inhibitor/antagonist) or receptor neutralizing antibody for at least 45 min before activation. The inhibitors, antagonists and neutralizing antibodies used, their target, and working concentration can be found in **Table 2**. References and vendors are in **Annex 1**.

**Table 2: Pharmacological inhibitors, neutralizing antibodies and antagonists used in this study.**

NAME	TARGET	WORKING CONCENTRATION	DILUENT
CAY10614	Antagonist of lipid A activation of TLR4	5 $\mu$ M	DMSO
IFNAR monoclonal antibody	IFNAR1/2	5 $\mu$ g/mL	Endotoxin-free water
Mouse IgG1	Isotype control	5 $\mu$ g/mL	Endotoxin-free water
LY294002	PI3K inhibitor	50 $\mu$ M	DMSO
NF- $\kappa$ B SN50	NF- $\kappa$ B translocation inhibitor	50 $\mu$ g/mL	Endotoxin-free water
Noggin	BMP antagonist	470 ng/mL	Endotoxin-free water
PD98059	MEK1/2 inhibitor	50 $\mu$ M	DMSO
PX-478	HIF-1 $\alpha$ inhibitor	1-80 $\mu$ M	M199
Ruxolitinib	JAK1/JAK2 inhibitor	6 $\mu$ M	DMSO
SB203580	p38 $\alpha$ / $\beta$ inhibitor	10 $\mu$ M	DMSO
SP600125	JNK 1/2/3 inhibitor	10 $\mu$ M	DMSO
Tofacitinib	JAK1/TYK2 inhibitor	6 $\mu$ M	DMSO

## **M.5-Quantitative reverse transcription polymerase chain reaction (RT-qPCR)**

RT-qPCR is a method designed to analyse mRNA levels based on the amplification of a cDNA template previously generated by retro-transcription of total RNA and monitoring the incorporation of a fluorophore within each DNA amplification cycle.

### **M.5.1-RNA purification**

Total RNA was extracted with TRI reagent following manufacturer's protocol. For valve tissue RNA extraction, a proportion of 1 mL of TRI Reagent per 50 mg of tissue was added followed

by mechanical disintegration with an Omni tissue homogenizer (Omni International). For cells, total RNA was extracted using 1 mL of reagent per approximately 300,000 cells.

Then, chloroform extraction was performed using 200  $\mu$ L of chloroform per mL of reagent. After mixing thoroughly, samples were centrifuged at 12,000 rpm for 12 min. The aqueous phase was extracted by gently pipetting and mixed with 500  $\mu$ L of isopropanol, followed by centrifugation at 12,000 rpm at 4 °C for 10 min. The supernatant was discarded, and the pellet was washed twice with 75% ethanol and then air-dried. RNA was resuspended into 20  $\mu$ L of diethyl pyrocarbonate (DEPC)-treated water, previously prepared by treating water with 0.1% DEPC for 2 h at 37 °C and subsequently autoclaved to remove the DEPC. Total RNA was quantified by spectrophotometry (Nanodrop 1000, Thermo Scientific, Waltham, MA, USA).

### **M.5.2-Retrotranscriptase reaction**

1.5  $\mu$ g of RNA were used to synthesize first-strand complementary DNA by the reverse transcription reaction. First, the RNA was mixed with 300 ng of random primers, 1  $\mu$ L of 10 nM triphosphate deoxyribonucleotides mix (dNTPs) and sterile distilled water up to 12  $\mu$ L. The mixture was heated for 5 min at 65 °C followed by a quick chill on ice to allow primer annealing. Then, 4  $\mu$ L of 5X First-Strand Buffer, 1  $\mu$ L of ribonucleases inhibitor (RNasin®) and 2  $\mu$ L of 2 mM dithiothreitol (DTT) were added. The mixture was gently homogenized and incubated at 37 °C for 2 min. Finally, 1  $\mu$ L of 200 U/ $\mu$ L Moloney Murine Leukemia Virus retro-transcriptase (M-MLV) was added to a final volume of 20  $\mu$ L and incubated as follows: 10 min at room temperature; 50 min at 37 °C; 15 min at 70 °C. Generated cDNA was stored at -20 °C until use.

### **M.5.3-Quantitative PCR**

cDNA was amplified by real-time PCR using a KAPA SYBR® FAST qPCR master mix (2X) kit. A total of 20 ng of cDNA generated in the previous step were added in a final volume of 20  $\mu$ L. For each target gene, 0.4  $\mu$ L of 10  $\mu$ M of the corresponding primers (Sigma-Aldrich, St.Louis, MO) were used. Primers previously reported and showing a 100% of complementarity with the target gene in a bioinformatics tool (<https://www.ncbi.nlm.nih.gov/tools/primer-blast/>) were used. All the primers used in the study are listed in **Table 3**. The qPCR reaction was carried out using a LightCycler480® (Roche Diagnostics, Rotkreuz, Switzerland) under the following conditions: (i) 5 min of denaturalization at 95 °C; (ii) 45 cycles of 15 seconds at 95 °C, 20 seconds at 60 °C, and 5 seconds at 72 °C; and (iii) a final cycle of 5 seconds at 95 °C and 1 minute at 55 °C, followed by 10

seconds at 4 °C. Two technical replicates were performed for each condition. Basal transcript levels were referred to the housekeeping gene glyceraldehyde-3 phosphate dehydrogenase (GAPDH) value as ( $2^{-\Delta Ct}$ , Ct = cycle threshold value). Relative transcript levels were calculated based on the  $2^{-\Delta\Delta Ct}$  method (relative to GAPDH and to basal conditions).

**Table 3: PCR primers used in the study.**

<b>Gene name</b>	<b>Forward primer sequence (5'-3')</b>	<b>Reverse primer sequence (5'-3')</b>	<b>Size (bp)</b>
<i>ACAN</i>	ACTCTGGGTTTTTCGTGACTCT	ACACTCAGCGAGTTGTCATGG	81
<i>AKT1</i>	AGCGACGTGGCTATTGTGAAG	GCCATCAATTCTTGAGGAGGAAGT	97
<i>BCL-2</i>	GGTGGGGTCATGTGTGTGG	CGGTTTCAGGTAAGTTCAGTCATCC	89
<i>BMP2</i>	ACCCGCTGTCTTCTAGCGT	CTCAGGACCTCGTCAGAGGG	140
<i>CNMD</i>	CTGGATCACGAAGGAATCTGT	ACCATGCCCAAGATACGGG	176
<i>GAPDH</i>	TGCCAAATATGATGACATCAAGAA	GGAGTGGGTGTCGCTGTTG	121
<i>HIF1A</i>	AGTGTACCCTAACTAGCCGA	GTGCAGTGCAATACCTTCC	70
<i>IBSP</i>	CCCCACCTTTTGGGAAAACCA	TCCCCGTTCTCACTTTCATAGAT	109
<i>IFNARI</i>	TGCCATGCCAGAAGATAGTG	TTAGGTGCTCAGGCTTCCAG	156
<i>IFN<math>\beta</math></i>	CAACTTGCTTGGATTCTTACAAAG	TATTCAAGCCTCCATTCAATTG	81
<i>IFNGR1</i>	AAAGTCAGAAGAATTTGCTGTAT	ACTGAAGGGTGAAATATGTC	108
<i>IL6</i>	CACCTCTTCAGAACGAATTG	CTAGGTATACTCAAACCTCC	239
<i>IL8</i>	ATGACTTCCAAGCTGGCCGT	TCCTTGGCAAACTGCACCT	82
<i>IRF1</i>	TTCCCTCTTCCACTCGGAGT	GATATCTGGCAGGGAGTTCA	378
<i>IRF3</i>	TCTGCCCTCAACCGCAAAGAAG	TACTGCCTCCACCATTTGGTGTC	151
<i>IRF8</i>	GCTGATCAAGGAGCCTTCTG	ACCAGTCTGGAAGGAGCTGA	98
<i>MSX2</i>	TGCAGAGCGTGCAGAGTTC	GGCAGCATAGGTTTTGCAGC	144
<i>MGP</i>	CTTAGCGGTAGTAACTTTGTG	AGAGCCTTCTCGGATCCTCTC	151
<i>NOS3</i>	CCAGCTAGCCAAAGTCACCAT	GTCTCGGAGCCATACAGGATT	354
<i>OSX</i>	TGCTTGAGGAGGAAGTTCAC	AGGTCACTGCCACAGAGTA	148
<i>RUNX2</i>	TGGTTACTGTCATGGCGGGTA	TCTCAGATCGTTGAACCTTGCTA	101
<i>SMURF1</i>	TGTGAAAAACACATTGGACCCA	ACGCTAATGGTTATCGAATCCG	81
<i>SOST</i>	CCGGAGCTGGAGAACAACAAG	GCACTGGCCGGAGCACACC	186
<i>SOX9</i>	AGCGAACGCACATCAAGAC	CTGTAGGCGATCTGTTGGGG	85
<i>TNAP</i>	CAAAGGCTTCTTCTTGCTGGT	AAGGGCTTCTTGTCTGTGTC	258
<i>VEGFA</i>	ATCTGCATGGTGATGTTGGA	GGGCAGAATCATCACGAAGT	218

## **M.6-Protein analysis by immunoblot (Western Blot)**

This technique, based on the detection of target proteins with specific antibodies, consists on the separation of protein by size using electrophoresis, and their transfer to a membrane for the subsequent immunologic detection. In this study we followed the original sodium dodecyl sulphate (SDS)-PAGE method described by Laemmli in 1970,<sup>173</sup> used in previous reports from our laboratory.<sup>164,174</sup> Buffers composition is indicated in **Annex 1**.

### **M.6.1-Protein extraction and quantitation by the bicinchoninic acid (BCA) assay**

Cells were grown to confluence in 6- or 12-well plates and treated as previously indicated. Before the lysis, supernatants were removed and stored at -80 °C until use and cells were washed with cold PBS.

Whole cell extracts: Cells were lysed with TNE buffer plus phosphatase inhibitors: (1 mM Na<sub>3</sub>VO<sub>4</sub>; 5 mM NaF) and protease inhibitors (10 µg/mL aprotinin, 10 µg/mL leupeptin; 1 mM phenylmethylsulfonyl fluoride (PMSF)). Typically, 75 µL of lysis buffer were used for 6-well plates and 50 µL for 12-well plates, and a cell scraper was used to facilitate cellular detachment and lysis. Cell extracts were centrifuged at 13,200 rpm for 12 min at 4 °C and the supernatant containing solubilized proteins was collected to assay protein concentration.

Cytoplasmic and nuclear extracts: Cells were lysed using the Active Motif Nuclear and cytoplasmic extract kit following manufacturer`s protocol.

Protein extracts from valve leaflet tissue: Specimens were first powdered using a mortar and a pestle with liquid nitrogen, and then resuspended in RIPA lysis buffer supplemented with protease/phosphatase inhibitors as previously indicated in a proportion of 5 µL of buffer per mg of tissue.

BCA protein assay: Total protein content of cell extracts was calculated using the BCA assay, which is based on the capacity of proteins to reduce Cu<sup>2+</sup> to Cu<sup>+</sup> in an alkaline environment. For the measurement, a Pierce™ BCA protein assay kit was used with some modifications of the manufacturer`s procedures for microplate applications. Briefly, 5 µL of each sample were incubated with 100 µL of the working BCA solution (mixing 50 parts of reagent A containing bicinchoninic acid in alkaline buffer and 1 part of reagent B containing cupric sulphate) for 30 min at 37 °C. The absorbance at 570 nm was determined using a Versamax microplate reader (Molecular Devices,

Sunnyvale, CA). Protein concentration was determined by interpolation in a standard curve with known concentrations of BSA.

### **M.6.2-Western blot procedure: SDS-PAGE and transfer**

For Western blot analysis, usually 25 µg of protein were mixed with Laemli buffer, then heated at 100 °C for 5 min and stored at -20 °C until use.

Protein separation was carried out in denaturing conditions in polyacrylamide gels, typically 8%-10% acrylamide depending on the proteins of interest. Electrophoretic separation was carried out applying a constant power of 25 mA for each gel using a power source (Bio-Rad, Hercules, CA). A molecular weight protein ladder was included for use as a size standard. Proteins were then transferred to hybond polyvinylidene difluoride membranes that had been previously activated in methanol for 1 min followed by rewetting in distilled water for 2 min. A wet-transfer system (Bio-Rad, Hercules, CA) was used at 400 mA for 2 h.

### **M.6.3-Protein immunodetection and visualization by chemiluminescence**

Non-specific binding was prevented by incubating the membrane with blocking buffer containing TBS-0.5% Tween buffer (TTBS) plus either 5% of non-fat milk or BSA, the latter for phospho-antibodies, for 1 h at room temperature on a rocker platform. Primary antibodies were prepared as indicated by the manufacturer, typically in 5% milk or BSA in TTBS supplemented with 0.02% sodium azide. The membranes were incubated overnight with the primary antibody and later washed 3 times for 10 min each in TTBS, followed by 1 h incubation at room temperature with the appropriate horseradish peroxidase-conjugated secondary antibody in 3% milk in TTBS. A compilation of primary and secondary antibodies used in the study is shown in **Table 4**. Antibody-labelled proteins were then detected by chemiluminescence reaction by using horseradish peroxidase blotting substrate ECL. Blots were exposed to autoradiography films and developed in a dark chamber. Signals were scanned with a densitometer GS-800 (Bio-Rad, Hercules, CA) and analysed by Quantity One software (Bio-Rad, Hercules, CA). Results were expressed as arbitrary units (a.u) normalized to the corresponding loading control ( $\beta$ -tubulin or actin) and to basal conditions.

If necessary, a harsh stripping buffer solution containing  $\beta$ -mercaptoethanol and SDS was used to eliminate previous signals from overlapping proteins following a protocol available online (<https://www.abcam.com/protocols/western-blot-membrane-stripping-for-restaining-protocol>).

Briefly, membranes were incubated in harsh stripping buffer for 45 min at 50 °C under shaking

conditions, then rinsed in tap water, and later washed extensively in TTBS. Before reusing the blot, it was incubated with blocking buffer.

**Table 4: Primary and secondary antibodies used for Western Blot. References and vendors in Annex 1.**

<b>Immunoblot human primary antibodies</b>		
<b>Target protein (human)</b>	<b>Molecular weight (kDa)</b>	<b>Working dilution</b>
<b>Actin</b>	42	1:1000
<b>eNOS</b>	140	1:1000
<b>HIF-1<math>\alpha</math></b>	120 / 110	1:1000
<b>Histone-H3</b>	17	1:500
<b>ICAM-1</b>	100	1:100
<b>NF-<math>\kappa</math>B-p65</b>	65	1:500
<b>pAkt (Ser473)</b>	65	1:500
<b>pp44/42 MAPK (Erk1/2) (Thr202/Tyr204)</b>	44 / 42	1:1000
<b>pNF-<math>\kappa</math>B-p65 (Ser536)</b>	65	1:1000
<b>pp38 (Tyr182/Thr180)</b>	38	1:1000
<b>pSAPK/JNK (Thr183/Tyr185)</b>	54 / 46	1:1000
<b>pSTAT1 (Ser727)</b>	95	1:1000
<b>pSTAT1 (Tyr701)</b>	95	1:1000
<b>pSTAT3 (Tyr705)</b>	90	1:1000
<b>RUNX2</b>	65	1:1000
<b>STAT1</b>	95	1:1000
<b>STAT3</b>	95	1:1000
<b><math>\beta</math>-tubulin</b>	55	1:20000
<b>VCAM-1</b>	110	1:200
<b>Immunoblot secondary antibodies (Horseradish peroxidase-conjugated)</b>		
<b>Target primary</b>	<b>Working dilution</b>	
<b>Goat-anti-mouse IgG</b>	1:3000	
<b>Goat anti-rabbit IgG</b>	1:2000	

## **M.7-Enzyme-linked immunosorbent assay (ELISA)**

One application of this antibody-based technique is the detection and quantification of secreted proteins. The antigen of interest is usually immobilized on a solid surface and then complexed with an antibody conjugated to an enzyme, typically HRP. In the assay, detection is accomplished by assessing the conjugated enzyme activity by oxidation of chromogenic reagents by a peroxidase like 3,3',5,5'-tetramethylbenzidine producing a detectable signal, most commonly a colour change. Quantification of the target protein is done based on a standard curve made of known concentrations of the protein of interest.

Protein secretion was evaluated in the supernatants of cells activated with the corresponding stimuli for 24-48 h, typically 1 mL/well (6-well plate) of cell activation medium. Collected supernatants were analysed by ELISA following manufacturer's protocol. A Versamax microplate reader (Molecular Devices, Sunnyvale, CA) was used to measure absorbance at 450 nm. Sample concentration was calculated by extrapolation from the standard curve, and values were normalized to total cell protein content. For prostaglandin E<sub>2</sub> (PGE<sub>2</sub>) analysis, an online free software (<https://www.myassays.com/arbor-assays-pge2-enzyme-immunoassay-kit-k051-h.assay>). was used to perform the calculations. All the commercial ELISA kits are listed in **Table 5**.

**Table 5: Commercial ELISA kits used in the study.**

<b>Target protein</b>	<b>Supernatant dilution</b>
BMP2	No dilution
IFN- $\beta$	Untreated and stimulated: 1/10
IL-6	Untreated: 1/20 Stimulated: 1/100
IL-8	Untreated: No dilution Stimulated: 1/40
IP-10	Untreated: No dilution Stimulated: 1/40
MMP-1	No dilution
PGE <sub>2</sub>	No dilution
VEGF-A	Untreated: 1/2 Stimulated: 1/5

## **M.8-Proliferation assay**

Cell proliferation was assayed by an indirect method based on the conversion of 3-(4,5-dimethylthiazol-2-yl)-2,5-diphenyltetrazolium bromide (MTT) into a purple and insoluble product named formazan by the activity of mitochondrial enzymes of living cells.<sup>175</sup>

For the assay, 2,500 cells were first seeded in 96-well plates. The following day, cells were stimulated in 200  $\mu$ L of activation media for 12 days, changing medium and stimuli every 3 days. At day 12, cells were visually examined, washed with PBS, and incubated with 100  $\mu$ L of phenol-red-free M199 medium supplemented with MTT at a final concentration of 1 mg/mL for 4 h at 37 °C /5 % CO<sub>2</sub>. Formazan crystal extraction was performed by adding 100  $\mu$ L of an SDS-HCl solution (10% SDS in 0.01 N HCl) followed by a 4 h incubation at 37 °C. Results were evaluated by measuring the absorbance at 570 nm and 630 nm (background) in a Versamax Microplate reader (Molecular Devices, Sunnyvale, CA). Data were expressed as  $A_{570}-A_{630}$  at day 12.

## **M.9-*In vitro* calcification assays**

*In vitro* calcification assays were performed in high-phosphate and low serum conditions following previously reported protocols.<sup>176</sup> VIC grown until reaching approximately 90% of confluence in 6- or 12-well plates, were incubated in calcification medium (M199 containing 1% FBS, 3 mmol/L Pi and 1% antibiotic-antimycotic solution) for a period ranging from 7 to 21 days, depending on the stimuli and the experiment design. Medium and treatments were replaced every 3 days. Evaluation of calcification was later performed by using two different and independent protocols and technical replicates, as indicated below.

### **M.9.1-Staining of calcium-phosphate crystals with Alizarin Red dye**

An anthraquinone derivative, alizarin red (AR), was used for visualization and semi-quantitation of calcification nodules in VIC. Cells, previously washed with PBS, were incubated with a dye solution (1.4% AR in water, pH 4.2 adjusted with NH<sub>4</sub>OH) for 2 min unless otherwise indicated. Then, cells were washed at least 3 times with PBS and visualized under a phase-contrast microscope (Nikon Eclipse TS100) connected to a digital camera. AR dye was then extracted following the acetic acid extraction protocol described by Gregory *et al.*<sup>177</sup> Briefly, cells were incubated in 10% acetic acid for 2 h at room temperature and then harvested by scraping. Later, the solution was heated at 85 °C for 15 min, followed by cooling on ice for 10 min. After centrifugation,

the aqueous phase was extracted and neutralized with 1M NH<sub>4</sub>OH. Absorbance at 450 nm was measured with a Versamax Microplate reader (Molecular Devices, Sunnyvale, CA). Data were expressed as a fold increase of absorbance referred to basal conditions.

### **M.9.2-Calcium deposits quantification**

A quantitative colorimetric calcium Quantichrom™ kit, based on the binding of a phenolsulphonophthalein dye to free calcium forming a very stable blue coloured complex, was used to quantify calcium deposits. Briefly, cells were first washed once with PBS and calcium deposits were then extracted with 0.6 N HCl for 24 h at 4 °C. Supernatants were collected and 5 µL were used to quantitate calcium deposits following manufacturer's protocol. The intensity of the colour at 612 nm, which is directly proportional to the calcium content of the sample, was evaluated. Cells were lysed in 0.1 N NaOH with 0.1% SDS and total protein concentration was determined using the BCA assay. Data were expressed as mg/dL of calcium and normalized to total protein content.

It should be noted that calcium quantitation cannot be performed in AR-stained plates; therefore, cells in separate plates were processed in parallel and assayed for each method.

### **M.10-Apoptosis/necrosis assay by flow cytometry**

Annexin V and propidium iodide staining followed by flow cytometry analysis was used to evaluate cell apoptosis and necrosis. The principle of annexin V assay is based on the capacity of this protein to bind with high affinity to phosphatidylserine residues exposed to the cell surface in the presence of calcium, a phenomenon occurring at the early stages of canonical apoptosis.<sup>178</sup> Propidium iodide is a cell membrane-impermeant dye binding to double-stranded DNA that is generally excluded from viable cells and can be excited at 488 nm thus emitting at a maximal wavelength of 617 nm.

For the assay, approximately 100,000 cells were grown to confluence and then treated with the indicated ligands for 7 days in calcification medium. Medium was replaced every 2 days. To avoid cell death caused by trypsinization, cells were detached using StemPro Accutase. Then, cells were spun down and resuspended in Annexin V binding buffer. Cell staining was performed following manufacturer's protocol by incubating with FITC ApoScreen® annexin V for 15 min on ice followed by two washes and staining with ApoScreen® propidium iodide. Immediately, stained cells were analysed by a Gallios™ Flow Cytometer (Beckman Coulter Inc, US). Data analysis was

performed using Kaluza® Flow Analysis Software (Beckman Coulter Inc, US). The percentage of apoptotic cells was calculated based on the number of annexin-V positive cells (B1+B2 quadrants).

## **M.11-Ectopic phosphatase activity**

Ectopic phosphatase activity assessment was based on the conversion of *p*-nitrophenyl phosphate to *p*-nitrophenol by extracellular phosphatases and the detection of the generated chromogenic product by measuring the absorbance at 405 nm.<sup>179</sup>

For the assay, cells cultured in 12-well plates were activated in M199 medium supplemented with 1% FBSi and 1% antibiotic/antimycotic solution for 21 days in an incubator at 37 °C with 5% CO<sub>2</sub> and humidified atmosphere. Medium and stimuli were replaced every 3 days. For the enzymatic assay, cells were incubated with 10 mmol/L of *p*-nitrophenyl phosphate in phenol-red-free M199 medium for 12 h at 37 °C. Then, absorbance at 405 nm was measured and phosphatase activity was calculated using the Beer-Lambert law and a specific molar extinction coefficient of 18.75 mM<sup>-1</sup> x cm<sup>-1</sup> for *p*-nitrophenyl phosphate. Data were expressed as nmol/min and normalized to µg of total protein content determined by the BCA assay.

## **M.12-HIF-1α detection by immunofluorescence**

Immunofluorescence staining was used to analyse the cellular location of HIF-1α protein and to confirm its nuclear translocation upon cell activation. A total of 10,000 VIC seeded on uncoated coverslips overnight were then activated with the corresponding stimuli for 24 h. The staining protocol and fluorescence quantitation was as the used for α-SMA detection (**Section M.3.1**). Primary antibody was rabbit anti-human HIF-1α antibody (1:100 in PBS-1% BSA); Secondary antibody was an Alexa Fluor 488 goat anti-rabbit IgG antibody (1:1000 in PBS-1% BSA).

## **M.13-Dynamic adhesion assays in side-specific VEC**

Dynamic VEC-monocyte adhesion assays were based on the simulation of different flow patterns in the edge compared to the centre of a 6-well plate.<sup>172</sup> This system simulated a flow pattern comparable to the one on the ventricular side of the valve (unidirectional and higher-magnitude shear stress, edge of the well) or the aortic side of the valve (multidirectional and lower-magnitude shear stress, centre of the well), although the flow magnitude was lower than the physiological in each side. A total of 5 independent pairs of aVEC and vVEC monolayers were treated with IFN-γ and/or

TNF- $\alpha$ , and then analysed for adhesion to the monocytic cell line THP-1, which were previously stained with calcein.

For the assay, approximately 150,000 side-specific VEC were seeded in 6-well plates pre-coated with 1% gelatin. The next day, medium was replaced with 1.9 mL of EGM-2 growth medium and sheared on an orbital shaker set at the angular velocity of 150 rpm for 48 h. Stimuli were added to VEC monolayers, which were sheared for additional 24 h before performing the THP-1 adhesion assay.

Before the assay, THP-1 cells (ATCC®; Middlesex, UK; Ref. TIB-202™) were cultured in RPMI-1640 medium supplemented with 1% L-glutamine and 10% FBSi. For the adhesion assay, THP-1 cells resuspended in pre-warmed RPMI medium at  $10^6$  cells/mL of density were stained with calcein-AM (1:1000 dilution) for 30 min at 37 °C / 5% CO<sub>2</sub>. Then, THP-1 cells were washed 3 times with pre-warmed EGM-2 medium and added to VEC monolayers at a density of  $10^6$  cells in 1.5 mL of EGM-2 medium without supplements. Cells were then incubated for 1 h at 37 °C without swirling. After 3 washes with pre-warmed medium, cells were fixed for 10 min with 4% *p*-formaldehyde. Non-adhered THP-1 cells were removed by washing twice with PBS. Fluorescence microscope images were taken using a Nikon DMx1200 camera (Nikon Instruments, Melville, NY) coupled on a Zeiss Axioscope Microscope (Carl Zeiss, Oberkochen, Germany). Images, 115X magnification, were captured using NIS elements software (Nikon Instruments, Melville, NY). Ten pictures were taken using a custom guide to discern the edge and the centre of the wells.

In parallel, an additional 6-well plate with VEC monolayer in a was used to evaluate cell number by nuclei staining with DAPI for 10 min. Calcein stained THP-1 counting and VEC nuclei counting were performed using a custom-made macro in ImageJ (U.S., NIH). Data were expressed as total number of THP-1 cells adhered, total number of VEC, and normalized adhesion, THP-1/VEC ratio.

## **M.14-Migration (wound healing) assay in side-specific VEC**

For migration assays, cells were seeded in 6-well plates for 36 h and then serum-starved overnight in EGM-2 supplemented with 2% FBSi. The following day a scratch was generated using a P200 pipette tip from the top to the bottom of each well. Cells were washed twice with pre-warmed medium to eliminate the dead ones and stimulated in 1.9 mL of starvation medium for 24 h. Next, cells were washed twice with pre-warmed medium, and microphotographs of the scratch area were

taken at 0 and 24h to calculate the wound healing. ImageJ software was used to measure the area of the wound. Data were expressed as % of wound healing as compared to the initial area as follows:

$$\% \text{ wound healing} = \frac{\text{Original area (time 0)} - \text{Treatment area (time x)}}{\text{Original area (time 0)}} \times 100$$

## **M.15-RNA interference assays**

For loss-of-function experiments, VIC were transiently transfected with small interference RNAs (siRNA) directed against the target gene. The siRNA have a length of 20-25 nucleotides complementary to the sequence of the mRNA of the target gene, preventing its translation to protein.

For the assay, approximately 50,000 VIC were seeded in 12-well plates and cultured for 3 days. Cells uniformly distributed and reaching a confluence of 75% were transfected for 72 h before stimulation. Ambion® Silencer® selected pre-designed and validated siRNA duplexes against *HIF1A*, *STAT1*, and *STAT3* genes or unspecific Silencer® target were used. The siRNA were first resuspended in 100 µL of provided nuclease-free water obtaining a 50 µM stock dilution that was kept at -20 °C until use. A final working concentration of 10 nM of siRNA was used.

The transient transfection of siRNA was performed using a lipid-based reagent, Dharmafect, as previously reported.<sup>174</sup> Briefly, 2 µL of the corresponding siRNA duplexes were diluted in 100 µL of Optimem medium. Additionally, 3 µL of Dharmafect-1 reagent were diluted in 100 µL of Optimem medium. Both solutions were incubated for 5 min at room temperature. Then, the siRNA dilution was gently added into the Dharmafect dilution and incubated for 20 min at room temperature to allow the formation of RNA-lipid complexes. Next, 800 µL of M199 medium supplemented with 10% FBSi and without antibiotics were added to each tube. Cells were then incubated with the corresponding mixture for 24 h to allow the transfection. Medium was then replaced by growth medium (M199 plus 10% FBSi and antibiotic-antimycotic solution), and cells were cultured for additional 48 h. Then, the medium was replaced, and cells were activated for 24 h before assayed for protein expression by Western Blot.

## **M.16-Conditioned medium experiments**

To study paracrine interactions between activated VIC and VEC, conditioned-medium (CM) experiments were performed. For this purpose, cultured VEC (mixed populations of aortic and ventricularis) were incubated with conditioned M199 medium from either stimulated or untreated

VIC. As shown in **Figure XIII**, VIC were cultured for 3 h in activation medium in an incubator at 37 °C and 5% of CO<sub>2</sub>, with or without stimulation with IFN- $\gamma$ +LPS. Cells were then washed to remove the stimuli and incubated for additional 24 h in 1 mL of medium. After that, conditioned supernatants were harvested and kept at -80 °C until use. VEC were then treated for 24 h with the supernatants (untreated or IFN- $\gamma$ +LPS-CM) and harvested as previously indicated for RT-qPCR or Western Blot analysis. Non-conditioned cell activation medium was used as control.

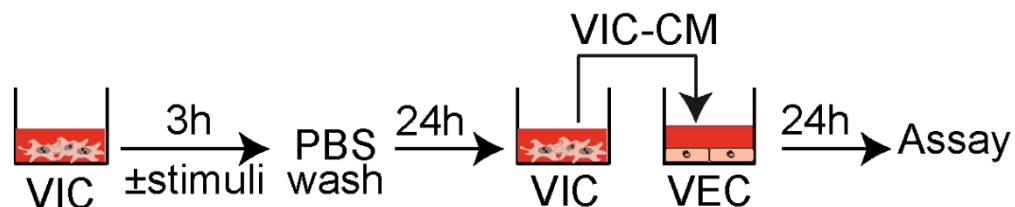


**Figure XIII: Flow chart of conditioned medium experiments.**

---

## **M.17-Statistical analysis**

All data are represented as dot plot overlaid to bar graphs indicating the mean  $\pm$  standard deviation (SD). Each dot represents data from either a valve cell isolate or valve tissue from one different and independent donor. For the analysis of two data sets, unpaired and two-tailed test were performed as follows: if data followed normal distribution, normal t-test was used for data with comparable SD, whereas a t-test with Welsch`s correction was used for data with unequal SD; if data did not follow normal distribution, a Mann-Whitney test was performed. To analyse 3 or more levels, analysis of variance (ANOVA) for either 1 factor (treatment), or 2 factors (treatment and sex; treatment and valve side) was performed. Repeated measures 1-way ANOVA or 2-way ANOVA were performed for data following a normal distribution and homoscedasticity requirements. In case of non-normal distributed or unequal variances data, logarithmic transformation was previously applied. Statistical significance was considered for  $p < 0.05$  values.

For 2 group comparison, the statistics for the 2-way ANOVA are presented in a box above the corresponding graph. If the interaction factor reached statistical significance, a *post-hoc* test was performed to analyse specific differences among groups. *Post hoc* test included the Benjamini-Hochberg *post-hoc* procedure that corrects for multiple comparisons by controlling the false discovery rate to reduce type I error (false positives).

Patient features included in **Tables 6-8** were analysed using the Student t test for categorical variables and the Fisher exact test (frequency under 5) or  $X^2$  test for continuous variables. All the statistics were performed using GraphPad Prism 7 software (La Jolla, CA).

## **RESULTS**



# RESULTS

---

The results of the thesis are presented in six sections:

**R.1:** “**Common effects of type I and II IFN in human VIC**”. In the first part of the study we investigated the effects of IFN- $\alpha$  and IFN- $\gamma$  on VIC isolated from non-mineralized valves. Here, we also explored the regulation of the TLR-induced effects by IFN. Our research was mainly focused on IFN-activated signalling pathways as well as their implication in CAVD relevant pathological processes such as inflammation and calcification.

**R.2:** “**Specific mechanisms of IFN- $\alpha$  in VIC**”. In this part, we focused on the understanding of the mechanism by which IFN- $\alpha$  exerts its effects on VIC, especially on calcification.

**R.3:** “**Specific mechanisms of IFN- $\gamma$  in VIC**”. The goal was to analyse the specific mechanisms for the interplay between IFN- $\gamma$  and LPS and its implication on VIC angiogenesis and calcification.

**R.4:** “**Basal findings in valve tissue**”. The aim was to explore whether the results of the previous sections correlated with findings on valve tissue from both control and calcified valves.

**R.5:** “**Type I IFN signalling mediates Poly(I:C) effects in VIC**”. We aimed to elucidate the underlying mechanisms of TLR3-induced inflammation and calcification.

**R.6:** “**VIC-VEC interactions and side-specific effects of IFN- $\gamma$  and TNF- $\alpha$  in VEC**”. The first part of this section shows the effects of VIC-conditioned medium in mixed VEC populations. The second part comprises the results obtained in valvular endothelial cells isolated specifically from the aortic or the ventricular side of the valve.

To note, at the beginning of each section, patients’ demographics are presented on a table, except for the case of side-specific VEC, which were obtained from deceased patients (without valve disease).

## **R.1-Common effects of type I and II IFN in human VIC**

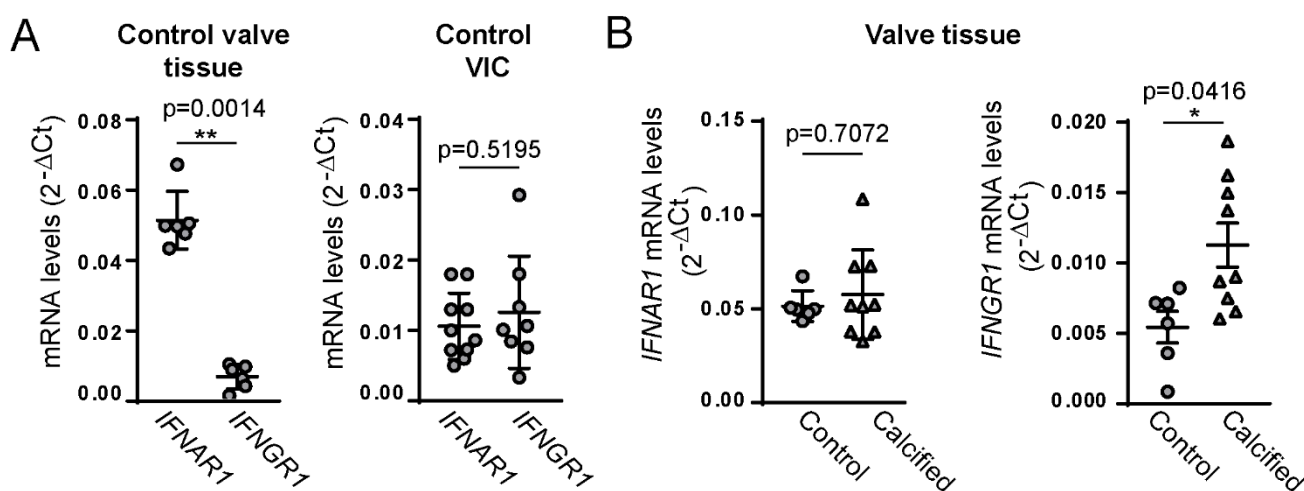
The overall effects of IFN on the pathophysiology of CAVD were investigated in a cellular model of VIC isolated from control non-calcified aortic valves from males and females. In addition, calcified valve tissue from male patients was also used. Clinical features of both groups were compared as indicated in **Methods**. Characteristics and comorbidities were not significantly different between male and female control groups (**Table 6**). All patients were Caucasian, and all female donors were post-menopausal.

**Table 6: Clinical features of the patients whose valves were included in section 1 of the study.**

Patient characteristics	Control valves			Calcified valves
	Male n=16	Female n=7	p-value	Male n=9
Age	61 ± 2	58 ± 3	0.48	77 ± 3
Hypertension	3 (19%)	0	0.53	3 (33%)
Hypercholesterolemia	4 (25%)	1 (14%)	0.56	3 (33%)
Diabetes mellitus	5 (31%)	3 (43%)	0.66	2 (22%)
Smoking	4 (25%)	1 (14%)	0.56	3 (33%)
Renal failure	2 (13%)	0	0.32	1 (11%)
Aetiology of heart failure	7 idiopathic, 7 ischemic 1 alcoholic 1 sarcoidosis	4 idiopathic, 2 ischemic, 1 post-cardiotomy shock	0.31	-
Aortic valve area (cm <sup>2</sup> )	-	-	-	0.75 ± 0.11
Peak gradient (mmHg)	-	-	-	68.75 ± 18.77
Mean gradient (mmHg)	-	-	-	42.44 ± 14.88
Statins	-	-	-	6 (66%)

### R.1.1-Human aortic valve tissue and explanted cells express IFN receptors

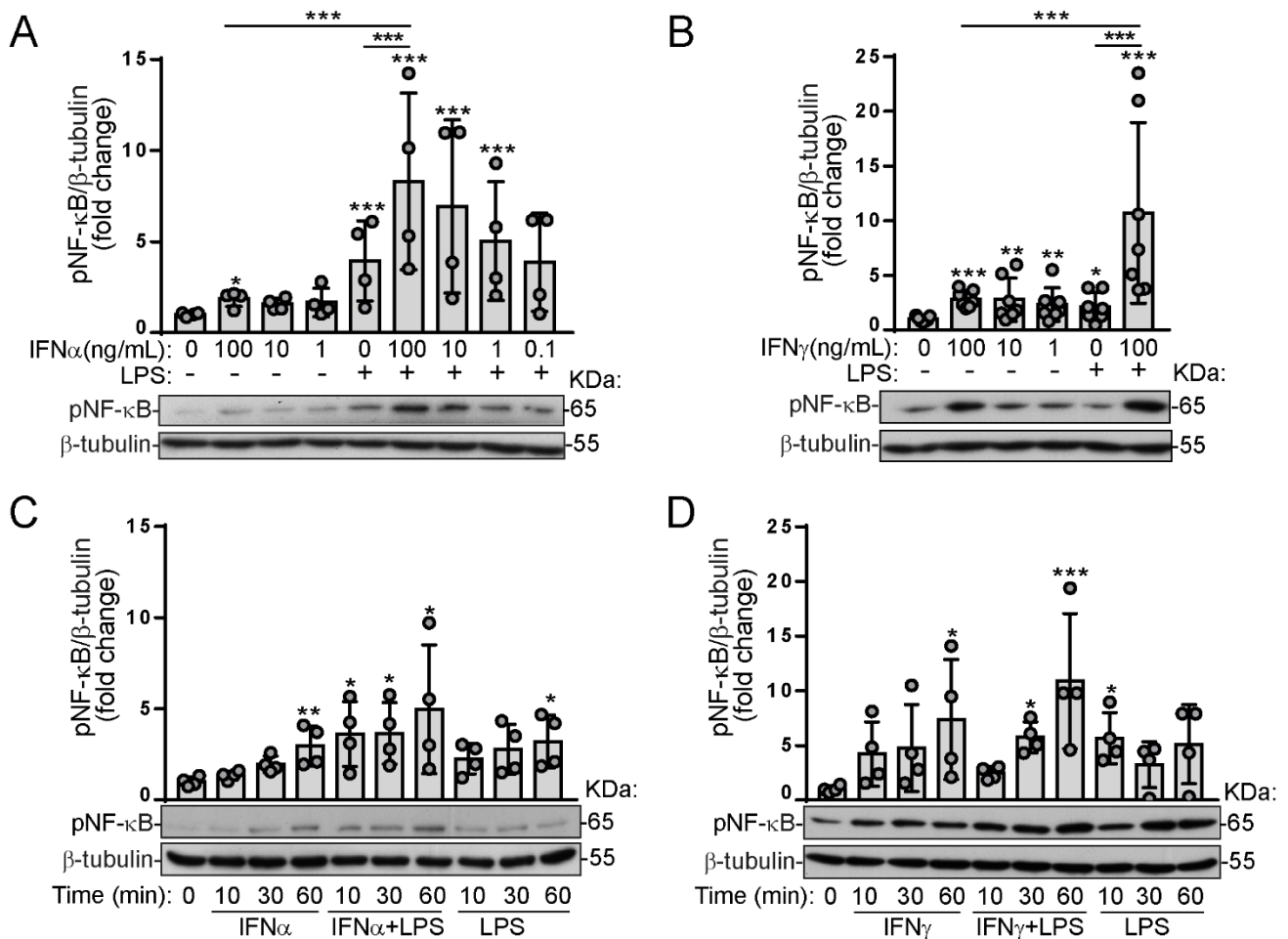
First, we analysed whether control human valve tissue and isolated VIC express IFN receptors. qPCR analysis revealed that non-calcified human aortic valve tissue expresses *IFNAR1* and *IFNGR1* genes, the former one showing higher transcripts levels (**Figure 1A, left panel**). However, the expression of both genes was similar in isolated VIC (**Figure 1A, right panel**). When comparing control and calcified valve tissue, similar transcript levels of *IFNAR1* gene were observed (**Figure 1B, left graph**), while *IFNGR1* expression was significantly higher in calcified valves (**Figure 1B, right panel**).



**Figure 1. Interferon receptors expression in valve tissue and VIC.** Total RNA was extracted from valve tissue and VIC and analysed by qPCR for type I and type II IFN receptor subunit 1 mRNA expression, *IFNAR1* and *IFNGR1*, respectively. (A) Receptor expression for control valve tissue (left panel) and isolated VIC (right panel);  $n \geq 6$  for each group. (B) *IFNAR1* (left panel) and *IFNGR1* (right panel) gene expression in control and calcified valve tissue;  $n \geq 6$  for each group. Grey dots, control male VIC or valve tissue; grey triangles, calcified male tissue. \* indicates statistical significance; \* $p < 0.05$ ; \*\* $p < 0.01$ .

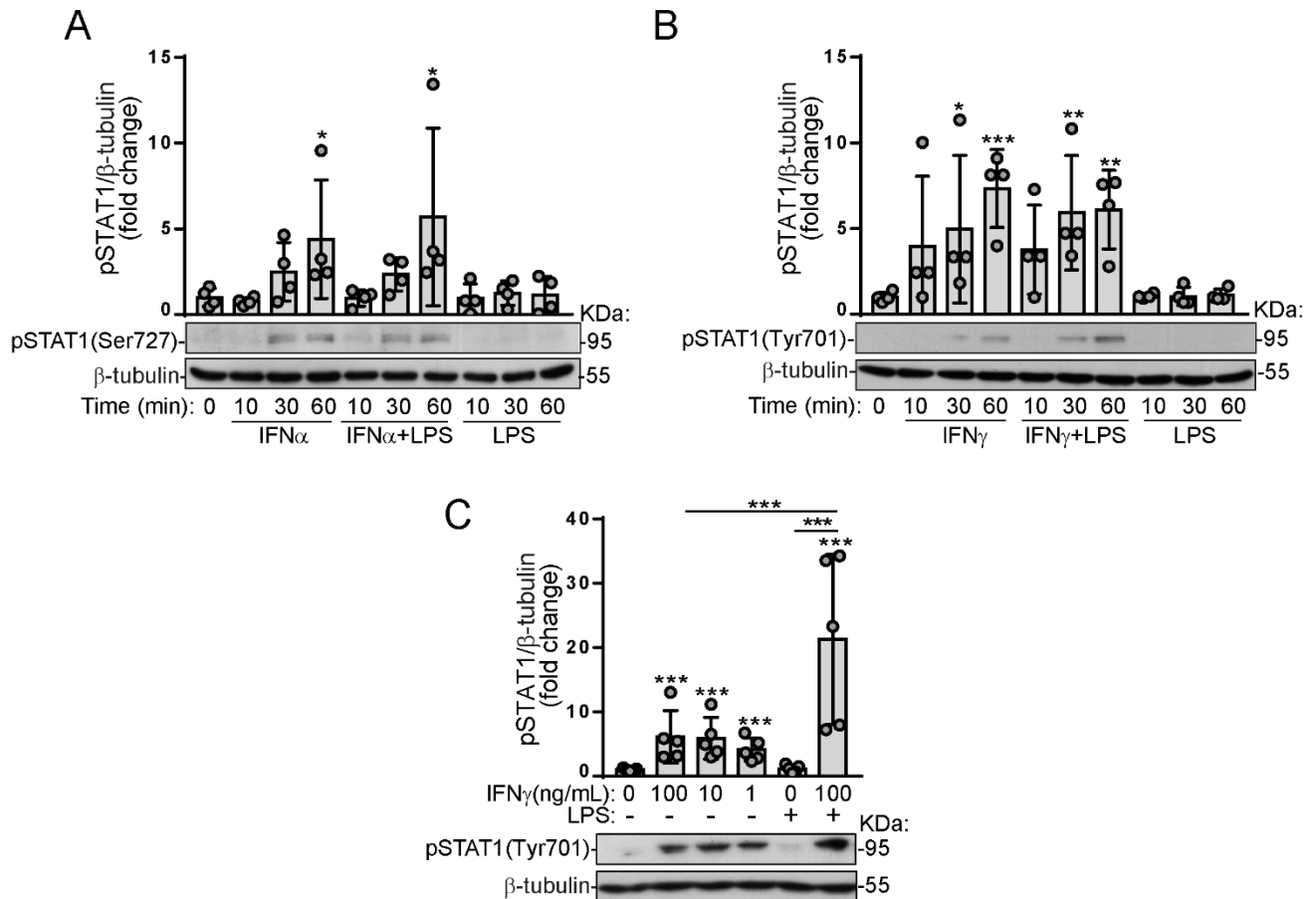
### R.1.2-IFN activate several signalling pathways in control VIC

Next, potential IFN-activated signalling pathways in VIC were explored. Given that inflammation plays a major role at the early stages of CAVD and that IFN are pro-inflammatory agents in some contexts, we examined the phosphorylation of the master transcription factor for inflammation, NF- $\kappa$ B. Data revealed that both recombinant type I (IFN- $\alpha$ ) and type II (IFN- $\gamma$ ) IFN promoted NF- $\kappa$ B-p65 phosphorylation at 24 h, being the effect enhanced upon co-stimulation with the TLR4 ligand LPS (**Figure 2A-B**). This effect was dose-dependent, reaching a maximum at a concentration of 100 ng/mL, a dose used throughout the study unless otherwise indicated. In addition, both IFN also promoted NF- $\kappa$ B-p65 phosphorylation at early times (0-60 min), although no significant potentiation in combination with LPS was observed (**Figure 2C-D**).



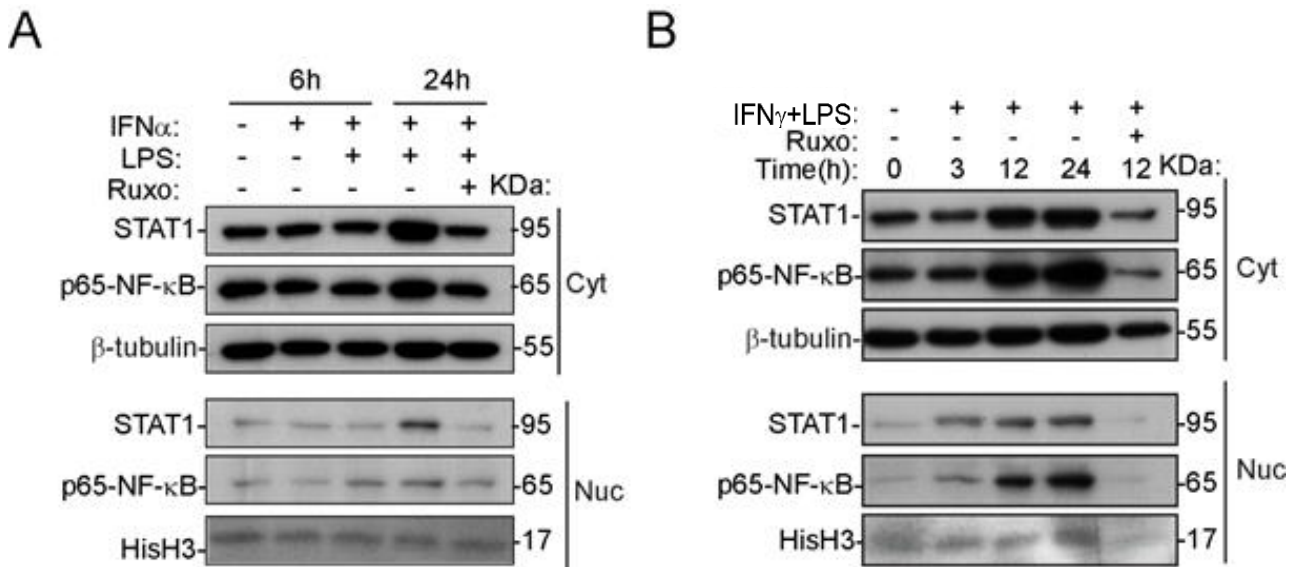
**Figure 2. Interferons promote NF-κB-p65 phosphorylation with further potentiation by LPS.** Control VIC from male patients were stimulated with the indicated ligands for either 24 h (A-B) or 0-60 min (C-D), and cell lysates analysed by Western Blot for NF-κB-p65 phosphorylation. Representative blots and densitometric analysis corresponding to the treatment with IFN-α (A, C) or IFN-γ (B, D); n≥4 for each treatment. Unless otherwise indicated, IFNα refers to 100 ng/mL IFN-α; IFNγ, 100 ng/mL IFN-γ; LPS, 1 μg/mL LPS. In the study, n indicates the number of VIC isolates from independent valve donors. \* indicates statistical significance as compared with basal conditions or as indicated by the line below; \*p<0.05; \*\*p<0.01; \*\*\*p<0.001.

Canonical IFN signalling pathways were then investigated first focusing on STAT1, which is known to play a major role on type I and II IFN signalling.<sup>112,111</sup> Western Blot analysis showed that both IFN-α and IFN-γ promoted STAT1 phosphorylation at different sites at early time points (0-60 min) (**Figure 3A-B**). In addition, IFN-γ strongly induced STAT1 activation at 24 h, with further potentiation in combination with LPS (**Figure 3C**).



**Figure 3. Interferons promote STAT1 phosphorylation with further potentiation by LPS.** Control VIC from male patients were stimulated with the indicated ligands for 0-60 min (A-B) or 24h (C). Cell lysates were analysed by Western Blot for STAT1 phosphorylation using antibodies specific for the serine 727 and tyrosine 701 phosphorylation sites. Representative blots and corresponding densitometric analysis;  $n \geq 4$ . Doses, n, statistics, and symbols as in Figure 2.

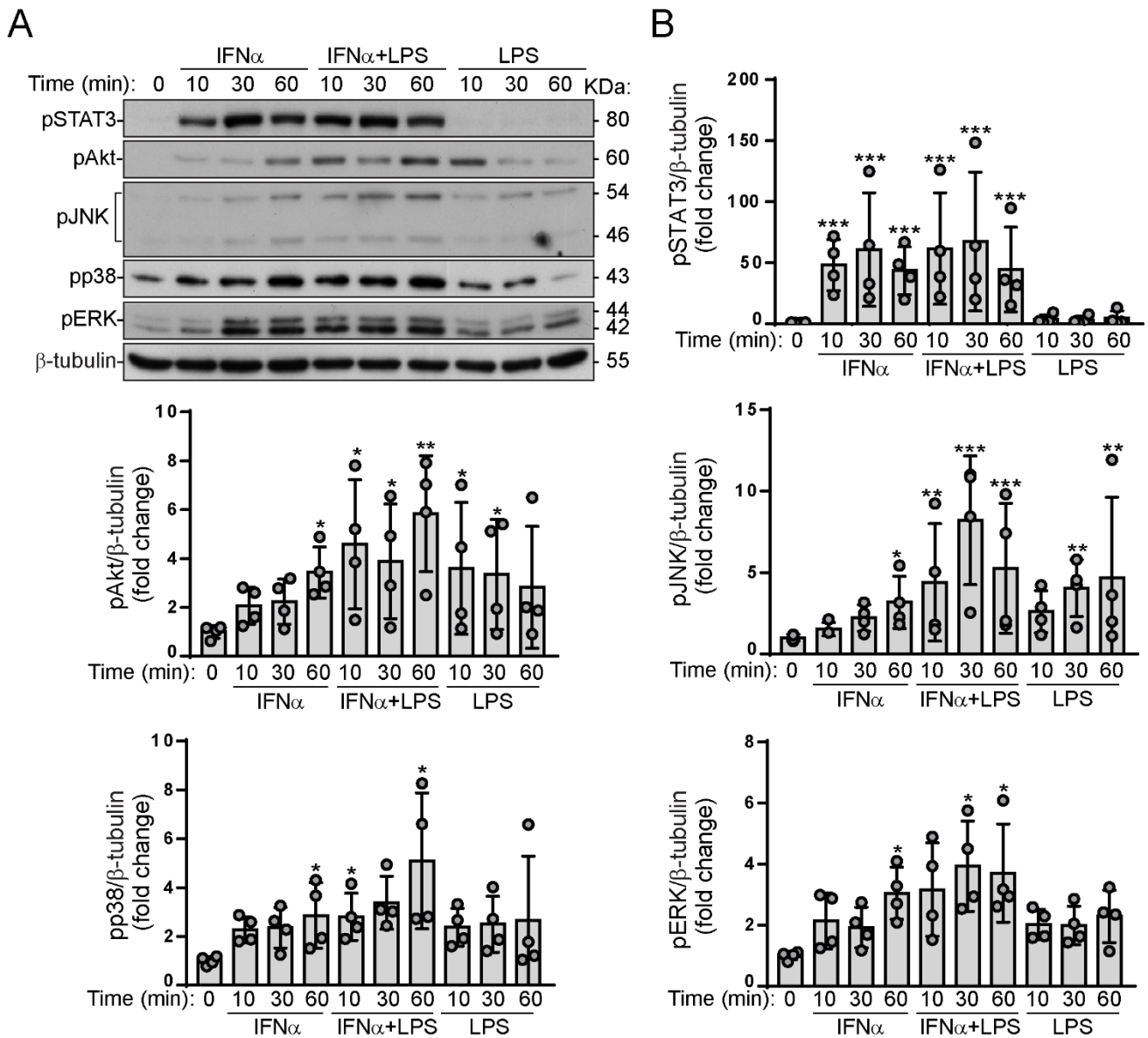
To further examine the activation of NF- $\kappa$ B-p65 and STAT1 transcription factors in stimulated VIC, we explored their nuclear translocation by analysing nuclear and cytoplasmic extracts. These experiments revealed that both transcription factors were present in the nucleus upon combined treatment of either IFN- $\alpha$  (**Figure 4A**) or IFN- $\gamma$  (**Figure 4B**) combined with LPS. Remarkably, pre-treatment with ruxolitinib, a JAK inhibitor,<sup>180</sup> abrogated the IFN+LPS-induced translocation of both transcription factors (**Figure 4A-B**).



**Figure 4. Interferons combined with LPS promote STAT1 and NF- $\kappa$ B translocation.** (A-B) Control VIC from males were stimulated with the indicated ligands and nuclear and cytoplasmic extracts were analysed by Western Blot. Representative blots after IFN- $\alpha$ +LPS (A) or IFN- $\gamma$ +LPS (B) treatment; n=3. Doses and n as in Figure 2. Ruxo indicates 6  $\mu$ M ruxolitinib; HisH3, histone-H3, used as nuclear loading control.

Finally, we explored additional pathways related to IFN and TLR signalling. Western blot analysis showed that IFN- $\alpha$  also promoted the early activation of STAT3 (**Figure 5**), a transcription factor with intriguing context-dependent effects given its reported role as promotor of tumour growth,<sup>126</sup> whereas it has cardioprotective effects.<sup>181</sup> In addition, IFN- $\alpha$  was also able to activate protein kinase B (Akt), a survival-promoting kinase whose activation triggers extracellular matrix deposition and whose overexpression prevents calcification in the valve context.<sup>182,100</sup> Moreover, results disclosed the early activation of the MAPK p38, ERK, and JNK (**Figure 5**), which have been associated to VIC calcification.<sup>183,166</sup>

Likewise, IFN- $\gamma$  induced the early activation of STAT3, Akt and MAPK p38, ERK, and JNK (**Figure 6**). It is noteworthy that LPS did not activate IFN-related transcription factors such as STAT1 (**Figure 3**) and STAT3 (**Figures 5-6**). Collectively, data demonstrate the IFN-mediated activation of several intracellular signalling routes in VIC.



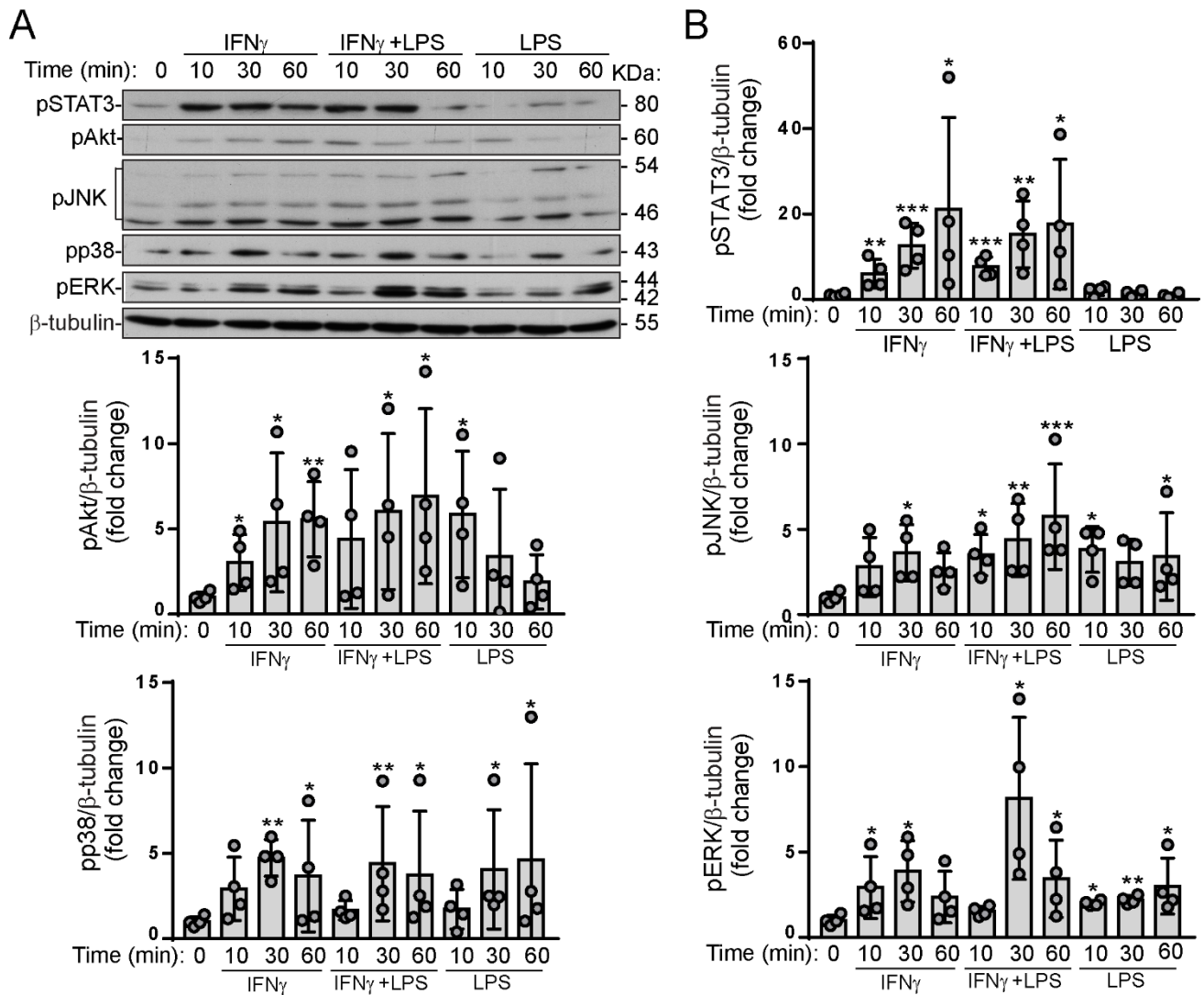


**Figure 6. Additional signalling pathways activated by IFN- $\gamma$  and LPS in VIC.** Control male VIC were stimulated with the indicated ligands and whole cell extracts were analysed by Western Blot. (A) Representative blots for the indicated proteins; n=4. (B) Densitometric analysis corresponding to the phosphorylation of STAT3, Akt, ERK, JNK and p38. Doses, statistics, n, and symbols as in Figure 2.

### R.1.3-IFN cooperate with LPS to induce a pro-inflammatory phenotype in VIC

Next, we sought to determine the effects of the IFN-mediated activation of NF- $\kappa$ B and STAT on downstream inflammatory molecules with a reported role on CAVD.<sup>56</sup> Our group previously described that VIC secrete considerable amounts of IL-6 and IL-8 upon TLR4 activation with LPS.<sup>164</sup> In the present study, ELISA analysis revealed that IFN- $\alpha$  and IFN- $\gamma$  slightly induced IL-6 (Figure 7A) but not IL-8 secretion in VIC (Figure 7B). Conversely, both IFN potentiated the LPS-induced secretion of IL-6 and IL-8 (Figure 7A-B). Strikingly, statistical analysis revealed unexpected sex-differences in IL secretion in response to LPS alone or combined with IFN- $\alpha$  (Figure 7A-B, left panels).

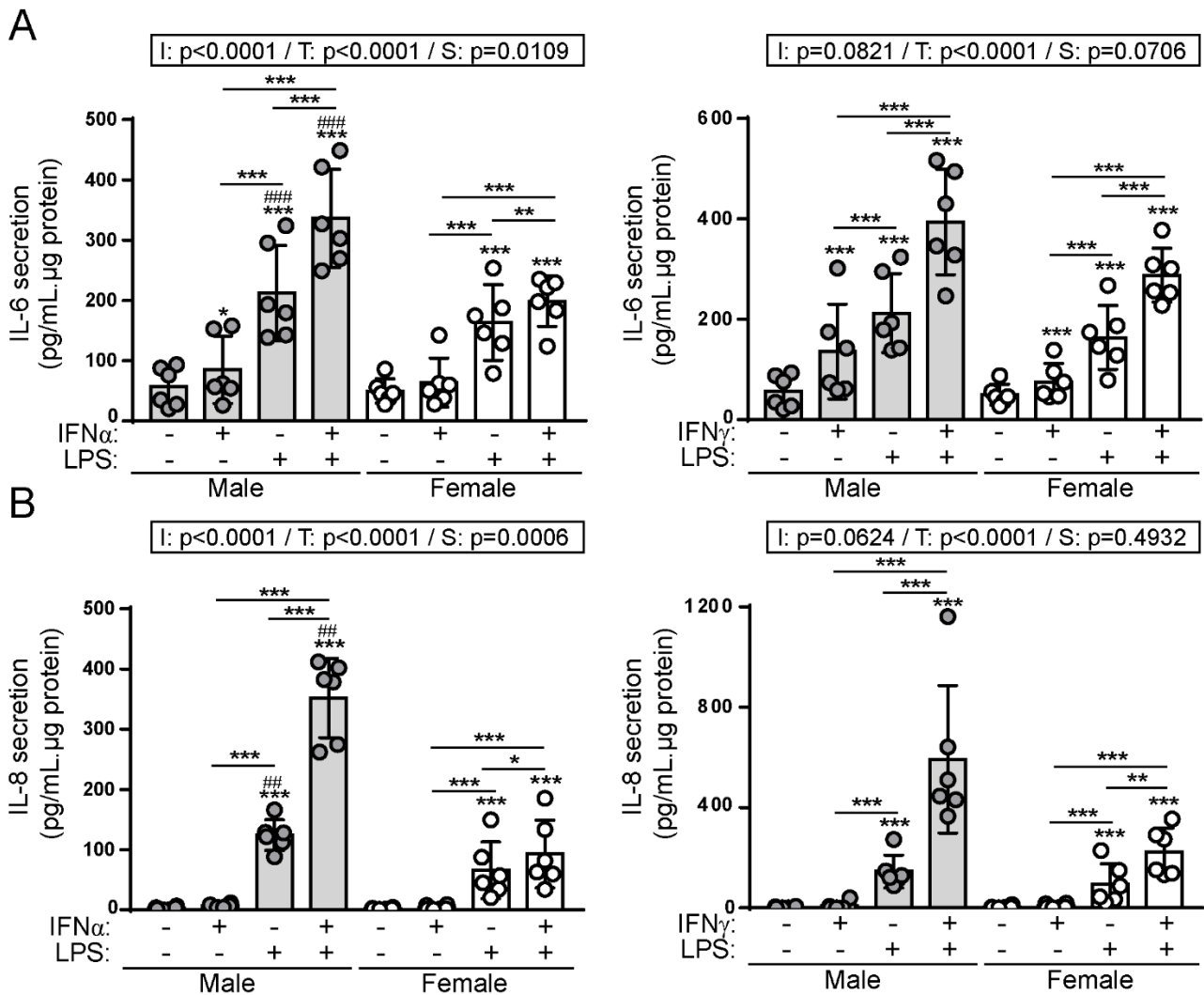


**Figure 7. Interferons enhance the LPS-induced secretion of IL-6 and IL-8 in VIC.** Control male and female VIC were treated with the indicated ligands for 24 h and supernatants collected to assay cytokine secretion by ELISA. (A) IL-6 secretion upon treatment; n=6. (B) IL-8 secretion upon treatment; n=5. Data were normalized to total protein content in each sample. Grey dots and bars, control male AVIC; white dots and bars, control female VIC. IFN $\alpha$  refers to 100 ng/mL IFN- $\alpha$ ; IFN $\gamma$ , 100 ng/mL IFN- $\gamma$ , LPS, 1  $\mu$ g/mL LPS. \* indicates statistical significance compared to the corresponding untreated conditions or as indicated by the line below. # indicates statistical significance compared to the same treatment of the other group. \* $\#$ P<0.05, \*\* $\#$ P<0.01, \*\*\* $\#$ P<0.001. Two-way ANOVA statistics are shown on the box above each plot: I indicates interaction; T, treatment; S, sex. n indicates the number of independent pairs of male/female VIC isolates from different donors.

Additionally, we evaluated adhesion molecule expression because the serum levels of ICAM-1 and VCAM-1 are increased in patients with non-rheumatic valve disease.<sup>184</sup> Immunoblot experiments revealed that VIC stimulation with IFN- $\alpha$  and IFN- $\gamma$  triggered ICAM-1 and VCAM-1 protein expression at 24 h. Strikingly, co-treatment with LPS resulted in a greater induction of adhesion molecule expression (**Figure 8A-C**). Moreover, statistical analysis revealed that, in contrast to IL secretion, no significant differences on adhesion molecule expression were found when comparing cells from males and females (**Figure 8B-C**).

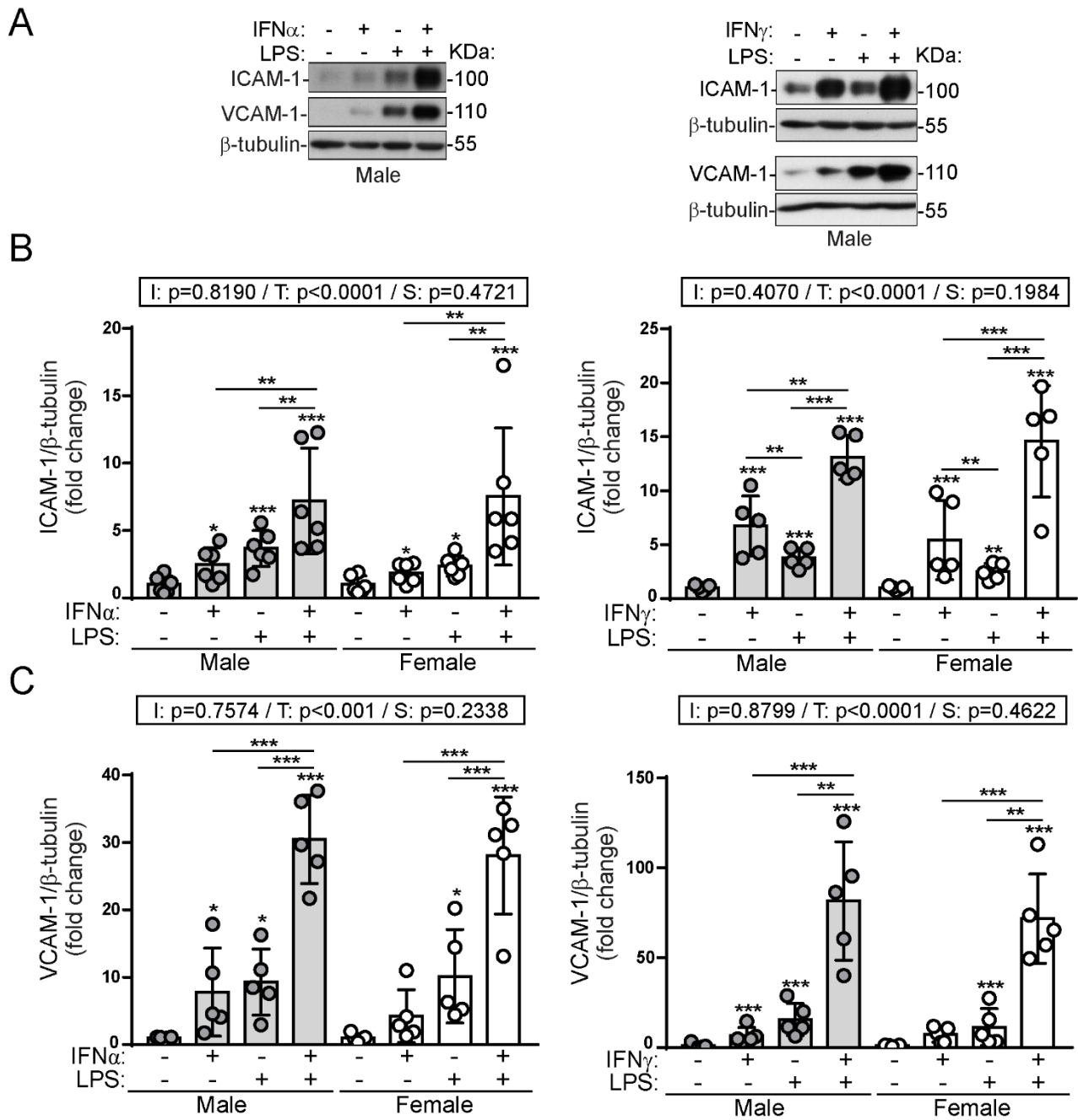


**Figure 8. Interferons induce adhesion molecule expression with further potentiation by LPS in VIC.** Control male and female VIC were treated with the indicated ligands for 24 h and whole cell lysates were analysed by Western Blot. (A) Representative blots of ICAM-1 and VCAM-1 protein levels in male cells. (B) Densitometric analysis of ICAM-1 expression for IFN- $\alpha$  (left panel, n=6) and IFN- $\gamma$  (right panel, n=5) in cells from males and females. (C) Densitometric analysis of VCAM-1 expression; n=5. Each pair of male and female VIC were analysed in the same blot. Doses, symbols, n, and statistics were as in Figure 7.

To further examine the role of IFN and the interplay with LPS on inflammation, we explored the secretion of inflammatory lipid mediators such as prostaglandin E<sub>2</sub>, which is induced upon TLR3/4 activation of human VIC.<sup>164</sup> ELISA analysis confirmed previous data demonstrating LPS-mediated induction of PGE<sub>2</sub> secretion and further disclosed that IFN did not promote PGE<sub>2</sub> secretion

but strongly potentiated the LPS-induced effect (**Figure 9**). No statistical differences among male and female cells in PGE<sub>2</sub> secretion were observed.

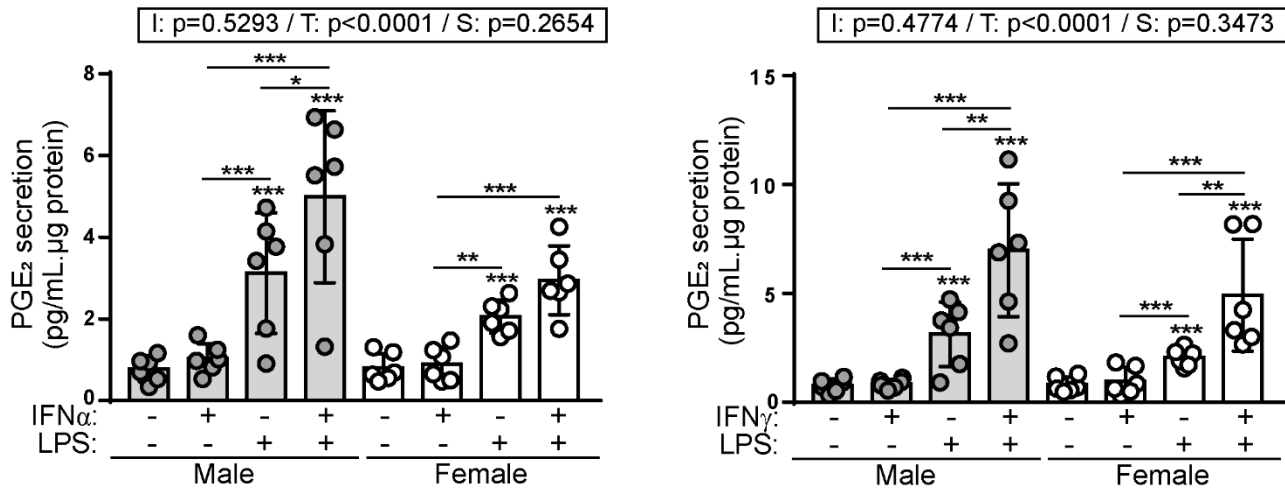


**Figure 9. Interferons enhance the LPS-induced secretion of PGE<sub>2</sub>.** Control male and female VIC were treated with the indicated ligands for 24 h and supernatants collected to assay PGE<sub>2</sub> secretion; n=6. Doses, symbols, n, and statistics were as in Figure 7.

Additionally, because fibrosis is another major mechanism of CAVD,<sup>43</sup> we explored whether IFN induce the secretion of matrix remodelling molecules such as MMP-1. The analysis of supernatants from activated VIC showed that neither IFN nor LPS alone induced MMP-1 secretion. Conversely, MMP-1 secretion was detected upon co-stimulation with both agents (**Figure 10**), suggesting an IFN-LPS interplay on matrix remodelling molecules. Moreover, the IFN- $\alpha$  and LPS interplay exhibited a sex-differential response, since the secretion of MMP-1 was only significant in male cells (**Figure 10, left panel**). In contrast, the combination of IFN- $\gamma$ -LPS did not show significant sex-differences (**Figure 10, right panel**).

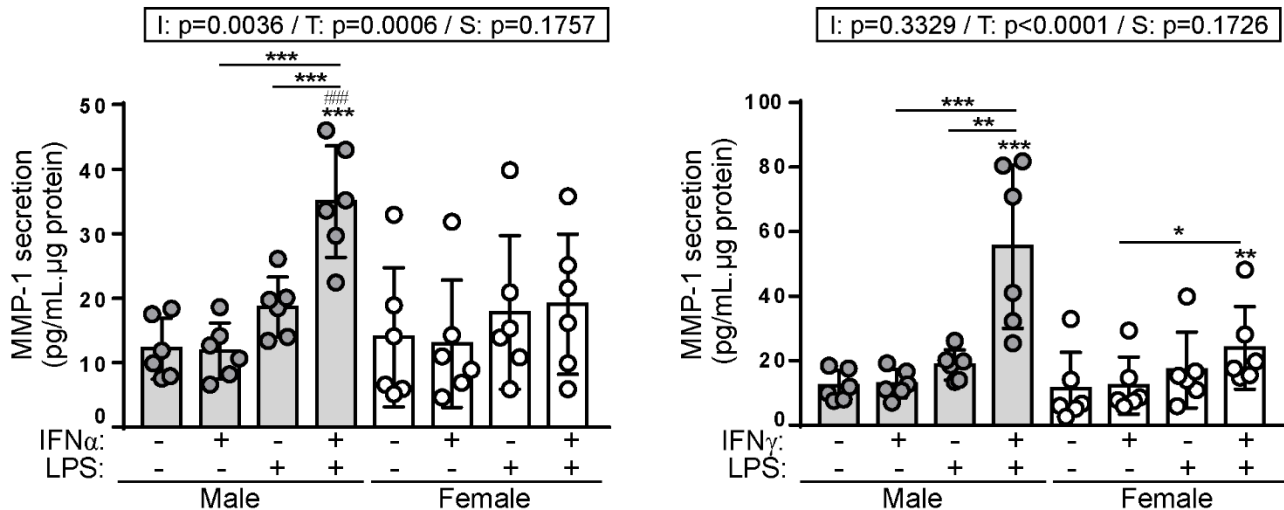


**Figure 10. Interferons and LPS cooperate to induce MMP-1 secretion.** Control male and female VIC were treated with the indicated ligands for 24 h and supernatants were collected to assay MMP-1 secretion; n=6. Doses, symbols, n and statistics were as in Figure 7.

To elucidate the signalling routes that control the interplay in inflammation among IFN and LPS, cells were pre-treated with different pharmacologic inhibitors of IFN, TLR, PI3K and MAPK pathways. Collectively, data disclosed a complex regulation of both adhesion molecule expression and IL secretion in VIC. The responses mediated by IFN- $\alpha$ +LPS were abrogated by JAK inhibitors (ruxolitinib and tofacitinib) as well as by different MAPK and Akt inhibitors (**Figure 11A-B**). Additionally, TLR signalling also played a role on VCAM-1 expression and IL-6/8 secretion since an antagonist of Lipid A activation of TLR4, CAY10614, blocked these responses (**Figure 11A-B**). Likewise, TLR and JAK signalling were significantly involved in IFN- $\gamma$ +LPS responses since not only Jakinibs, but also CAY10614, abrogated the effects (**Figure 12A-B**). Other pathways, such as MAPK and Akt were also involved in pro-inflammatory molecule expression upon IFN- $\gamma$ +LPS stimulation (**Figure 12A-B**).

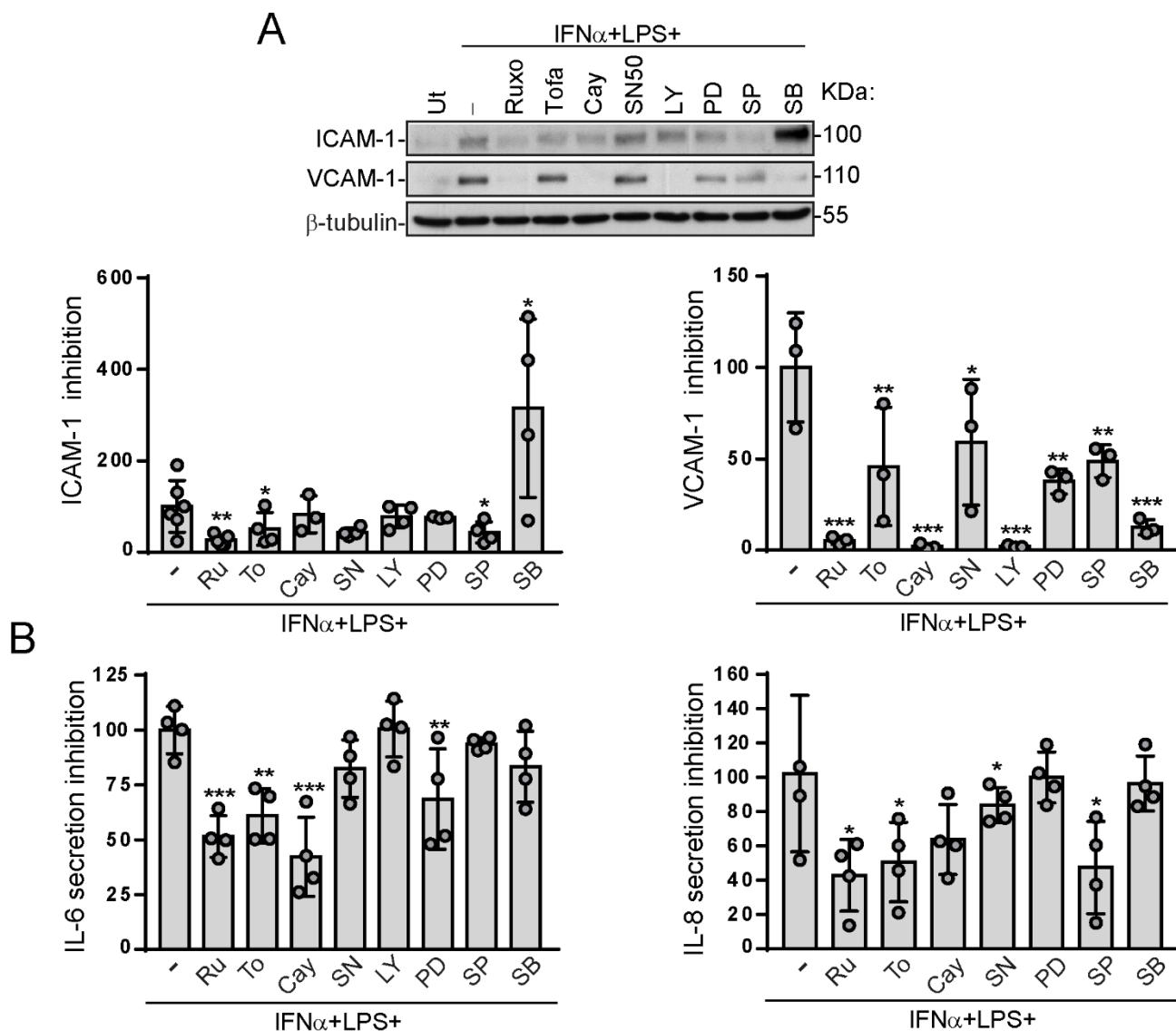
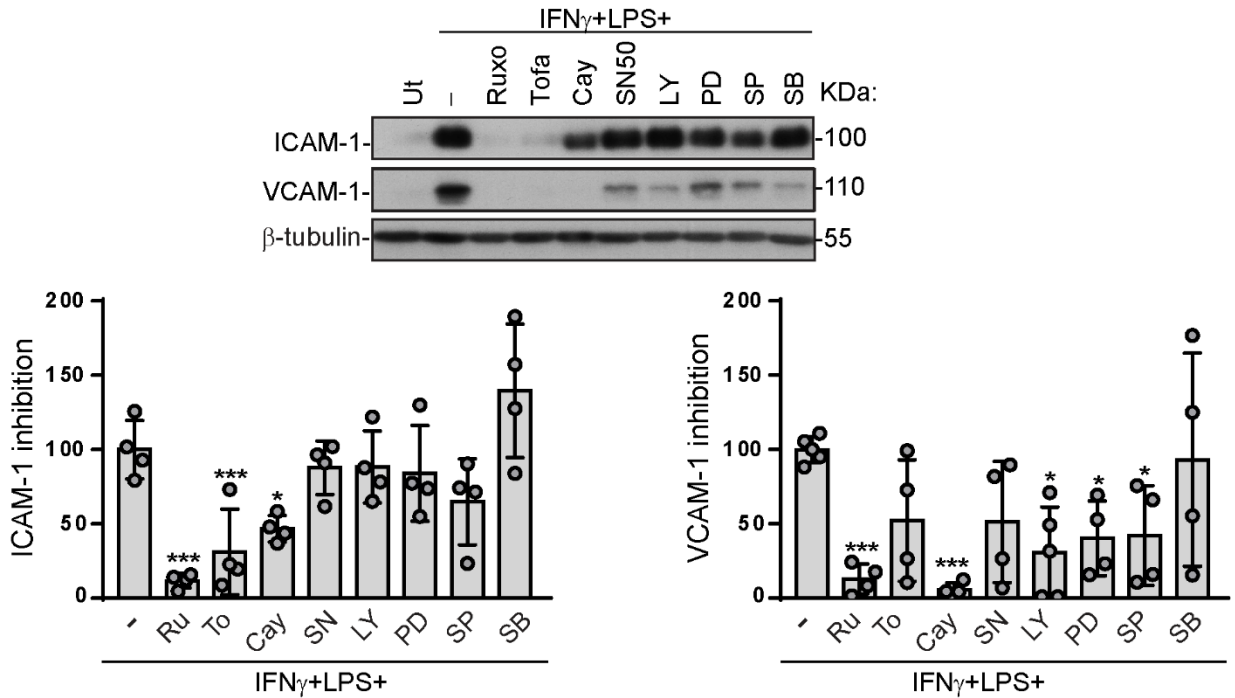


**Figure 11. Signalling routes involved on the IFN- $\alpha$ +LPS-mediated induction of pro-inflammatory molecules.** Control male VIC were pre-treated for at least 45 minutes with the indicated inhibitors and then activated for 24 h. Whole cell lysates were analysed by Western blot and supernatants by ELISA. (A) Representative image and densitometric analysis of ICAM-1 and VCAM-1 expression; n=3-4. (B) Supernatants were analysed for the secretion of IL-6 and 8 by ELISA; n=3-4. Data were normalized to IFN- $\alpha$ +LPS value (100%). Cay indicates 5  $\mu$ M CAY10614; LY, 50  $\mu$ M LY294002; PD, 50  $\mu$ M PD98059; Ruxo/Ru, 6  $\mu$ M ruxolitinib; SB, 10  $\mu$ M SB203580; SN50, 50  $\mu$ g/ml NF- $\kappa$ B SN50; SP, 10  $\mu$ M SP600125; Tofa, 6  $\mu$ M tofacitinib. Ut, untreated conditions. Doses, statistics, n and symbols as in Figure 2.

A



B

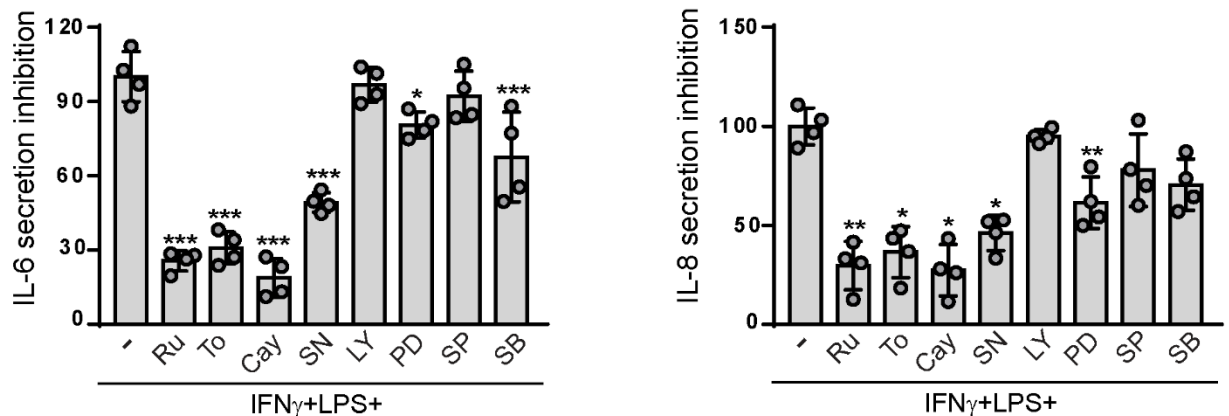


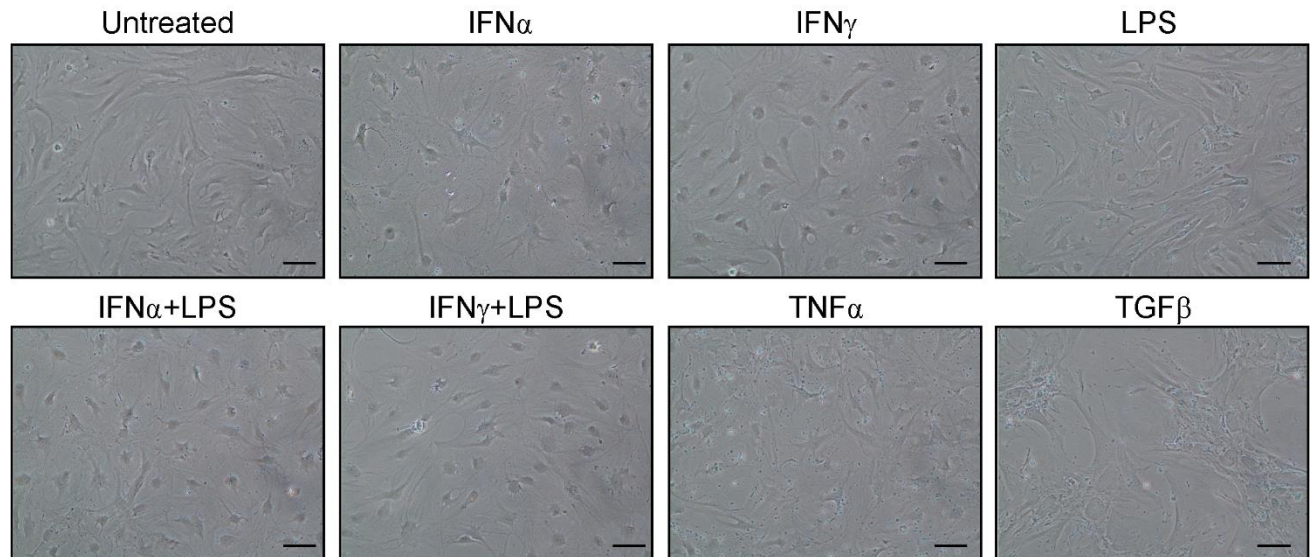
**Figure 12. Signalling routes involved on the IFN- $\gamma$ +LPS-mediated induction of pro-inflammatory molecules.** Control male VIC were pre-treated for at least 45 minutes with the indicated inhibitors and then activated for 24 h. Whole cell lysates were analysed as in Figure 11. (A) Representative image and densitometric analysis of ICAM-1 and VCAM-1 expression; n=4. (B) Secretion of IL-6 and IL-8; n=4. Data were normalized to IFN- $\gamma$ +LPS value (100%). Inhibitor/antagonist abbreviations and doses were as in Figure 11. Statistics, n, and symbols were as in Figure 2.

### R.1.4-IFN drive VIC differentiation towards a pro-osteogenic phenotype

Nowadays it is widely accepted that inflammation triggers pro-osteogenic responses in resident valve cells.<sup>57,56,41,82</sup> On this basis, we explored whether IFN can induce pro-calcifying responses in VIC. Our experiments showed that 12 days treatment of cells with IFN promoted marked morphological changes, characterized by a prominent nuclei and round shape. We used TNF- $\alpha$  and TGF- $\beta$  as controls for cell differentiation (**Figure 13A**). Given that IFN are well known

regulators of cell cycle and cell differentiation, we therefore explored VIC proliferation by using the MTT assay. Formazan formation at 12 days showed that IFN-treated cells exhibited reduced growth, whereas LPS-treated or untreated cells proliferated at a normal rate (**Figure 13B**).

**A**



**B**

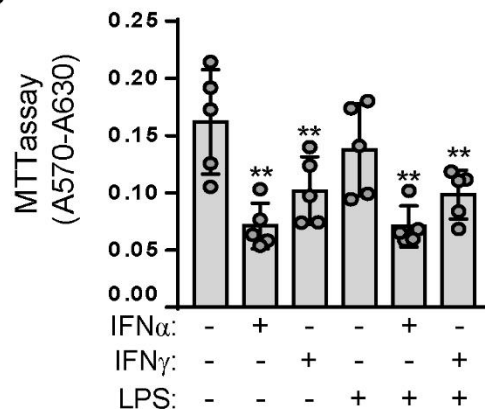


**Figure 13. Interferons promote morphological changes and exert anti-proliferative effects in VIC.** (A) Confluent male cell cultures were treated for 12 d replacing medium and stimuli every 3 d. Microscopic images were taken to visualize cell morphology. Representative microphotographs of n=5. Black line indicates 50  $\mu$ m. (B) Non-confluent cell cultures were grown for 12 d, replacing medium and stimuli every 3 days, and cell viability was tested by MTT assay as indicated in Methods; n=5. Doses, statistics, n, and symbols were as in Figure 2.

Considering these findings, we sought to explore whether IFN induce VIC differentiation towards a pro-calcifying phenotype. The gene expression profile for pro- and anti-osteogenic molecules was checked. As shown in **Figure 14A**, the exposure of VIC to both IFN- $\alpha$  and IFN- $\gamma$  as well as to LPS induced a marked increase in the expression of *Bone sialoprotein-2 (IBSP)*, an osteoblastic extracellular matrix gene upregulated in CAVD.<sup>185</sup> In addition, the mRNA levels of the anti-calcifying gene *Matrix-Gla protein (MGP)*<sup>102</sup> were also downregulated upon IFN and LPS

treatment (**Figure 14B**). Intriguingly, in both cases, cells from males showed an increased pro-osteogenic phenotype as compared to cells isolated from female donors (**Figure 14A-B**).

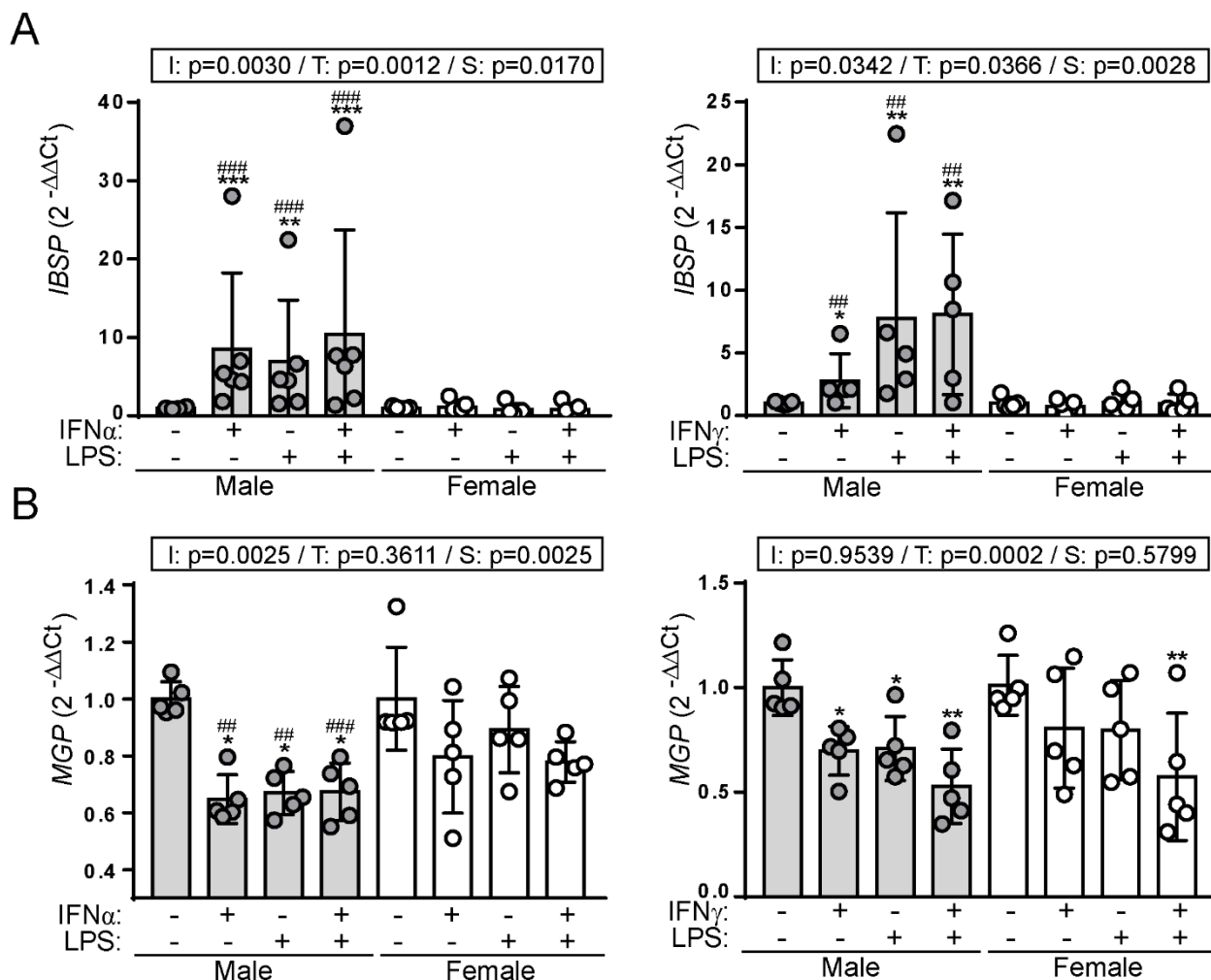


**Figure 14. Interferons induce a pro-osteogenic phenotype in VIC.** Control male and female VIC were treated with the indicated ligands for 24 h and mRNA was analysed by RT-qPCR. (A) *IBSP* transcript levels. (B) *MGP* mRNA levels; n=5. Doses, symbols, n, and statistics were as in Figure 7.

### R.1.5-IFN and LPS induce VIC calcification to a higher extent in male cells

Our next step was to study whether the stimulation with IFN promoted VIC calcification. For this purpose, a calcifying medium based on high phosphate and low serum concentrations was used as previously described.<sup>176</sup> *In vitro* calcification was evaluated by Alizarin Red staining (ARS) of calcific nodules and by assaying calcium deposits. Notably, both IFN- $\alpha$  and LPS induced calcific nodule formation and calcium deposition upon 21 days of treatment (**Figure 15A-C**). Moreover, these effects were potentiated when both stimuli were combined. Interestingly, and consistent with

sex differences on osteogenic molecule induction (**Figures 14**), male cells exhibited significantly higher levels of calcification than female cells (**Figure 15A-C**).

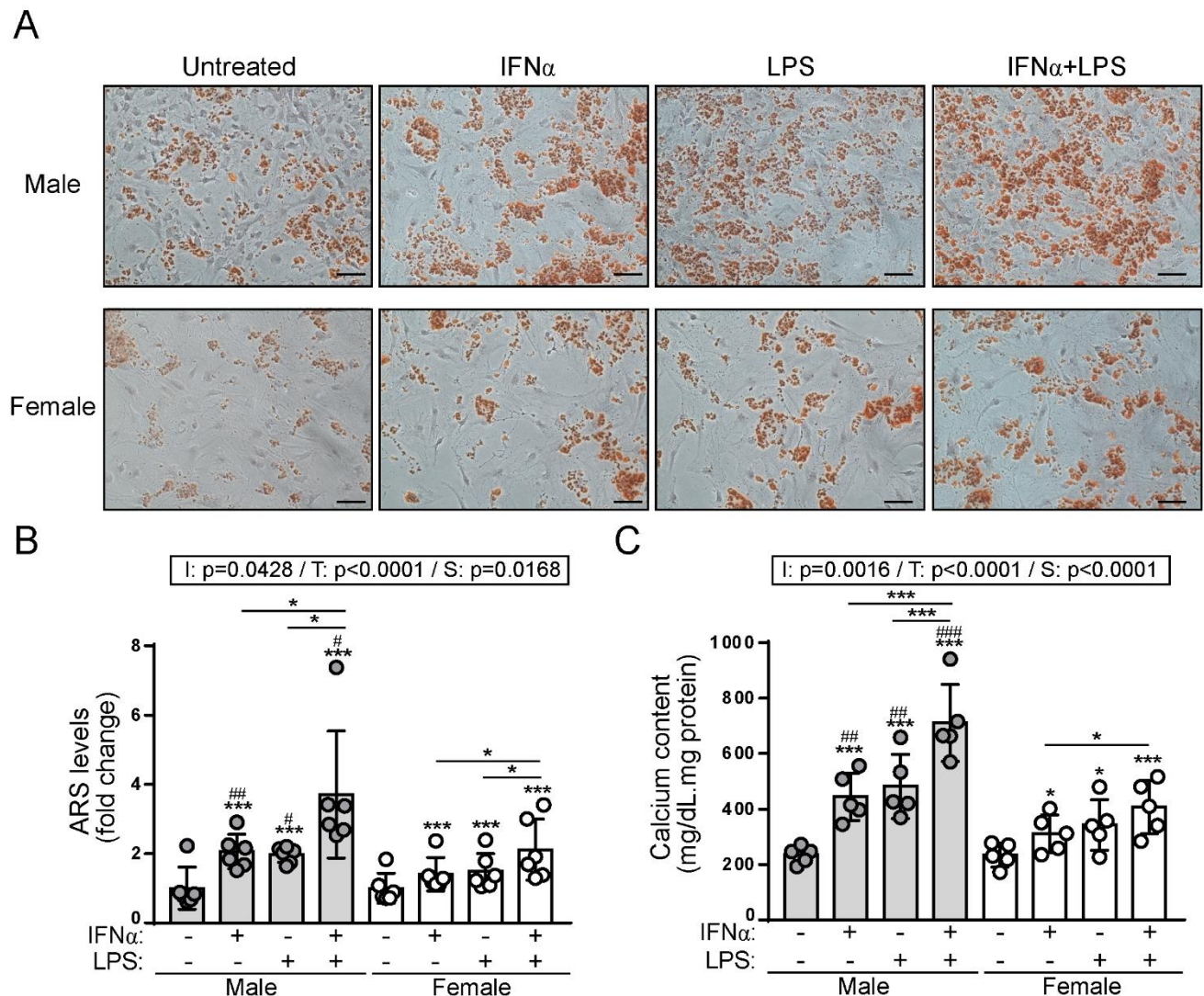


**Figure 15. IFN- $\alpha$  and LPS promote VIC calcification to a higher extent in cells from males.** Control male and female VIC were treated with the indicated ligands for 21 days in calcification medium containing 3 mmol/L of Pi and 1% FBSi and calcification was assessed by two methods. (A-B) Representative images of alizarin red staining (ARS) (A), and ARS levels, expressed as fold increase as compared to untreated conditions (B); n=6. (C) Calcium content evaluated using a commercial kit was normalized to total protein content; n=5. Doses, statistics, n, and symbols as in Figure 7.

Next, we sought to investigate the effects of IFN- $\gamma$  on VIC calcification. ARS and calcium quantification demonstrated that IFN- $\gamma$  also induce significant VIC calcification after 14 days of treatment. To note, IFN- $\gamma$ +LPS combination strongly potentiated VIC calcification. In keeping with IFN- $\alpha$  data, significant sex-differences for IFN- $\gamma$ -induced calcification were found (**Figure 16A-C**). Collectively, these findings demonstrate a pro-osteogenic role of IFN in VIC with sex differences in the response.

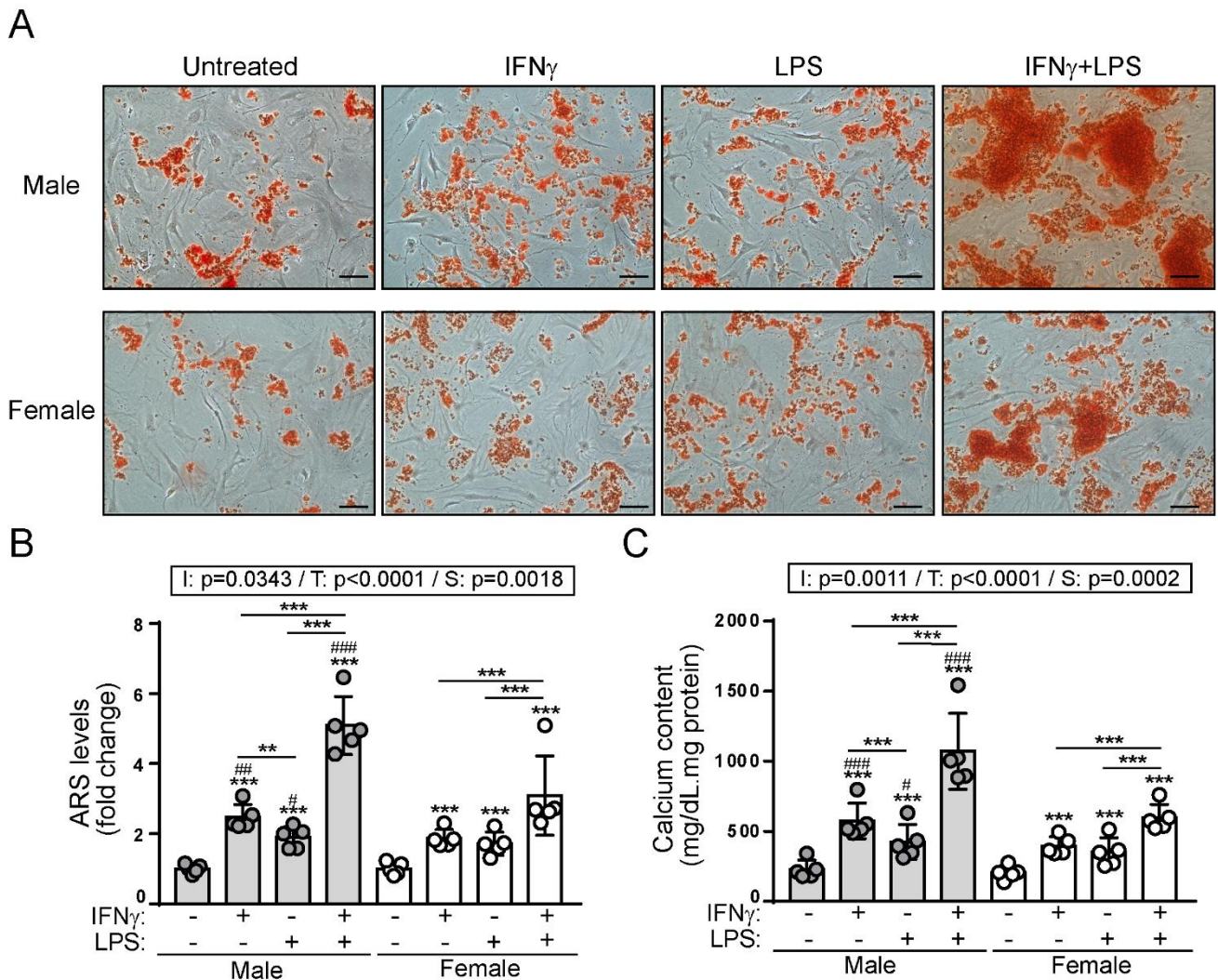


**Figure 16. IFN- $\gamma$  and LPS induce VIC calcification to a higher extent in cells from males.** Control male and female VIC were treated with the indicated ligands for 14 days in calcification medium and analysed as in Figure 15. (A-B) Representative microphotographs (A) and staining level quantitation of ARS (B); n=5. Black line indicates 50  $\mu$ m. (C) Calcium deposition quantification was normalized to total protein content; n=5. Doses, statistics, n and symbols were as in Figure 7.

To investigate whether IFN-induced calcification was receptor-mediated and could be pharmacologically targeted, we used Jakinibs, which reduced the IFN+LPS-induced inflammation (**Figures 11-12**). VIC were pre-treated with tofacitinib and ruxolitinib before stimulation in calcifying medium. Notably, the JAK1/TYK2 inhibitor tofacitinib dramatically reduced calcification in cells treated with either IFN- $\alpha$  alone or combined with LPS (**Figure 17A-C**).

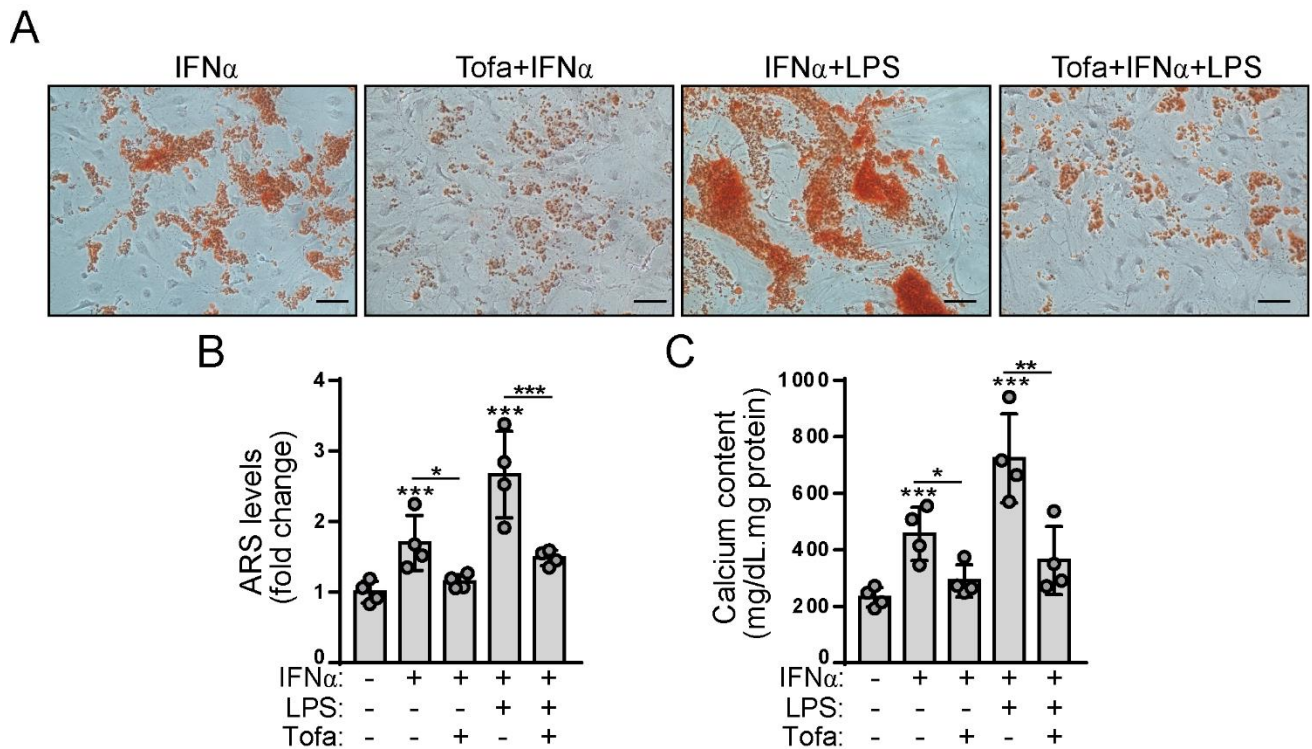


**Figure 17. Tofacitinib dramatically decreases IFN- $\alpha$ -induced calcification.** (A-C) Control male VIC were pre-treated or not with tofacitinib, stimulated for 21 days in calcifying medium and analysed as in Figure 15. (A-B) Representative microphotographs of ARS (A) and ARS quantitation (B). Black line indicates 50  $\mu$ m. (C) Calcium deposition; n=4 VIC. Tofa indicates 6  $\mu$ M tofacitinib. Doses, statistics, n, and symbols as in Figure 2.

Likewise, the pre-treatment with the JAK1/2 inhibitor ruxolitinib strongly decreased both nodule formation and calcium deposition induced by IFN- $\gamma$  alone and in combination with LPS (**Figure 18A-C**). Together, data revealed that IFN-mediated calcification of VIC can be pharmacologically blocked by Jakinibs currently used in therapy.

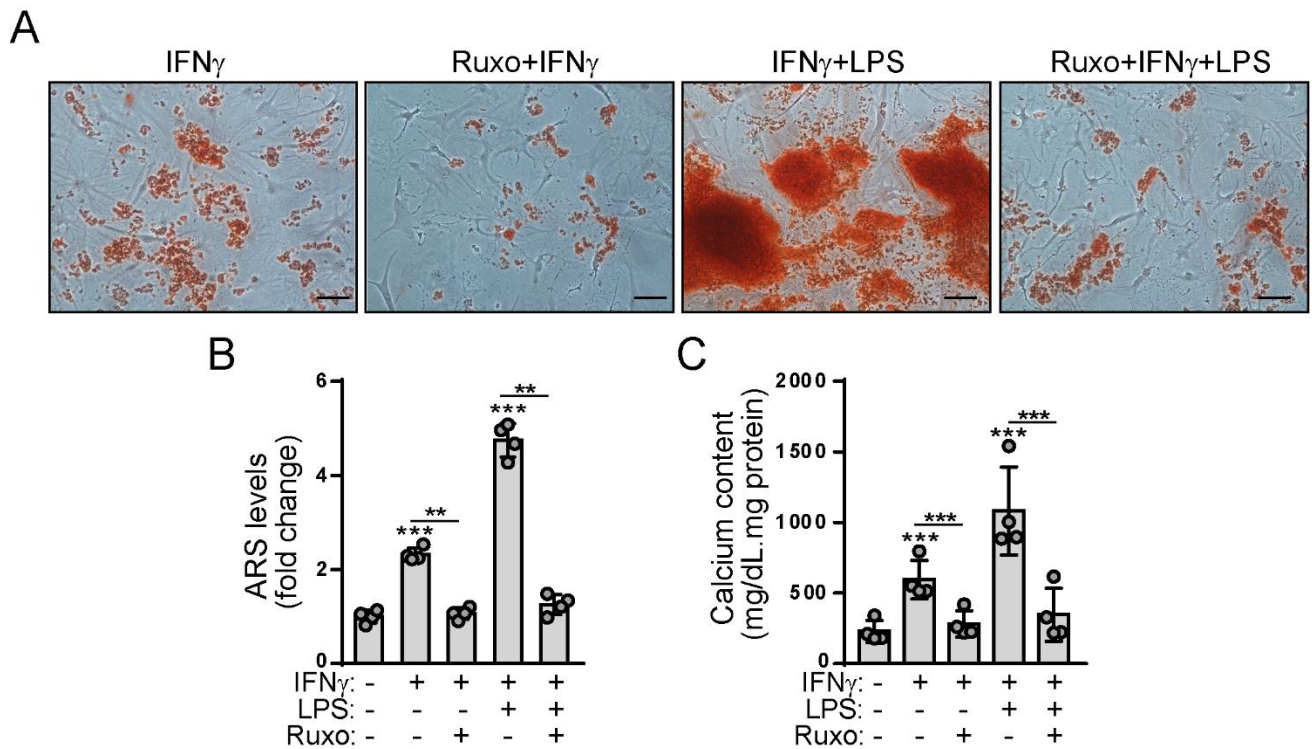


**Figure 18. Ruxolitinib markedly decreases IFN- $\gamma$ -induced calcification.** (A-C) Control male VIC were pre-treated or not with ruxolitinib and stimulated for 14 days in calcifying medium and analysed as in Figure 15. (A-B) Representative microphotographs (A) and quantitation of ARS (B); n=4. Black line indicates 50  $\mu$ m. (C) Calcium deposition quantification; n=4. Ruxo indicates 6  $\mu$ M ruxolitinib. Doses, statistics, n, and symbols as in Figure 2.

The next aim was to explore the mechanisms leading to IFN-mediated calcification under high-phosphate conditions. It is known that both osteogenic and dystrophic calcification play a role on phosphate-induced calcification of vascular cells.<sup>186,187</sup> A potential role for dystrophic osteogenesis in VIC calcification was explored by assessing apoptosis and necrosis by flow cytometry. Data showed that not IFN- $\alpha$  neither LPS alone induced VIC apoptosis. However, both stimuli together significantly increased cell death. Strikingly, sex-differences were observed for IFN- $\alpha$ +LPS treatment, given that it increased apoptosis only in male VIC (**Figure 19A-B**).

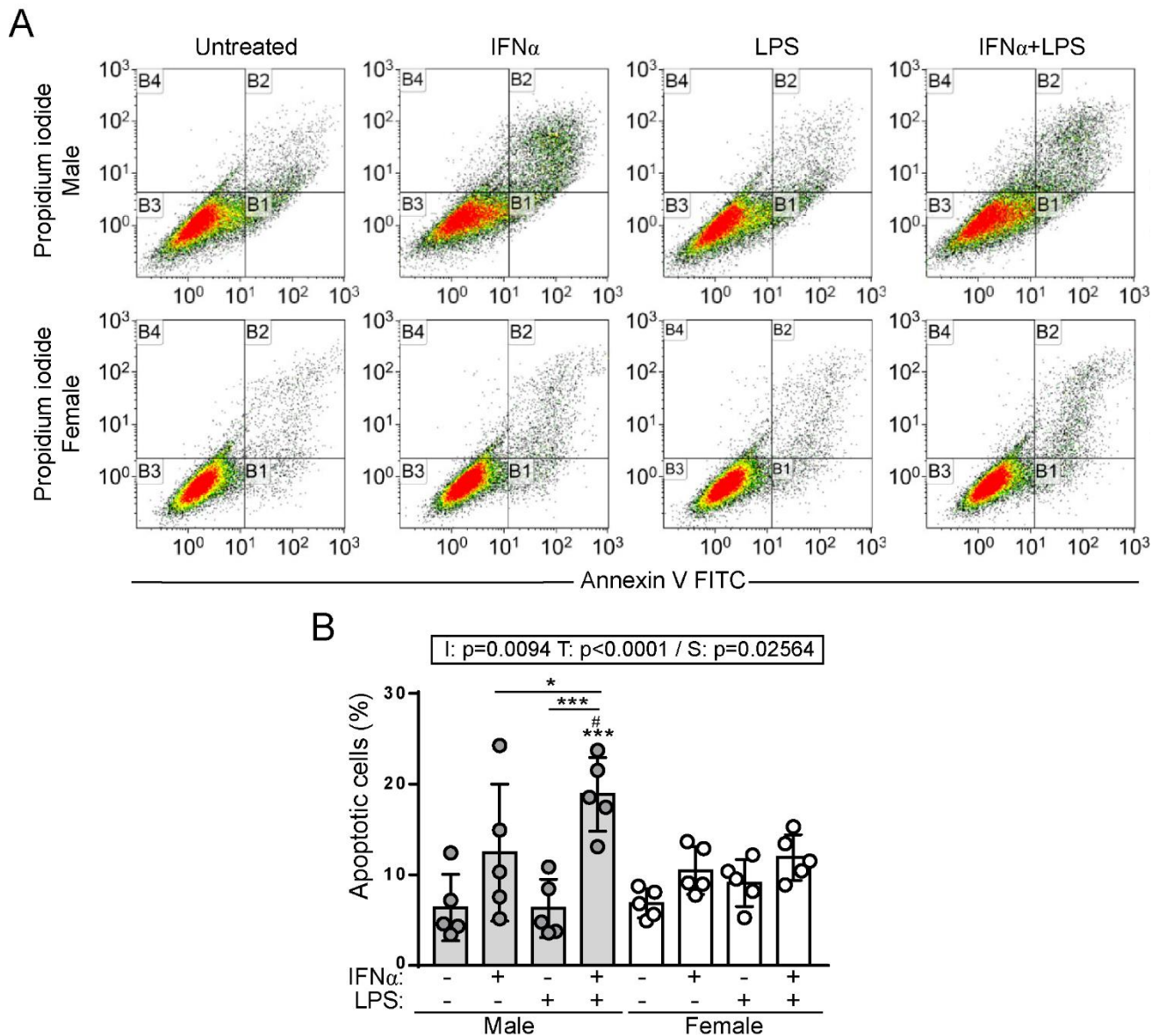


**Figure 19. IFN- $\alpha$  and LPS combination induces apoptosis in male VIC.** Male and female VIC were treated for 7 days in calcifying medium and then analysed by flow cytometry for Annexin V-FITC and propidium iodide staining. (A) Representative flow cytometry plot. (B) Statistical analysis of apoptotic cells counts (B1+B2 quadrants);  $n=5$ . Doses, statistics,  $n$ , and symbols as in Figure 7.

Conversely, under the same conditions, IFN- $\gamma$  alone and together with LPS statistically increased apoptosis in male and female VIC, although a higher effect was found for IFN- $\gamma$  in male cells (**Figure 20A-B**). Finally, Jakinibs significantly decreased IFN-induced apoptosis in male cells (**Figure 21A-B**). Collectively, data suggest a role for apoptosis in IFN-mediated calcification.

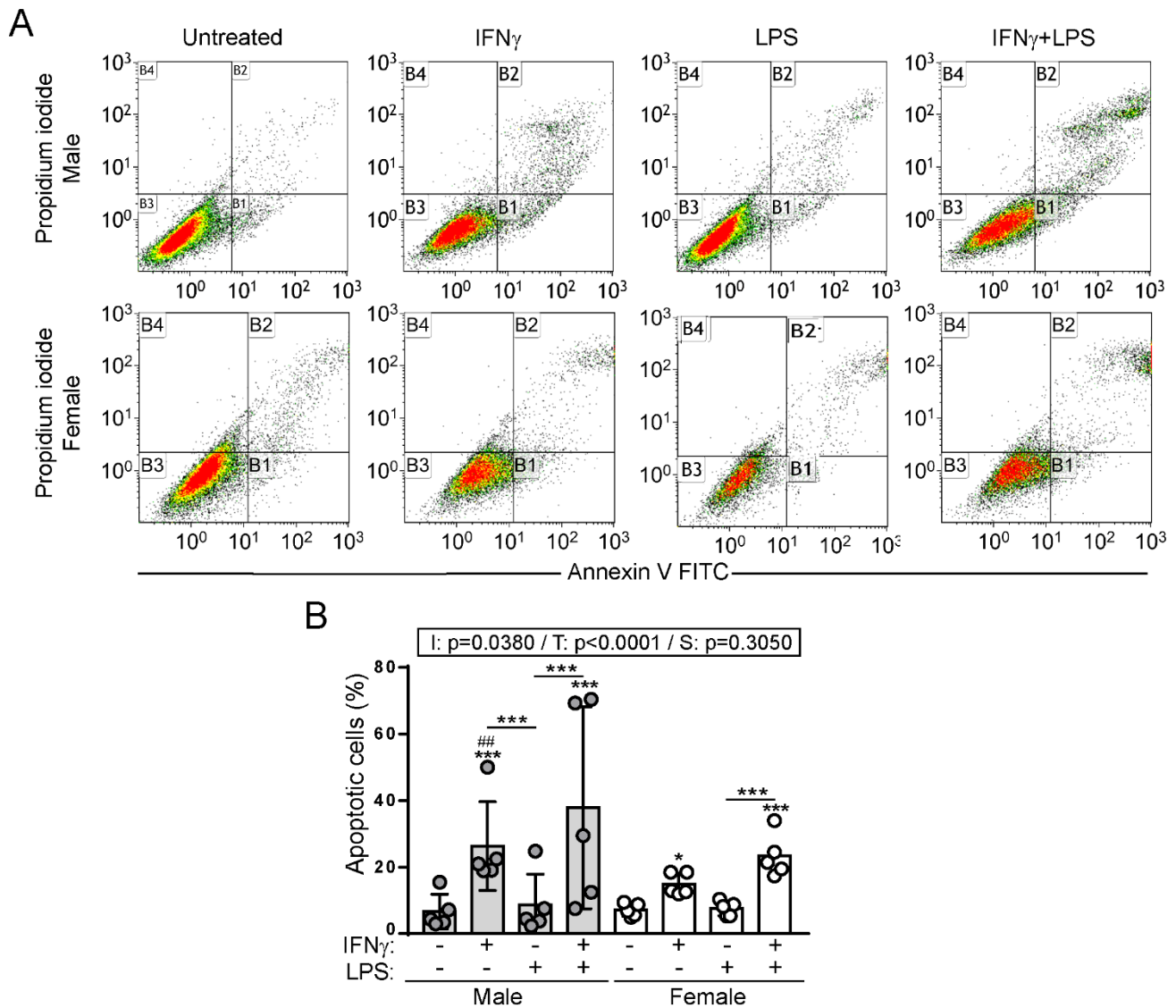


**Figure 20. IFN- $\gamma$  alone and together with LPS induces apoptosis in male and female VIC.** Male and female VIC were cultured and treated for 7 days in calcifying medium and then analysed by flow cytometry for Annexin V-FITC and propidium iodide staining. (A) Representative flow cytometry plot. (B) Statistical analysis of apoptotic cells counts (B1+B2 quadrants);  $n=5$ . Doses, statistics,  $n$ , and symbols as in Figure 7.

To note, calcification assays (**Figures 15-16**) and flow cytometry analysis (**Figures 19-20**) revealed similar responses in cells from both sexes in the absence of stimulus, thus suggesting a major role for IFN and LPS, but not for Pi, in the induction of the sex-differential responses.

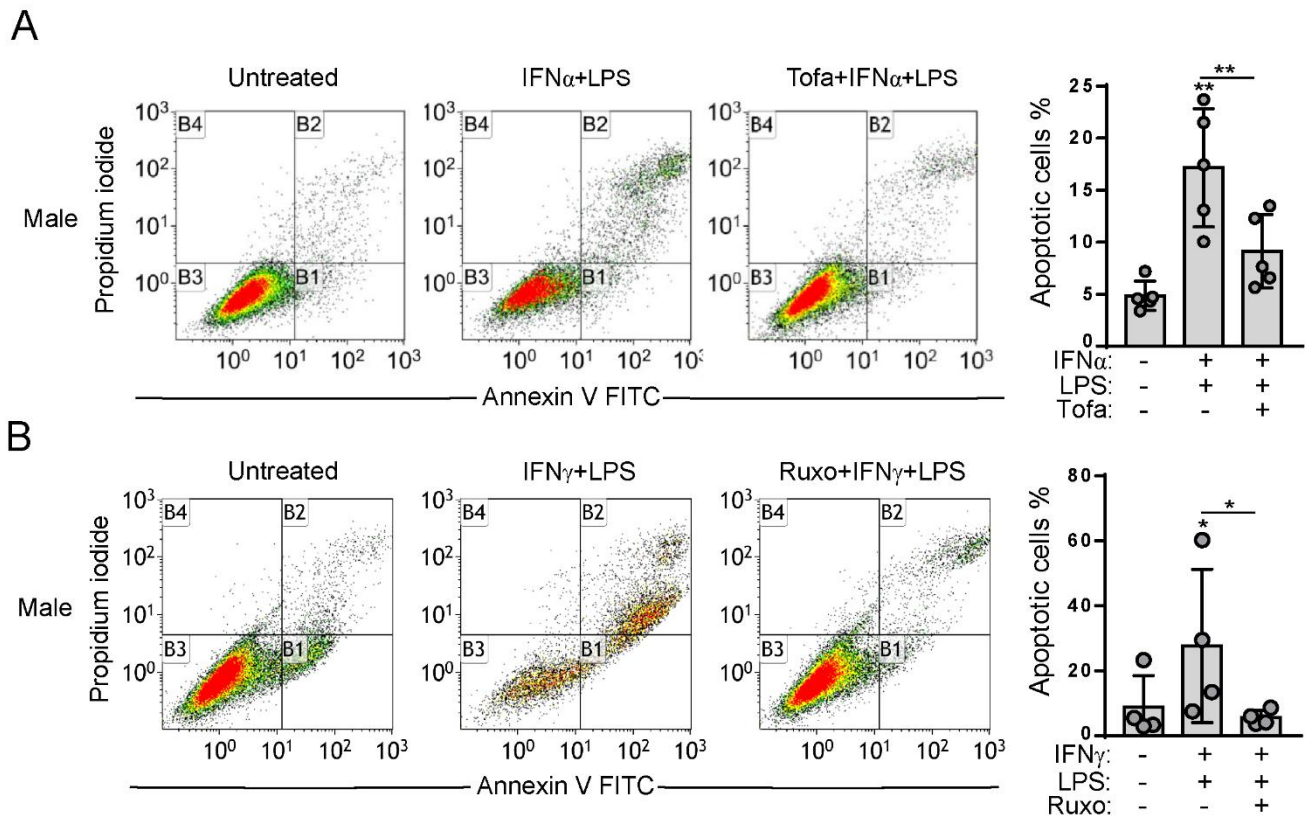


**Figure 21. Jakinibs reduce the IFN+LPS-mediated apoptosis of VIC.** (A-B) Male VIC were pre-treated with Jakinibs before stimulation and apoptosis analysis was performed as in Figure 19. Representative flow cytometry plot and statistical analysis of apoptotic cells counts (B1+B2 quadrants) for IFN- $\alpha$ +LPS (A) treatment (n=4) and for IFN- $\gamma$ +LPS treatment (n=4). Ruxo indicates 6  $\mu$ M ruxolitinib, Tofa, 6 $\mu$ M tofacitinib. Doses, statistics, n, and symbols and as in Figure 2.

Taken together, results from this section demonstrate that type I and II IFN promoted common effects on CAVD relevant pathologic processes in a cellular model of valve cells. The major findings include the induction of pro-inflammatory and pro-osteogenic responses on VIC that exhibited sex differences and can be abrogated by FDA-approved Jakinibs. Additionally, a marked positive interplay with the TLR4 ligand LPS was disclosed. Moreover, IFN alone and combined with LPS lead to an increased Pi-induced calcification that was significantly higher in cells obtained from males, thus correlating with clinical findings in calcified aortic valves.<sup>188</sup>

## **R.2-Specific mechanisms of IFN- $\alpha$ in VIC**

In this part of the study, the specific mechanisms by which IFN- $\alpha$  exerts its effects on VIC and the interplay with TLR ligands were investigated. The analysis was performed in VIC isolated from control valves from male and female patients. As shown in **Table 7**, patient characteristics and comorbidities were not significantly different between sex groups. To note, all patients were Caucasian, and female donors were post-menopausal.

**Table 7: Clinical features of the patients included in the section 2 of the study.**

<b>Patient characteristics</b>	<b>Control valves</b>		
	<b>Male n=14</b>	<b>Female n=6</b>	<b>p-value</b>
<b>Age</b>	60 $\pm$ 7	57 $\pm$ 9	0.49
<b>Hypertension</b>	2 (14%)	1 (16%)	0.89
<b>Hypercholesterolemia</b>	4 (28%)	1 (16%)	0.57
<b>Diabetes mellitus</b>	4 (28%)	2 (33%)	0.8
<b>Smoking</b>	4 (28%)	0	0.14
<b>Renal failure</b>	2 (14%)	0	0.32
<b>Aetiology of heart failure</b>	7 idiopathic, 5 ischemic 1 alcoholic 1 sarcoidosis	4 idiopathic 2 ischemic	0.41

## R.2.1-IFN- $\alpha$ and TLR cooperation is specific for TLR2-4 ligands

Considering the cooperation between IFN- $\alpha$  and LPS on VIC inflammation (**Figures 2, 7-9**), we explored potential interplay with other TLR ligands. Interestingly, NF- $\kappa$ B was activated upon combination of IFN- $\alpha$  with several TLR agonists, namely Pam<sub>2</sub>CSK<sub>4</sub> (a TLR2/6 ligand) and the dsRNA analogous Poly(I:C) (a TLR3 ligand) (**Figure 22**). Conversely, Flagellin (a TLR5 ligand) and Imiquimod (a TLR7 ligand) did not show significant cooperation with IFN- $\alpha$  (**Figure 22**), although Flagellin+IFN- $\alpha$  treatment increased NF- $\kappa$ B phosphorylation in almost all experiments. Together, data suggest that IFN- $\alpha$ -TLR cooperation is more prominent for TLR2-4 ligands in VIC.

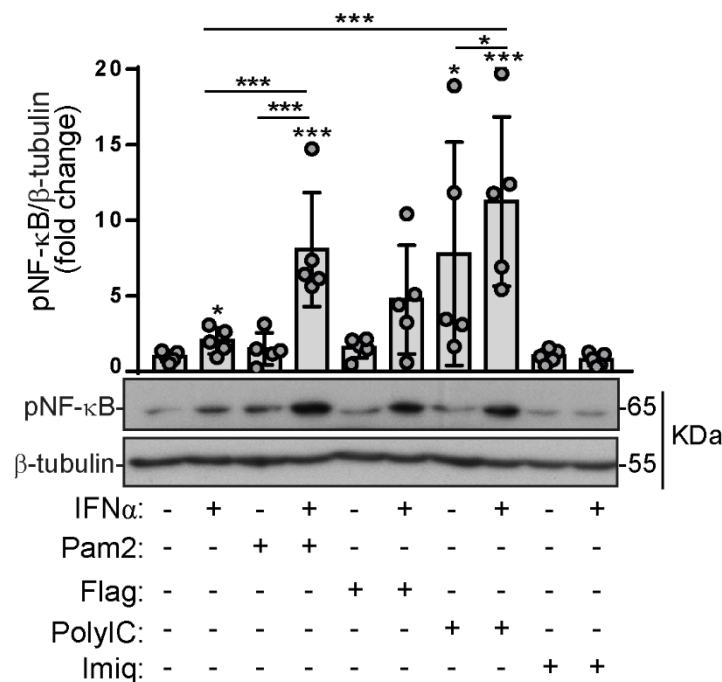


**Figure 22. IFN- $\alpha$  cooperates with TLR2/6 and TLR3 ligands to phosphorylate NF- $\kappa$ B in VIC.** Cells from control male valves were stimulated with the indicated TLR ligands for 24 h and whole cell lysates were analysed by Western Blot; n=5. Pam2 (TLR2/6) refers to 100 ng/mL of Pam<sub>2</sub>CSK<sub>4</sub>; Flag (TLR5), 1  $\mu$ g/mL flagellin; IFN $\alpha$ , to 100 ng/mL IFN- $\alpha$ ; Imiq (TLR7), 5  $\mu$ g/mL Imiquimod; PolyIC (TLR3), 1  $\mu$ g/mL polyinosinic:polycytidylic acid. Statistics, n, and symbols as in Figure 2.

## R.2.2-IFN- $\alpha$ drives VIC differentiation towards an osteoblast-like phenotype

As shown in **Figure 13**, the exposure of VIC to IFN- $\alpha$  resulted on marked changes on cell morphology. To demonstrate the IFN- $\alpha$ -mediated cell differentiation, and because VIC resemble an activated myofibroblast phenotype in our culture conditions,<sup>189</sup> we analysed the expression of the myofibroblast marker  $\alpha$ -SMA. Immunofluorescence analysis revealed that the protein levels of  $\alpha$ -SMA decreased after 48 h of treatment, with no apparent differences between male and female cells

(Figure 23A-B). Together, these findings demonstrate the IFN- $\alpha$ -mediated loss of myofibroblast phenotype, thus supporting the hypothesized VIC differentiation upon activation.

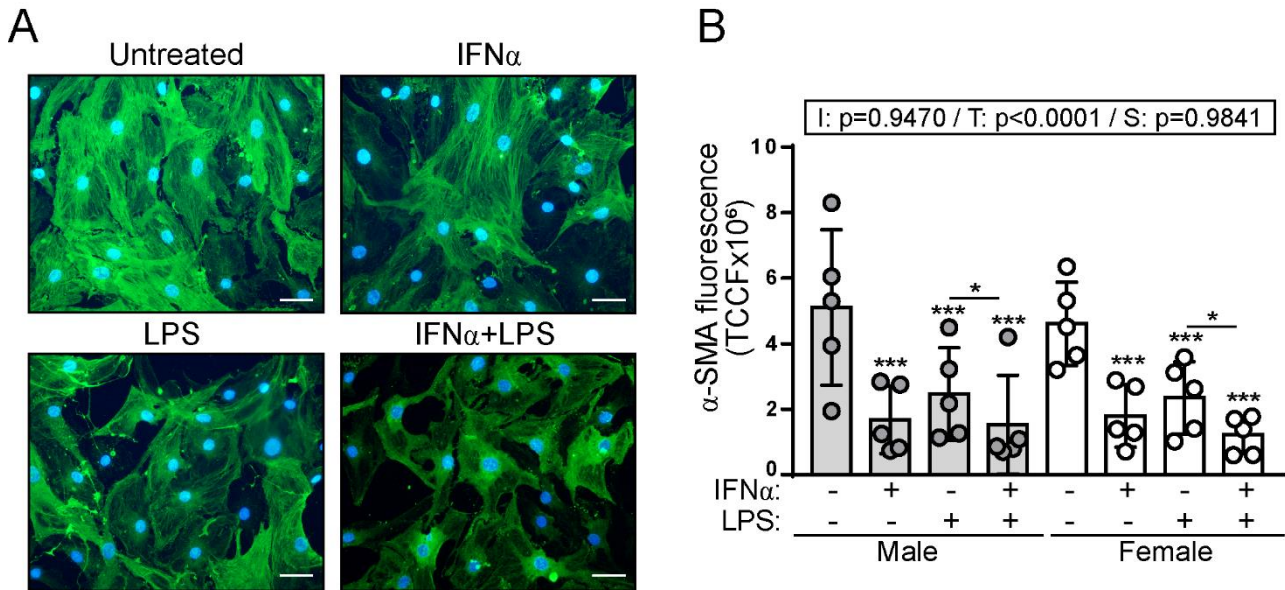


**Figure 23. IFN- $\alpha$  and LPS promote  $\alpha$ -SMA downregulation in VIC.** Control male and female VIC were treated with the indicated ligands for 48 h and  $\alpha$ -SMA protein levels were analysed by immunofluorescence. (A) Images are representative of male VIC. Green, FITC; blue, DNA staining (DAPI); white line indicates 50  $\mu$ m. (B) Total corrected cellular fluorescence (TCCF) was calculated as indicated in Methods; n=5. Doses, statistics, n, and symbols as in Figure 7.

Because osteoblastic differentiation is a common finding in calcified human valves,<sup>190</sup> we analysed the gene expression profile of different bone-related transcription factors and osteocyte markers. qPCR analysis revealed that the co-stimulation with IFN- $\alpha$  and LPS resulted in a male-specific upregulation of *Sclerostin (SOST)*, an osteocyte marker increased in CAVD patients' serum<sup>191</sup> (Figure 24A). In the attempt to better understand the VIC phenotype, we investigated the most important osteoblastic transcription factors reported to play a role in CAVD. Consistent with *SOST* induction, only in male VIC IFN- $\alpha$ +LPS treatment upregulated the expression of *RUNX2/CBFA1* gene (Figure 24B), which is the master transcription factor for osteoblastic differentiation that has been associated to VIC differentiation.<sup>91</sup> Then, we explored additional osteoblastic transcription factors and found that the mRNA levels of *MSX2*, a gene associated to valve calcification,<sup>192</sup> were not increased by IFN- $\alpha$  but by LPS treatment in both male and female VIC at 24 h (Figure 24C). Otherwise, the expression of *OSX* gene, which has also been related associated to CAVD,<sup>89</sup> was only upregulated in male cells specifically after IFN- $\alpha$  treatment (Figure 24D). Together, these results are consistent with a differentiation process accelerated by the combination of IFN- $\alpha$  with LPS and exhibiting sex-differences.

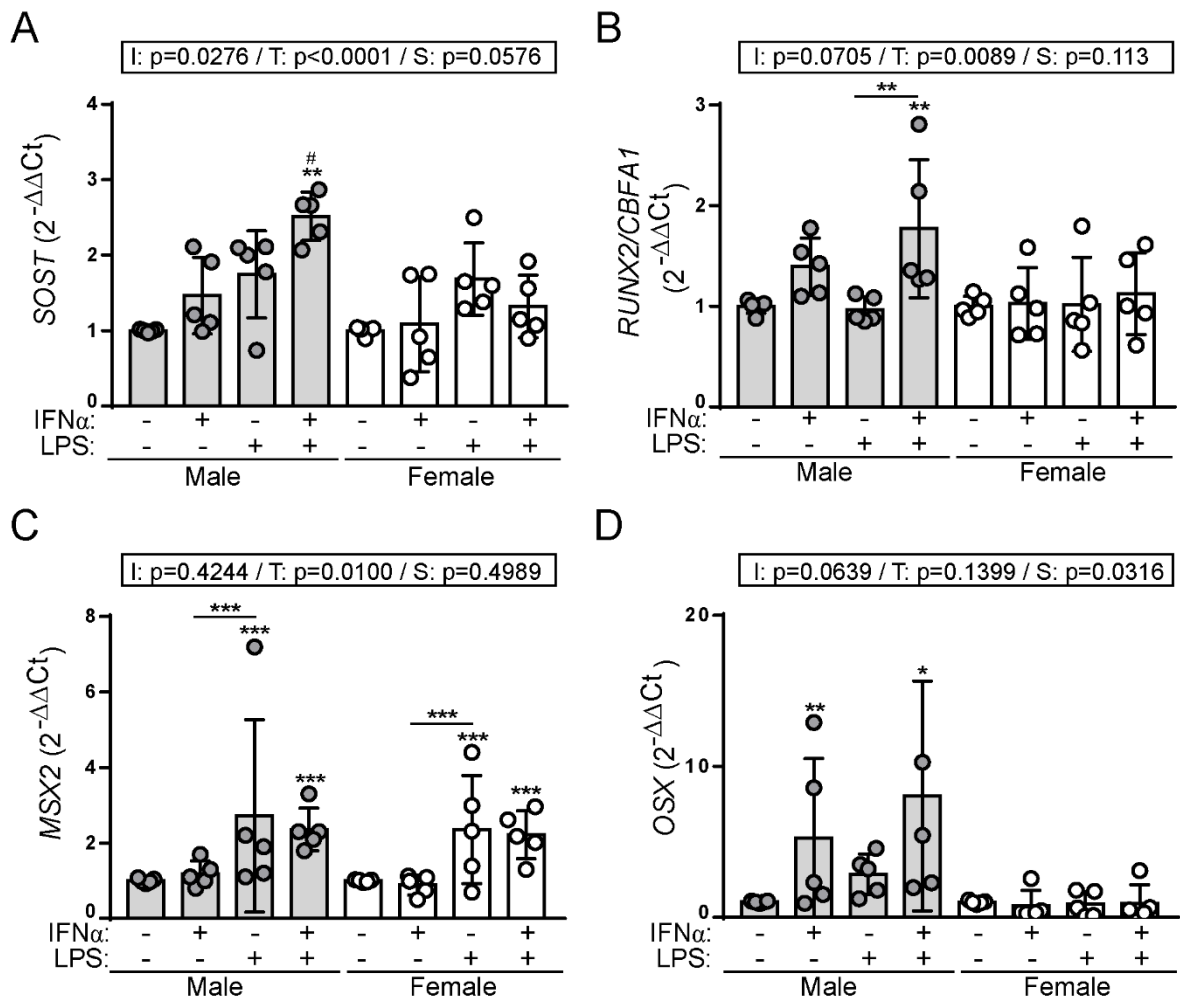


**Figure 24. IFN- $\alpha$  and LPS interplay potentiates VIC differentiation.** Control male and female VIC were treated with the indicated ligands for 24 h and mRNA extracted for qPCR experiments. (A) Relative *SOST* expression. (B-D) Relative expression of the osteoblastic transcription factors *RUNX2* (B), *MSX2* (C) and *OSX* (D);  $n=5$ . Doses, statistics,  $n$ , and symbols as in Figure 7.

Based on the fact that ectopic phosphatase activity is necessary for osteoblastic extracellular matrix formation,<sup>101</sup> the effects of IFN- $\alpha$  on *TNAP* expression were investigated. Herein, qPCR analysis revealed the upregulation of *TNAP* mRNA levels upon exposure of male cells to IFN- $\alpha$  and LPS for 24 h (**Figure 25A**). Conversely, no effect was observed in female VIC, thus confirming sex differences at early times (**Figure 25A**). Based on this result, we performed a long-term functional assay for ectopic phosphatase activity. After 21 days of treatment in activation medium, IFN- $\alpha$  or LPS alone and the combination of both stimuli significantly increased phosphatase activity in both male and female cells (**Figure 25B**). Collectively, these findings and previous data suggest that female cells also suffered an osteoblast-like differentiation process that seems to be delayed at early times.

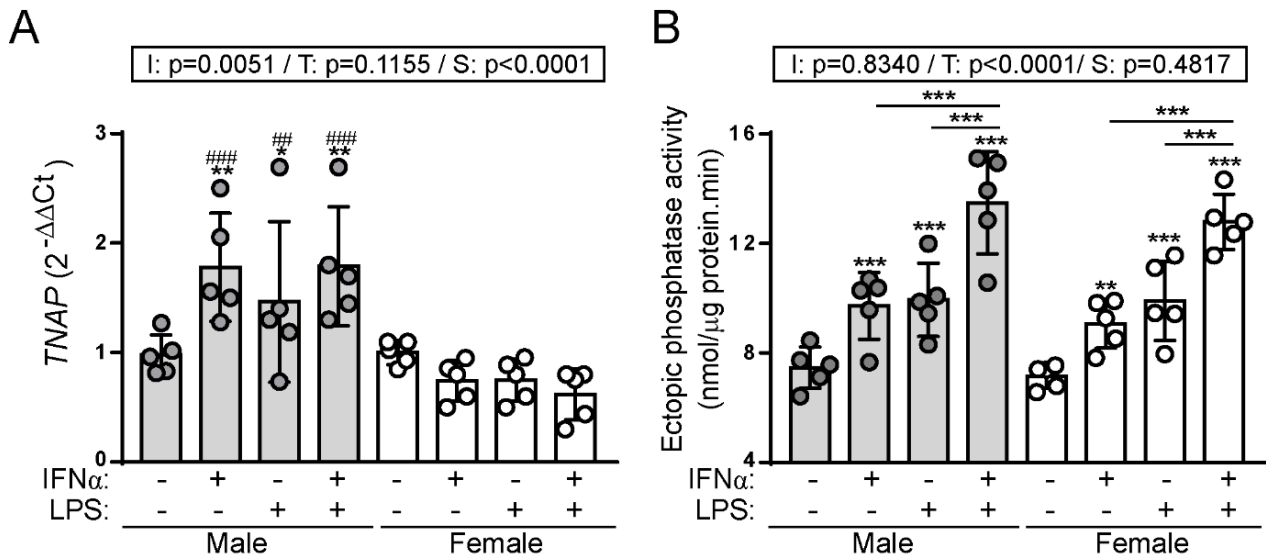


**Figure 25. IFN- $\alpha$  and LPS increase ectopic phosphatase activity.** (A) Control male and female VIC were treated with the indicated ligands for 24 h and mRNA extracted for qPCR analysis of *TNAP* expression; n=5. (B) Cells were treated for 21 days in growth medium and ectopic phosphatase activity assessed by colorimetric conversion of *p*-nitrophenyl phosphate. Data are expressed as nmol/min of formed product and normalized to total protein content; n=5. Doses, statistics, n, and symbols as in Figure 7.

### R.2.3-BMP-2 signalling plays a role on male preferential calcification

To investigate potential mechanisms accounting for sex-differences in calcification, we focused on BMP-2 signalling since it has been reported to be necessary for aortic valve calcification *in vitro* and *in vivo*.<sup>92</sup> Here, we found by ELISA analysis that IFN- $\alpha$  alone or together with LPS induced BMP-2 secretion at 24 h in male but not in female VIC (**Figure 26A**). Based on this sex-differential secretion of BMP-2, we then assessed the role of this pathway in calcification using a BMP antagonist named noggin, which has been reported to block the osteogenic activation of VIC.<sup>193</sup> In calcification assays, noggin pre-treatment significantly reduced calcific nodule formation in male cells, as demonstrated by ARS and calcium deposits quantification (**Figure 26B-D**). These findings demonstrate the involvement of BMP-2 on IFN- $\alpha$ -mediated calcification and suggest that it is a mechanism accounting for sex differences in osteogenesis.

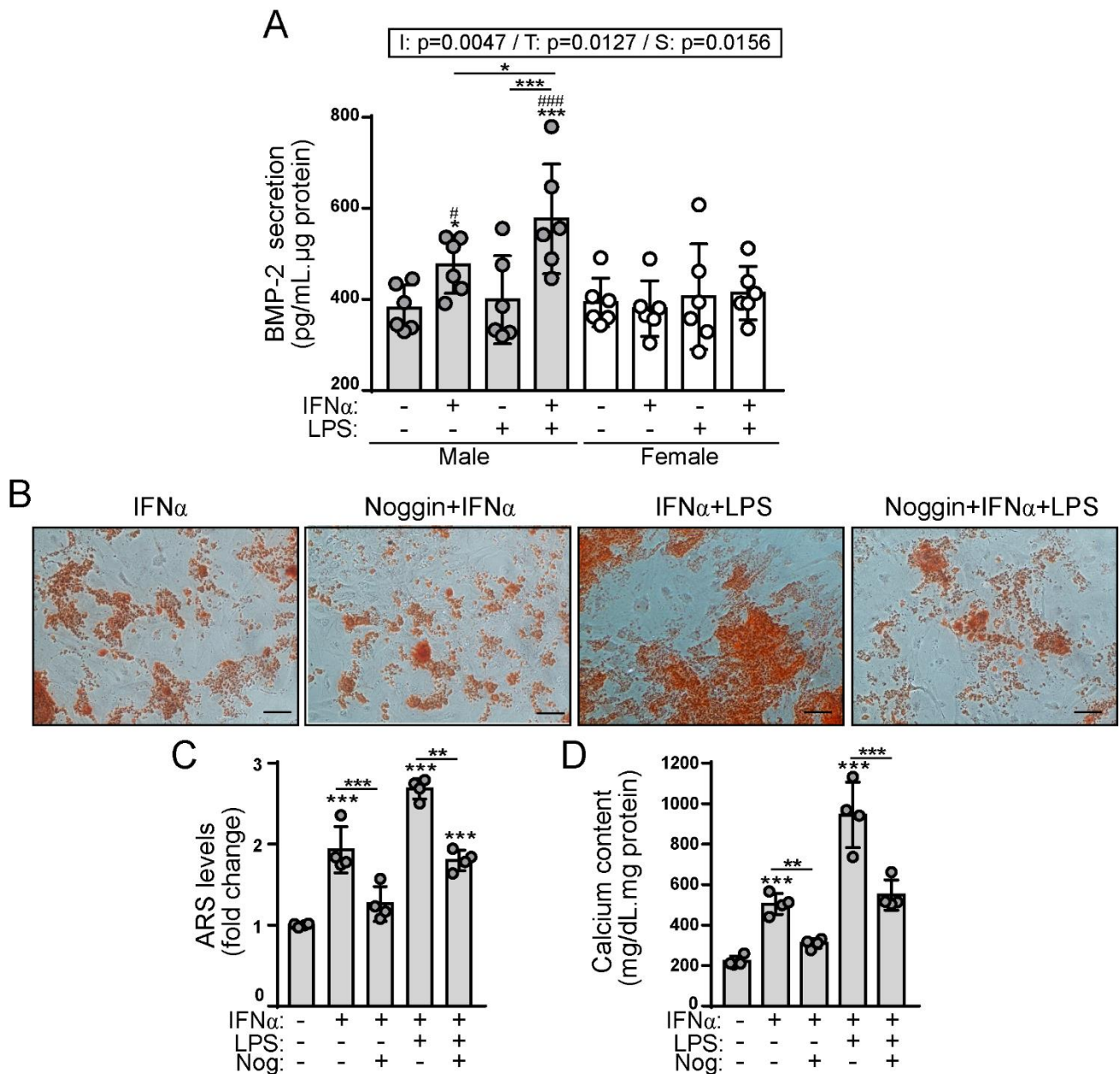


**Figure 26. IFN- $\alpha$  induces BMP-2 secretion only in male cells and BMP-2 signalling blockade attenuates IFN- $\alpha$ -mediated calcification.** (A) Control male and female VIC were treated with the indicated ligands for 24 h and supernatants collected for assaying BMP-2 secretion; n=6. (B-D) *In vitro* calcification experiments were performed in male cells pre-treated or not with the BMP antagonist noggin before stimulation. ARS extraction and calcium deposits measurements were performed in n=4 male isolates. Nog indicates 470 ng/mL noggin. Doses, statistics, n, and symbols as in Figure 7.

We then investigated BMP-2 downstream effectors. Given that BMP-2 up-regulates RUNX2 protein levels in VIC,<sup>91</sup> and our previous results demonstrating the upregulation of *RUNX2* gene transcripts by IFN- $\alpha$ +LPS in male cells (**Figure 24B**), we further explored the involvement of this osteoblastic transcription factor on cell differentiation. Unexpectedly, nuclear and cytoplasmic extract analysis revealed that RUNX2 was in the nucleus of male VIC and not present in the

cytoplasm even in basal conditions (**Figure 27A**). Moreover, its nuclear protein levels were downregulated by IFN- $\alpha$ +LPS treatment for 24 h (**Figure 27A**). In order to confirm this striking finding, cells were stimulated for 12 days, and the pro-osteogenic cytokine TNF- $\alpha$ <sup>194</sup> and the morphogen TGF- $\beta$ 1<sup>195</sup> were used as controls. Whole cell lysates analysis showed that IFN- $\alpha$  promoted RUNX2 downregulation, and both LPS and TNF- $\alpha$  showed no effects, whereas TGF- $\beta$ 1 was the only stimuli inducing an increase in RUNX2 protein levels (**Figure 27B**). Altogether, these data suggest a basal nuclear location of RUNX2 in cultured VIC in our conditions and a complex regulation of this transcription factor upon stimulation with different cytokines. As a potential mechanism explaining the IFN- $\alpha$ -induced RUNX2 downregulation, we found that this cytokine triggered the expression of *Smad ubiquitination regulatory factor* (**Figure 27C**), an ubiquitin E3 ligase that promotes RUNX2 degradation.<sup>196</sup>

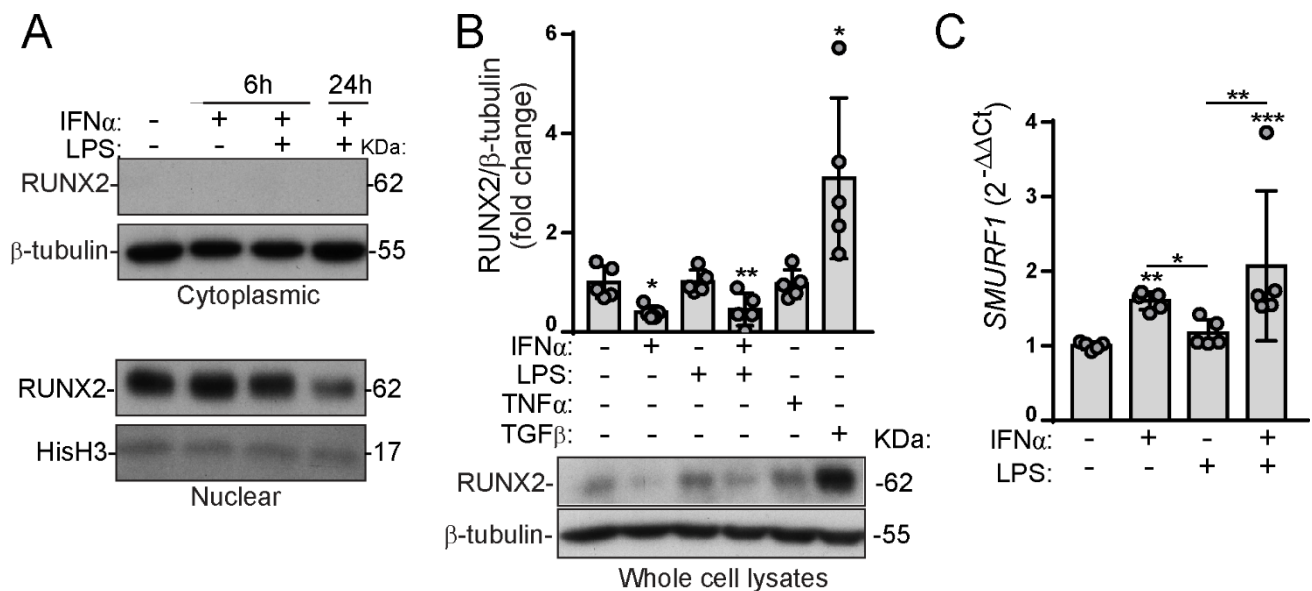


**Figure 27. RUNX2 is basally located in the nucleus of cultured VIC, being its protein levels downregulated by IFN- $\alpha$ .** (A) Control male VIC were treated with the indicated ligands for either 6 or 24 h and nuclear/cytoplasmic extracts analysed by Western Blot for RUNX2; n=3. (B) Male cells were treated with the indicated ligands for 12 days and whole cell extracts analysed by Western Blot. Densitometric analysis and representative blot of n=4. (C) *Smad ubiquitination regulatory factor* (*SMURF1*) transcripts levels after 24 h of treatment; n=4. TGF $\beta$  indicates 10 ng/mL TGF- $\beta$ 1; TNF $\alpha$ , 25 ng/mL TNF- $\alpha$ . Doses, n, statistics and symbols as in Figure 2.

Other BMP-2 downstream mediator like *OSX* was also upregulated by IFN- $\alpha$  (**Figure 24D**), while *MSX2* was not (**Figure 24C**), thus suggesting the potential involvement of *OSX* in IFN- $\alpha$ -induced osteogenic differentiation of VIC. Collectively, data demonstrate that BMP-2 signalling plays a role on male preferential calcification, and further studies are needed to elucidate the involvement of downstream effectors.

## R.2.4-Female-specific Akt activation is a protective mechanism for calcification

The next step was to explore additional signalling pathways accounting for sex-differences in calcification. Our previous findings showed that IFN- $\alpha$  induced early Akt phosphorylation in male VIC (**Figure 5**). Strikingly, we found a female-specific activation of Akt upon treatment with either IFN- $\alpha$ , LPS or both combined for 24h (**Figure 28A**). Since the Akt pathway is known to be involved in cell survival, we also explored the expression of the anti-apoptotic gene *B-cell lymphoma-2* (*BCL2*). RT-qPCR data disclosed differential IFN- $\alpha$ -mediated responses between sexes, being *BCL2* gene upregulated only in male cells (**Figure 28B**), which could be a counteracting mechanism against apoptosis.

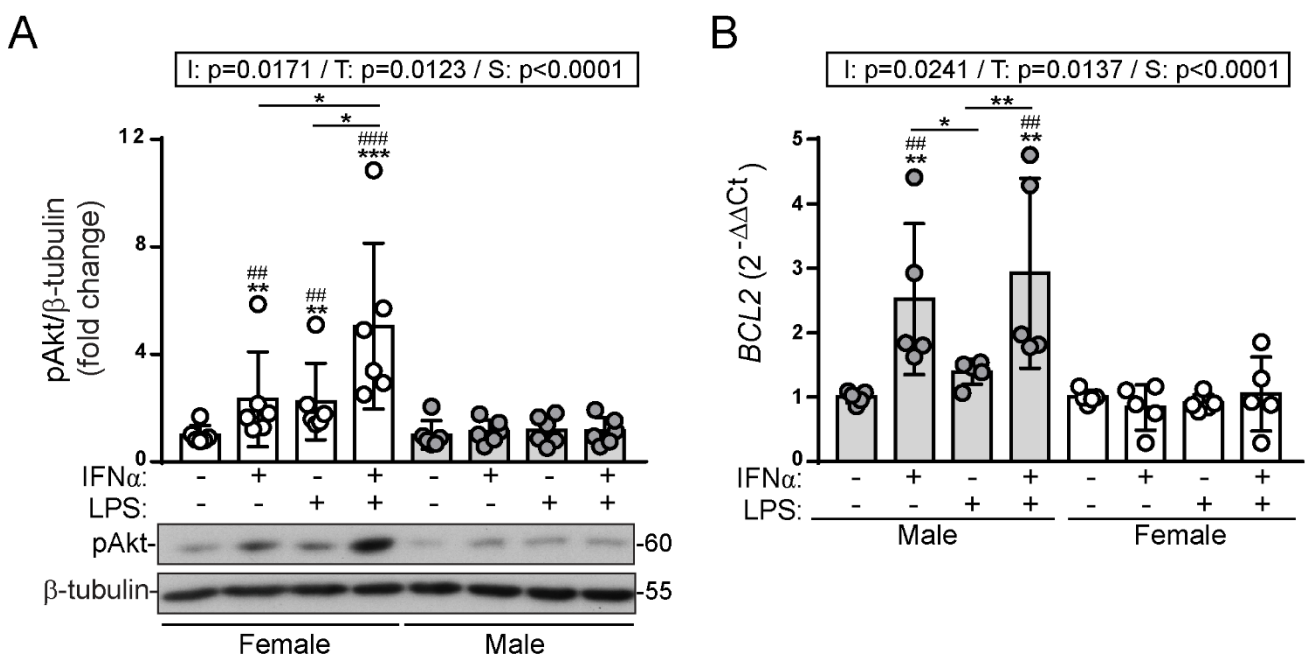


**Figure 28. IFN- $\alpha$  and LPS promote a female-specific activation of Akt.** (A) Female and male VIC were treated with the indicated ligands for 24 h, and whole cell lysates analysed for Akt phosphorylation. Representative blot and densitometric analysis of n=6. (B) Male and female cells treated for 24 h were analysed for *BCL2* expression; n=5. Doses, statistics, n, and symbols as in Figure 7.

As previously shown, female VIC were less prone to mineralization (**Figure 15**) and apoptosis in calcifying conditions (**Figure 19**). Since the Akt pathway is involved in cell survival and it has been described as a protective mechanism in Pi-induced calcification,<sup>100</sup> we addressed its role on calcification experiments in female VIC using a pharmacological approach. Strikingly, Akt activation blockade by the PI3K inhibitor LY294002 significantly increased female VIC calcification in both basal and activated conditions (**Figure 29A-C**). These data together with literature evidences support the notion of Akt as a protective pathway in Pi-induced calcification that could explain the lower apoptosis of female VIC shown upon IFN- $\alpha$ +LPS treatment. In addition, these results are

consistent with the emerging role of apoptosis as an underlying cause of sex-differences in cardiovascular diseases.<sup>197</sup>

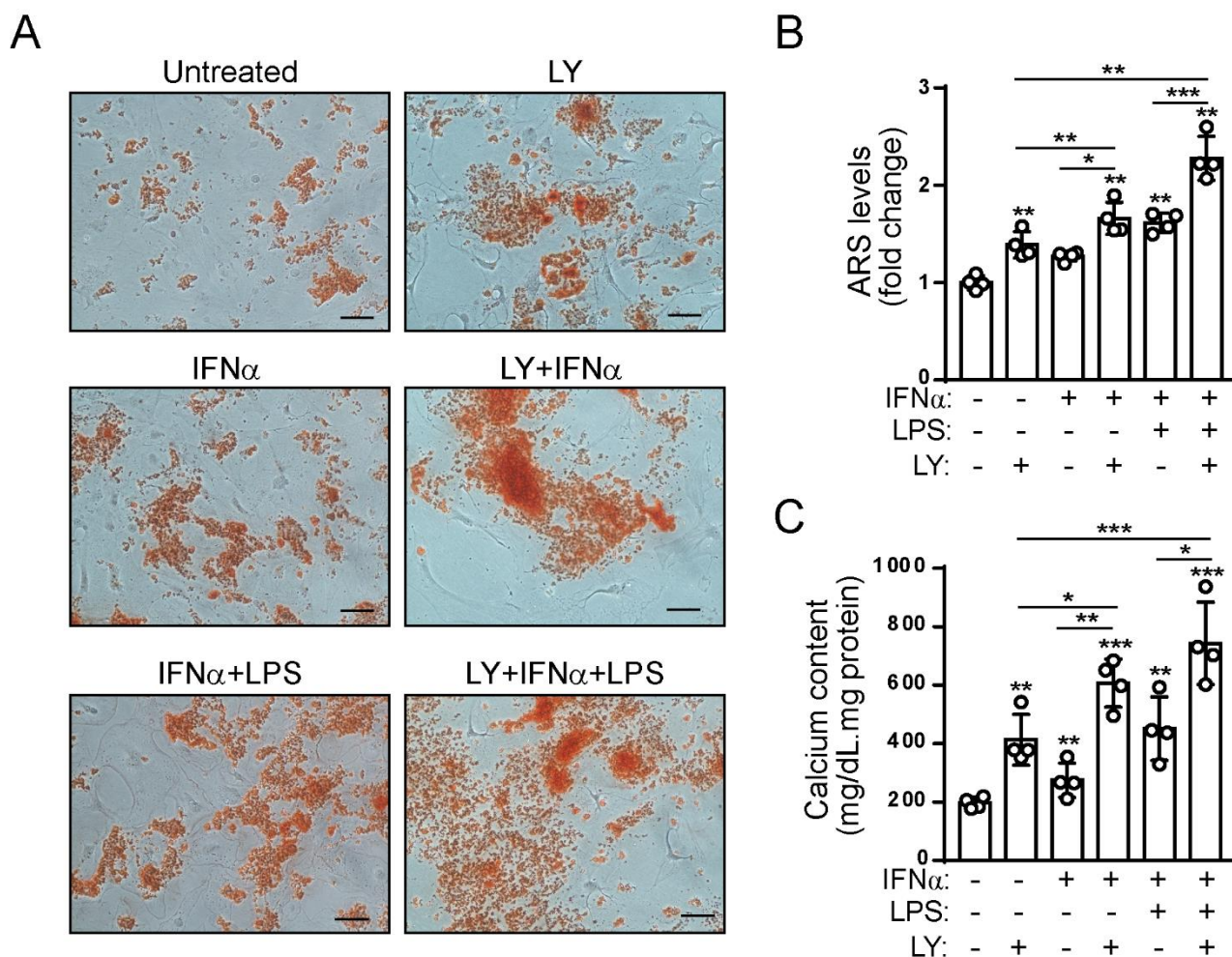


**Figure 29. Akt activation blockade increases calcification in female cells.** (A-C) Female VIC cultured for 14 days in calcifying conditions were pre-treated or not with the PI3K inhibitor LY294002 before stimulation. ARS representative microphotographs (A) and levels (B). Calcium deposits quantitation (C). LY indicates 50  $\mu$ mol/L LY294002; n=4. Doses, symbols, n, and statistics as in Figure 2.

In conclusion, data shown on this section reveal IFN- $\alpha$ -specific mechanisms in VIC. The major findings include the osteoblastic differentiation of VIC triggered by IFN- $\alpha$ , which is delayed in female cells; and the identification of BMP-2 signalling and female-specific Akt activation as mechanisms that account for male-preferential calcification. Additionally, the data suggest that RUNX2 regulation is a complex process that merits further investigations in the complex context of valve calcification.

### **R.3-Specific mechanisms of IFN- $\gamma$ in VIC**

The aim of this section was to analyse the specific mechanisms for the IFN- $\gamma$ -TLR interplay and its impact on VIC angiogenesis and calcification. The study was performed in VIC isolated from control valves from male and female patients that had similar characteristics and comorbidities (**Table 8**). All patients were Caucasian, and female donors were post-menopausal.

**Table 8: Clinical features of the patients whose valves were included in section 3.**

<b>Patient characteristics</b>	<b>Control valves</b>		
	<b>Male n=12</b>	<b>Female n=6</b>	<b>p-value</b>
<b>Age (Range)</b>	60 $\pm$ 8	57 $\pm$ 9	0.46
<b>Hypertension</b>	3 (25%)	1 (16%)	0.68
<b>Hypercholesterolemia</b>	5 (41%)	1 (16%)	0.28
<b>Diabetes mellitus</b>	5 (41%)	2 (33%)	0.73
<b>Smoking</b>	1 (8%)	0	0.46
<b>Renal failure</b>	0	0	1.00
<b>Aetiology of heart failure</b>	4 idiopathic, 7 ischemic, 1 hypertrophic	4 idiopathic, 2 ischemic	0.22

### R.3.1-IFN- $\gamma$ and LPS interplay promotes HIF-1 $\alpha$ induction in VIC

As noted in the introduction, the master transcription factor for angiogenesis, HIF-1 $\alpha$ , has been found in calcified valves co-localizing with calcifying nodules,<sup>107</sup> but little is known about the underlying mechanisms of its expression. As expected, Western Blot analysis of VIC revealed no expression of HIF-1 $\alpha$  in basal conditions (**Figure 30A**). However, we found that exposing VIC to IFN- $\gamma$  slightly induced HIF-1 $\alpha$  protein levels under normoxic conditions. Remarkably, this effect was strongly potentiated by LPS (**Figure 30A**). Moreover, the interplay with LPS on HIF-1 $\alpha$  induction was specific for IFN- $\gamma$ , since it was not observed with IFN- $\alpha$  (**Figure 30B**). Together, data disclose an immune, non-hypoxic, and IFN- $\gamma$ -specific mechanism of HIF-1 $\alpha$  induction.

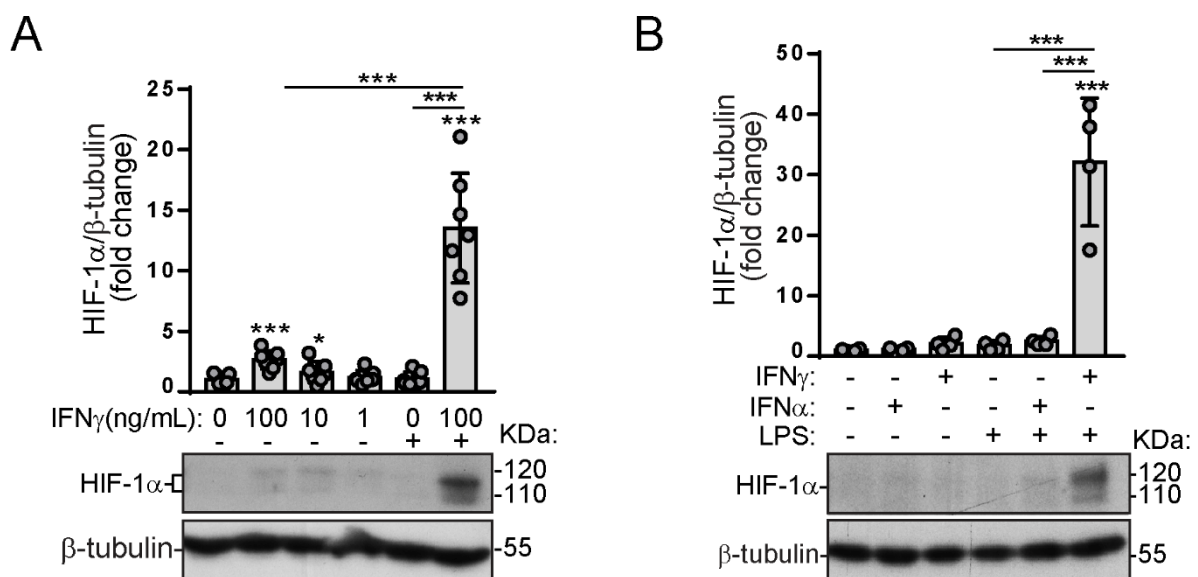


**Figure 30. IFN- $\gamma$  and LPS co-stimulation promotes HIF-1 $\alpha$  protein stabilization.** (A-B) Control male VIC were treated with the indicated ligands for 24 h and whole cell lysates analysed for HIF-1 $\alpha$  protein levels. Representative blots and densitometric analysis of n=4-7. Doses, symbols, n, and statistics as in Figure 2.

We next analysed HIF-1 $\alpha$  nuclear translocation as an indicator of its activation. Two independent methods of cellular localization, cell immunostaining and Western blot analysis of nuclear and cytoplasmic extracts, demonstrated that HIF-1 $\alpha$  was present in the nucleus upon co-stimulation of VIC with IFN- $\gamma$  and LPS (**Figure 31A-C**). Remarkably, ruxolitinib pre-treatment abrogated HIF-1 $\alpha$  nuclear translocation (**Figure 31C**). These data are consistent with a JAK/STAT-mediated activation of HIF-1 $\alpha$ .

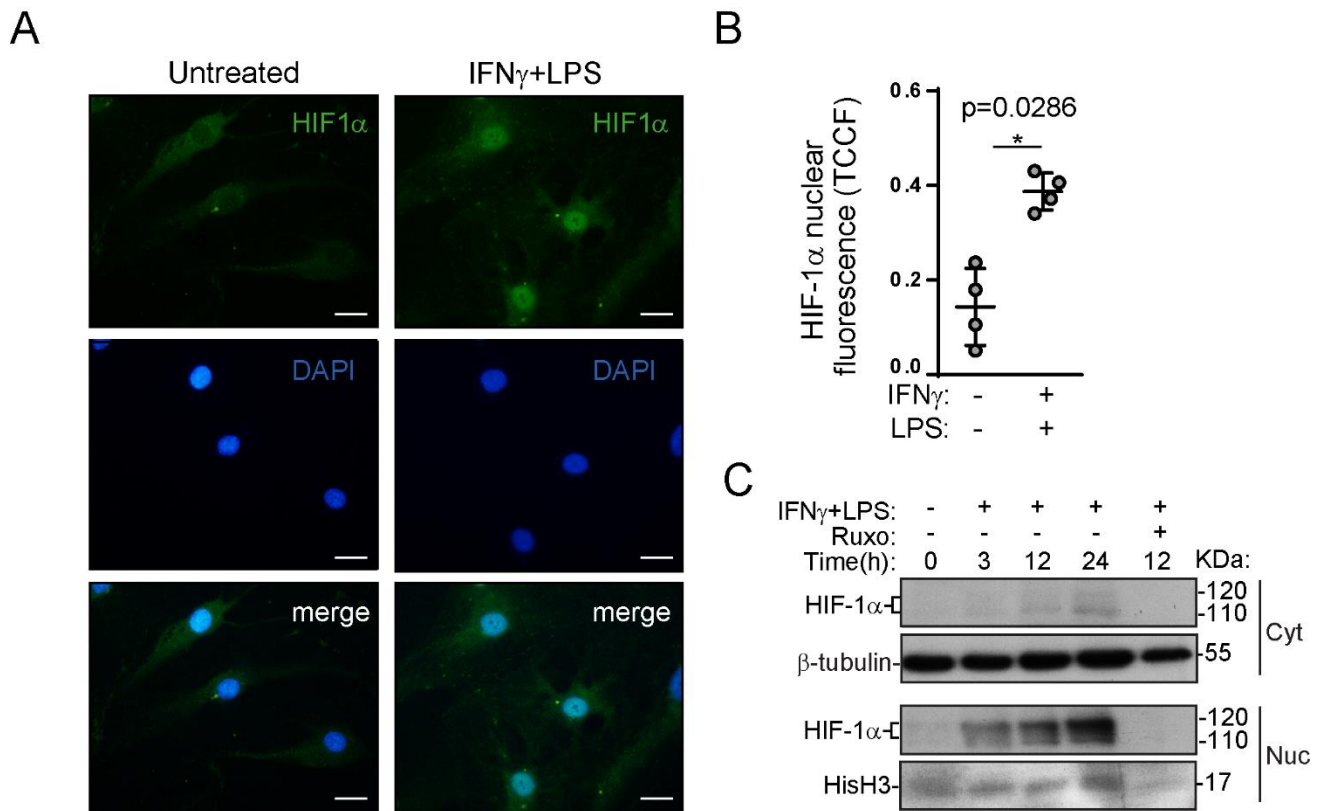


**Figure 31. HIF-1 $\alpha$  is translocated to the nucleus upon IFN- $\gamma$  and LPS co-treatment of VIC under normoxic conditions.** (A-B) Male VIC seeded on coverslips were treated for 24 h with IFN- $\gamma$ +LPS and HIF-1 $\alpha$  protein was analysed by immunostaining as described in Methods. Representative microphotographs of HIF-1 $\alpha$  (green) and DAPI (blue) staining, either separated or merged (A), and statistics of n=4 (B). Total corrected cellular fluorescence (TCCF) was calculated as indicated in Methods. White line indicates 50  $\mu$ M. (C) Male VIC were treated for the indicated times and nuclear (Nuc) and cytoplasmic (Cyt) extracts analysed by Western Blot. HisH3 indicates histone-H3; Ruxo, 6  $\mu$ M ruxolitinib. Doses, statistics, n, and symbols as in Figure 2.

Once confirmed the immune-mediated activation of HIF-1 $\alpha$ , we explored its regulation. RT-qPCR data showed that the treatment with IFN- $\gamma$  and/or LPS did not alter *HIF1A* gene expression in VIC (**Figure 32A**), thus correlating with its well-known post-transcriptional regulation by stabilization via prolyl hydroxylase inhibition.<sup>198</sup> Next, we used a pharmacological approach of several signalling routes that revealed a complex regulation of HIF-1 $\alpha$  induction in VIC. First, the effect was receptor-dependent since HIF-1 $\alpha$  protein induction was abrogated by the inhibition of both JAK and TLR activation (**Figure 32B**). Additionally, several downstream pathways, such as NF- $\kappa$ B, Akt and MAPK, played a role on HIF-1 $\alpha$  induction (**Figure 32B**). Among HIF-1 $\alpha$  selective inhibitors available, we tested a drug named PX-478<sup>199</sup> that is currently used in a clinical trial for cancer treatment. Western Blot analysis revealed that this drug inhibited the IFN- $\gamma$ +LPS-mediated expression of HIF-1 $\alpha$  in a dose-dependent manner (**Figure 32C**). Given that PX-478 exerts some

potential off-target effects in transcription at high doses,<sup>199</sup> the minimal dose exhibiting inhibitory effects in VIC, 40  $\mu$ M, was chosen for the subsequent experiments.

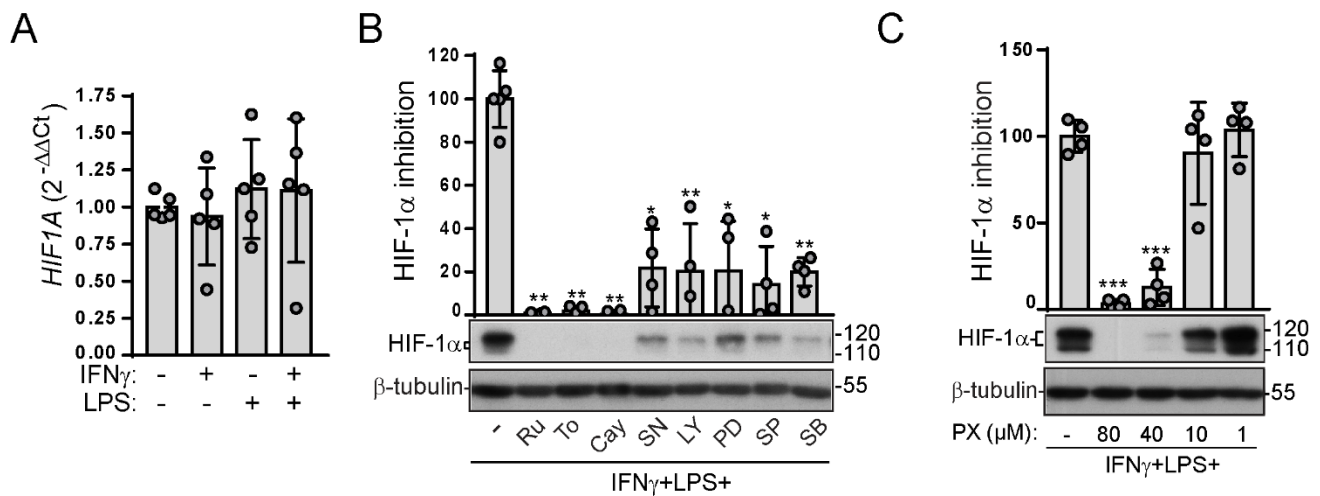


**Figure 32. Immune induction of HIF-1 $\alpha$  protein is controlled by several signalling pathways and abrogated by PX-478.** (A) Male VIC were treated for 24 h and *HIF1A* mRNA levels analysed by qPCR; n=5. (B-C) Cells were pre-treated with the indicated inhibitors and activated for 24 h with IFN- $\gamma$ +LPS for the analysis of HIF-1 $\alpha$  protein levels. Representative blots and densitometric analysis of n=3-4. Data were normalized to IFN- $\gamma$ +LPS induction (100%). Inhibitors and antagonist abbreviations and doses as in figure 11. PX indicates PX-478. Statistics, n and symbols as in Figure 2.

To accurately elucidate the pathway controlling HIF-1 $\alpha$  expression, gain and loss of function experiments were performed. First, we used cobalt chloride (CoCl<sub>2</sub>) a well-known chemical stabilizer of HIF-1 $\alpha$ .<sup>200</sup> Western Blot analysis revealed that treatment of male VIC with CoCl<sub>2</sub> induced HIF-1 $\alpha$  protein expression in a dose-dependent manner (**Figure 33A-B**). Conversely, chemical stabilization of HIF-1 $\alpha$  did not induce either STAT1 or STAT3 phosphorylation (**Figure 33A-B**). These findings, together with HIF-1 $\alpha$  induction blockade by Jakinibs (**Figure 32B**), suggest that this transcription factor is downstream of JAK/STAT signalling. Given the pro-apoptotic effects of CoCl<sub>2</sub> reported in mitral valve interstitial cells at doses above 100  $\mu$ M,<sup>201</sup> the dose of 100  $\mu$ M was selected for the subsequent experiments.

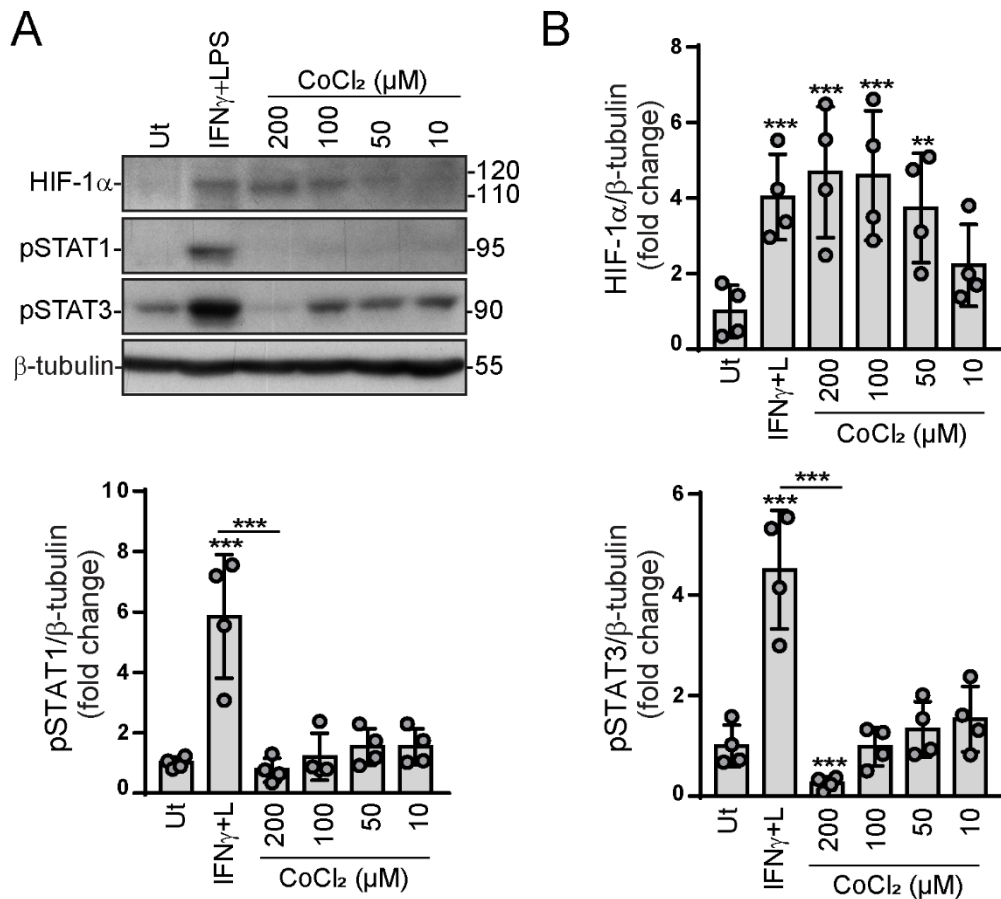


**Figure 33. CoCl $_2$  induces HIF-1 $\alpha$  expression but not STAT1/3 activation.** Male VIC were treated for 24 h with the indicated ligands and whole cell lysates analysed by Western Blot. (A) Representative blot for HIF-1 $\alpha$ , pSTAT1 (Tyr701), and pSTAT3 (Tyr705) levels. (B) Densitometric analysis and statistics; n=4. L indicates LPS; Ut, untreated. Doses, n, statistics and symbols as in Figure 2.

We then performed loss of function experiments using a siRNA Silencer® select pre-designed and validated siRNA duplexes for *STAT1*, *STAT3* and *HIF1A* genes that were used to clearly define the signalling pathways involved in IFN- $\gamma$ +LPS effects. Western blot analysis confirmed gene knockdown, since siRNA duplexes for *STAT1* and *STAT3* genes markedly reduced their protein levels, to an 18% and 5% respectively (**Figure 34A**). Based on these set-up experiments, the time of 72 h post-transfection was chosen for the silencing experiments. The efficiency of *HIF1A* silencing was demonstrated by analysing HIF-1 $\alpha$  protein expression upon VIC stimulation with both immune and chemical inducers for 24 h (**Figure 34B**). *HIF1A* knockdown completely depleted both the CoCl $_2$  and IFN- $\gamma$ +LPS-mediated induction of HIF-1 $\alpha$  protein (**Figure 34B**). Then, the effects of silencing *STAT1/3* and *HIF1A* genes were analysed.

Remarkably, data disclosed that *STAT1* gene silencing completely abrogated HIF-1 $\alpha$  protein induction upon cell activation with IFN- $\gamma$ +LPS and CoCl $_2$  (**Figure 34B**). In contrast, *HIF1A*

knockdown did not statistically affect either STAT1 protein levels or its phosphorylation (Tyr701) upon cell stimulation (**Figure 34B**).

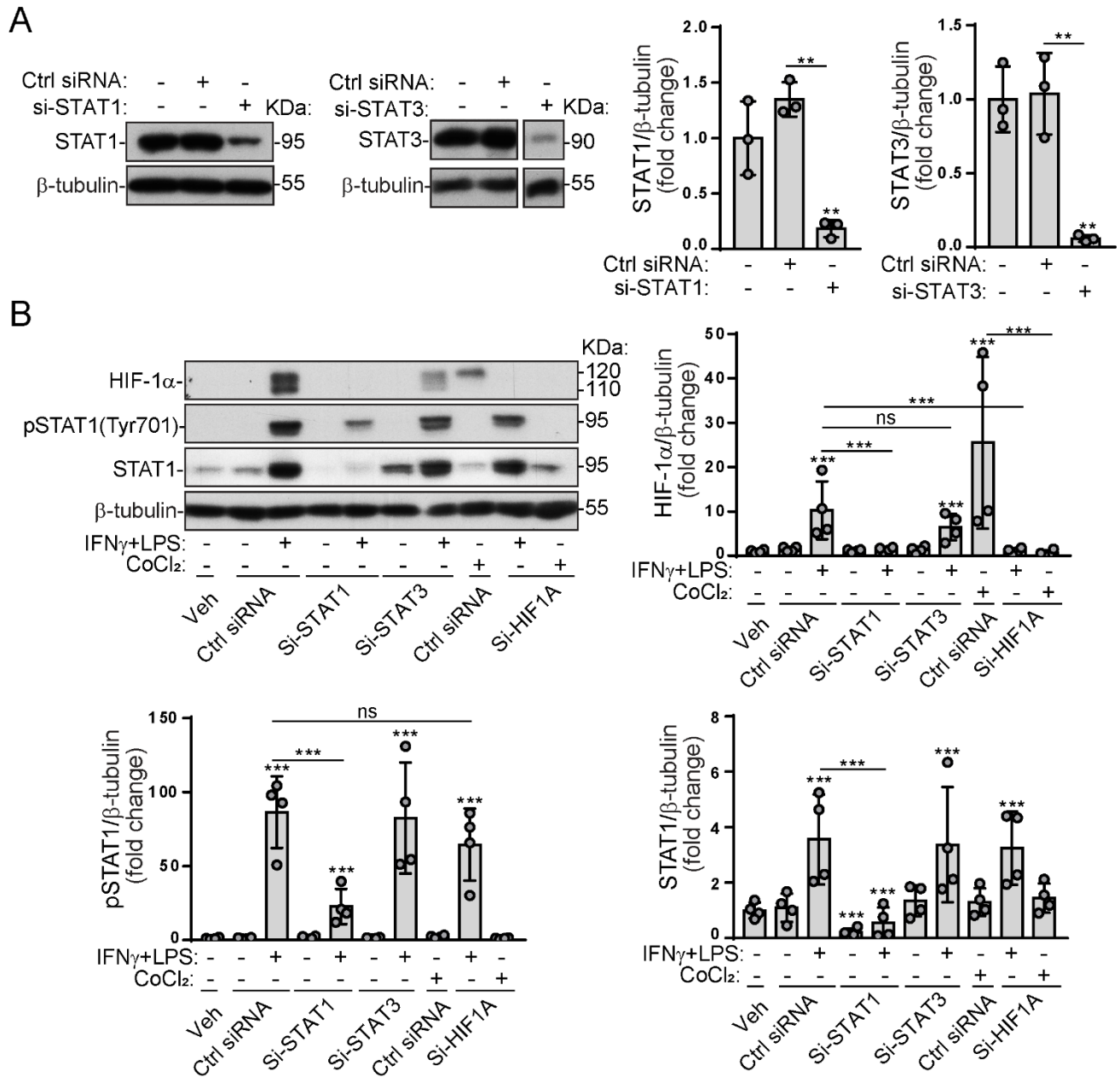


**Figure 34. *STAT1*, but not *STAT3*, gene knockdown depletes HIF-1 $\alpha$  induction by IFN- $\gamma$ +LPS.** Gene silencing experiments were performed as described in Methods. siRNA duplexes for *STAT1* (si-STAT1), *STAT3* (si-STAT3), and *HIF1A* (si-HIF1A) genes, and siRNA negative control (Ctrl siRNA) were used. (A) Representative blot and densitometric analysis confirming STAT1/3 gene knockdown at 72 h; n=3 male VIC. (B) Male VIC transfected as indicated for 72 h were activated with IFN $\gamma$ +LPS or 100  $\mu$ M CoCl<sub>2</sub> for 24 h; n=4. Representative blot and densitometric analysis of n=4. Doses, statistics, n, and symbols as in Figure 2.

Next, *STAT3* knockdown showed a trend to reduce the stimuli-mediated HIF-1 $\alpha$  induction, but data did not reach statistical significance (**Figure 34B**). Finally, HIF-1 $\alpha$  knockdown did not significantly affect either STAT3 protein levels or its activation upon cell stimulation (**Figure 35**).

Altogether these data demonstrate that HIF-1 $\alpha$  is downstream of STAT signalling. Moreover, STAT1 is the main transcription factor controlling the induction of HIF-1 $\alpha$  expression by JAK/STAT and TLR pathways interplay.

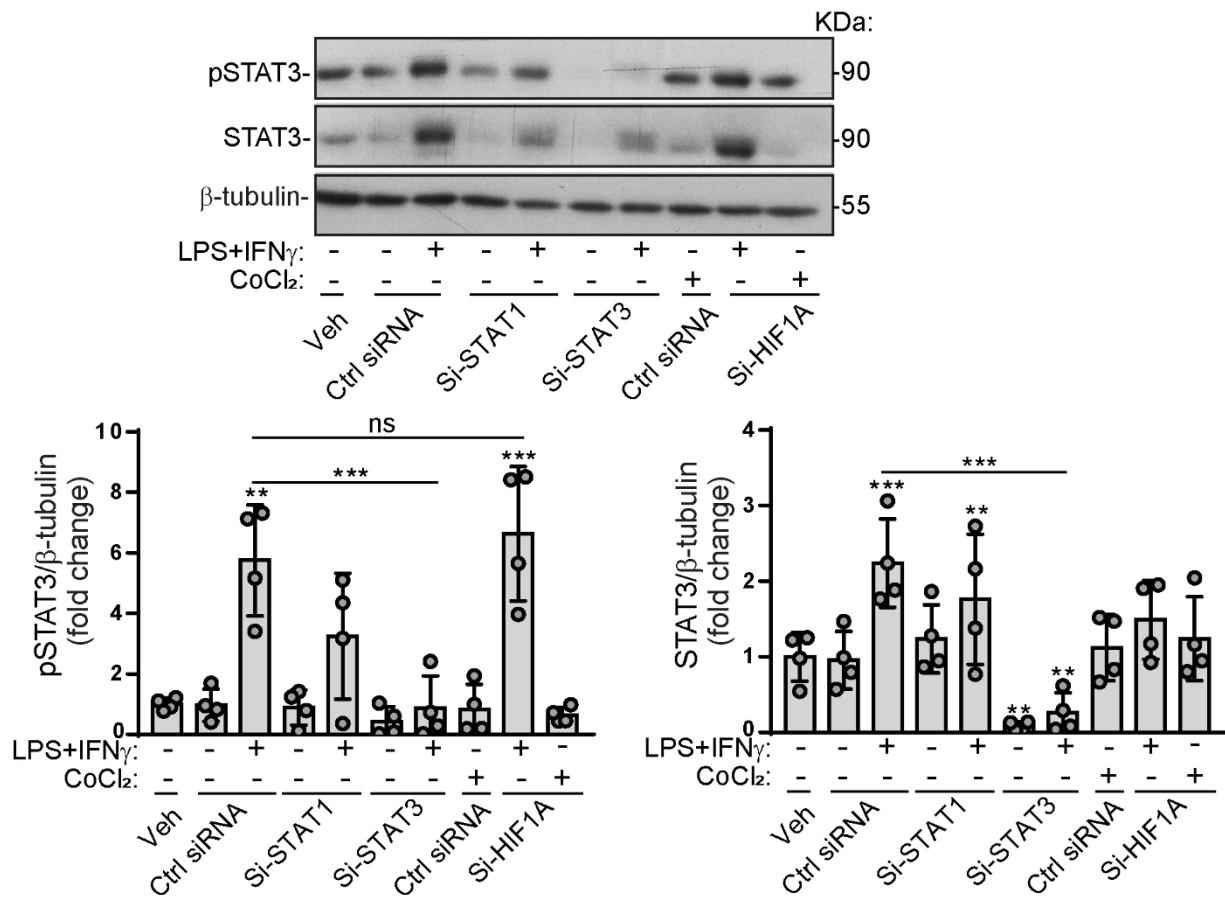


**Figure 35. HIF1A and STAT1 knockdown does not affect STAT3 signalling upon stimulation.** Gene silencing experiments were performed as described in Methods; siRNA duplexes and activation were as in Figure 34. Representative blots and the corresponding densitometric analysis of n=4. Doses, n, statistics, and symbols as in Figure 2.

Densitometric analysis of knockdown experiments showed that STAT1 and STAT3 protein levels were statistically increased after 24 h of treatment with IFN- $\gamma$ +LPS and negative control siRNA (**Figures 34B and 35**). These unexpected findings lead us to speculate whether these stimuli would increase STAT1 protein levels in non-transfected cells as an additional mechanism of regulation beyond its phosphorylation. The data revealed that cell activation for 24 h also significantly increased STAT1 total protein levels (**Figure 36**). This finding parallels previous reports, pointing to total STAT1 total protein levels increase as a mechanism of prolongation of STAT1 signalling and the expression of IFN-induced genes, apart from its phosphorylation.<sup>202</sup>

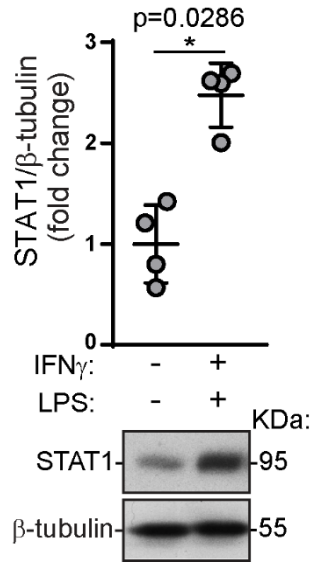


**Figure 36. IFN- $\gamma$  and LPS co-stimulation increases STAT1 total protein levels.** Male VIC were treated with IFN- $\gamma$ +LPS for 24 h and whole cell lysates analysed by Western Blot. Representative blot and densitometric analysis of n=4. Doses, n, statistics, and symbols as in Figure 2.

### R.3.2-IFN- $\gamma$ treatment induces a pro-angiogenic phenotype in male VIC

Because HIF-1 $\alpha$  is the master transcription factor for angiogenesis, we next explored its downstream molecules and their involvement on VIC responses. Among the molecules downstream of HIF-1 $\alpha$  with a crucial role on angiogenesis is VEGF-A, whose expression is increased in calcified valves.<sup>107</sup> We found that VEGF-A was secreted by male VIC in response to IFN- $\gamma$ , LPS, and the combination of both stimuli (**Figure 37A**). Additionally, significant sex-differences were observed since IFN- $\gamma$  did not induce VEGF-A secretion in female cells, which also displayed lower secretion upon IFN- $\gamma$ +LPS treatment (**Figure 37A**). In keeping with JAK and HIF-1 $\alpha$ -mediated effects, pharmacological intervention with ruxolitinib and PX-478 blocked VEGF-A secretion induced by IFN- $\gamma$ +LPS in male VIC (**Figure 37B**).

To confirm the pro-angiogenic state induced by stimuli in VIC, we also explored the expression of the anti-angiogenic gene *CNMD*, which is known to maintain the valvular function by preventing angiogenesis.<sup>105</sup> As shown in **Figure 37C**, *CNMD* expression was significantly reduced upon treatment with IFN- $\gamma$  alone or combined with LPS in male VIC. Additionally, female VIC showed a high variation in the response but not statistically significant differences between activated and untreated conditions (**Figure 37C**). Together, data suggest that IFN- $\gamma$ +LPS treatment triggered pro-angiogenic effects in VIC with the involvement of JAK and HIF-1 $\alpha$  pathways and sex-differential responses.

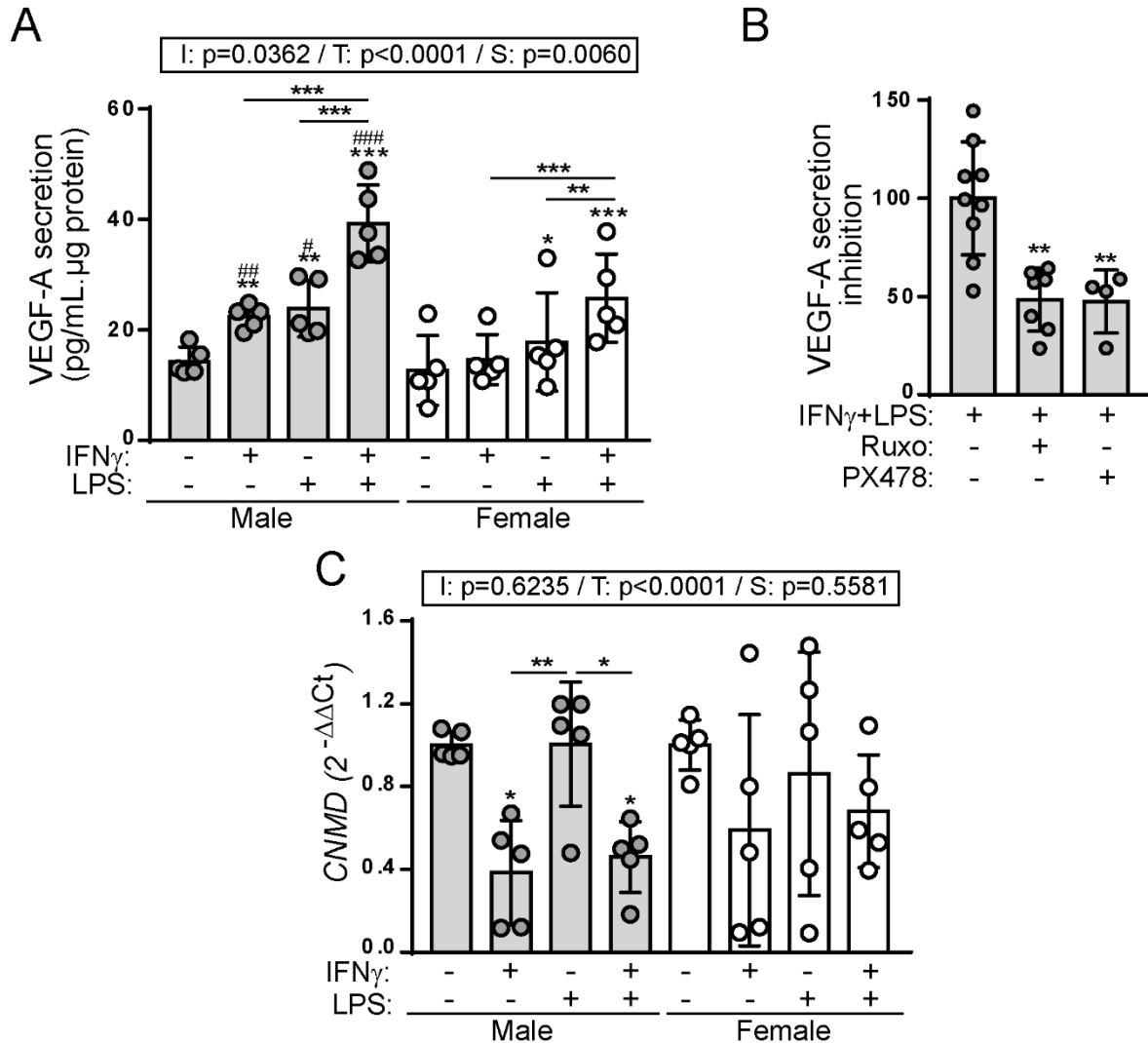


**Figure 37. IFN- $\gamma$  induces a pro-angiogenic phenotype potentiated by LPS via HIF-1 $\alpha$  in male VIC.** (A) Male and female VIC were treated with the indicated ligands for 48 h and supernatants collected for assaying VEGF-A secretion; n=5. (B) Male cells were pre-treated or not with ruxolitinib or PX-478 before activation and VEGF-A secretion was quantitated as in A; n=5-7. Data were normalized to IFN- $\gamma$ +LPS value (100%). (C) Male and female VIC were treated for 24 h and *CNMD* gene expression was assessed by qPCR; n= 5 for each group. Doses, colour code, symbols, n, and statistics as in Figure 7.

### R.3.3-Chemical stabilization of HIF-1 $\alpha$ increases VIC calcification

To elucidate the role for HIF-1 $\alpha$  on calcification, we performed calcification assays exposing cells to CoCl<sub>2</sub>. The chemical induction of HIF-1 $\alpha$  significantly increased calcification levels in VIC, although it was less potent than the immune stimulation with IFN- $\gamma$ +LPS (Figure 38A-C). These data disclosed a role for HIF-1 $\alpha$  on the induction of VIC calcification.

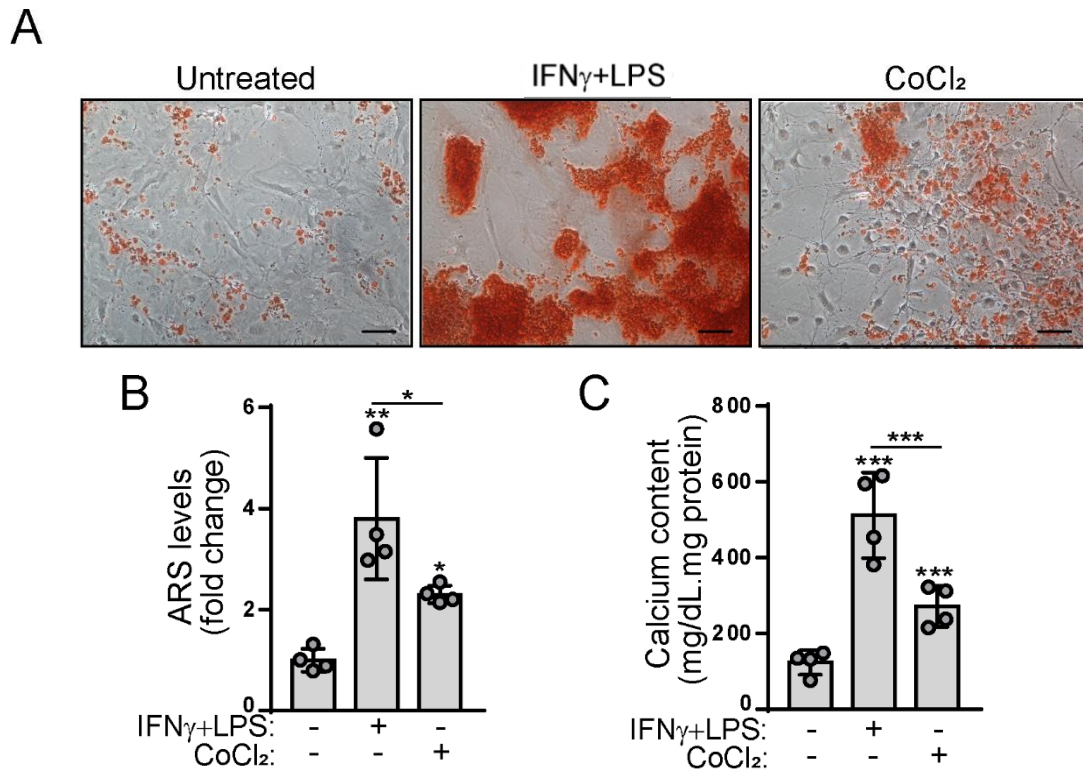


**Figure 38. Chemical induction of HIF-1 $\alpha$  increases VIC calcification levels.** Male VIC were treated with either IFN- $\gamma$ +LPS or CoCl $_2$  for 7 days in calcifying medium. (A-B) Representative microphotographs (A) and quantification of the relative ARS levels (B); n=4. (C) Calcium deposits measurements; n=4. Doses were as in Figure 34. Statistics, n and symbols as in Figure 2.

### R.3.4-Signalling pathways involved in sex-differences upon IFN- $\gamma$ +LPS treatment

Next, we explored the signalling pathways that could account for sex differences in VIC responses to IFN- $\gamma$ +LPS. We found that the ERK was differentially activated in male and female cells, the former ones having a statistically greater phosphorylation of these kinases (**Figure 39A**), which have been previously described as pro-calcifying pathways in the valve context.<sup>91,166</sup>

Given the differences on the pro-angiogenic profile between male and female VIC (**Figure 37**), we also explored potential sex differences on HIF-1 $\alpha$  induction as the upstream explanation. Strikingly, after 48 h, IFN- $\gamma$ +LPS treatment resulted in a greater induction of HIF-1 $\alpha$  in male cells (**Figure 39B**), thus confirming sex differences at this level.

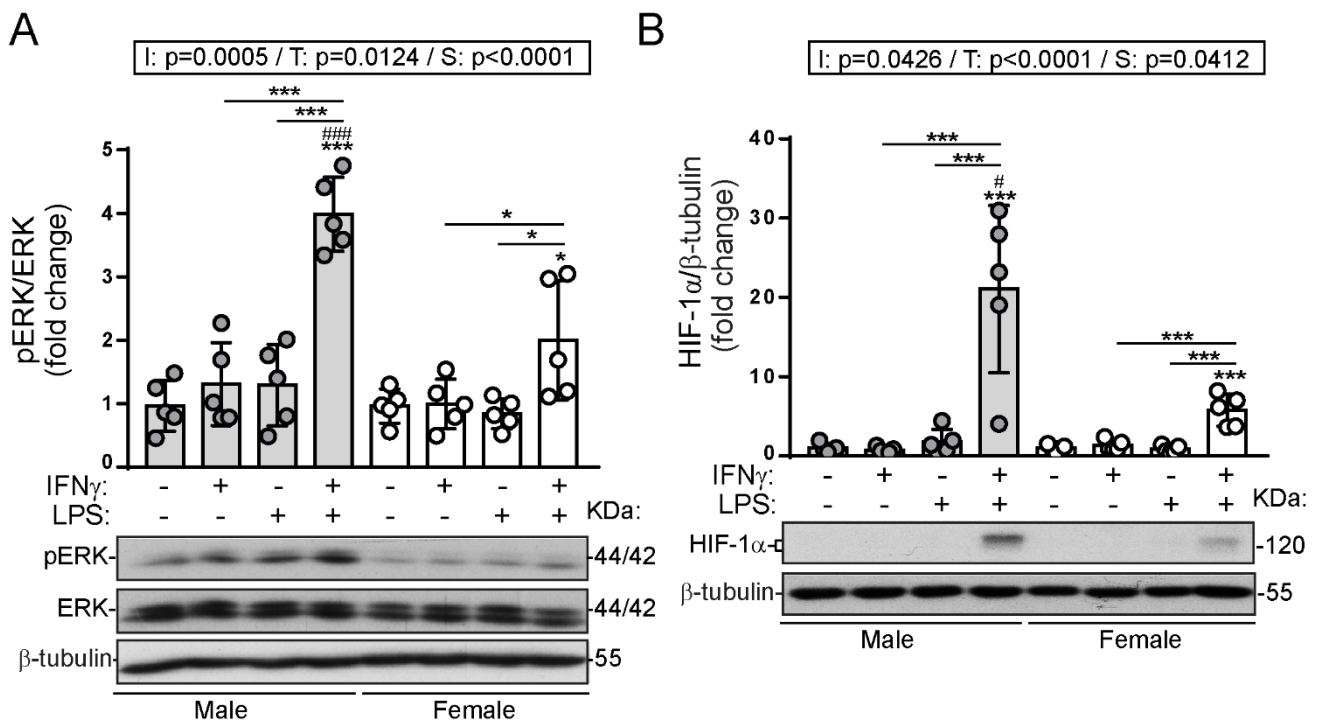


**Figure 39. HIF-1 $\alpha$  and ERK are preferentially activated in male VIC upon IFN- $\gamma$  and LPS treatment.** Male and female VIC were treated with the indicated ligands for 24 h (A) or 48 h (B) and whole cell lysates analysed by Western blot. (A) Representative blot of ERK phosphorylation and densitometric analysis of the bands normalized to total ERK content; n=5. (B) Representative blot of HIF-1 $\alpha$  protein induction and densitometric analysis of n=5. Doses, statistics, n, and symbols as in Figure 7.

Based on the differential activation of ERK and HIF-1 $\alpha$ , we aimed to determine their role on VIC calcification. A pharmacological approach disclosed that inhibition of HIF-1 $\alpha$  by PX-478 and ERK activation blockade with PD98059 decreased the calcification levels induced by IFN- $\gamma$ +LPS (**Figure 40A-C**). Data obtained with the HIF-1 $\alpha$  inhibitor are in line with the increased calcification showed upon chemical stabilization of HIF-1 $\alpha$  with CoCl<sub>2</sub> (**Figure 38**) and suggest a role of HIF-1 $\alpha$  on the immune-induced calcification. Altogether, these data suggest that the sex-biased activation of ERK and HIF-1 $\alpha$  may be mechanisms accounting for the differential calcification levels in male and female VIC.

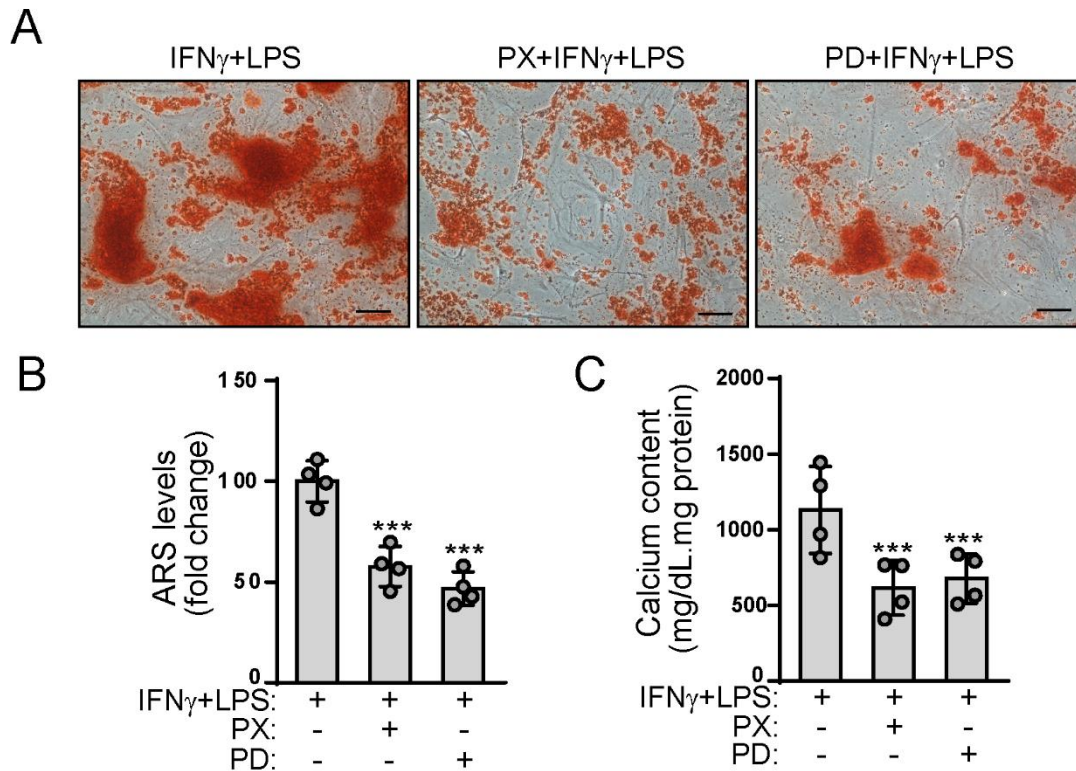


**Figure 40. HIF-1 $\alpha$  and ERK activation plays a role on the IFN- $\gamma$ +LPS-induced calcification.** (A-C) Male VIC were pre-treated with HIF and ERK inhibitors before activation in calcification medium for 9 days. Representative microphotographs (A) and quantification of ARS levels (B); n=4. Calcium deposits quantitation (C); n=4. PX indicates 40  $\mu$ M PX-478; PD, 50  $\mu$ M PD98059. Doses, statistics, n, and symbols as in Figure 2.

### R.3.5-Mechanistic differences of IFN in osteogenic differentiation

Previous data have shown common effects of IFN- $\alpha$  and IFN- $\gamma$  including the induction of marked morphological changes and a pro-calcifying phenotype in VIC (**Figures 13-16**), although some differences were observed. Additionally, data shown in **Figure 26** demonstrated a role of BMP-2 on IFN- $\alpha$ -induced calcification. These findings prompted us to explore whether the osteogenic phenotype triggered in VIC by IFN- $\gamma$  was also dependent on the BMP-2 pathway. Strikingly, IFN- $\gamma$  alone and combined with LPS strongly induced *BMP2* gene expression with marked sex-differences upon IFN- $\gamma$ +LPS treatment, since male VIC exhibited significantly higher levels of transcripts (**Figure 41A**). However, in contrast to IFN- $\alpha$  (**Figure 26**), no BMP-2 secretion was detected after IFN- $\gamma$ +LPS treatment for 24h (**Figure 41B**). Data suggest differences between IFN in the regulation of the expression and/or secretion of BMP-2 in VIC.

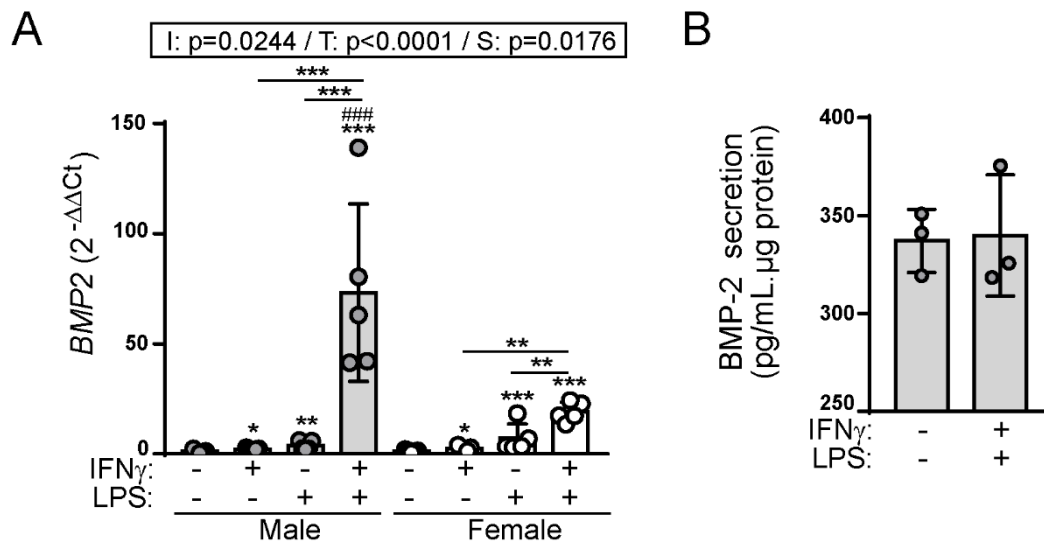


**Figure 41. Induction of *BMP2* gene expression but not BMP-2 secretion by IFN- $\gamma$  and LPS.** Male and female VIC were treated the indicated ligands for 24 h. (A) mRNA was extracted for *BMP2* gene expression analysis. Representative of n=5. (B) Supernatants from male VIC were analysed for BMP-2 secretion at 24 h; n=3. Doses, n, statistics, and symbols as in Figure 7.

This striking finding led us to think that type I and type II IFN could be driving VIC differentiation towards distinct osteogenic pathways. To confirm this hypothesis, different genes involved in osteo-chondrogenic differentiation were analysed by qPCR. Data shown in **Figure 42A** revealed that IFN- $\alpha$  upregulated *RUNX2* gene expression at 24 h, whereas IFN- $\gamma$  exhibited opposite effects. The gene profiling analysis also disclosed differences between IFN for the expression of the chondrogenic transcription factor *SRY-related high mobility group-box gene 9 (SOX9)* as well as the chondrocyte extracellular matrix *aggrecan (ACAN)* genes, which were upregulated by IFN- $\alpha$ , but not by IFN- $\gamma$  (**Figure 42A**).

Additionally, we found a different effect of type I and II IFN on *BCL2* expression, arguing for potential differences in the regulation of apoptosis (**Figure 42B**). Collectively, these data indicate mechanistic differences of IFN on osteogenic differentiation and apoptosis in human VIC.

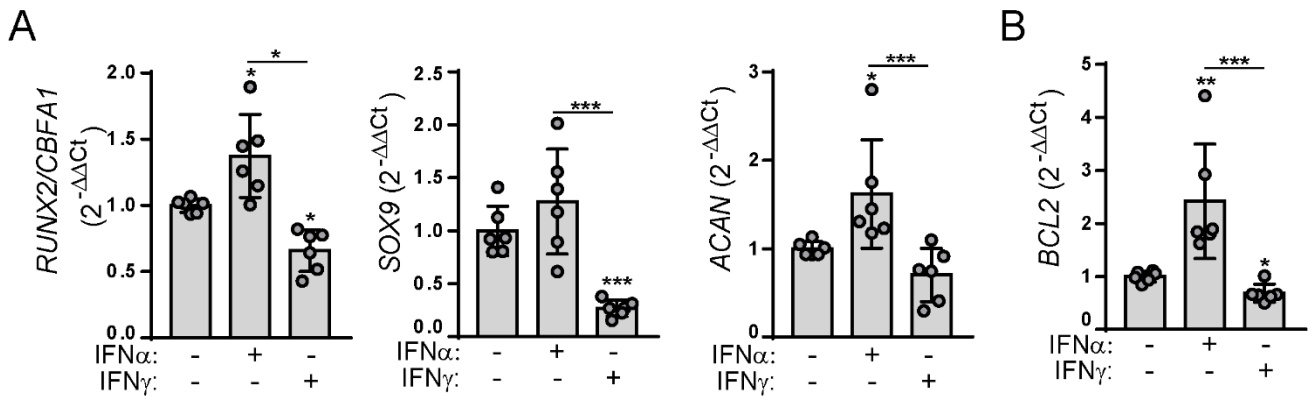


**Figure 42. IFN- $\gamma$  and IFN- $\alpha$  trigger different osteogenic and apoptotic profiles in VIC.** (A-B) Male cells were treated with IFN for 24 h and analysed by qPCR for the expression of the indicated differentiation markers (A) as well as *BCL2* gene (B); n=6. Doses, statistics, n, and symbols as in Figure 2.

Finally, based on the sex-specific differences observed, we also explored potential intrinsic sex dissimilarities in gene expression of IFN receptors and antiapoptotic genes. The gene profiling analysis of male and female VIC from control valves revealed that the levels of *IFNGR1* transcripts were greater in male VIC. In contrast, female VIC presented higher basal levels of the anti-apoptotic gene *BCL2* (Figure 43A-B).

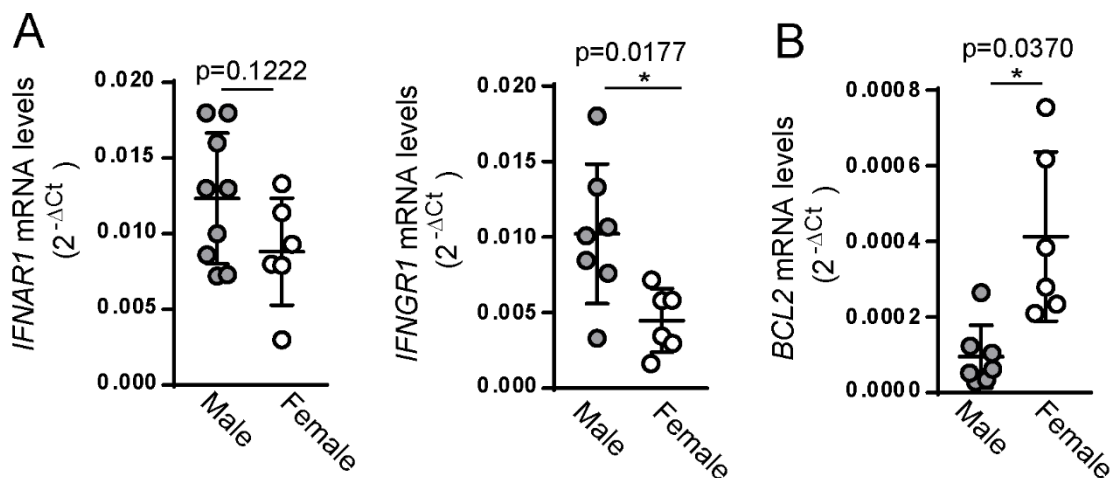


**Figure 43. Intrinsic differences among control male and female VIC in *IFNGR1* and *BCL2* expression.** Basal expression levels of male and female control VIC were analysed by qPCR; n=6-7 in each group. Grey dots, control male VIC; white dots, control female VIC.

In conclusion, the major findings of this section include the demonstration of a non-hypoxic and immune induction of HIF-1 $\alpha$  in VIC upon concomitant activation of IFNGR and TLR4 pathways with consequences in the induction of a pro-angiogenic and pro-osteogenic phenotype. Strikingly, male cells showed higher *IFNGR1* expression and exhibited greater responses to IFN- $\gamma$ +LPS, being HIF-1 $\alpha$  and ERK signalling involved on the sex-differences.

## **R.4-Correlation of IFN findings in intact valve tissue**

In this part of the study, major findings from sections R.2 and R.3 disclosed in cultured valve cells, were evaluated in valve tissue. For this purpose, we analysed non-calcified valves from males, and calcified valves from males and females (**Table 9**). As shown in the table, clinical features and comorbidities were similar between sex groups except for hypertension, which was significantly higher in female than in male with CAVD. All patients were Caucasian, and all female donors were post-menopausal.

**Table 9: Clinical features of the patients whose valves were included in the section 4 of the study.**

Patient characteristics	Control valves	Calcified valves		p-value
	Male n=6	Male n=9	Female n=9	
Age (Range)	56 ± 9	77 ± 3	80 ± 4	0.20
Hypertension	1 (16%)	3 (33%)	8 (88%)	*0.04
Hypercholesterolemia	1 (16%)	3 (33%)	2 (22%)	0.59
Diabetes mellitus	0	2 (22%)	2 (22%)	1.00
Smoking	0	3 (33%)	0	0.05
Renal failure	0	1 (11%)	0	0.30
Aetiology of heart failure	3 ischemic, 2 idiopathic, 1 hypertrophic	-	-	-
Aortic valve area (cm <sup>2</sup> )	-	0.75 ± 0.11	0.67 ± 0.12	0.4870
Peak gradient (mmHg)	-	68.7 ± 18.77	73.5 ± 15.9	0.6270
Mean gradient (mmHg)	-	42.4 ± 14.88	42.4 ± 8.9	0.9834
Statins	-	4 (44%)	5 (55%)	0.63

### R.4.1-Expression of IFN receptors, HIF-1 $\alpha$ and related molecules in control and calcified valves from males

We have previously shown that the expression levels of *IFNGR1*, but not *IFNAR1*, were upregulated in calcified valves compared to control valves (**Figure 1B**). Since previous findings pointed to a role of HIF-1 $\alpha$  and downstream molecules on the IFN- $\gamma$ -mediated pro-angiogenic and calcific phenotypes in activated control VIC (**Figure 37, 39-40**), we explored whether those genes were altered in CAVD. In keeping with a report detecting HIF-1 $\alpha$  expression and co-localization with calcific nodules in human valve tissue by immunohistochemistry,<sup>107</sup> Western blot data confirmed that this transcription factor is expressed in tissue homogenates from calcified valves (**Figure 44A**). In addition, qPCR analysis of valve tissue showed that the mRNA levels of *HIF1A* (**Figure 44B**) and the angiogenic molecule *VEGFA* (**Figure 44C**) genes were upregulated in calcified valves as compared to non-stenotic valves. In contrast, the expression of the anti-angiogenic gene *CNMD* was higher in control valves (**Figure 44D**). Together, the pro-angiogenic profile of calcified valves correlate with the one induced in cultured VIC exposed to IFN- $\gamma$ +LPS.

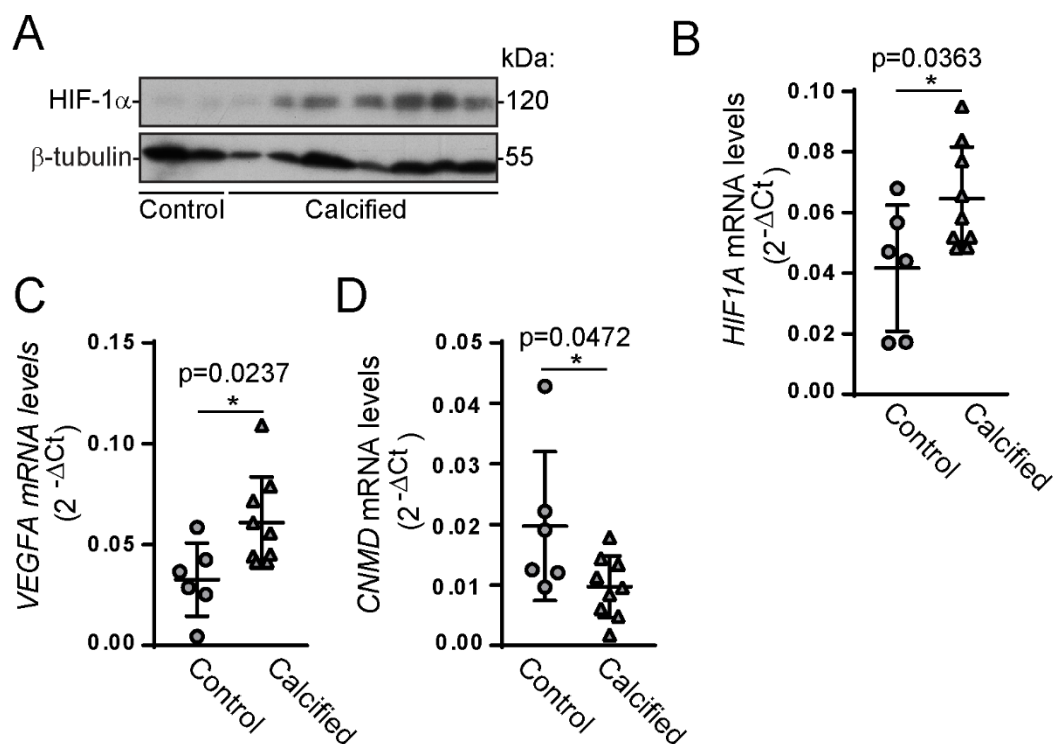


**Figure 44. Calcified valves exhibit HIF-1 $\alpha$  expression and a greater pro-angiogenic gene expression profile compared to control valves.** (A-D) Valve tissue from control and calcified male valves was homogenized for protein (A) or mRNA analysis (B-D); n=6 control valves, 9 calcified valves. Grey dots, control male valve tissue; grey triangles, calcified male valve tissue. \* indicates statistical significance. \*p<0.05.

## R.4.2-Intrinsic sex-differences in calcified valve tissue

Our next step was to explore whether the sex-differential mechanisms in control VIC correlated with different profiles on calcified tissue from male and female patients. Unfortunately, the comparison between sexes in control valves could not be performed due to the low number of female control valve tissue specimens available.

Regarding sex differences in the response to IFN uncovered in R.1 and 2 sections, we found a higher expression of *IFNAR1* in calcified valves from males (**Figure 45A**). Based on sex-specific differences in cell survival observed in VIC, we also evaluated apoptosis-related proteins in stenotic valve tissue. The mRNA levels of *AKT1* did not significantly differ between males and females (**Figure 45B**). However, the expression of the anti-apoptotic gene *BCL2* was increased in female tissue (**Figure 45C**), thus correlating with the resistance to apoptosis and the activation of survival pathways observed in cultured female VIC (**Figures 19-20, 28-29**).

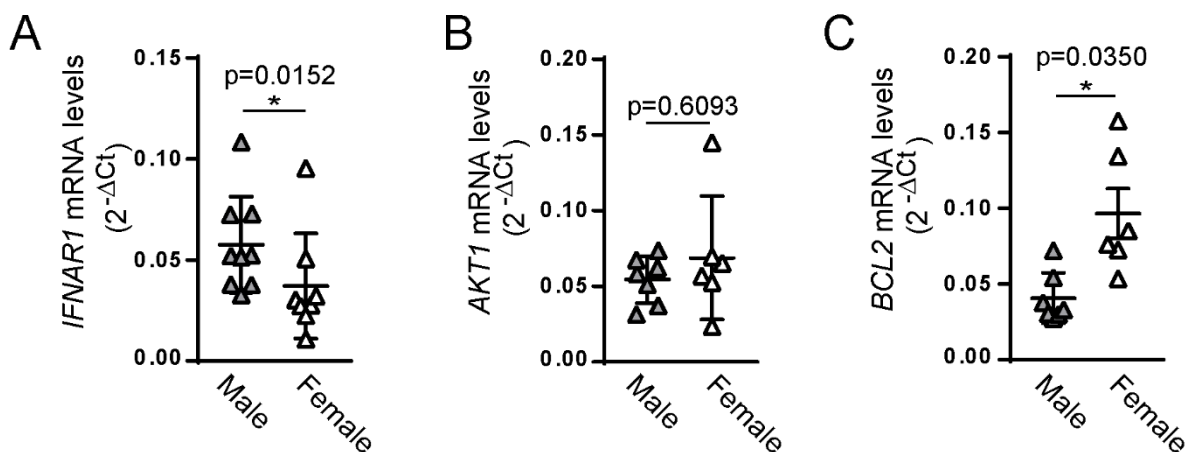


**Figure 45. Sex differences in IFN receptors and survival-related proteins in calcified valve tissue.** (A-C) Tissue homogenates from male and female calcified valves were used for mRNA analysis of the indicated genes; n=9 in each group. Grey triangles calcified male valve tissue; white triangles, calcified female valve tissue. \*p<0.05.

Next, we analysed the expression of type II IFN receptor and pro-angiogenic molecules related with the sex dissimilarities found in the section R.3 of the study. Gene profiling analysis disclosed a higher expression of *IFNGR1* in calcified valves from males (**Figure 46A**), thus mirroring with IFN- $\gamma$ -mediated effects more potent in male VIC. The data also disclosed similar levels of *HIF1A* transcripts between sexes (**Figure 46B**). Conversely, higher levels of the proangiogenic gene *VEGFA* were detected in male valves (**Figure 46C**).

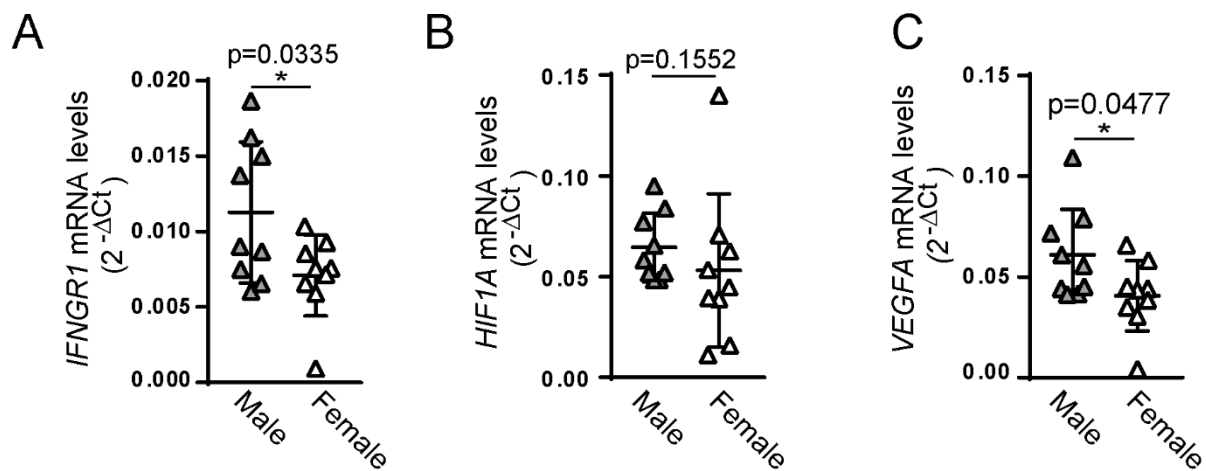


**Figure 46. Sex differences in *IFNGR* and angiogenesis-related genes in calcified tissue.** (A-C) Tissue homogenates from male and female calcified valves were used for mRNA analysis of the indicated genes; n=9 for each group. Symbols and statistics as in Figure 45.

We also studied the protein levels of two relevant transcription factors for the IFN-mediated effects in VIC, namely STAT1 and HIF-1 $\alpha$ . Western Blot analysis of tissue homogenates showed that the expression of HIF-1 $\alpha$  was variable between samples from males and females, and its basal expression showed no apparent significant differences between sexes (**Figure 47A-B**). Although, it should be noted the low number of female available for this analysis and we cannot rule out possible technical issues that may affect HIF-1 $\alpha$  protein stability. Remarkably, total STAT1 protein levels were significantly higher in valve tissue homogenates from males (**Figure 47B**), consistent with the higher IFN-mediated effects in male VIC.

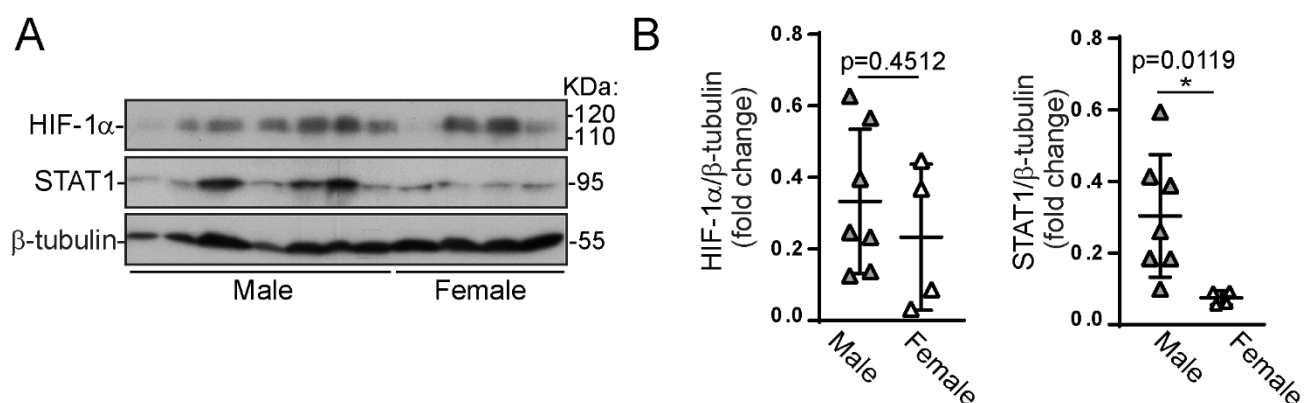


**Figure 47. Sex differences in STAT1 protein levels and variable expression of HIF-1 $\alpha$  among calcified valves.** (A-B) Tissue homogenates from male and female calcified valves were analysed for protein expression. Representative blot (A) and densitometric analysis of the indicated proteins; n $\geq$ 4 in each group. Symbols and statistics as in Figure 45.

We finally explored the expression of inhibitors of calcification (*MGP*) and angiogenesis (*CNMD*) downregulated in VIC upon IFN treatment (**Figures 14B and 37C**). We found that the

expression of both inhibitors was higher in female calcified valves (**Figure 48A-B**). These data support the notion of the maintenance of protective mechanisms in female valves, which correlates with the increased downregulation of these genes in male VIC upon stimulation with inflammatory molecules.

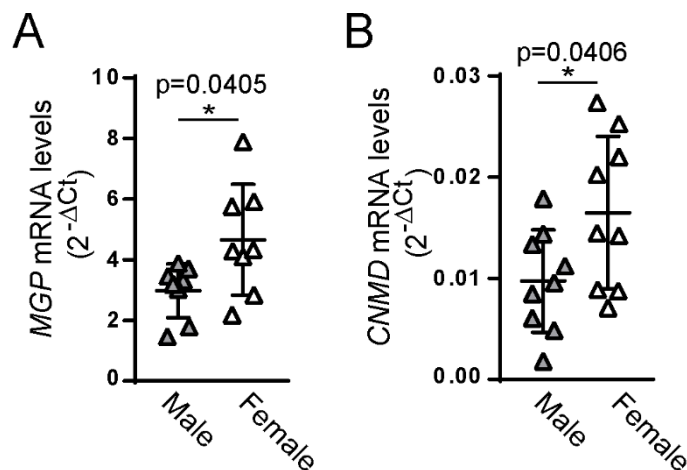


**Figure 48. Sex differences in anti-calcification and anti-angiogenic genes among calcified valves.** (A-B) Tissue homogenates from male and female calcified valves were used for mRNA analysis of the indicated genes; n=9 for each group. Symbols and statistics as in Figure 45.

Altogether, the data on this chapter show basal differences between male control and calcified valves that correlate to findings on cultured VIC activated with IFN. Moreover, data argue for some intrinsic differences between sexes in valves. Sex differences in the response of control VIC to IFN also correlate with some findings in calcified valves such as lower *MGP* and *CNMD* in females and higher *VEGFA* in males. In addition, *STAT1* protein levels are higher in calcified valves from males, suggesting a potential role for JAK/STAT on sex-differences in CAVD. Collectively, these intrinsic differences suggest protective or delaying mechanisms in females that could explain the sex-differential clinical outcomes. However, these findings warrant further investigation with more accurately techniques such as immunohistochemistry or transcriptomic/proteomic analysis.

## **R.5-Type I IFN signalling mediates Poly(I:C) effects in VIC**

In this section of the study, the evaluation of TLR3 signalling and interplay with IFN pathways was performed in VIC from control non-mineralized male valves. **Table 10** includes the characteristics of all the patients, which were all Caucasian.

**Table 10: Clinical features of the patients whose valves were included in this section of the study.**

	<b>Control valves</b>
<b>Patient characteristics</b>	<b>Male n=9</b>
<b>Age (Range)</b>	57 ± 9
<b>Hypertension</b>	1 (11%)
<b>Hypercholesterolemia</b>	2 (22%)
<b>Diabetes mellitus</b>	0 (0%)
<b>Smoking</b>	0 (0%)
<b>Renal failure</b>	0 (0%)
<b>Aetiology of heart failure</b>	5 idiopathic, 3 ischemic, 1 hypertrophic

### **R.5.1-dsRNA treatment activates IFN signalling in VIC**

Emerging evidences point to an important role of viral or cell-derived dsRNA in cardiovascular diseases.<sup>203</sup> Previous data from our group disclosed that the dsRNA analogous poly(I:C) promotes the secretion of inflammatory and anti-viral molecules by VIC, including IFN- $\beta$  and IFN-related proteins.<sup>164</sup> Additionally, Meng and colleagues have recently demonstrated that poly(I:C)-induced inflammatory and osteogenic effects are mainly mediated by the TLR3-IRF3 axis on VIC,<sup>204,205</sup> although the underlying mechanisms are not well understood. Our data from **sections R.1 and R.2** demonstrated that type I IFN promote inflammatory and osteogenic responses in VIC. Based on these evidences, we hypothesized that TLR3 effects are mediated by type I interferon secretion and the ensuing activation of JAK/STAT pathways.

First, we tested the overall effects of dsRNA in VIC using Poly(I:C) as a potent inducer of TLR3 activation. In addition, we also explored a potential TLR3-IFN- $\gamma$  interplay. The MTT assay showed that Poly(I:C) significantly reduced VIC proliferation after long-term treatment (**Figure 49A**), in contrast to the TLR4 ligand LPS, which showed no significant effects in VIC growth (**Figure 13B**). In addition, qPCR analysis disclosed that Poly(I:C) treatment strongly increased *TLR3* expression, (**Figure 49B**), thus suggesting a potential autocrine loop promoting a prolonged activation.

Because Poly(I:C) is known to induce VIC calcification,<sup>164</sup> we explored pro-osteogenic and myofibroblast markers as indicators of cell differentiation. Poly(I:C) markedly increased *BMP2* expression, whereas it triggered the downregulation of the calcification inhibitor *MGP* and the myofibroblast marker *ACTA2*, although no interplay with IFN- $\gamma$  was observed (**Figure 49C**). These findings are consistent with a dsRNA-mediated induction of VIC differentiation. Strikingly, data resemble the IFN- $\alpha$ -induced effects, which were characterized by BMP-2 upregulation (**Figure 26**), proliferation inhibition (**Figure 13**), and *MGP* gene and  $\alpha$ -SMA protein expression downregulation (**Figures 14 and 23**).

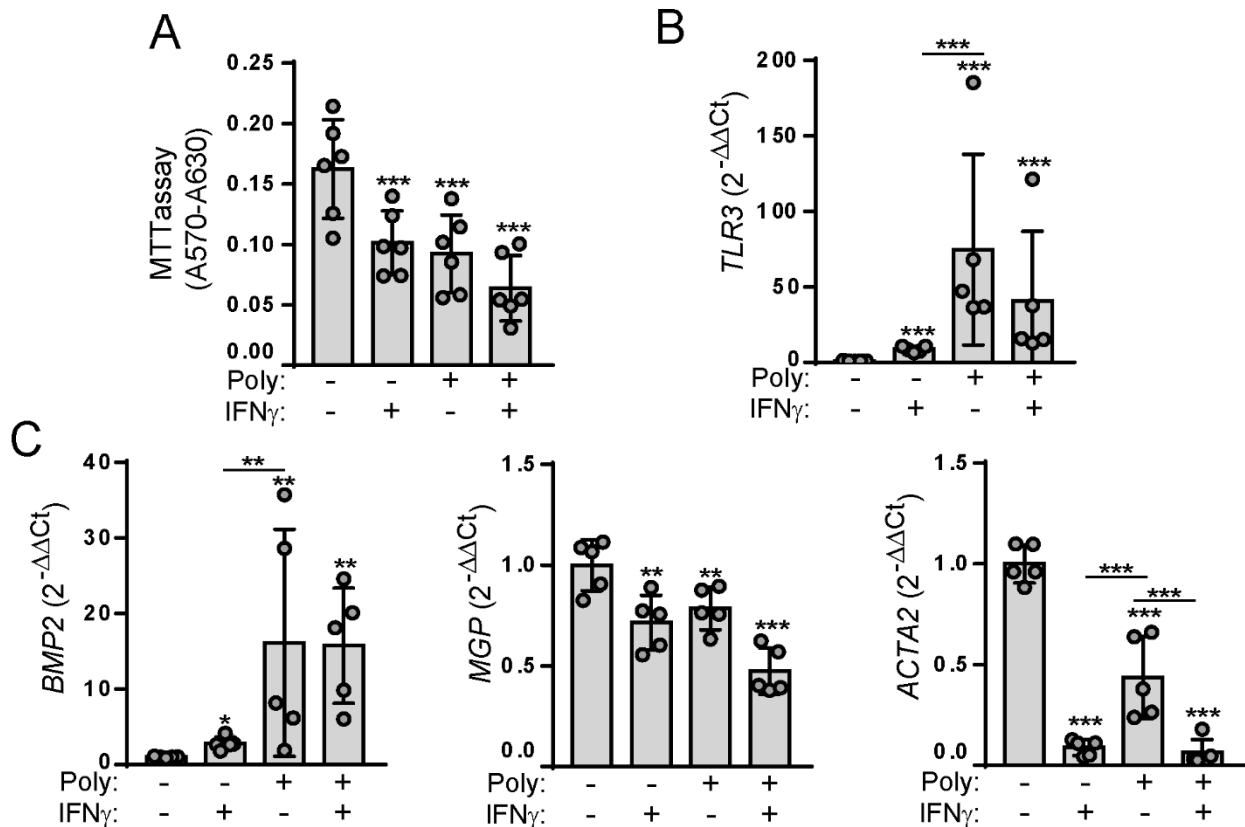


**Figure 49. Poly(I:C) treatment reduces cell proliferation and promotes cell differentiation and TLR3 expression.** (A) Non-confluent cells were grown for 12 days, replacing medium and stimuli every 3 days; n=6 male VIC. (B-C) Male VIC were treated for 24 h with the indicated ligands and harvested for qPCR analysis of *TLR3* (B) and the indicated differentiation markers expression (C); n=4-5. Poly indicates 1  $\mu$ g/mL of polyinosinic:polycytidylic acid. IFN $\gamma$ , 100 ng/mL IFN- $\gamma$ . Doses, n, color code, and \* as in Figure 2.

Next, we sought to investigate whether Poly(I:C) could activate IFN-related signalling. Gene expression analysis revealed that VIC exposure to this ligand induced a strong upregulation on *IFNB1* gene expression (**Figure 50A**). The secretion of this cytokine was then assayed in supernatants from activated cells. Strikingly, Poly(I:C), as well as IFN- $\gamma$ , significantly induced IFN- $\beta$ 1 secretion, although no interplay between stimuli was observed (**Figure 50B**). Moreover, upregulation of IFN signalling was further demonstrated by analysing the expression of downstream transcription factors from the *IRF* family. As shown in **Figure 50C**, *IRF1*, 3 and 8 mRNA levels were significantly increased after Poly(I:C) treatment, although no interplay with IFN- $\gamma$  was found. Together, data disclose type I IFN secretion and the upregulation of IFN signalling molecules upon VIC exposure to synthetic dsRNA.

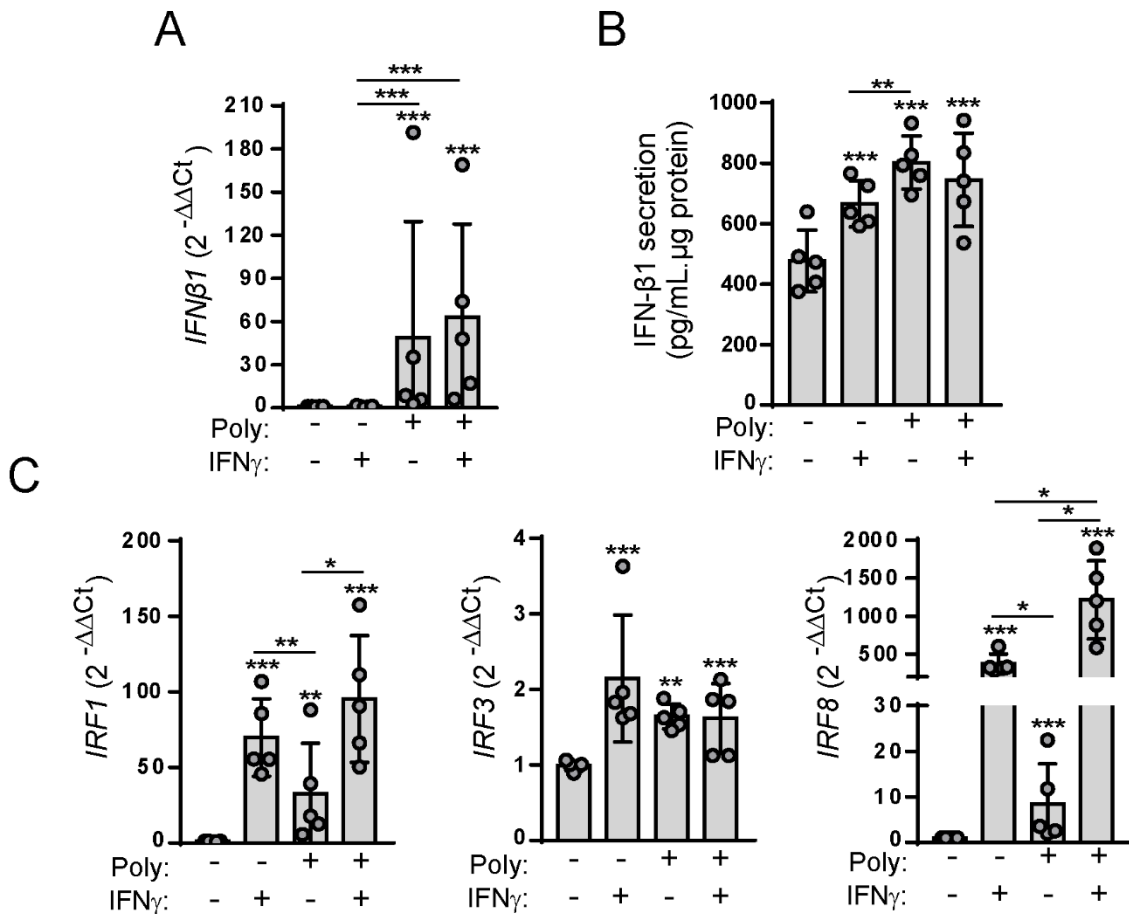


**Figure 50. Poly(I:C) treatment promotes IFN- $\beta$ 1 expression and secretion and IRF upregulation in VIC.** (A-C) Male VIC were treated with the indicated ligands for 24 h. mRNA was analysed for IFN-related genes by qPCR (A, C), and IFN- $\beta$  was assayed in cell supernatants by ELISA (B); n=5. Doses as in Figure 49; n, symbols, and statistics as in Figure 2.

Finally, we investigated IFN signalling cascade activation. As shown by Western Blot, TLR3 activation resulted in a marked phosphorylation of STAT1 (**Figure 51**). Strikingly, STAT1 activation was blocked by ruxolitinib, indicating a role of JAK signalling on the Poly(I:C)-mediated activation of STAT1. Overall, data demonstrate that a synthetic dsRNA triggers IFN- $\beta$  secretion and the subsequent activation of IFN-related signalling pathways in VIC.

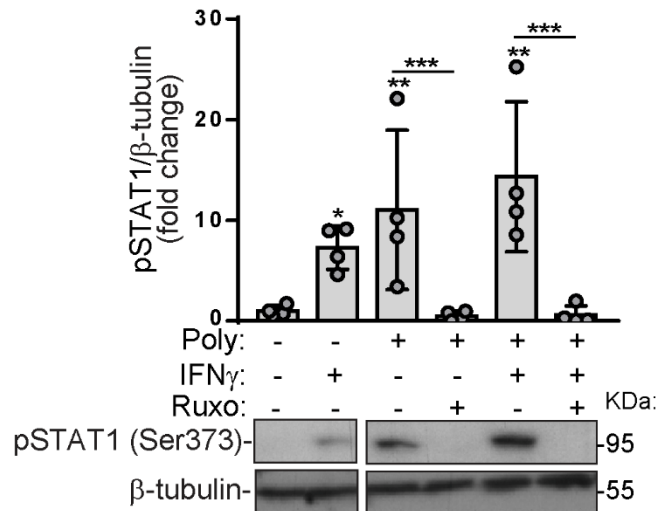


**Figure 51. Poly(I:C) treatment promotes STAT1 activation.** Male VIC were treated with the indicated ligands for 24 h and whole cell lysates analysed by Western Blot for STAT1 phosphorylation. Representative blot and densitometric analysis of n=4. Ruxo indicates 6  $\mu$ M ruxolitinib. Doses as in Figure 49; n, symbols, and statistics as in Figure 2.

### R.5.2-JAK/STAT signalling blockade reduced Poly(I:C)-induced effects

Given the previous findings, we sought to demonstrate a role for JAK/STAT signalling on the reported Poly(I:C)-induced responses in VIC, namely inflammation and calcification.<sup>164</sup> Initially, we studied the master transcription factor for inflammation and found that Poly(I:C) induced a strong activation of NF- $\kappa$ B (**Figure 52A**).

Then, we explored adhesion molecules downstream this factor. Our data confirmed that Poly(I:C) is a strong inducer of ICAM-1 (**Figure 52B**), as previously reported by our group,<sup>164</sup> and uncovered the upregulation of VCAM-1 protein levels (**Figure 52C**). Remarkably, the pre-treatment with ruxolitinib completely depleted the marked Poly(I:C)-mediated activation of NF- $\kappa$ B (**Figure 52A**), and strongly reduced adhesion molecule expression (**Figure 52B-C**). Together, data are consistent with JAK/STAT involvement in dsRNA-mediated pro-inflammatory responses in VIC.

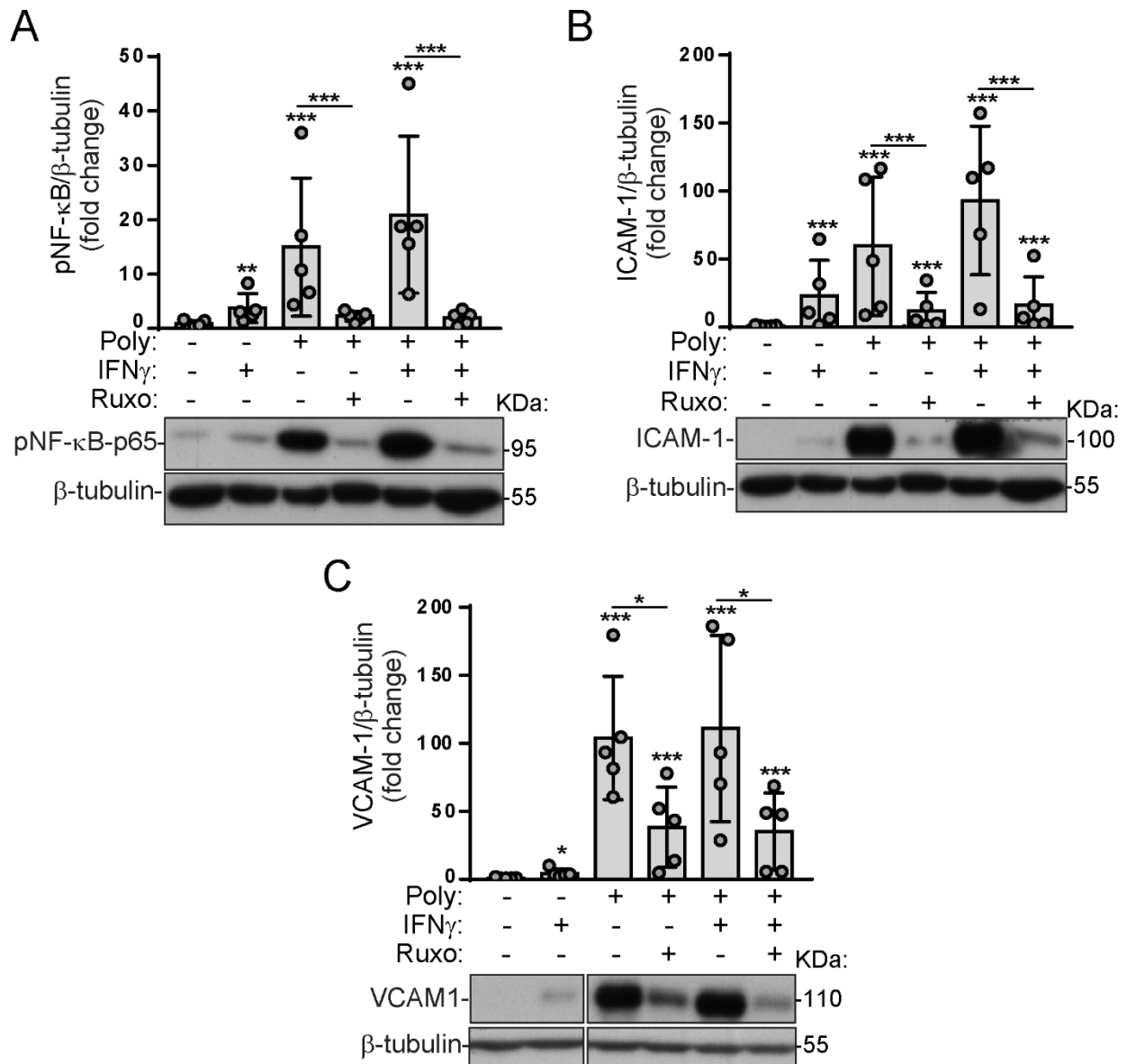


**Figure 52. Poly(I:C) treatment induces inflammatory molecules, being its effects reduced by ruxolitinib pre-treatment.** (A-C) Male VIC were treated with the indicated ligands for 24 h and whole cell lysates analysed by Western Blot for NF- $\kappa$ B activation (A) and adhesion molecule expression (B-C); n=4. Ruxo indicates 6  $\mu$ M ruxolitinib. Doses as in Figure 49; n, symbols, and statistics as in Figure 2.

Our group previously described the cytokine profile induced by Poly(I:C), which is characterized by IL-6 and 8 secretion as well as the secretion of an IFN-related cytokine, interferon gamma-induced protein 10 (IP-10), also known as C-X-C motif chemokine 10.<sup>164</sup> In this basis, we analysed whether JAK/STAT signalling activation mediates Poly(I:C)-induced cytokine profile. As shown in **Figure 53**, ruxolitinib pretreatment markedly abrogated IL secretion (**Figure 53A**) and completely depleted IP-10 secretion in VIC (**Figure 53B**), further demonstrating a role for JAK/STAT pathways in the inflammatory responses upon TLR3 activation.

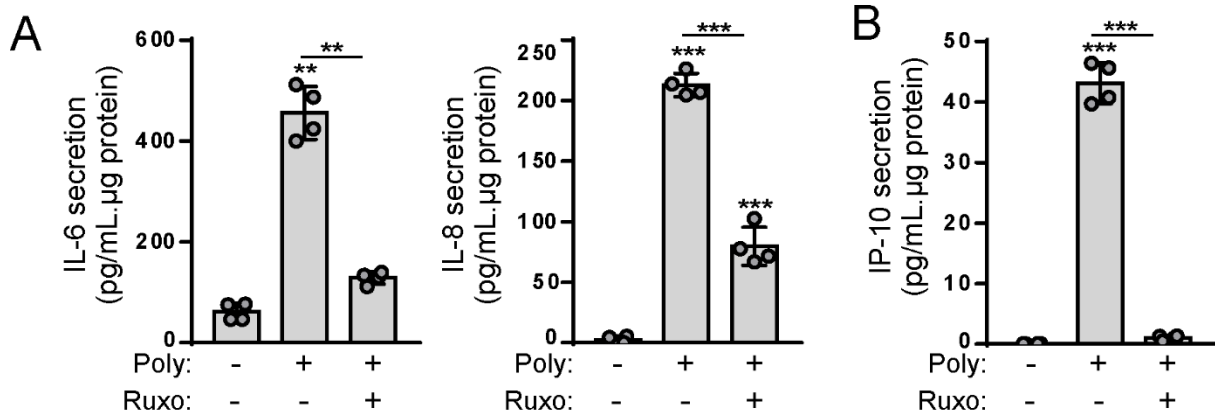


**Figure 53. Ruxolitinib pre-treatment blunts the Poly(I:C)-induced cytokine profile in VIC (A-B)** Male VIC were treated with the indicated ligands for 24 h and supernatants were collected to assess cytokine secretion; n=4. Ruxo indicates 6 µM ruxolitinib. Doses, symbols, n, and statistics as in Figure 2.

Our next step was to investigate the effects of Poly(I:C) on calcification under high phosphate conditions. Calcification assays revealed that Poly(I:C) is a strong inducer of VIC calcification, being its effects more robust than the induced by IFN- $\gamma$  (Figure 54A-C). To note, nodule formation and calcium deposition were observed at relatively short times (7-9 days) as compared to type I and type II IFN-mediated calcification (Figures 15-16). Strikingly, VIC calcification was strongly potentiated upon combination of Poly(I:C) with IFN- $\gamma$  (Figure 54A-C), thus indicating an interplay between Poly(I:C) and IFN- $\gamma$  on VIC calcification in high phosphate conditions.

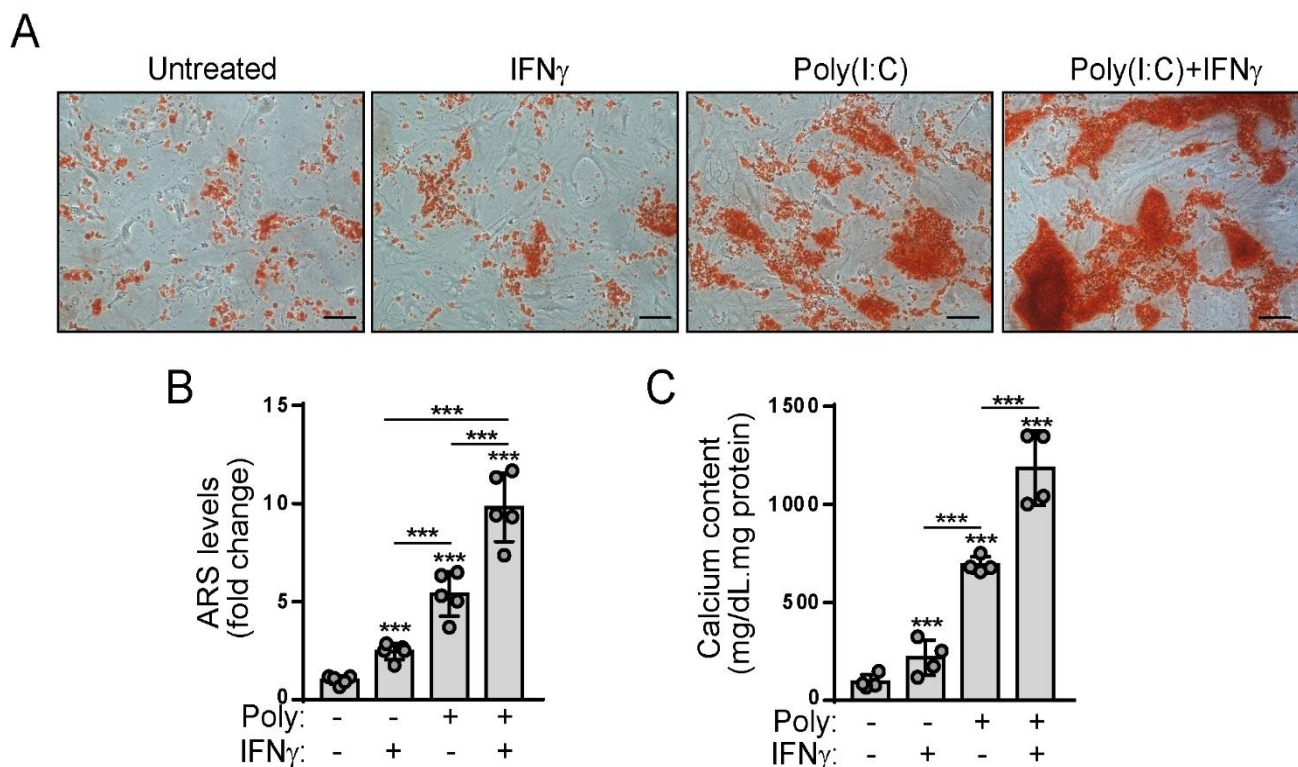


**Figure 54. Poly(I:C) treatment induces VIC calcification with further potentiation by IFN- $\gamma$ .** (A-C) VIC were treated with the indicated ligands for 9 days in calcification medium and mineralization was evaluated by ARS (A-B) and calcium deposits quantitation (C); n=4. Doses, symbols, n, and statistics as in Figure 2.

Finally, to elucidate the underlying mechanism, we investigated whether type I IFN signalling blockade blunts Poly(I:C)-induced calcification. Remarkably, a type I IFN receptor neutralising antibody (IFNAR Ab) markedly reduced both nodule formation and calcium deposition upon Poly(I:C) treatment, while an isotype control had no significant effects (**Figure 55**). These findings support a major role for IFNAR signalling on TLR3-induced calcification under high phosphate conditions and unravel a mechanism accounting for the TLR3 agonist Poly(I:C)-mediated effects in VIC via Type I IFN/JAK/STAT pathways.

Data in this section showed that Poly(I:C) exerts similar anti-proliferative, pro-inflammatory and pro-osteogenic effects to those observed with IFN- $\alpha$  (**sections R.1 and R.2**) and exhibited differences in cell proliferation as compared to the TLR4 ligand LPS. The major findings are that Poly(I:C) mediates its marked effects, at least in part, by triggering type I IFN secretion and signalling in VIC, subsequently promoting inflammation and calcification that can be blocked by type I IFN signalling inhibition. Moreover, data disclosed a positive cooperation with IFN- $\gamma$  on VIC calcification.

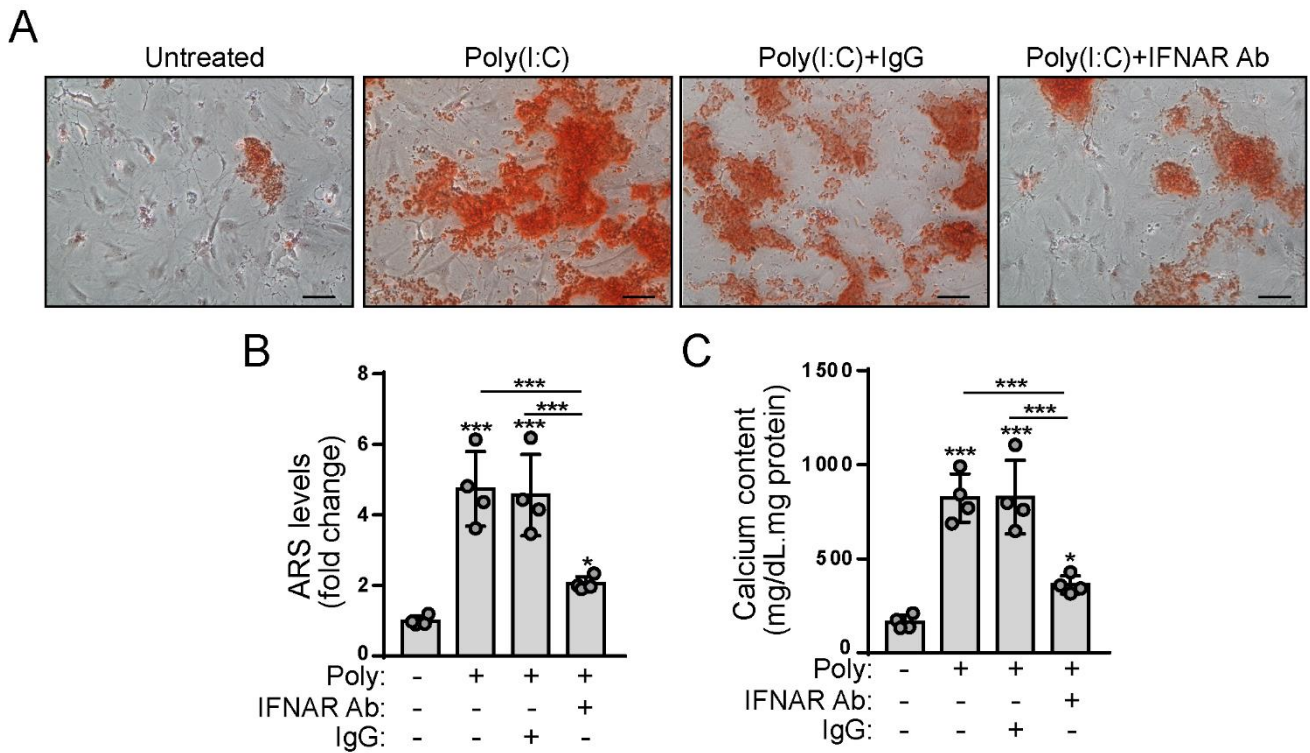


**Figure 55. Type I IFN receptor blockade strongly abrogates Poly(I:C)-mediated calcification.** (A-C) VIC were pre-treated with 5  $\mu\text{g}/\text{mL}$  of either IFNAR neutralising antibody (IFNAR Ab; 5  $\mu\text{g}/\text{mL}$ ) or its isotype control (IgG; 5  $\mu\text{g}/\text{mL}$ ) before activation with Poly(I:C) in calcification medium. ARS staining and quantitation (A-B) and calcium deposits measurement (C);  $n=4$ . Doses as in Figure 49, symbols,  $n$  and statistics as in Figure 2.

## **R.6-Relevance of IFN- $\gamma$ +LPS effects in the AV context and VEC side-specific effects**

### **R.6.1-Effects of secreted factors by VIC activated with IFN- $\gamma$ +LPS in VEC**

To investigate the relevance of IFN effects on AV physiopathology, we used VIC and VEC explanted from control male patients whose features are indicated in **Table 11**. It is important to note that VEC cultures used in these experiments consist of a mixed population of both aortic and *ventricularis* endothelial cells.

**Table 11: Clinical features of the patients whose valves were included in the section R.6.1 of the study.**

	<b>Control valves</b>
<b>Patient characteristics</b>	<b>Male n=6</b>
<b>Age</b>	59 $\pm$ 11
<b>Hypertension</b>	2 (33%)
<b>Hypercholesterolemia</b>	1 (16%)
<b>Diabetes mellitus</b>	1 (16%)
<b>Smoking</b>	0
<b>Renal failure</b>	0
<b>Aetiology of heart failure</b>	3 idiopathic, 3 ischemic

First, we investigated if supernatants from activated VIC could trigger VEC damage. For this purpose, VIC were previously treated as indicated in **Methods (Figure XIII)**, and conditioned medium from both untreated (untreated-CM) or activated (IFN- $\gamma$ +LPS-CM) VIC was collected. Next, VEC monolayers were exposed to either CM or to endothelial growth medium (Ctrl medium) for 24 h. Remarkably, CM from activated VIC promoted marked morphological changes on VEC, which were characterized by an enlarged shape as well as the loss of intercellular connections (**Figure 56A**). Conversely, VEC exposed to untreated-CM exhibited similar features than the ones cultured in control growth medium. Moreover, gene profiling analysis revealed genotypic changes in VEC. As shown in **Figure 56B**, CM from activated, but not untreated, VIC significantly induced *VEGFA* and *IL6* gene expression in VEC, consistent with a pro-angiogenic and pro-inflammatory gene profile. Finally, CM from activated VIC also promoted *NOS3* downregulation (**Figure 56B**), which has been previously related to an increase in oxidative stress and VIC calcification.<sup>50</sup>

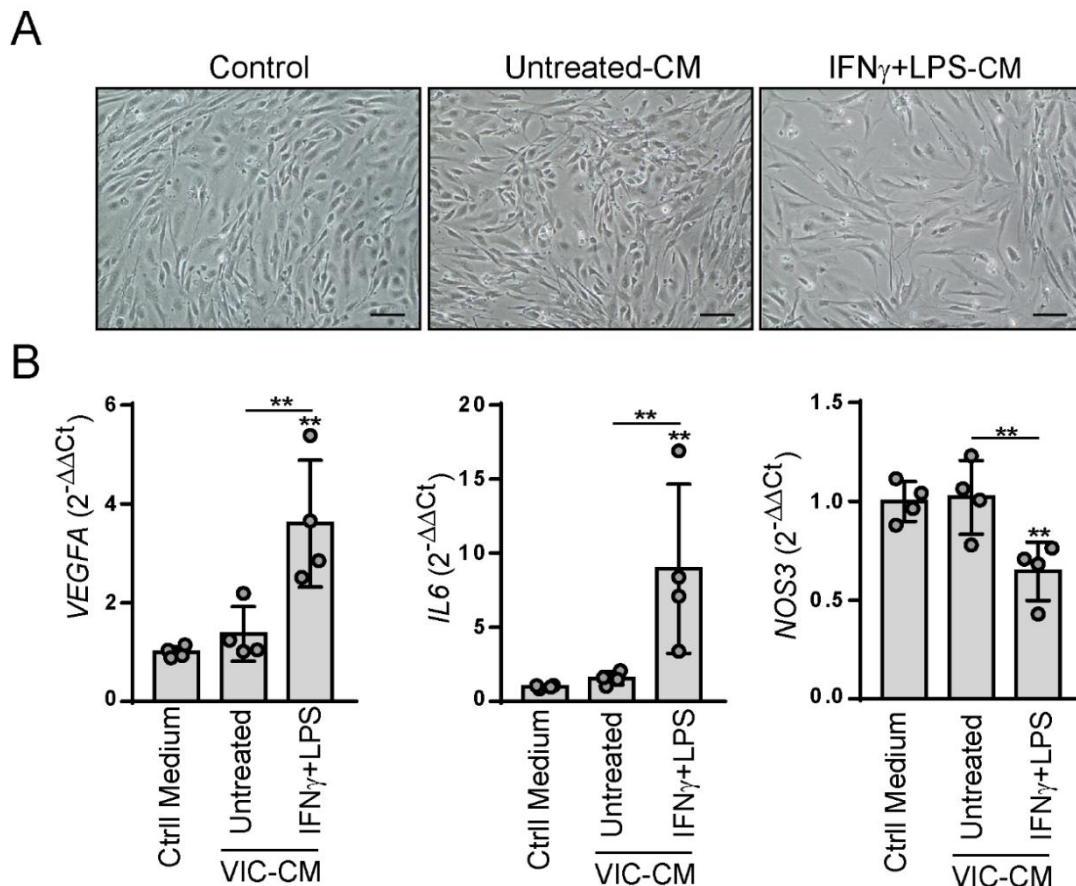


**Figure 56. VEC exposed to conditioned medium from activated VIC exhibit morphological and genotypic changes in genes associated to endothelial inflammation and damage.** (A-B) VEC monolayers were incubated with conditioned medium from untreated VIC (Untreated-CM) or treated VIC (IFN $\gamma$ +LPS-CM) for 24 h, or with VIC growth medium (Control, Ctrl medium). Representative microphotographs of cells (A) and qPCR analysis for the indicated genes (B); n=4. Black line indicates 50  $\mu$ M. Statistics and n as in Figure 2.

Finally, given the importance of immune cell infiltration in valves at early stages of CAVD,<sup>13</sup> the expression of adhesion molecule in VEC was investigated. Data revealed that both ICAM-1 and VCAM-1 protein levels were markedly increased upon treatment with IFN- $\gamma$ +LPS-CM (**Figure 57**).

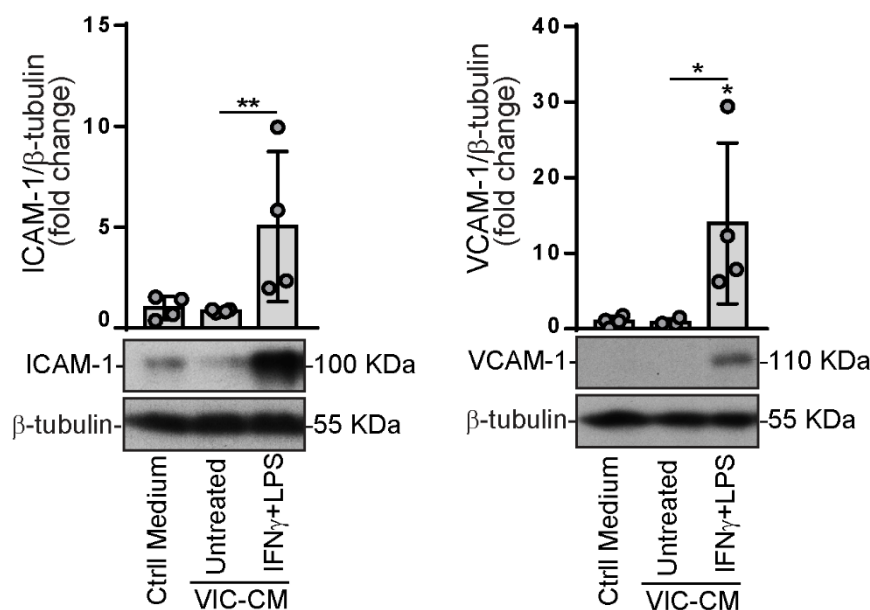


**Figure 57. VEC exposed to conditioned medium from activated VIC exhibited adhesion molecule upregulation.** VEC monolayers were incubated with conditioned medium from either untreated VIC (Untreated-CM) or treated VIC (IFN $\gamma$ +LPS-CM) or with VIC growth medium (Ctrl medium). Western Blot analysis of adhesion molecule expression in n=4 experiments. Doses, statistics, n, and symbols as in Figure 2.

Overall, data revealed a role of IFN- $\gamma$ +LPS-mediated secretion of factors in aortic valve physiopathology. The major findings are that IFN- $\gamma$ +LPS activated VIC secrete mediators promoting genotypic and phenotypic changes in VEC associated with endothelial inflammation and damage, which are key events in CAVD initiation.<sup>43,41</sup>

## R.6.2-Effects of IFN- $\gamma$ and TNF- $\alpha$ in side-specific VEC

The next part of the study was focused on the effects of IFN in VEC. We first checked whether mixed VEC populations from the aortic and ventricular side of the valve can sense both Type I and II IFN. qPCR analysis showed that VEC respond to recombinant IFN- $\alpha$  and IFN- $\gamma$ , both inducing *IL6* expression, whereas *IL8* expression was only induced by IFN- $\alpha$  (**Figure 58A**). We also found that IFN did not induce *VEGFA* expression (**Figure 58B**) but promoted *NOS3* gene expression downregulation (**Figure 58C**), which is associated to endothelial damage and oxidative stress.<sup>50</sup>

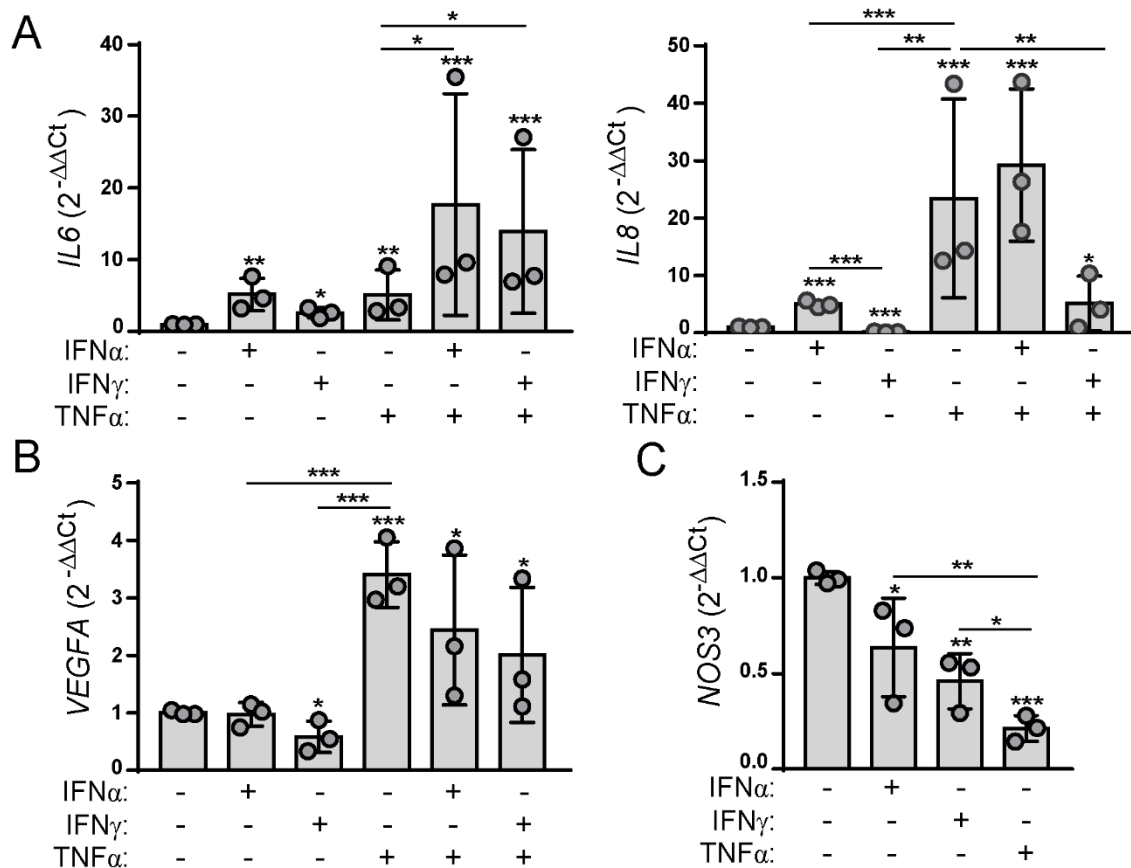


**Figure 58. Type I and II IFN induce cytokine expression and *NOS3* downregulation in mixed VEC populations.** VEC were isolated as indicated in Methods and challenged for 24 h with the indicated stimuli under static conditions. mRNA was extracted to assess *IL6*, *IL8*, *VEGFA* and *NOS3* gene expression; n=3. IFN $\alpha$  indicates 100 ng/mL IFN- $\alpha$ , IFN $\gamma$ , 100 ng/mL IFN- $\gamma$ ; TNF $\alpha$ , 5 ng/mL TNF- $\alpha$ . Statistics, and n as in Figure 2.

Based on the previous results, we next tested the effects of IFN in VEC isolated specifically from either the aortic (aVEC) or the ventricular side of the valve (vVEC). Growing evidence point to different behaviours of aVEC compared to vVEC, which has been related to the fibrosa layer preferential calcification.<sup>206,207,208</sup> However, potential side-specific differences in the response to inflammatory stimuli have not been addressed yet, which could shed light on VEC roles in the

disease pathogenesis and its underlying mechanisms. The next goal of the study was to explore putative side-differential effects of IFN- $\gamma$ , which is secreted by infiltrated T lymphocytes during CAVD,<sup>138</sup> and TNF- $\alpha$  in aVEC and vVEC. These experiments were performed at the Magdi Yacoub Institute under the supervision of Professor Sir Magdi Yacoub and Dr. Adrian H. Chester. To note, the non-mineralized valves were from deceased patients without valve disease. Initially, we investigated whether IFN- $\gamma$  induced adhesion molecule expression in side-specific VEC, and explored potential cooperation with TNF- $\alpha$ , which has been reported to promote inflammation and eNOS downregulation in VEC.<sup>52</sup> To simulate conditions that reproduce more accurately the physiological state, a swirling system previously reported in a vascular context was used.<sup>172</sup> Western Blot showed that IFN- $\gamma$  significantly induced ICAM-1 and VCAM-1 expression to the same extent in aVEC and vVEC under shear conditions, but did not potentiate the TNF- $\alpha$ -mediated effects. To note, we also tested the effects of chemical stabilization of HIF-1 $\alpha$  with CoCl<sub>2</sub>, which did not affect adhesion molecule expression in VEC (**Figure 59**).

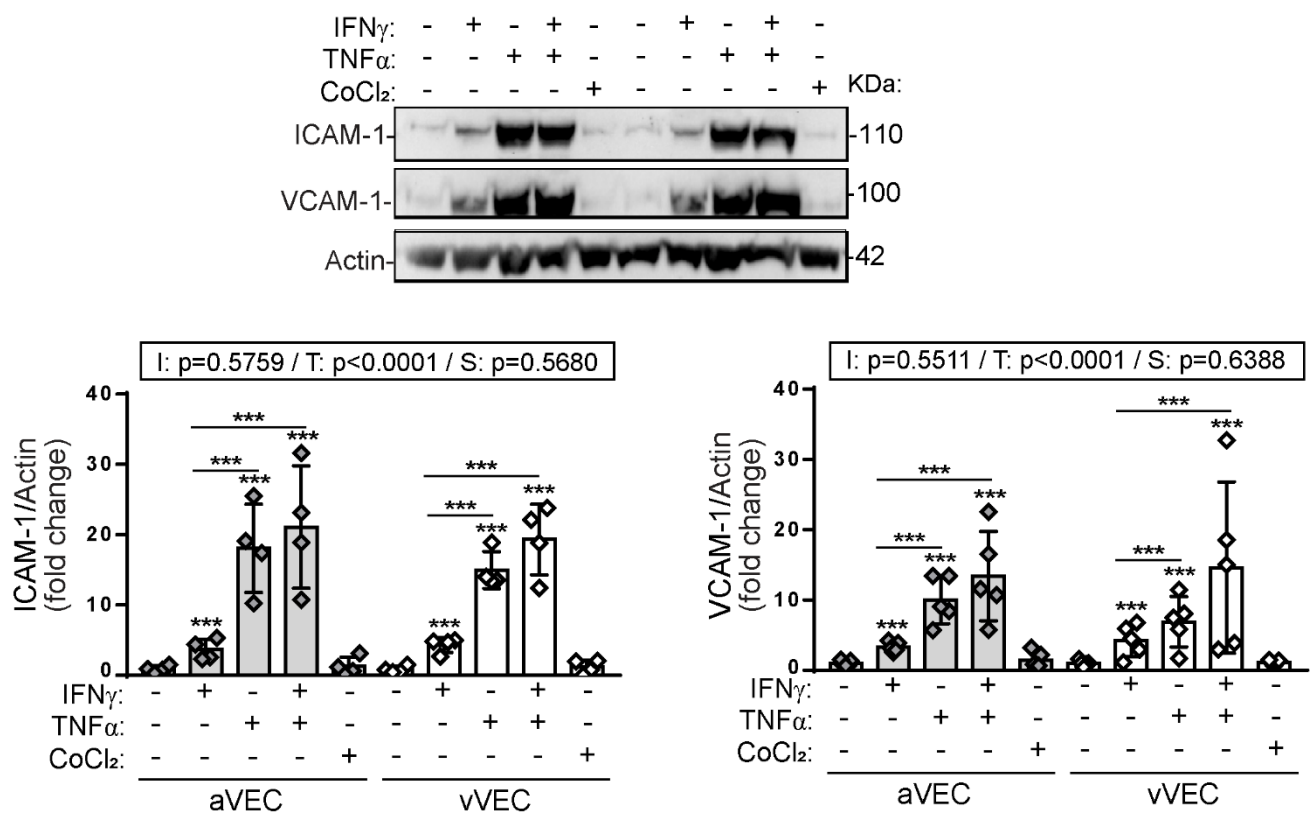


**Figure 59. IFN- $\gamma$  and TNF- $\alpha$  induce adhesion molecule expression on side-specific VEC.** aVEC and vVEC were sheared for 72 h and treated during the last 24 h with the indicated ligands. Whole cell extracts were analysed by Western Blot for ICAM-1 and VCAM-1 expression. Densitometric analysis and representative blot of n=4-5 aVEC and vVEC from independent deceased valve donors. Grey diamond, aVEC, white diamond, vVEC. CoCl<sub>2</sub> indicates 100  $\mu$ M cobalt chloride; IFN $\gamma$ , 100 ng/mL IFN- $\gamma$ ; TNF $\alpha$ , 5 ng/mL TNF- $\alpha$ . Statistics as in Figure 7. I=interaction; T=treatment; S=valve side (aortic or ventricular).

We next tested the cytokine profile induced by pro-inflammatory cytokines in side-specific VEC. ELISA analysis revealed that IFN- $\gamma$  and TNF- $\alpha$  induced IL-6 secretion in both aVEC and vVEC (**Figure 60A**). However, only TNF- $\alpha$  induced IL-8 secretion (**Figure 60A**), which mirrors the gene expression profile induced by these cytokines in mixed VEC populations (**Figure 58**). To note, no side-differential responses were detected for these cytokines. In addition, IP-10 was strongly secreted upon IFN- $\gamma$  and TNF- $\alpha$  challenging in aVEC and vVEC. Remarkably, IP-10 secretion was significantly higher in aVEC in response to IFN- $\gamma$  alone compared to vVEC (**Figure 60B**). Finally, we also tested VEGF-A secretion, but surprisingly, VEC did not secrete VEGF-A not basally neither upon stimulation (**Figure 60C**). These findings support the concept of IFN- $\gamma$  as a pro-inflammatory stimulus in VEC and point to side-differential secretion of IP-10.

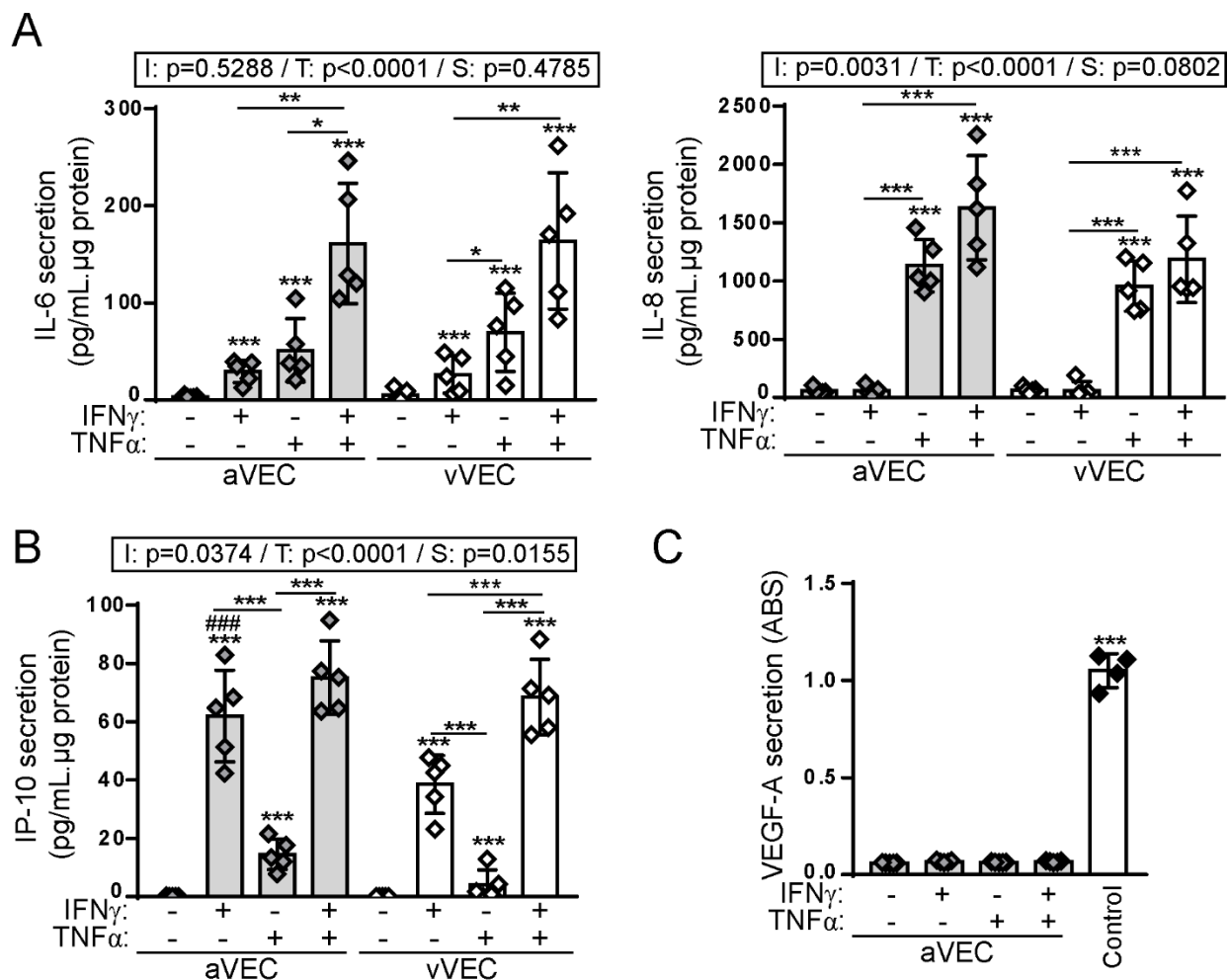


**Figure 60. IFN- $\gamma$  induces cytokine secretion in both aVEC and vVEC.** (A-C) aVEC and vVEC were sheared for 72 h and treated during the last 24 h with the indicated ligands. Supernatants were collected and assayed for cytokine (A-B) and VEGF-A (C) secretion. (A-B) Data were normalized to total protein content. (C) Data are expressed as raw absorbance (ABS). Positive control refers to EGM-2 medium supplemented with recombinant VEGF-A; n=5 for each group. Doses, n, symbols and statistics as in Figure 59.

Since valve endothelial-derived NO is known to be an important regulator of valve pathophysiology and eNOS expression is reduced in CAVD in a side-specific manner,<sup>206</sup> we explored the effects of IFN- $\gamma$  on eNOS protein levels. As shown in **Figure 61A**, upon 24 h of treatment under shear conditions, IFN- $\gamma$  did not induce eNOS downregulation. In keeping with previous reports performed in porcine VIC at 48 h,<sup>50</sup> TNF- $\alpha$  decreased eNOS protein levels in human cells at shorter times (**Figure 61A**). Given the IFN- $\gamma$ +LPS interplay on HIF-1 $\alpha$  induction in VIC, we looked for similar mechanisms on VEC. Strikingly, TNF- $\alpha$ , but not IFN- $\gamma$ , increased HIF-1 $\alpha$  protein levels in aVEC, which mirrors the immune-mediated mechanism in VIC. In addition, IFN- $\gamma$  and TNF- $\alpha$  combination stabilized HIF-1 $\alpha$  protein levels in both aVEC and vVEC (**Figure 61B**).

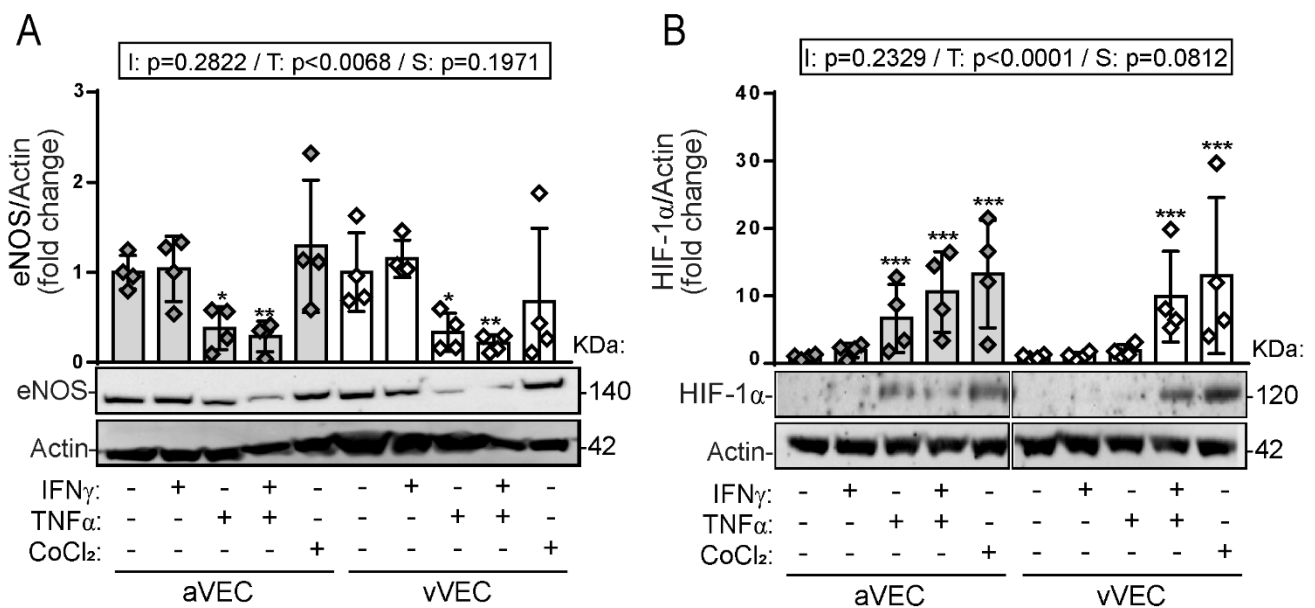


**Figure 61. TNF- $\alpha$ , but not IFN- $\gamma$ , promoted a decrease on eNOS protein levels as well as an immune induction of HIF-1 $\alpha$  in aVEC.** (A-B) aVEC and vVEC were seeded for 72 h as indicated in Methods and treated during the last 24 h with the indicated ligands. Cells were then lysed and whole cell extracts analysed by Western Blot for eNOS (A) and HIF-1 $\alpha$  (B) protein expression. Densitometric analysis and representative blot of n=4. Doses, n, statistics, and symbols as in Figure 59.

Immune cell infiltration is one of the earliest events in CAVD.<sup>209</sup> Prompted by findings on cytokine-induced adhesion molecule expression (**Figure 59**), we performed VEC-monocyte adhesion assays under shear stress conditions mimicked by a swirling system creating a multidirectional and low magnitude flow at the centre, and a laminar flow at the edge of the well.<sup>172</sup> Strikingly, both IFN- $\gamma$  and TNF- $\alpha$  increased THP-1 adhesion at both the centre and the edge of the well, with no further potentiation when both stimuli were combined (**Figure 62**). Remarkably, in the centre of the well we found a statistically higher monocyte adhesion in aVEC compared to vVEC (**Figure 62**), thus pointing to side-differential responses.

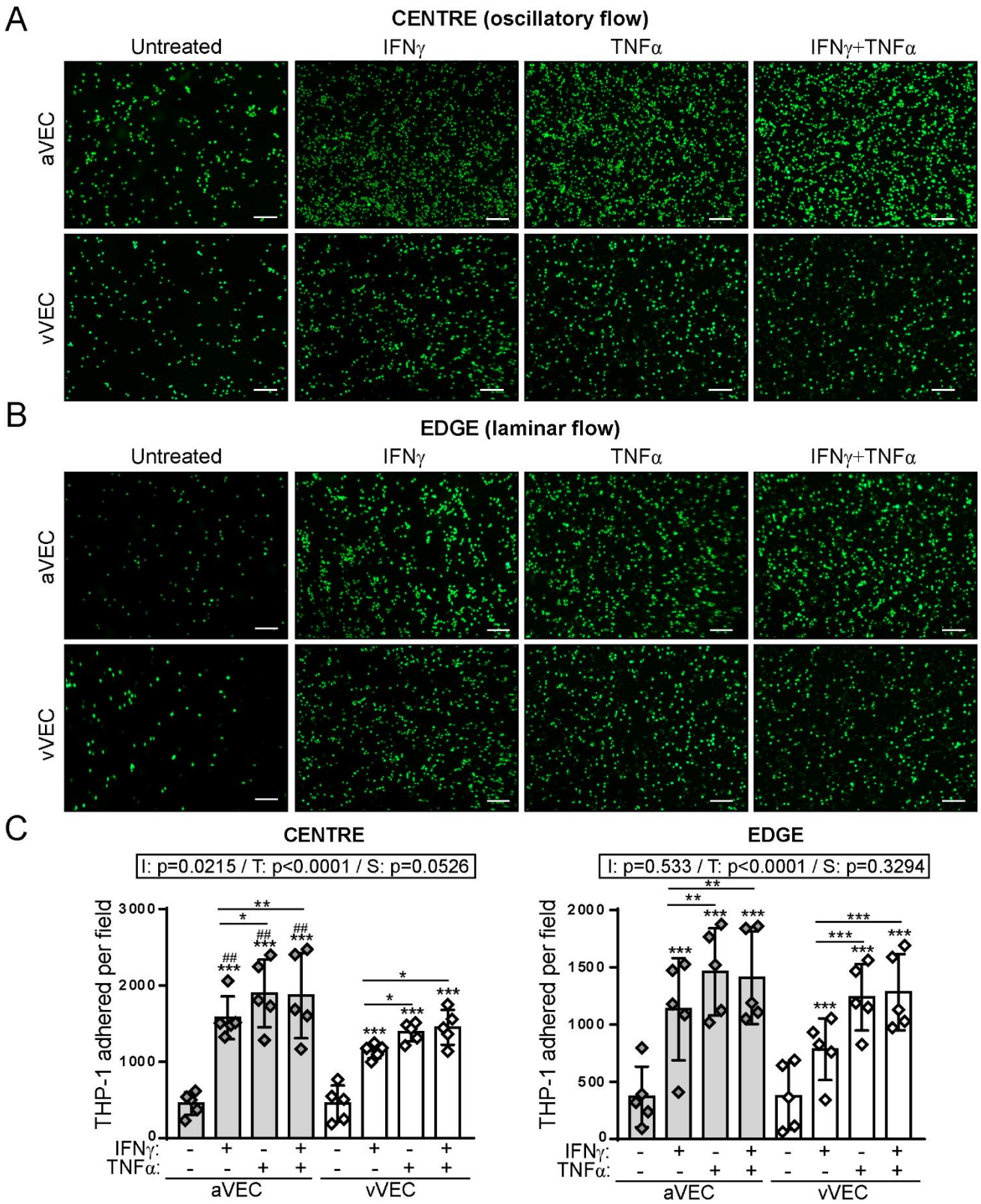


**Figure 62. aVEC exposed to a multidirectional flow are more prone to monocyte adhesion upon IFN- $\gamma$  and TNF- $\alpha$  treatment.** (A-C) aVEC and vVEC were seeded and seared in parallel and adhesion assays performed as indicated in Methods. Representative microphotographs of stained THP-1 cells adhered to aVEC and vVEC at the centre (A) and at the edge of the well (B). White line indicates 20  $\mu$ m. (C) Data correspond to total THP-1 cell counting evaluated with ImageJ software; n=5 Doses, n, statistics, and symbols as in Figure 59.

Under the conditions of the swirling system used, Ghim et al reported differences in the number of vascular endothelial cells HUVEC comparing the edge and the centre of the wells due to the different flow patterns, therefore normalization of cell adhesion to the number of endothelial vascular cells was performed.<sup>172</sup> Based on these findings, we performed parallel experiments under the same conditions analysing the number of VEC by DAPI staining. Strikingly, VEC number density did not show significant differences when comparing the edge and the centre of the well (**Figure 60**), in contrast to data reported in vascular cells.<sup>172</sup> This evidence further supports the notion of different behaviours between vascular and valvular endothelial cells under similar flow patterns.

It is noteworthy that the combination of stimuli, TNF- $\alpha$ +IFN- $\gamma$ , significantly reduced aVEC and vVEC number at both the centre and the edge of the wells (**Figure 63**). Whether the combination of both stimuli induce VEC apoptosis and monolayer reorganisation should be explored in future studies.

THP-1-VEC monolayer adhesion data normalised to VEC density confirmed the IFN- $\gamma$  and TNF- $\alpha$ -mediated adhesion to monocytes and valve side differences. Moreover, given the lower VEC number detected upon TNF- $\alpha$ +IFN- $\gamma$  treatment, data further disclosed cooperation between cytokines on monocyte adhesion per endothelial cell (**Figure 64**). To note, more studies are needed to reach a conclusion on this interplay. Together, data demonstrate a cytokine-mediated VEC-monocyte adhesion with aortic-side VEC more prone to adhesion under multidirectional flow, which could be relevant to the preferential calcification in the aortic side of the valve.

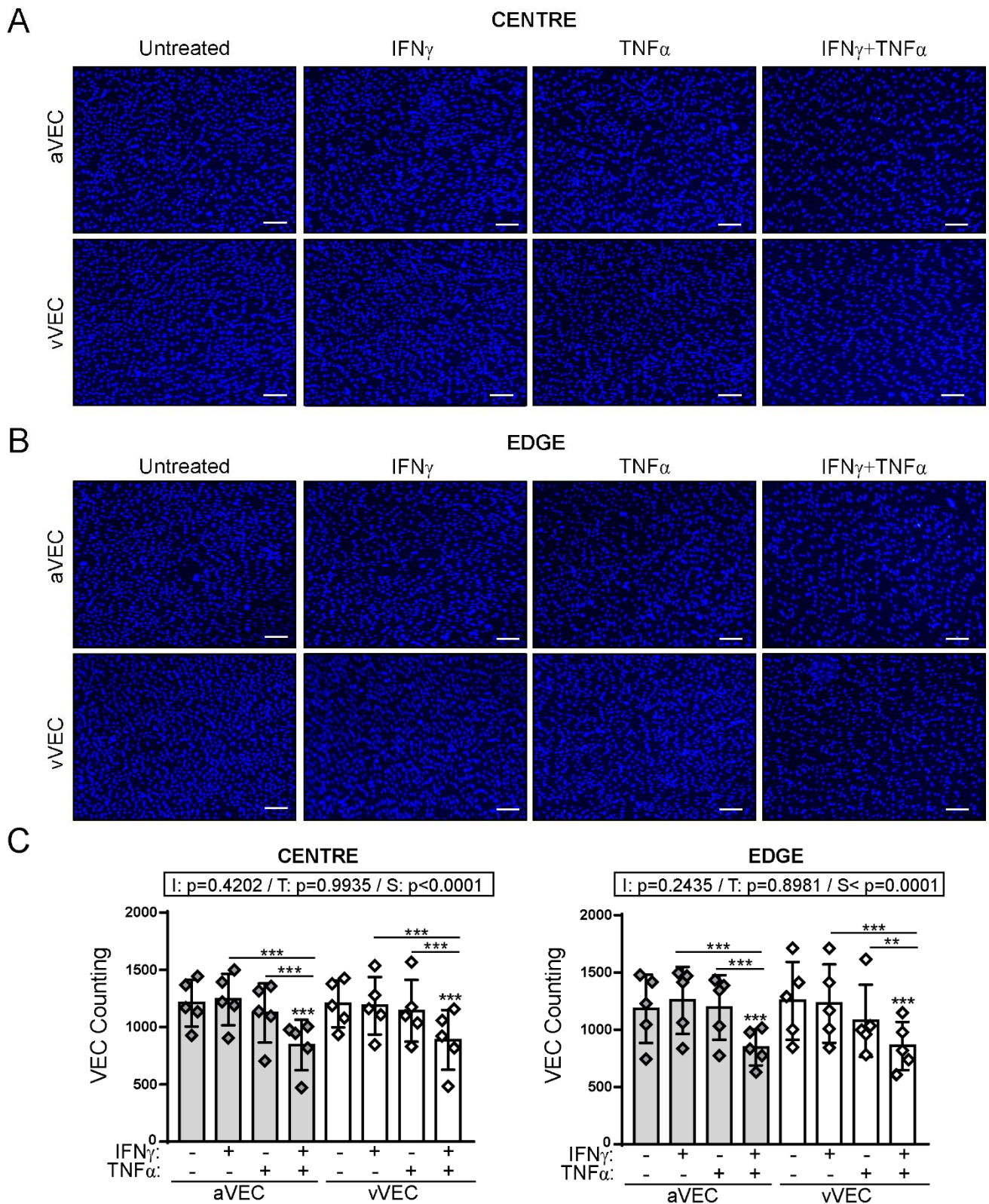


**Figure 63. Shearing conditions do not alter VEC density at the centre and the edge of the well.** (A-C) aVEC and vVEC were seeded and activated as in Figure 59. Then, DAPI staining was performed. Representative microphotographs of DAPI-stained aVEC and vVEC at the centre (A) or the edge of the well (B). Total number of VEC per field and statistics of n=5 (C). Doses, statistics, n and symbols as in Figure 59.

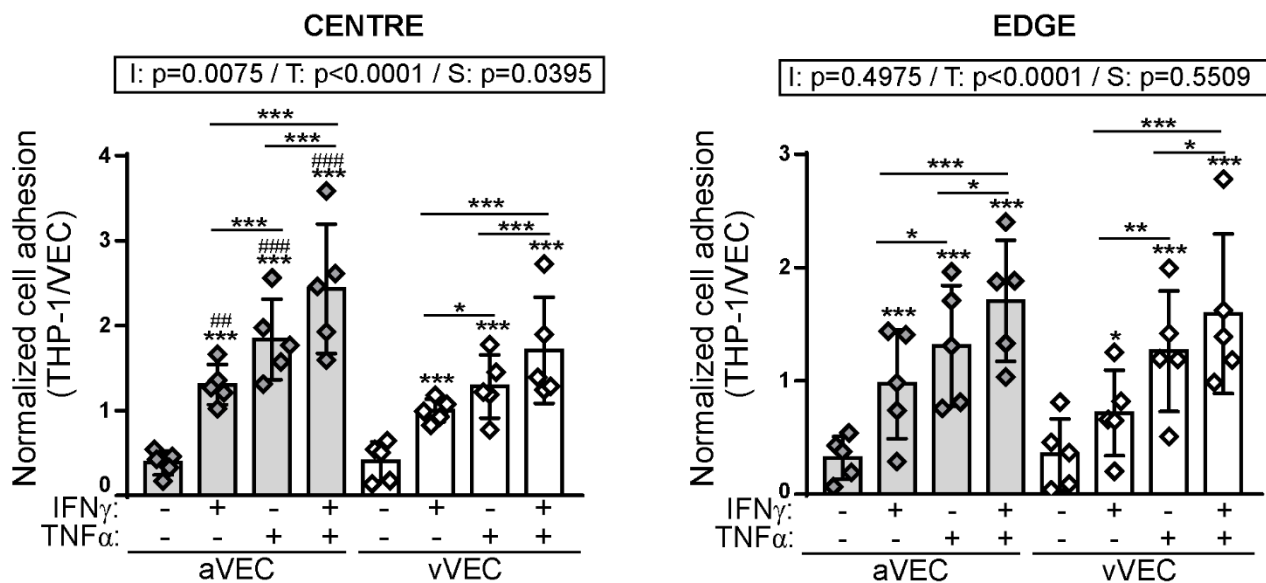


**Figure 64. THP-1 adhesion normalised to total VEC number confirmed cytokine-mediated induction of monocyte adhesion and side-specific effects.** Values from Figures 59 and 60 were used to calculate the adhered THP-1/VEC ratio; n=5 pairs of aVEC-vVEC from independent donors.

Given the intriguing differences on cell adhesion between aVEC and vVEC, we next performed preliminary migration assays performed with the scratch assay.<sup>210</sup> Due to technical limitations, the scratch wound analysis was only performed at the middle of the wells. Cells were sheared as usual and scratched just before the stimulation. Then, pictures were taken at 24 h to measure the % of wound healing compared to an average of the initial scratch in 6 different random pictures (time 0). Given that HIF-1 $\alpha$  is also known to regulate cell migration,<sup>211</sup> we also used CoCl<sub>2</sub> as stimuli. Strikingly, at 24 h, the wound was completely closed in aVEC activated with either TNF- $\alpha$  or CoCl<sub>2</sub> (**Figure 65**), further supporting side specific effects. Conversely, IFN- $\gamma$ -treated cells, aVEC and vVEC, showed no healing after 24 h, suggesting that this cytokine either inhibit or delay the wound healing (**Figure 65**). Collectively, data argue for cytokine differences and valve side specific responses, although more studies are needed to confirm and further explore this finding.

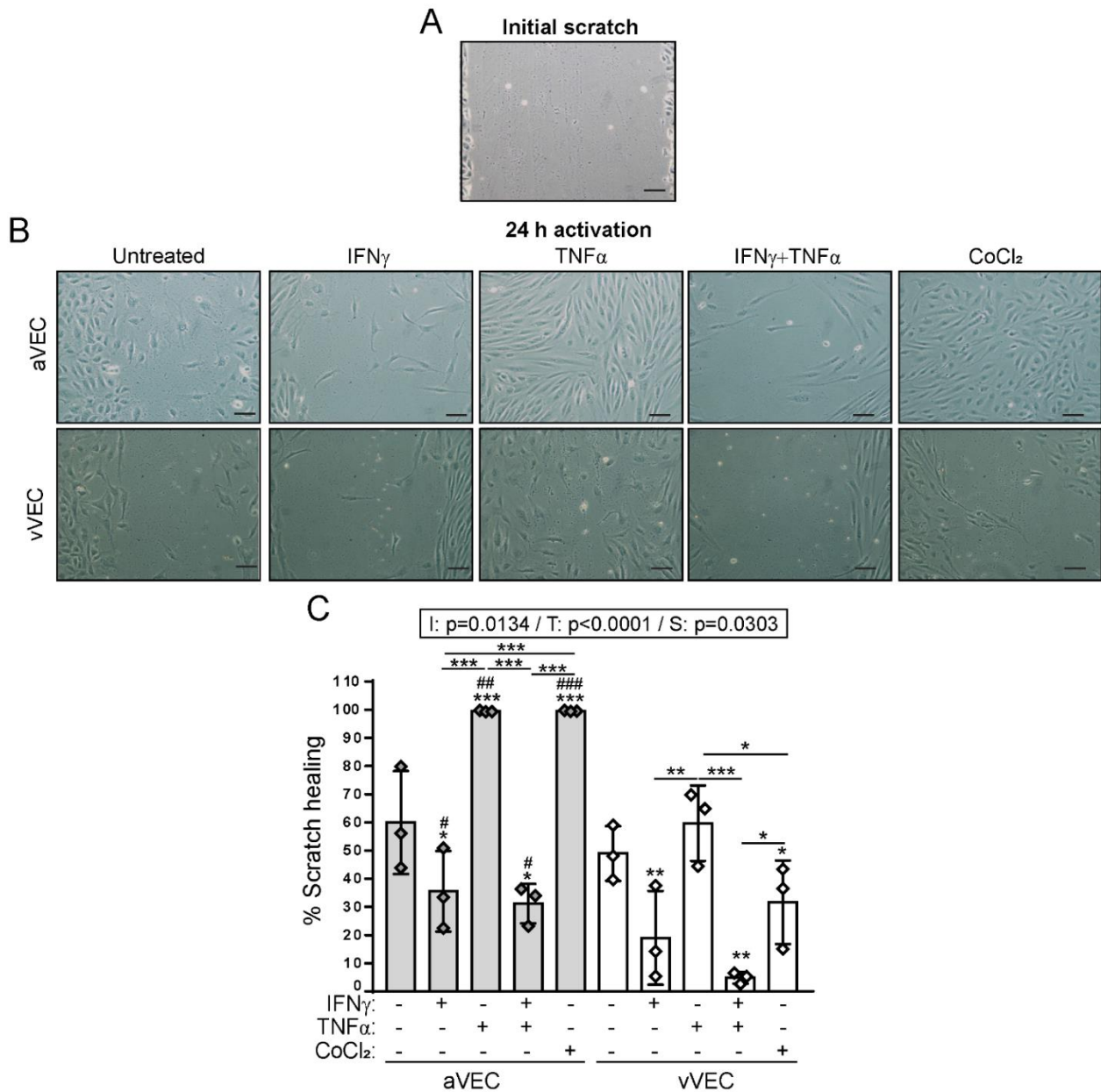


**Figure 65. IFN- $\gamma$  reduces cell migration while TNF- $\alpha$  and CoCl $_2$  induce cell migration in aVEC under multidirectional flow.** aVEC and vVEC were seeded and sheared in parallel and the scratch wound healing assay performed as indicated in Methods. (A) Representative image of the scratch size at time 0 in aVEC, which was used to calculate % of scratch healing as indicated in Methods. (B) Representative images of the wound size after 24 h of activation in aVEC and vVEC. (C) % scratch healing was measured in 3 pictures for each condition in n=3 experiments performed in independent pairs of aVEC-vVEC. CoCl $_2$  indicates 100  $\mu$ M cobalt chloride. Doses, statistics, n, and symbols as in Figure 60.

Major findings of this section include that IFN- $\gamma$  acts as a pro-inflammatory cytokine in VIC and, while inhibiting wound healing. Data also disclosed a novel immune induction of HIF-1 $\alpha$  by TNF- $\alpha$  in the aortic valve context. Finally, data reveal functional differences in cytokine-mediated adhesion and migration between aVEC and vVEC that could be relevant for the fibrosa layer preferential calcification found in CAVD.

## **DISCUSSION**



# DISCUSSION

---

The results presented in this study unravel a novel role for IFN on the physiopathology of the AV via JAK/STAT pathways. Our findings highlight that IFN are inducers of inflammation and calcification in VIC explanted from patients with no aortic valve disease and disclose and interplay between JAK/STAT and TLR signalling pathways, with the involvement of STAT, NF- $\kappa$ B and HIF-1 $\alpha$  transcription factors and the osteogenic mediator BMP-2. Clinically significant findings of our study include the blockade of these immune-mediated responses by Jakinibs currently used for the treatment of autoimmune diseases, pointing to JAK/STAT as a therapeutically relevant target. In addition, this study provides several new insights about the sex-differences reported in CAVD, with unexpected greater responses to IFN in male cells and sex-differences in gene expression profile in calcified tissue correlating with lower calcification in female patients. The identified underlying sex-differential molecular mechanisms include higher Akt activation/survival signals in females and higher osteogenic signalling and HIF-1 $\alpha$ /ERK activation in males. Furthermore, our work demonstrates a role for type I IFN signalling on the TLR3-mediated effects in VIC. Finally, we also describe some side-specific differences in the monocyte adhesion to VEC monolayers response to IFN- $\gamma$  and TNF- $\alpha$  with potential relevance in CAVD pathogenesis.

## **D.1-IFN as pro-inflammatory and osteogenic cytokines in VIC**

In the first part of the study we disclosed the overall effects of IFN- $\alpha$  and IFN- $\gamma$  as inducers of inflammation and calcification in VIC, which supports the model of inflammation-mediated calcification. These data are relevant since these cytokines could be potential candidates to act as endogenous initiators of CAVD by triggering changes leading to the calcification of the AV cusps.

### **D.1.1-IFN- $\alpha$ effects in VIC**

A striking finding and pathogenic clue that prompted us to study the role of type I IFN on VIC calcification was the link between an enhanced type I IFN activity and the early onset of ectopic calcifications in non-skeletal tissues found in patients with the Singleton-Merten syndrome (reviewed in<sup>212</sup>). In addition to these rare mutations, the AV cusps could be exposed to type I IFN from different sources:

- i. The bloodstream. During viral and bacterial infections, immune cells release IFN to plasma, and these cytokines could be sensed by resident valve cells. Although there is not a straightforward association of infections to valve calcification, several evidences support this theory. For example, patterns from *Chlamydia pneumoniae* and different virus have been detected in calcified valves in the fibrosa layer, where the calcifications are mainly located.<sup>68</sup> Additionally, the inoculation of oral bacteria strains triggers valve calcification in an animal model.<sup>70</sup>
- ii. Secreted by infiltrated immune cells activated with either cytokines, molecular patterns from pathogens, or endogenous damage molecules via TLR signalling.<sup>213,111</sup>
- iii. Secreted by resident valve cells upon viral/bacterial stimulation, as reported in VIC upon stimulation with TLR agonists.<sup>164</sup>

The study revealed mild pro-inflammatory effects of IFN- $\alpha$  in human VIC. Evidences in the literature disclose context-dependent responses to this cytokine. Consistent with our data, a great amount of evidences supports the notion of type I IFN as enhancers of chronic inflammatory responses.<sup>214</sup> However, type I IFN has also been shown to exert anti-inflammatory and protective effects for a wide variety of diseases.<sup>213,215</sup> Thus, these intriguing context-dependent effects point to type I IFN pathway as a central and pleiotropic regulator of cell fate and inflammatory responses. Our collective data unveil an IFN- $\alpha$ -triggered inflammatory phenotype in VIC characterized by the early and late activation of NF- $\kappa$ B, as well as the subsequent induction of downstream proteins such as adhesion molecules ICAM-1 and VCAM-1 and slight secretion of IL-6, which resembles, in part, the pro-inflammatory phenotype induced upon TLR engagement.<sup>153</sup>

In keeping with type I IFN-specific signalling, we demonstrated the activation of STAT transcription factors in VIC. Notably, our data unravel the specific IFN- $\alpha$ -mediated phosphorylation of STAT1 at the Serine 727, which requires p38 activation.<sup>216</sup> IFN- $\alpha$  also promoted STAT3 phosphorylation, whose role is likely to be protective since its activation has been described as a counter-acting mechanism of STAT1-induced inflammatory responses.<sup>217</sup> Consistent with this notion, a recent report in VIC showed that rapamycin exerts a protective function for cell calcification via the activation of STAT3 through the Akt pathway.<sup>218</sup> In addition, in VIC, type I IFN is also capable of activating Akt, a pathway reported to exert an essential role on mRNA translation of IFN-stimulated genes.<sup>219</sup> Finally, MAPK are also activated by IFN- $\alpha$ . These pathways are known to be not only essential regulators for innate immunity and inflammatory responses activated in a large subset of inflammatory responses,<sup>220</sup> but also pro-calcifying pathways in the AV context.<sup>183,166</sup>

The data presented here are among the first evidences linking type I IFN signalling with ectopic calcification of soft tissue and support the notion of inflammation-induced calcification. The differentiation of VIC toward an osteoblast-like phenotype is a well-described phenomenon, but the exact mechanisms and endogenous factors involved remain largely unknown. The present study highlights the role of IFN- $\alpha$  on VIC differentiation and points to this cytokine as an endogenous candidate to initiate phenotypic changes in VIC. The exposure of these cells to recombinant IFN- $\alpha$  decreased their proliferation, thus correlating with the well-known role of this cytokine as inhibitor of cell proliferation,<sup>111</sup> while promoting morphological changes. Strikingly, in growth medium, we found that IFN- $\alpha$  triggers male VIC differentiation towards an osteoblastic-like phenotype, a mechanism reported to occur in approximately 15% of resected AV.<sup>74,77</sup> Moreover, we elucidated the IFN- $\alpha$ -mediated differentiation profile, which is characterized by the downregulation of the myofibroblast marker  $\alpha$ -SMA and the induction of a subset of osteoblastic features previously reported in CAVD.<sup>43</sup> We also demonstrated that IFN- $\alpha$  induces BMP-2 secretion in VIC, a morphogen which is likely to play a key role on VIC differentiation because it is essential for calcification both in *in vitro* and *in vivo* models of CAVD.<sup>92,185</sup>

RUNX2, the master transcription factor of osteogenic differentiation,<sup>88</sup> has been proposed as the downstream effector of BMP-2 signalling in the context of the AV.<sup>185,91</sup> Strikingly, when we explored the regulation of this transcription factor by IFN- $\alpha$  at the protein level in VIC, we found its unexpected basal nuclear localization as well as the reduction of its protein expression upon long-term stimulation. These results seem at first glance a matter of controversy with the early upregulation of osteoblastic differentiation genes after IFN- $\alpha$  stimulation. To address this question, we compared the effects of other reported osteogenic inducers in VIC and found that only TGF- $\beta$  upregulated RUNX2 protein levels, in keeping with previous reports.<sup>221</sup> LPS and TNF- $\alpha$  did not alter RUNX2 protein expression. One hypothesis explaining the IFN- $\alpha$ -induced RUNX2 downregulation is that it may act as an early osteogenic factor upregulated in early stages of osteoblastic differentiation but not essential for the maintenance of major bone matrix gene expression, as previously reported in other models.<sup>88</sup> Also, the discordance on RUNX2 expression with previous reports may also be explained since most studies analysed *RUNX2* transcript levels as a marker of cell differentiation but neither its protein expression nor its localisation. Based on our data, we propose two potential theories that could explain these controversial results: i) The IFN- $\alpha$ -mediated differentiation of VIC is independent of RUNX2. ii) Additional and unexplored regulations of this master transcription factor could take place during the IFN-induced differentiation. Given that in our culture conditions VIC are in an activated state termed aVIC,<sup>189</sup> one could hypothesize that RUNX2

nuclear translocation could be involved in the phenotypic transition from qVIC to aVIC. Finally, the lack of correlation between *RUNX2* mRNA and protein levels, upregulated and downregulated by IFN- $\alpha$  respectively, suggests a posttranscriptional regulation of this transcription factor, as it has been reported.<sup>222</sup>

Osteoblastic differentiation is tightly regulated and other BMP-2 downstream effectors, such as osterix, have been reported to be essential for this process<sup>223</sup> and upregulated in CAVD.<sup>89</sup> In fact, *OSX* transcript levels induction by IFN- $\alpha$  in VIC suggests that this transcription factor could also play a role on the differentiation process. Conversely, an alternative BMP-2 effector acting via non-canonical pathways is *MSX2*, which was not upregulated by IFN- $\alpha$  but by LPS, in keeping with previous reports showing the MyD88-dependent activation of *MSX2* in AV cells.<sup>224</sup> Together, data suggest a role for BMP-2 canonical pathways on the IFN- $\alpha$ -mediated differentiation, although further studies are needed to elucidate the regulation by downstream effectors.

A novel finding of this study is that IFN- $\alpha$  can induce calcific nodule formation, a conclusion demonstrated in high-phosphate calcifying medium by two independent methods. Two main calcifying mediums are commonly used in cardiovascular research. First, calcification assays based on high Pi concentrations, which have been extensively used in both vascular<sup>176</sup> and valvular<sup>225</sup> mineralization studies. Second, the classically-used OM composed of organic phosphate in the form of  $\beta$ -glycerolphosphate and supplemented with ascorbic acid and dexamethasone.<sup>226</sup> As noted in the introduction, the mineral found in calcified valves is composed of calcium hydroxyapatite, whose formation is dependent on the nucleation of calcium phosphate.<sup>41</sup> Several clinical and *in vitro* evidences support the role of Pi as a key regulator of cardiovascular and valvular calcification: (i) High serum Pi levels within the normal range have been linked to an increased predisposition for valve calcification in the Cardiovascular Health Study<sup>99</sup> and the Multi-Ethnic Study of Atherosclerosis (MESA).<sup>227</sup> (ii) High calcium serum levels were not associated with CAVD development in the Cardiovascular Health Study.<sup>99</sup> (iii) Pi signalling has been previously demonstrated as an important pro-mineralizing pathway in VIC.<sup>98</sup> (iv) The calcification induced by OM has been described as dependent on VIC passage, whereas Pi-induced calcification was independent of passage.<sup>226</sup> Previous studies in our laboratory showed scarce calcific nodule formation after 28 days of stimulation in OM, being the potential explanation the high passage of used VIC as recently demonstrated,<sup>226</sup> since our low sample availability prevented us to perform the experiments with passage 4 or less isolates. (v) Whereas OM is used for the study of cell transition of VIC into osteogenic cells,<sup>226</sup> the Pi-induced calcification *in vitro* is thought to be dependent on both osteogenic and dystrophic processes (reviewed in <sup>228</sup>), thus mirroring the main mechanisms driving

most cases of AV calcification. vi) In our model and conditions, stimuli induced VIC osteoblastic differentiation in regular activation medium (M199 supplemented with 2% FBSi), as demonstrated by osteoblastic gene expression, BMP-2 upregulation and  $\alpha$ -SMA decrease. However, the high-Pi calcification medium also presents limitations that should be considered for a more cautious interpretation of data. First, the phosphate concentration used (3 mM Pi) is not physiologically found in healthy subjects but in hyperphosphatemia patients.<sup>229</sup> Second, the *in vitro* calcification method based on high Pi has been shown to be dependent on pH changes and variable experimental conditions, which could affect data interpretation and *in vivo* extrapolation.<sup>230</sup> Despite these limitations, we thought that a calcification assay based on high-phosphate concentrations would be a good model for performing functional and mechanistic mineralization assays in VIC since covers a wide range of CAVD underlying processes.

Regarding the mechanisms underlying the IFN- $\alpha$ -induced calcification in high Pi conditions, our data unveil an important contribution of BMP-2 signalling, supported by the marked reduction in calcification levels upon BMP antagonism with noggin. Otherwise, IFN- $\alpha$  did not significantly alter cell death after 7 days of treatment in calcifying conditions. Taken together, data suggest that osteogenic, but not dystrophic, processes are the major contributors for IFN- $\alpha$ -induced calcification in VIC in high Pi conditions. More importantly, calcification blockade by pre-treatment with tofacitinib, a JAK inhibitor currently used in clinics,<sup>231</sup> demonstrated that the IFN- $\alpha$ -induced calcification depends on JAK/STAT signalling.

In conclusion, our study provides evidence that VIC can sense type I IFN, which could be an endogenous initiator of CAVD-related processes in the early stages of the disease. It is plausible to think that the repeated exposure of the AV to immune conditions may promote VIC differentiation and favour calcium deposition leading to CAVD.

### **D.1.2-IFN- $\gamma$ effects in VIC**

IFN- $\gamma$  is a cytokine secreted mainly by immune cells, being the major sources natural killer cells in whole blood although its receptor IFNGR is known to be widely expressed.<sup>112</sup> In the AV context, our study demonstrates that resident valve cells are able to sense this cytokine. Valve cusps could be exposed to type II IFN from different sources:

- i. The bloodstream upon viral infection. Exposure of valve cells to IFN- $\gamma$  is likely to happen during infection courses when IFN- $\gamma$  is secreted by natural killer cells and T lymphocytes.<sup>232,233</sup>

- ii. From activated infiltrated T cells. Some evidences suggest that VIC could also be exposed to IFN- $\gamma$  secreted by infiltrated immune cells, as demonstrated by different reports on the literature. First, Olsson and colleagues demonstrated that T lymphocyte infiltrates are present in tricuspid non-rheumatic aortic valves.<sup>234</sup> More recently, Nagy and colleagues demonstrated that infiltrated CD8+ T lymphocytes are activated in calcified human aortic valves and secrete active IFN- $\gamma$  that subsequently impairs the calcium resorption potential of osteoclasts.<sup>138</sup> Therefore, the inhibition of IFN- $\gamma$  effects on the AV could be advantageous from two different and complementary points of view since it could restore the osteoclastic potential of infiltrated cells and also inhibit pro-osteogenic responses in resident valve cells.

Similarly to type I IFN, IFN- $\gamma$  exerts striking context-dependent effects on inflammation.<sup>235</sup> In human VIC, IFN- $\gamma$  behaves as a potent inducer of pro-inflammatory effects, characterised by NF- $\kappa$ B activation as well as the induction of adhesion molecule expression and IL-6 secretion. Our results are consistent with the reported pro-inflammatory effects of this cytokine in mouse embryonic fibroblasts through a mechanism involving autophagy.<sup>236</sup> Moreover, IFN- $\gamma$  is also able to activate its canonical signalling in VIC, which is STAT1 phosphorylation at Tyr701.<sup>112</sup> In our study, IFN- $\gamma$  promotes STAT3 phosphorylation in VIC, whereas it triggers STAT3 dephosphorylation in human prostatic metastatic cancer cell lines,<sup>237</sup> further reinforcing the notion of the context-dependent effects of this cytokine. Additional signalling pathways such as Akt and MAPK are also activated by IFN- $\gamma$  in VIC at early times, consistent with the IFN- $\gamma$ -mediated activation of ERK and JNK reported in murine macrophages.<sup>238</sup>

Our findings reveal the induction of a pro-angiogenic phenotype in VIC by IFN- $\gamma$ . In this line, context-dependent effects of IFN- $\gamma$  on angiogenesis have been reported. It is a well-known inhibitor of tumour growth and migration,<sup>239</sup> but some pro-angiogenic effects have also been found in human retinal and corneal cells.<sup>240</sup> One of the striking findings in this study is the slight induction of HIF-1 $\alpha$  in normoxic conditions upon IFN- $\gamma$  treatment in VIC. As noted earlier, this regulator of angiogenesis has been detected in calcified valves in areas of neoangiogenesis and calcification.<sup>107</sup> Consistent with HIF-1 $\alpha$  induction, VIC secrete VEGF-A in response to IFN- $\gamma$ . Reminiscent with these data, the depletion of IFN- $\gamma$ -secreting NK cells reduced angiogenesis in a laser-induced choroidal neovascularization mouse model.<sup>241</sup> The pro-angiogenic status induced by IFN- $\gamma$  in VIC included not only VEGF-A secretion but also *CNMD* downregulation, which is an important anti-angiogenic factor widely expressed on adult valves.<sup>105,106</sup> One might hypothesize that IFN- $\gamma$  could

play a role on angiogenesis in the AV by altering the homeostatic balance of angiogenic and angiogenic-inhibitory factors.

Herein, our data demonstrate a novel role for IFN- $\gamma$  as a pro-osteogenic agent in VIC, as demonstrated by osteogenic marker expression upregulation in cell growth medium and a potent induction of calcific nodule formation in high-Pi conditions. Increasing evidences support the notion of IFN- $\gamma$  as a pro-osteogenic cytokine. Intriguingly, IFN- $\gamma$  induces basal ganglia calcification that subsequently promotes the development of neurologic disorders.<sup>242</sup> In keeping with a role for IFN- $\gamma$  on cardiovascular calcification, elevated serum levels of IFN- $\gamma$ -related cytokines have been proposed as biomarkers for coronary artery calcification.<sup>243</sup> In addition, a genetic polymorphism leading to increased IFN- $\gamma$  activity has been recently linked to a higher predisposition for valvular damage at early ages in Turkish patients with rheumatic heart disease.<sup>244</sup>

Regarding the mechanisms of IFN- $\gamma$ -induced calcification, we found a marked increase on VIC apoptosis in high Pi conditions after IFN- $\gamma$  challenge. These results are in line with the consistent role of this cytokine as an inducer of apoptosis in a wide variety of cell types including joint capsule myofibroblasts.<sup>245</sup> More importantly, our data agree with a report showing that transgenic mice overexpressing IFN- $\gamma$  present marked dystrophic calcifications in the myocardium.<sup>246</sup> Therefore, it is plausible to think that IFN- $\gamma$  could be an initiator of dystrophic calcification in the AV. Repeated exposure of the AV cells to this cytokine may favour VIC differentiation and calcium deposition leading to CAVD.

### **D.1.3-Mechanistic differences between type I and II IFN**

Our collective data disclosed pro-inflammatory, pro-osteogenic and anti-proliferative activities for both type I and II IFN, however, some differences in the extent of some responses and the underlying mechanisms arise. In fact, regarding inflammation, IFN- $\gamma$  is a more potent inducer of NF- $\kappa$ B activation than IFN- $\alpha$ , which could explain the larger induction of adhesion molecules expression and IL-6 secretion triggered by this cytokine.

The major differences between IFN are related to the osteogenic signalling and markers. Our data showed that the IFN- $\alpha$ -induced differentiation features include BMP-2 secretion, which plays a role for calcific nodule formation. In contrast, IFN- $\gamma$  promoted an increase on *BMP2* gene expression in VIC, which did not turn into BMP-2 secretion even in combination with LPS, a result that does not parallel the IFN- $\gamma$ -induced BMP-2 expression and secretion reported in pancreatic cells.<sup>247</sup> Strikingly, the osteogenic gene profile of VIC revealed opposing effects of IFN on the expression of

the osteoblastic gene *RUNX2* and the chondrogenic markers *ACAN* and *SOX9*. Therefore, the IFN- $\alpha$ -mediated upregulation of these markers would agree with an osteochondrogenic differentiation. However, the exact mechanistic pathways for IFN- $\gamma$ -mediated osteogenic differentiation are still not clear and merit future investigations.

In high Pi conditions, we demonstrated a major role for BMP-2 osteogenic signalling in IFN- $\alpha$ -induced calcification. However, we did not find evidences of dystrophic mechanisms induced by this cytokine. At the contrary, IFN- $\gamma$  induced VIC apoptosis in high-Pi medium, a finding suggesting that dystrophic mechanisms could be the major mediators of the IFN- $\gamma$ -induced calcification as previously discussed.

## **D.2-Novel insights into TLR4/3 ligands in VIC**

In the present work, the comparison between IFN and TLR ligands revealed differences according to the responses analysed. While IFN are less potent pro-inflammatory agents than TLR4/3 agonists, IFN- $\gamma$  and Poly(I:C) are the most potent inducers of osteogenesis in VIC. Moreover, this study disclosed new findings on the activation of TLR by PAMP associated to bacterial and viral infections in VIC that strengthen and further deepen prior observations.

Our group and others had previously done an extensive work regarding the effects of TLR signalling in VIC and their implications in inflammation and calcification (reviewed in<sup>71</sup>). Importantly, TLR pathways have been reported to be upregulated in an elegant study by Schlotter and colleagues. In this study, the authors used cutting-edge proteomic and transcriptomic techniques to disclose that TLR signalling is strongly increased in areas of calcification from calcified valves as compared with other areas and with control valves.<sup>160</sup> The current study provides clear evidences that further support the relationship between TLR activation and calcification in the aortic valve context.

### **D.2.1-Novel insights into LPS effects in VIC**

Our data confirmed previous observations on the LPS-mediated effects in VIC, (reviewed in<sup>71</sup>) and further disclosed novel insights on the role of this prototypic TLR4 ligand on inflammation and angiogenesis. Among the novel findings is the potent LPS-mediated induction of VCAM-1 expression in VIC, while previous studies had focused on the induction of another adhesion molecule, ICAM-1.<sup>164,163</sup> This finding is relevant since the expression of both adhesion molecules is increased in calcified valves<sup>248</sup> and soluble VCAM-1 has also been associated to CAVD progression in patients with coronary artery disease.<sup>249</sup> In addition, higher circulating levels of the soluble form

of these proteins were found in serum from CAVD patients.<sup>184</sup> Finally, VCAM-1 has also been linked to oxidative stress in the AV endothelium.<sup>50</sup> Our collective data suggest that both IFN and LPS are among the potential inducers of the high levels of adhesion molecules found in serum from CAVD patients.

Our data unveil some differences in the pro-inflammatory phenotype induced by TLR4 and IFN receptor activation in VIC. In fact, LPS triggers marked IL-6/8 and prostaglandin E<sub>2</sub> secretion, consistent with previously reported data (reviewed in<sup>71</sup>). Additionally, marked dissimilarities on VIC proliferation and differentiation were found since LPS does not affect VIC proliferation. Interestingly, data pointed to different osteogenic mechanisms given that LPS, but not IFN- $\alpha$ , induces *MSX2* gene expression. This finding is in line with a previous report indicating that MyD88 silencing decreased *MSX2* basal expression in VIC.<sup>224</sup> We also demonstrated the downregulation of the calcification inhibitor *MGP* by LPS, suggesting that it could be a novel mechanism contributing to the LPS-mediated calcification. Finally, we revealed increased VEGF-A secretion upon TLR4 activation, which does not agree with previous reports of our laboratory indicating that LPS required co-stimulation with the lipid mediator sphingosine-1 phosphate to induce VEGF-A secretion in VIC.<sup>250</sup> This apparent discrepancy could be explained by the different time course, 48 h of activation in the current study, while 24 h in the previous report. Interestingly, LPS promoted VEGF-A secretion but did not induce HIF-1 $\alpha$  protein levels, a finding suggesting that it could be other pathways or transcription factors regulating VEGF-A secretion in VIC. Thereby, new studies are warranted to elucidate the mechanism underlying the LPS-induced VEGF-A secretion and the putative role of LPS on angiogenesis.

A remarkable finding was also disclosed in the analysis of IFN signalling pathways. It has been previously described that LPS is able to phosphorylate STAT1 at either the Ser727<sup>216</sup> or the Tyr 701 sites in macrophages.<sup>251</sup> In contrast, in VIC, neither STAT1, nor STAT3 were phosphorylated by LPS at early or longer time points, thus suggesting that the regulation of STAT pathways is cell and tissue-specific since it differs between VIC and immune cells.

### **D.2.2-Type I IFN signalling mediates Poly(I:C) effects in VIC**

In the cardiovascular field, self-recognition of DNA or RNA has been associated to arterial and venous thrombosis, atherosclerosis and ischemia-reperfusion injury (reviewed in<sup>252</sup>). Related to CAVD pathogenesis, a synthetic analogue of dsRNA, high-molecular weight Poly(I:C), was previously reported to induce potent pro-inflammatory and pro-osteogenic responses in VIC,

characterized by cytokine secretion, osteogenic protein upregulation and calcium deposits formation (reviewed in<sup>71</sup>). In a previous study, Zhan and colleagues disclosed that TLR3 is the major sensor of dsRNA in VIC<sup>205</sup> and that its downstream MyD88-independent signalling include the adaptor protein TRIF and the ensuing activation of NF- $\kappa$ B, IRF-3 and MAPK. However, the underlying mechanisms remained unknown.

In this study, we demonstrated that Poly(I:C) effects in VIC strongly resemble those of IFN- $\alpha$  on osteogenic differentiation, i.e., *BMP2* gene upregulation, proliferation inhibition, and downregulation of *MGP* and *ACTA2* genes, supporting the notion of TLR3 activation as a potent mechanism of VIC calcification.<sup>205,164</sup> In keeping with our findings, it has been reported that TLR3 activation leads to osteogenesis in mesenchymal stromal cells with variable potency depending on the cell type and tissue of origin.<sup>253</sup> As mentioned above, Poly(I:C), but not LPS, inhibited cell proliferation, suggesting that there are some additional mechanisms accounting for the TLR3-mediated proliferation inhibition. This finding is reminiscent with the negative regulation of cell proliferation by Poly(I:C) in different cancer cell lines.<sup>254</sup>

In our model, we found that IFN- $\beta$  is secreted in response to Poly(I:C) stimulation of VIC. IFN- $\beta$  secretion is a common outcome of TLR3 engagement in a wide variety of *in vitro* and *in vivo* models. For example, in human gingival epithelial cells, the activation of TLR3, but not TLR4, leads to IFN- $\beta$  secretion via phosphorylation of IRF3.<sup>255</sup> Regarding *in vivo* evidences, type I IFN secreted in response to TLR3 activation is the major mediator of the protection against *Coxsackievirus* A16 infection in young mice.<sup>256</sup> Strikingly, there is a cell and context specificity in the TLR3-induced responses, i.e., substantial differences between myeloid cells and non-myeloid on the extent of IFN secretion.<sup>257</sup> In this study we demonstrate how IFN-related genes are overexpressed after Poly(I:C) treatment in VIC, which promoted the ensuing secretion of IFN- $\beta$ 1 and subsequent activation of STAT1. Therefore, the TLR3-induced IFN- $\beta$  secretion might be the underlying mechanism of the induction of inflammation and calcification in VIC by TLR3 activation. However, in other systems, such as a caerulein-induced mouse model of pancreatitis,<sup>258</sup> the activation of TLR3 seems to be protective. These differences could be directly related with the pro- or anti-inflammatory effects of the secreted type I IFN in each specific context.

Regarding inflammation, in keeping with previous reports,<sup>204,164</sup> Poly(I:C) was a strong inducer of NF- $\kappa$ B phosphorylation and subsequent adhesion molecule expression and cytokine secretion in VIC. A novel finding of this study is the induction of VCAM-1 by Poly(I:C) treatment in VIC. Similar results have been found in corneal fibroblasts, in which Poly(I:C) induced both ICAM-

1 and VCAM-1 expression via NF- $\kappa$ B activation.<sup>259</sup> To note, the use of the JAK1/2 inhibitor ruxolitinib inhibited both NF- $\kappa$ B activation and inflammatory molecule expression in VIC, demonstrating a role for JAK/STAT signalling on Poly(I:C)-induced inflammation.

Strikingly, in our hands the calcification potential of Poly(I:C) seems to be very high when compared to IFN- $\gamma$ +LPS. In addition, based on our own results, the endogenously secreted IFN- $\beta$  seems to be more potent than the recombinant IFN- $\alpha$ . In fact, the calcification induced by Poly(I:C) in 9 days, reached over two times the calcification levels of IFN- $\alpha$  in 21 days. These data could be explained by higher local concentrations of IFN, or most likely, by the participation of additional mechanisms potentiating the effect. Given that Poly(I:C) strongly induces IL-6 secretion in VIC,<sup>164</sup> and the pro-osteogenic effects of this cytokine,<sup>59</sup> it is plausible to think that increased IL-6 secretion could account for the larger effects of dsRNA in calcification as compared to recombinant IFN- $\alpha$ .

Altogether, these results suggest that TLR3 activation by long-chain dsRNA in VIC results in the secretion of IFN- $\beta$ , which is the major mediator of subsequent responses. A relevant and novel finding of this study is the blockade of Poly(I:C)-induced inflammation by ruxolitinib and calcification by IFNAR blocking antibody, which reinforces the importance of the JAK/STAT system in VIC biology. JAK/STAT signalling could be a potential therapeutic target for the dsRNA-induced inflammation and calcification in the AV context.

### **D.3-JAK/STAT and TLR interplay in VIC**

Our study provides evidence of a functional interplay between IFN receptors and TLR4 signalling in resident valve cells, further contributing to potentiate, extend and expand the processes associated to CAVD pathogenesis.

The occurrence of concomitant activation of IFN receptors, IFNAR or IFNGR, and TLR4 in the valve may take place during infections or after tissue damage, including endothelial valve layer injury. It should be noted that TLR4 signalling is not only triggered by PAMP but also by DAMP that are not necessarily linked to an infectious state. The so-called sterile inflammation could be triggered for example by matrilin-2, an extracellular matrix protein upregulated in calcified valves that signals via TLR2/4 in VIC thus promoting the subsequent inflammatory and osteogenic responses.<sup>167</sup> These evidences point to the likelihood of concomitant activation of IFN- $\alpha$  and TLR signalling pathways in the AV context.

### D.3.1-IFN- $\alpha$ and LPS interplay on inflammation and osteogenesis

A major finding of this study is the positive interplay between JAK/STAT and TLR pathways in VIC on processes relevant to CAVD, i.e. inflammation and osteogenesis. Our data point to a strong potentiation of the LPS-induced inflammation by IFN- $\alpha$  in VIC. Cooperation of both stimuli resulted in a marked increase in NF- $\kappa$ B activation and the ensuing upregulation of a subset of inflammatory molecules such as adhesion molecules, PGE<sub>2</sub> and IL-6/8, which correlates with an enhanced profile of the LPS-induced inflammatory response.<sup>153</sup> Strikingly, the IFN- $\alpha$ -LPS interplay promoted MMP-1 secretion, which could be involved on the higher levels of this metalloproteinase found in calcified valves.<sup>83</sup> One may think that type I IFN secreted upon TLR activation may activate an autocrine loop thus amplifying and sustaining inflammation as well as remodelling of the valve cusps.

Remarkably, the IFN- $\alpha$ -LPS interplay results in the potentiation of VIC differentiation, characterized by a marked upregulation of *SOST* and *RUNX2* expression, thus suggesting that VIC differentiation may occur faster than the observed with the ligands alone. Regarding Pi-induced calcification, different potential mechanisms were identified: (i) BMP-2 secretion, potentiated when IFN- $\alpha$  was combined with LPS, may account for the IFN- $\alpha$ +LPS-induced calcification as demonstrated by BMP-2 blockade with noggin. These results are in line with the important role of this osteogenic mediator in the induction of AV calcification both *in vitro* and *in vivo*.<sup>92</sup> (ii) Dystrophic calcification could be also playing a role, since IFN- $\alpha$ +LPS treatment triggered a significant increase in VIC apoptosis as compared to the ligands alone, a process that resembles the induction of dystrophic calcification by TGF- $\beta$  via apoptosis of VIC.<sup>62</sup>

This dual cytokine and PAMP/DAMP receptor synergism has been reported to occur in other cell lines and diseases. Consistent with our data and with a role for the type I IFN-TLR interplay on the cardiovascular system, IFN- $\alpha$  has been reported to act as an inflammatory amplifier by a mechanism involving TLR4 upregulation and the increased production of cytokines involved in plaque destabilization.<sup>134</sup> Additional mechanisms for TLR potentiation by type I IFN include the IFN- $\alpha$ -mediated upregulation of MyD88 described in macrophages.<sup>260</sup> Moreover, a recent study showed how type I IFN amplified cardiac inflammation after myocardial infarction by triggering deleterious effects via IRF3 in mice.<sup>261</sup> Our data also demonstrate a cooperation between IFN- $\alpha$  and TLR2/TLR3 ligands on the master regulator on inflammation and key mediator of the TLR responses, NF- $\kappa$ B.<sup>153</sup> The specific regulation and effects of the TLR2/6-IFNAR and the

TLR3/IFNAR interplay should be further studied. Altogether, these evidences and our work expand the emerging role of JAK/STAT and TLR interplay in the cardiovascular pathophysiology.

### **D.3.2-IFN- $\gamma$ and LPS interplay on inflammation, angiogenesis and osteogenesis**

The present study discloses a positive interplay between type II IFN receptor and TLR4 with robust pro-angiogenic, pro-inflammatory and pro-osteogenic effects in VIC. Similarly to type I IFN, a strong cooperation between IFN- $\gamma$  and LPS was found, particularly on VIC calcification. These data are in agreement with the current notion of IFN- $\gamma$  as a key modulator of other cytokines and inflammatory pathways.<sup>262</sup> Notably, the IFN- $\gamma$ -LPS interplay induced a similar pro-inflammatory profile in VIC than the IFN- $\alpha$ +LPS co-stimulation, but strikingly, it reached higher levels of adhesion molecule expression and cytokine secretion. These data are reminiscent of IFN- $\gamma$  as an amplifier of TLR signalling by promoting ligand-receptor interactions as well as downstream signalling routes via the inactivation of TLR-induced feedback inhibitory loops, reported in macrophages.<sup>263</sup> In VIC, gene silencing experiments identified STAT1 as the main transcription factor involved in IFN- $\gamma$  and LPS positive interplay. Consistently, in the cardiovascular system, STAT1 has been pointed out as the major factor integrating IFN- $\gamma$  and TLR signalling, which promotes a pro-atherogenic state in VSMC and vascular endothelial cells.<sup>264</sup>

We also disclosed a novel immune and non-hypoxic induction of HIF-1 $\alpha$  by IFN- $\gamma$ +LPS with consequences on angiogenesis and osteogenesis in VIC. Although HIF-1 $\alpha$  is canonically activated in response to hypoxia,<sup>198</sup> here we show its activation under normoxic conditions. Calcified valves are known to exhibit a pathologic new vessel formation and angiogenesis-related molecules. Histological and immunohistochemical analyses of valve cusps revealed that infiltrated T lymphocytes colocalized with areas of new vessel formation and surrounding calcific nodules,<sup>171</sup> and the colocalization of the pro-angiogenic molecule VEGF-A as well as HIF-1 $\alpha$  with calcific nodules within calcified valves.<sup>107</sup> It is therefore very likely that the axis HIF-1 $\alpha$ /VEGF-A plays a major role on the pathological neoangiogenesis found in calcified valves. In addition, HIF-1 $\alpha$  could also be involved in extracellular matrix remodelling since it has been described as the key mediator of the hypoxia-induced secretion of extracellular matrix proteins in mitral valve interstitial cells.<sup>201</sup>

The most accepted theory explaining HIF-1 $\alpha$  expression in CAVD is based on a passive process consequence of valve thickening and impairment of O<sub>2</sub> diffusion to layers underneath the endothelium. Here, we focused on the pathway controlling HIF-1 $\alpha$  expression in VIC in an inflammatory milieu and normoxic conditions. Our findings support the emerging role of non-

hypoxic mechanisms of HIF-1 $\alpha$  activation in cardiovascular pathophysiology, since recent reports have demonstrated the stimulation of HIF-1 $\alpha$  by mechanical low shear stress at atheroprone regions of arteries,<sup>265</sup> and by mimicking disturbed flow in porcine valvular cells and human valves.<sup>266</sup>

We elucidated the pathway underlying the non-canonical and immune-mediated induction of HIF-1 $\alpha$  in VIC using pharmacological and gene silencing approaches. Remarkably, we found that the immune-induced HIF-1 $\alpha$  expression is largely dependent on a dual-receptor challenge, since it is inhibited by Jakinibs as well as TLR4 activation signalling blockade. Knockdown and gain of function experiments unveiled STAT1 as the major transcription factor controlling HIF-1 $\alpha$  expression upon IFN- $\gamma$ +LPS treatment in VIC. However, STAT3 does not seem to play a major role. Intriguingly, in contrast to our results, STAT1 promoted the repression of HIF-1 $\alpha$ -dependent transcription in tumour cells, which reinforces the context-dependent effects of JAK/STAT signalling.<sup>267</sup> Altogether, our data demonstrate that JAK/STAT1 is the main pathway regulating the immune-induced HIF-1 $\alpha$  expression in VIC.

Our study highlights a role for HIF-1 $\alpha$  on pro-angiogenic molecule expression and calcification in VIC. One could hypothesize that at the initial stages of the disease, the pro-inflammatory milieu could activate HIF-1 $\alpha$  in VIC via immune mechanisms, which would support the notion of HIF-1 $\alpha$  expression on the valve because of concomitant challenges occurring prior to hypoxia after valve thickening. It is well known that HIF-1 $\alpha$  expression is finely regulated under normoxic conditions, and although it is constitutively translated, the prolyl-4-hydroxylases inhibit its protein stabilization by inducing its ubiquitination and degradation.<sup>198,268</sup> The exact mechanism leading to HIF-1 $\alpha$  stabilization by IFN- $\gamma$ +LPS co-stimulation in VIC remains to be further explored. The use of the selective HIF-1 $\alpha$  inhibitor PX-478, which is currently in clinical trial for the treatment of solid tumors and lymphoma,<sup>199,269</sup> demonstrated a role for HIF-1 $\alpha$  on VEGF-A secretion and calcification of VIC. However, HIF-1 $\alpha$  may not be the only effector accounting for IFN- $\gamma$ +LPS interplay-mediated responses since the chemical induction of HIF-1 $\alpha$  mimics the effects only in part, thus suggesting that STAT1 signalling diverges to other pathways prior to HIF-1 $\alpha$  activation. As a potential mechanism, we found that ERK could partially contribute to the Pi-induced calcification, as demonstrated by pharmacological blockade of ERK activation.

In keeping with the immune induction of HIF-1 $\alpha$  reported here, IFN- $\gamma$ -stimulated macrophages challenged with *Mycobacterium tuberculosis* exhibited HIF-1 $\alpha$  protein upregulation accounting for the subsequent immune responses.<sup>270</sup> Our data also remind the Warburg effect reported in macrophages during microbial challenge, in which NF- $\kappa$ B promotes a glycolytic

metabolism via HIF-1 $\alpha$  activation, thus turning in VSMC to the production of angiogenic as well as pro-inflammatory molecules.<sup>271</sup> As it pertains to calcification, an elegant study has previously associated HIF-1 $\alpha$  with the development of extra-skeletal ossifications, being the effects abrogated by PX-478.<sup>272</sup> Moreover, our findings are consistent with a major role of HIF-1 $\alpha$  on Pi-induced calcification reported in VSMC.<sup>229</sup> Additional non-hypoxic mechanisms of HIF-1 $\alpha$  activation have been recently shown in a study performed in porcine and human valves demonstrating that disturbed flow increased ubiquitin E2 ligase C by regulating HIF-1 $\alpha$  stabilization, which subsequently leads to endothelial inflammation, EndMT, and the ensuing calcification of transformed cells.<sup>266</sup>

To note, STAT1 regulation by IFN- $\gamma$ -LPS interplay is not only dependent on its activation by phosphorylation at different sites, but also on the upregulation of its protein expression. This mechanism is similar to one reported in human fibroblastic cell lines, where IFN- $\gamma$  upregulated STAT1 protein expression that turned into a sustained and prolonged activation of the pathway beyond its phosphorylation.<sup>202</sup>

The relevance of our data resides in that the IFNGR-TLR4 interplay contributes to potentiate, extend and expand the IFN- $\gamma$  and LPS effects in human VIC, via enhanced activation of NF- $\kappa$ B and STAT1 transcription factors as well as the unexpected immune induction of HIF-1 $\alpha$ . A relevant finding is the blockade of these responses by the pre-treatment with Jakinibs, as well as the reduction of the angiogenic and calcific response by the HIF-1 $\alpha$  inhibitor PX-478, which identifies novel potential druggable targets for the disease.

## **D.4-Sex-differences in VIC responses**

A major and unexpected finding of the present study is the demonstration of sex-specific differences in response to IFN and LPS in the AV context that correlate with clinical findings. Male sex is known to be a risk factor for CAVD, although the exact underlying mechanisms remain unknown. The first evidences were reported in the “Cardiovascular Health Study” in 1997, in which male sex was associated with a two-fold increase in the risk of aortic valve disease.<sup>20</sup> More recently, a study performed in a larger cohort of patients confirmed male sex as a risk factor for CAVD and calcium deposition on the AV.<sup>273</sup>

Growing clinical evidences from male and female calcified valves support the notion of sex as an important biological variable in CAVD. The main difference found in diseased tissue is the higher valvular calcification normalized to body weight or surface in male valves.<sup>188,23</sup> Strikingly,

despite these differences in calcium score, female valves reach similar CAVD severity levels than male ones, which could be related to the results of a recent work revealing that valves from women exhibit more fibrosis as compared to men.<sup>23</sup>

The understanding of the underlying mechanisms leading to sex differences in CAVD is clinically relevant and could be of use for the design of potential sex-specific therapeutic targets for drug development.<sup>274</sup> To date, two main theories of sex-differences in CAVD have been proposed: i) CAVD is a pathologic process exhibiting sex differences from the onset. ii) The initial triggers of CAVD are common for both sexes, but lately diverge during its progression.<sup>26</sup>

In addition, several lines of *in vitro* evidences demonstrate sex-differences in CAVD. The first report showed intrinsic sex-differences in porcine VIC, particularly in the expression profile of genes associated with processes relevant to CAVD pathogenesis, namely proliferation, apoptosis, migration, calcification, angiogenesis, inflammation, and extracellular matrix remodelling. Moreover, these differences translated into sex-differences in VIC function with respect to cell behaviour *in vitro*, i.e. proliferation and apoptosis.<sup>24</sup> Later, Masjedi and colleagues reported additional differences in matrix remodelling, alkaline phosphatase content, and calcific nodule formation in osteogenic media in porcine VIC. That was the first evidence of a higher predisposition of male VIC to calcify in osteogenic conditions.<sup>25</sup>

Our study brings light into sex-differences in CAVD. This is the first evidence of dissimilarities according to sexes in response to immune stimuli in human VIC. We have demonstrated scarce intrinsic differences at both cellular and tissue levels and a good amount of intriguing sex-divergences in response to type I and II IFN, the TLR4 ligand LPS, and to the interplay among these pathways. All these differences will be discussed in the next paragraphs.

Osteogenic calcification, via osteoblastic-like differentiation, seems to be more prevalent in calcified valves from males compared to females.<sup>74,275</sup> Regarding our type I IFN results, we have demonstrated that IFN- $\alpha$  alone and combined with LPS triggered larger calcification in VIC isolated from valves of males. Mechanistically, we found that variances in MMP-1/BMP-2/IL-6 secretion may account for sex-differences in the response to type I IFN in VIC. Despite sex dissimilarities in osteogenic markers at early times, 24 hours, neither cell differentiation nor functional ectopic phosphatase activity showed differences among sexes after long-term exposure (21 days). These observations suggest that both male and female VIC differentiate to a pro-calcifying phenotype, but the process seems to be delayed in female cells.

One striking finding relating sex-differences was the female-specific activation of Akt upon stimulation with either IFN- $\alpha$  and LPS or combined. In keeping with previous reports,<sup>100</sup> our data highlight a role of Akt in modulating VIC mineralization. Our findings further pinpointed Akt/cell survival as a sex-differential mechanism with consequences in VIC calcification. Strikingly, Akt activation blockade turned into an increased female cell calcification even in basal conditions, suggesting that it is a protective pathway. In addition, Akt activation could play a role on the lower TNAP expression as well as IL-6 secretion in female cells. This hypothesis is further supported by the downregulation of Akt found in calcified valve tissue, and its reported negative role on VIC mineralization and apoptosis by modulating the Pi transporter SLC20A1.<sup>100</sup> Moreover, Akt signalling has been related to extracellular matrix protein deposition in VIC,<sup>182</sup> which could be an underlying mechanism explaining the greater levels of fibrosis found in calcified valves from females.<sup>22</sup> This kinase has been related to cell survival, so one may expect that this mechanism could contribute to sex differences on calcification, a hypothesis supported by our findings on the lower apoptosis in female cells under high-phosphate conditions. This notion is further reinforced by the sex-differences in *BCL2* expression upon IFN- $\alpha$  treatment, which is only upregulated in male cells, possibly as a potential counter-acting mechanism. Our results are reminiscent with the increased nuclear activity of Akt in females as compared to males reported in the myocardium.<sup>276</sup>

Several hypotheses arise to explain the reported sex-differences in cell survival: (i) Epigenome alterations by sex hormones exposure. This is supported by several evidences suggesting that estrogen receptor- $\alpha$  cooperates with coactivators to epigenetically regulate estrogen-responsive genes such as *BCL2* by mechanisms involving PI3K/Akt pathways and histone demethylation.<sup>277</sup> Moreover, testosterone exposure decreased myocardial Akt in male heart during cardiac ischemia reperfusion by mechanisms involving *BCL2* and transcriptional repressors with a key role for miRNA regulation.<sup>278</sup> Furthermore, several evidences may support a putative role of type I IFN-mediated epigenetic changes in sex-differential responses, since this cytokine modulates epigenetic modifications that persist beyond the original stimulus, and its effects can be inhibited by transcriptional repressors downstream of Akt like forkhead box protein O3 (reviewed in<sup>111</sup>). Collectively, these data converge on Akt and *BCL2* pathways as key mediators of sex-differences in cardiovascular diseases.<sup>197</sup> ii) miRNA regulation has emerged as a potential explanation for sex-biased diseases,<sup>279</sup> and several miRNA have been reported to play a role on CAVD progression as pointed out by recent reports.<sup>280,281</sup> Thus, sex-differential regulation of miRNA emerges as a plausible mechanism accounting for sex-differences in CAVD. Overall, our data further agree with evidences on the well-stabilised notion of estrogens as critical regulators of innate immunity cells

and responses,<sup>282</sup> although a direct role for estrogens on regulating VIC calcification should be addressed in next studies

Sex-differential responses to immune stimuli have been previously described in other systems. One example is the higher responsiveness of male human neutrophils to stimulation with LPS and IFN- $\gamma$ , which triggered higher TNF- $\alpha$  secretion.<sup>283</sup> In our study, VIC exhibited sex differences on angiogenesis and calcification in the response to IFN- $\gamma$ . The major sex-differences were found in the higher level of calcification reached by male cells, which could be explained, at least in part, by the major contribution of dystrophic mechanisms in male VIC as demonstrated by flow cytometry analysis of cell death. Remarkably, stronger evidences for sex differences in the interplay between IFN- $\gamma$  and LPS were found. The pro-angiogenic phenotype induced in VIC by the combination of both ligands was characterized by a significantly larger secretion of VEGF-A and lower expression of *CNMD* anti-angiogenic gene in male cells. Mechanistically, data disclosed sex differences in HIF-1 $\alpha$  and ERK pathways that could account for the lower calcification in high Pi conditions exhibited by female VIC. In line with our findings, HIF-1 $\alpha$  has been pointed as a key mediator of the sex-differences found in the expression and modulation of growth and differentiation factor 15 in neonatal hyperoxic injury.<sup>284</sup> Moreover, sex-differences on ERK pathways have been previously reported in porcine VIC, in which a gene microarray analysis revealed that MAPK/ERK route was overrepresented in male cells.<sup>24</sup> This evidence and the increased propensity for ERK activation by IFN- $\gamma$ +LPS activation in human male VIC, suggest that ERK pathway may contribute to produce an overall increased susceptibility in male VIC to becoming activated to diseased phenotypes.

The correlation of some major findings in intact valve tissue highlights the intrinsic differences between sexes that may contribute to male sex being a risk factor for CAVD. Strikingly, female calcified valves showed higher expression of “protective genes”, such as *MGP* and *CNMD*. In addition, higher levels of the anti-apoptotic gene *BCL2* were found in both control cells and calcified tissue from females, in accordance to the lower levels of *BCL2* associated to a higher predisposition for cell death found in cardiovascular diseases.<sup>197</sup>

Overall, we found striking sex-differences on inflammation and calcification that parallel those findings in calcified valves. However, further studies are needed to elucidate the exact mechanisms underlying these differences, and to shed light on whether CAVD has a different scenario in male and female patients. It should be noted that, in our study, race was not a variable accounting for potential sex-differences because all the patients were Caucasian. In addition, sex

groups were comparable in terms of age, characteristics and in most cases comorbidities. The only statistical difference among male and female groups was the significantly higher levels of hypertension found in the calcified female valves used in **section R.4**. It is important to note that the sex-differences were not an initial hypothesis of this work, but data later revealed striking lower responses in female cells that were then confirmed by statistical analysis. Therefore, no sex bias in either cell isolation or experiment procedures was added since all specimens and cells were processed in parallel and following the same protocols. In addition, male and female VIC populations showed similar levels of basal  $\alpha$ -SMA protein, which indicates a similar phenotype in basal conditions. In our opinion, these sex-differences may have gone previously unnoticed since most studies in VIC have been performed in cells isolated from mostly male patients.

## **D.5-VIC-VEC communication and its potential role for CAVD**

Even though endothelial dysfunction is the earliest event in CAVD that leads to immune cell infiltration as well as lipid deposition,<sup>48</sup> how the activated endothelium communicates to VIC is still poorly understood. Once an inflammatory response has been initiated within the valve, it would be of interest to understand whether activated VIC secrete factors affecting VEC behaviours and if these factors promote increased damage or in contrast help to resolve endothelial inflammation.

We addressed this question using CM experiments from VIC previously activated with IFN- $\gamma$ +LPS, stimuli that were then removed. Our data revealed that mediators secreted by activated VIC can induce endothelial damage and inflammation, as demonstrated by the increased expression of *NOS3*, *VEGFA*, and *IL6* genes. In addition, CM induced adhesion molecule expression in VEC, which could perpetuate the immune cell infiltration and therefore an unresolved chronic inflammation within the valve. Together, data point to an impact of IFN- $\gamma$  and LPS on the pathophysiology of resident valve cells and support the communication between VIC and VEC in an inflammatory milieu with consequences in AV physiopathology.

There are some studies addressing the complex VIC-VEC communications with different approaches. In our hands, factors secreted by stimulated VIC promoted changes in VEC consistent with endothelial damage and inflammation. However, using co-culture platforms, Hjortnaes and colleagues showed a protective role for VIC, which suppressed the EndMT induced by TGF- $\beta$  in VEC and the subsequent calcification.<sup>285</sup> Therefore, the regulation of VEC phenotype by VIC remains still unclear. VEC have been shown to regulate VIC phenotype under shear stress

conditions.<sup>286</sup> Loss of TGF- $\beta$  in the endothelium have been shown to induce VIC calcification by suppression of SOX9 expression.<sup>287</sup>

Our hypothesis supporting a pharmacological intervention of the initial inflammatory phase of CAVD is further reinforced by evidences indicating a chronic endothelial dysfunction in CAVD. In this regard, calcified particles have been reported to induce the loss of endothelial markers in VEC, which could be a continuous source of pro-calcifying cells via EndMT to osteogenic-like cells.<sup>86</sup> Overall, little is known about this matter and further studies are needed to understand how the interplay VIC-VEC is finely regulated in the complex context of the AV.

## **D.6-IFN- $\gamma$ and TNF- $\alpha$ effects in VEC**

Endothelium has been pointed as the key mediator of the mechanical properties of the AV cusps,<sup>288</sup> and as noted earlier, endothelium injury is a key event in CAVD initiation.<sup>48</sup> It is therefore essential to understand VEC biology and their responses to different stimuli that could account for endothelial damage.

CAVD occurs in a side-specific manner, with the fibrosa layer preferentially calcified. It is hypothesized that the fibrosa-preferential calcification is due to endothelial dysfunction in response to disturbed flow in the fibrosa, characterized by low magnitude and oscillatory shear stress.<sup>1</sup> Investigating putative differences between inflammatory responses on both sides of the valve could shed light on VEC roles in disease pathogenesis and its underlying mechanisms. Our preliminary experiments in mixed VEC populations under static conditions showed that they can sense both Type I and II IFN, which upregulated *IL6* expression and downregulated *NOS3* transcript levels, suggesting harmful effects of these cytokines. In the subsequent study we focused on IFN- $\gamma$  given its association to atherosclerosis,<sup>109</sup> and its presence in diseased valves.<sup>138</sup> Material and time unavailability issues did not allow us to further study the role of type I IFN on side-specific VEC, which should be addressed in future studies.

It has been previously reported that pro-inflammatory cytokines, i.e. TNF- $\alpha$ , promote adhesion molecule expression in endothelial cells.<sup>289</sup> Here we demonstrate that IFN- $\gamma$  act as a pro-inflammatory cytokine in both aVEC and vVEC, as demonstrated by the induction of adhesion molecules expression, and IL-6 and IP-10 secretion. However, IFN- $\gamma$  did not induce IL-8 secretion, which suggests a chemokine-specific pattern in response to IFN- $\gamma$  similar to the previously reported for human microvascular endothelial cells.<sup>290</sup> No major side-specific differences were found at the

inflammatory level when comparing aVEC to vVEC responses. Strikingly valve-side differential secretion of IP-10 in aVEC in response to IFN- $\gamma$  was observed. This finding may be relevant since IP-10 is known as a chemoattractant cytokine for monocytes and T cells and it also exerts pro-atherogenic effects in a mouse model by modulating the local balance of immune cells.<sup>291</sup>

In normal conditions, VEC secrete nitric oxide (NO) that has protective effects on the valve, however, in response to pathological challenges the homeostatic balance is disrupted, leading to subsequent damage by reactive oxygen species increase.<sup>50</sup> In our study, IFN- $\gamma$ , in contrast to TNF- $\alpha$ , did not affect eNOS protein expression in human aVEC and vVEC. Our results are in line with previous reports indicating that TNF- $\alpha$  promoted eNOS downregulation in porcine VEC after 48 h of treatment.<sup>292</sup> Our data confirmed these results in human aortic side-specific VEC and showed differences with other cytokines like IFN- $\gamma$ . However, more studies are needed to elucidate whether IFN- $\gamma$  is capable of regulating the TNF- $\alpha$ -induced impairment of eNOS activity, such as the inhibition of the TNF- $\alpha$ -mediated NO production by IFN- $\gamma$  reported in vascular endothelial cells.<sup>293</sup> Finally, whether other regulations of eNOS, such as coupling/uncoupling or phosphorylation, could be induced by IFN- $\gamma$  remains to be further explored.

Another important finding of the study in VEC is the non-hypoxic induction of HIF-1 $\alpha$ , which mirrors the results with LPS+IFN- $\gamma$  in VIC. Potential side-specific differences were found at this level since TNF- $\alpha$  alone induced HIF-1 $\alpha$  stabilization only in aVEC. In contrast, when TNF- $\alpha$  was combined with IFN- $\gamma$ , HIF-1 $\alpha$  is stabilized in both aVEC and vVEC. Our results remind the TNF- $\alpha$ -mediated stabilization of HIF-1 $\alpha$  in different cancer cell lines.<sup>294</sup> Regarding the cardiovascular system, the stabilization of this transcription factor via NF- $\kappa$ B in endothelial cells has been linked to endothelial dysfunction in atheroprone regions.<sup>295</sup> In the AV context, these results point to this master transcription factor as the potential regulator of VEC fate in response to cytokines, given that HIF-1 $\alpha$  stabilization by disturbed blood flow leads to EndMT and subsequent calcification.<sup>296</sup> Therefore, similar mechanisms involving HIF-1 $\alpha$  could be regulating the previously reported EndMT in aVEC in response to TNF- $\alpha$ .<sup>52,292</sup>

Immune cell infiltration is a predominant process at CAVD early stages. Strikingly, we found that under multidirectional shear stress simulating a disturbed flow (centre of the wells), monocyte adhesion was higher in aVEC compared to vVEC for both cytokines alone and combined. In contrast, under unidirectional shear flow conditions (edge of the wells), no significant differences were found between aVEC and vVEC. These data suggest that aVEC are more prone to immune cell infiltration upon inflammatory stimulation under oscillatory flow conditions. Supporting these data,

previous studies have shown that the adhesion molecule profile of PECAM-1,  $\beta$ 1-integrin, VE-cadherin, and vinculin are different between aVEC and vVEC under cyclic strain.<sup>297</sup> Furthermore, our data further support the notion of unidirectional and higher magnitude shear flow as a protective pattern in vascular and valvular endothelial cells.<sup>298,45</sup> Our study provides evidence indicating that aortic-sided endothelium is more prone to IFN- $\gamma$ -mediated monocyte adhesion. However, based on the similar profile of ICAM-1 and VCAM-1 expression upon stimulation in aVEC and vVEC, other adhesion molecules could be implicated in the IFN- $\gamma$ -induced THP-1 adhesion. Among the potential candidates is E-selectin, which was reported to be expressed in valves and serum levels of CAVD patients.<sup>248</sup> Another potential explanation is that our Western Blot lysates comprised the mixture of VEC from either the centre and the edges of the wells, therefore potential differences of cells on the centre could be masked by the similar adhesion profile of cells on the edge.

Our adhesion assay data also highlight differences between valvular and vascular endothelial cell in the response to shear stress. In contrast to the vascular cell line HUVEC,<sup>172</sup> in our hands there were no differences in VEC density comparing the centre to the edge of the well. This finding supports the theory of different behaviours between valvular and vascular endothelial cells based on their distinct gene expression profiles.<sup>7</sup> Moreover, it is important to note that cells orientate differently under the same shear flow, parallel to flow in vascular endothelium, or perpendicular in valve endothelium.<sup>4</sup> One may speculate that these differences may explain, at least in part, why some similarities in the initial stages of atherosclerosis and CAVD lead to dissimilarities on later stages, particularly on the calcification process.

Interestingly, wound healing assays point to intriguing side-specific differences between aVEC and vVEC as well as dissimilarities in the response to pro-inflammatory cytokines. Indeed, IFN- $\gamma$  markedly reduced the wound closure in both aVEC and vVEC, pointing to this cytokine as a potent inhibitor of VEC migration. Our data correlate with previous studies demonstrating that IFN- $\gamma$  is an anti-angiogenic agent and a promising target for tumor growth and migration inhibition,<sup>239</sup> but differs from the pro-angiogenic phenotype induced by this cytokine in VIC, further reinforcing the cellular specificity of its effects. One could hypothesize that IFN- $\gamma$  could either reduce or slow VEC migration therefore affecting the maintenance and repair of endothelium after injury. In contrast to IFN- $\gamma$ , TNF- $\alpha$  and CoCl<sub>2</sub> induced the complete wound closure only in aVEC. This higher migratory potential of aVEC could have important implication in the EndMT and angiogenesis of these cells preferentially in the aortic side of the valve. Damaged VEC can de-differentiate into progenitor cells that are a source for osteogenic cell phenotypes within the valve.<sup>52,292</sup> It should be noted that data are

preliminary due to the limited number of samples (n=3) used in these experiments, therefore these results should be further confirmed using complementary protocols to reach final conclusions.

Our collective data further shed light to the role of endothelium on CAVD by disclosing an increased induction of IP-10 secretion, HIF-1 $\alpha$  stabilization, monocyte adhesion and cell migration upon challenging with inflammatory stimuli in aVEC compared to vVEC. This could be of relevance in the aortic valve context since the calcifications are developed preferentially in the fibrosa layer. However, further studies are needed to deepen on the functional relevance of these results.

## **D.7-JAK/STAT as potential therapeutic targets for CAVD**

A therapeutically relevant finding of our work is that the use of two different Jakinibs can inhibit IFN-induced calcification and the enhanced responses by JAK/STAT-TLR interplay. It is noteworthy that these drugs are currently used in clinics and that JAK/STAT pathways, associated with disease such as cancer, autoimmune disorders or asthma, are targeted for therapeutic intervention (reviewed in<sup>299</sup>). Our findings prompted us to hypothesize that these pathways could be a potential therapeutic target for CAVD during the initial stages of the disease. The paragraphs below will discuss our current knowledge on the role of JAK/STAT in CAVD pathogenesis and whether these pathways are putative targets that will enable to decelerate or even halt its progression.

### **D.7.1-Type I IFN and CAVD**

Our study provide evidence suggesting that type I IFN/STAT could be potentially involved in the initiation of the disease, thus targeting these pathways in early stages may be therapeutically relevant. The JAK/STAT inhibitor tofacitinib was able to abrogate the IFN- $\alpha$ -induced effects in human VIC. 2-dimensional plastic surfaces *in vitro* data show that the use of tofacitinib efficiently reduced the inflammation and calcification induced by the combination of IFN- $\alpha$  and LPS. Additionally, as demonstrated in the present study, dsRNA analogue responses are mainly mediated by IFN- $\beta$ 1 secretion in VIC. The use of ruxolitinib or a blocking antibody abrogated Poly(I:C)-induced responses, demonstrating that JAK/STAT pathways could be also targeted to reduce TLR3 responses in VIC upon viral infection and/or endogenous damage and release of self-dsRNA.

Tofacitinib is currently used as therapy for rheumatoid arthritis because its capacity to inhibit the inflammatory responses associated to this condition. The drug is primarily directed against dendritic cells, CD4+ T cells and activated B cells to blunt the ensuing production of cytokines.<sup>129</sup> As an example, this drug was capable not only of inhibiting the production of IFN- $\alpha$  by immune cells

but also its anti-viral properties.<sup>300</sup> In regards to potential adverse effects, the use of this drug has been associated with a lower incidence of cardiovascular events in patients with rheumatoid arthritis after 6 months of treatment.<sup>301</sup> In addition, tofacitinib did not show any adverse cardiovascular event in recent clinical trials for the treatment of plaque psoriasis.<sup>302</sup> In general, tofacitinib treatment seems to be a safe therapeutic option regarding adverse cardiovascular outcomes, as demonstrated by a systematic literature review.<sup>303</sup>

Strikingly, the only evidence that we found on the literature regarding a direct relationship between tofacitinib and calcification-related diseases has been recently reported. It is a two-case report of patients with calcifications associated to dermatomyositis, who were treated during 28 weeks with tofacitinib, a treatment that stopped and even regressed calcification development. This study provides the first evidence of the potential of Jakinibs for calcification-related conditions in human subjects.<sup>304</sup> However, for its putative use in CAVD, the development of novel diagnostic tools seems to be mandatory to detect the disease initiation in the initial stages, in which the therapeutic intervention of JAK signalling could be clinically relevant.

### **D.7.2-Type II interferons and CAVD**

Our findings in VIC suggest that the IFN- $\gamma$  secreted by infiltrated T lymphocytes could be an important endogenous initiator of the disease, therefore JAK/STAT pathways could be potentially used as therapeutic strategies. The JAK1 and JAK2 inhibitor ruxolitinib is currently used for primary myelofibrosis,<sup>131</sup> and also polycythaemia vera.<sup>130</sup> In our study, this FDA-approved drug completely blocked IFN- $\gamma$ -induced effects alone or combined with LPS. Importantly, ruxolitinib has been reported to be safe in a 3-year follow-up study in patients with myelofibrosis, with low adverse events.<sup>305</sup>

The relevance of targeting JAK/STAT pathways in the AV context goes beyond IFN signalling since a wide variety of cytokines, some of them with a potential role on CAVD progression, signal through these pathways. The JAK/STAT pathways can sense other cytokines apart from IFN, such as IL-6 and IL-10 and IL-12 p70, thus regulating cell growth and differentiation in different conditions and cell types in the body.<sup>299</sup> In the cardiovascular system, the IL-6/STAT3 axis has recently been described to promote VSMC differentiation towards an osteoblast-like phenotype via a mechanism involving RUNX2.<sup>306</sup> In CAVD, IL-6, a cytokine known to activate JAK/STAT and other pathways,<sup>136</sup> has been described as a potent inductor of calcification in VIC.<sup>59</sup> Therefore, targeting JAK/STAT pathways could be also a therapeutic strategy for IL-6-induced

calcification. Overall, our data, summarized in **Figure 66**, suggest that the use of JAK/STAT signalling inhibitors could be a potential therapeutic option during the initial stages of CAVD, in which inflammation is a relevant pathogenic process. However, the development of new diagnostic techniques and the discovery of novel biomarkers is a mandatory step before the potential use of these drugs. In addition, to avoid off-target effects, the development of site-targeted vehicles would be necessary to direct the action of these compounds to the AV.

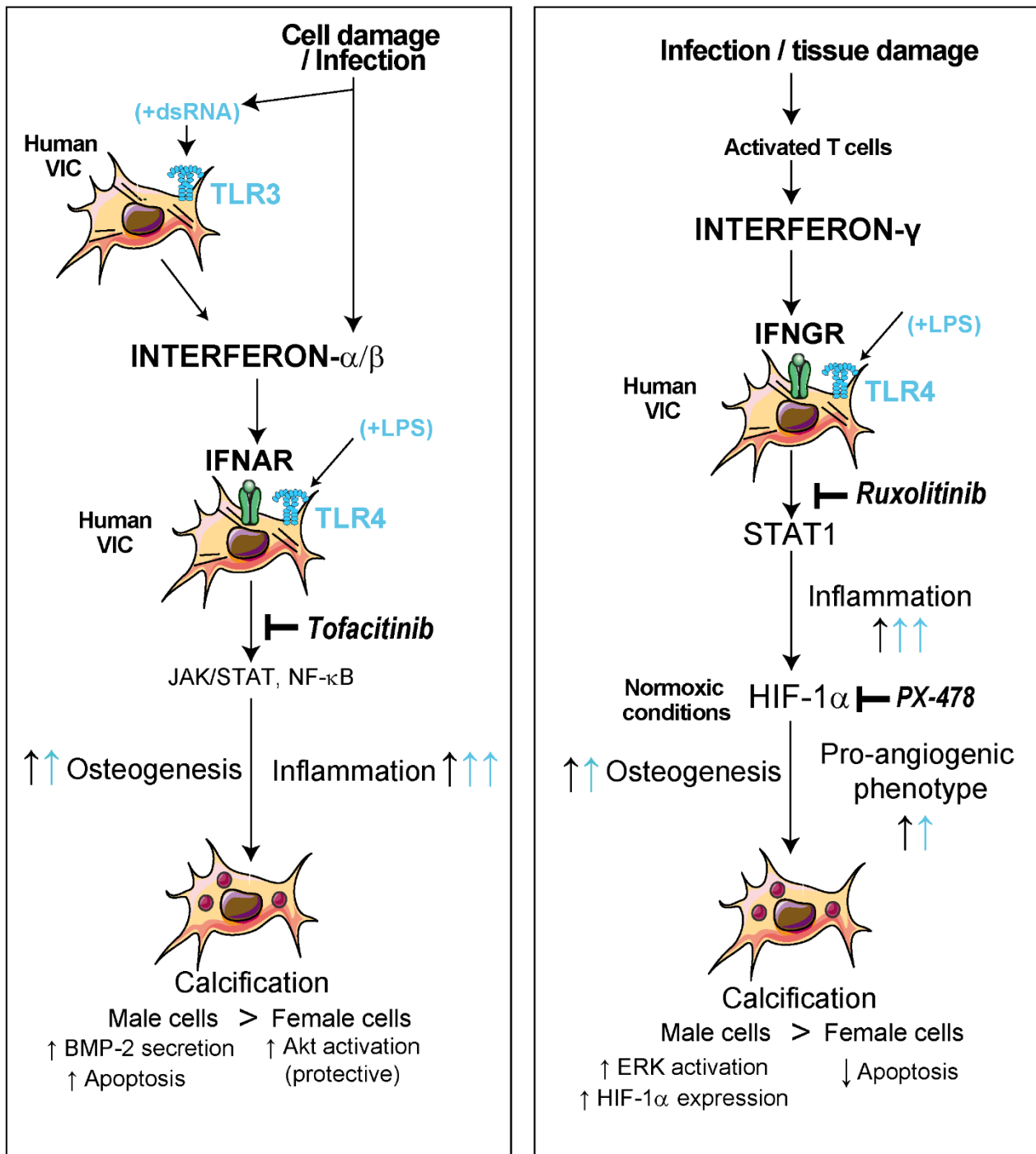


**Figure 66.** Schematic representation of IFN-induced effects in VIC, their mechanisms and the potential of Jakinib use in the aortic valve context.

## **D.8-Limitations of the study**

Apart from the low sample availability, especially limiting in the case of control valves from women given the low rate of cardiac transplantation in females, our study presents some technical and model limitations. The human cell culture model of CAVD used in the study has been extensively used over the last decades. Although many advances have been obtained, the culture of VIC on 2-dimensional plastic surfaces that are stiffer than the endogenous matrix it promotes the activation of the so-called qVIC to a myofibroblastic state termed activated aVIC.<sup>80</sup> Therefore, the control VIC used in the study, mostly myofibroblasts, exhibit a pre-pathological state of activation under our culture conditions. The use of 3D collagen culture models<sup>307</sup> or de-differentiating medium supplemented with insulin and fibroblast growth factor (FGF)-3<sup>189</sup> would have been a better model of the intact valve conditions. However, despite this limitation, to our understanding, a potential therapeutic intervention at the early stages of CAVD is only likely to be plausible when VIC are already activated since diagnostic tools and biomarkers for CAVD are far to detect its initiation during the initial transition of qVIC to aVIC.

Another limitation of the study is that our experiments with VIC were performed under static conditions that do not simulate the haemodynamics in the physiological state. Therefore, the experiments could have been performed under flow conditions, which would have allowed the interpretation of IFN effects under conditions that recapitulate more accurately the valve environment. In this line, the exposure of VIC to LPS under mechanical stress enhanced the response to this TLR agonist as compared to static conditions.<sup>308</sup> In addition, the application of shear stress in microfluidic devices also triggered porcine VIC activation, further supporting the potential effects of shear stress on VIC phenotype.<sup>309</sup> These recent evidences suggest an interplay between mechanical shear forces and inflammatory stimuli in VIC phenotype that could have been relevant for our study. Side-specific VEC experiments were performed under flow conditions that resemble to some extent the directionality of the flow within the AV on the aortic surface (oscillatory shear stress, centre of the well) and on the ventricular surface (laminar flow, edge of the well).<sup>172</sup> However, the magnitude of the shear stress was low compared to the real conditions of the valve. Therefore, the development and the use of more accurate flow systems such as microfluidic cardiac flow generators<sup>310</sup> mandatory to truly confirm the endothelial side-specific differences on immune cell adhesion.

Moreover the findings obtained in valve tissue by qPCR and Western Blot warrant further investigation with more accurately techniques such as immunohistochemistry or transcriptomic/proteomic analysis.

Finally, our findings are restricted to *in vitro* experiments and analysis of valve tissue. It would be of interest to check the effects of the immune mediators and inflammatory cytokines in appropriate animal models of the disease. Regarding this possibility, one important limitation is that there are not good animal models of CAVD to test the effects of inflammatory cytokines in conditions akin to human physiology.<sup>311</sup>



## **CONCLUSIONS**



# CONCLUSIONS

---

## Human aortic valve interstitial cells:

1. Aortic valve interstitial cells explanted from healthy valves express functional IFN receptors that activate several pathways such as canonical JAK/STAT routes, NF- $\kappa$ B, MAPK, and Akt.
2. Recombinant IFN- $\alpha$  and IFN- $\gamma$  induce a pro-inflammatory phenotype characterized by NF- $\kappa$ B activation and the subsequent induction of adhesion molecule expression and IL secretion. IFN trigger VIC differentiation towards an osteoblast-like phenotype and promote calcific nodule formation in high-phosphate conditions. The interplay between IFN and the TLR4 ligand LPS strongly potentiates the pro-inflammatory phenotype and accelerates both the osteogenic differentiation and calcification.
3. Differences between IFN consist of more robust effects of IFN- $\gamma$  and distinct mechanisms of osteogenesis. IFN- $\alpha$ -specific mechanisms include increased BMP-2 signalling. IFN- $\gamma$ -LPS interplay-specific mechanisms involve the non-hypoxic immune induction of HIF-1 $\alpha$  via STAT1, and the subsequent secretion of proangiogenic factors and calcification of VIC.
4. IFN- $\alpha$  and IFN- $\gamma$ -mediated responses, and their interplay with LPS, are abrogated by the JAK inhibitors tofacitinib and ruxolitinib, respectively.
5. IFN and LPS promote sex-differential responses, being VIC from male donors more responsive than cells from females, especially on the extent of calcification. Male-specific mechanisms include increased BMP-2, HIF-1 $\alpha$ , and ERK signalling pathways. Female-specific routes involve Akt/BCL2 as protective mechanisms.
6. The TLR3 ligand Poly(I:C) mediates pro-inflammatory and pro-osteogenic responses via type I IFN secretion and the subsequent activation of JAK/STAT.

## Human aortic valve endothelial cells:

7. Secreted factors from VIC activated with IFN- $\gamma$ +LPS promote endothelial damage and inflammation in VEC.
8. IFN- $\gamma$  act as a pro-inflammatory cytokine in VEC. IFN- $\gamma$  and TNF- $\alpha$  promote higher monocyte adhesion to aVEC compared to vVEC monolayers under oscillatory flow conditions.

### Human aortic valve tissue:

9. Calcified aortic valve tissue exhibits a pro-angiogenic profile compared to control valves, which includes HIF-1 $\alpha$  expression. Additionally, calcified valves from male donors express higher levels of pro-angiogenic genes and lower levels of calcification/angiogenesis inhibitors and anti-apoptotic genes.

### General conclusion:

10. Collectively, data reveal the complex regulation of immune pathways within the AV context that could be relevant at the early stages of CAVD. Data provide evidences supporting the current model of inflammation-induced calcification and the concept of additional active pro-angiogenic mechanisms beyond valve thickening and the subsequent hypoxia. Our results correlate with the higher calcification levels reported in AV from male patients and point to CAVD as a sex-divergent disease from the early inflammatory stages. Clinically relevant findings include the blockade of IFN-induced responses by Jakinibs currently used in clinics, and by a HIF-1 $\alpha$  inhibitor currently on clinical trials. JAK/STAT and HIF-1 $\alpha$  pathways emerge as potential therapeutic targets for CAVD during the initial-mid stages.

## **BIBLIOGRAPHY**



# BIBLIOGRAPHY

---

1. Sacks, M. S., Merryman, W. D. & Schmidt, D. E. ON THE BIOMECHANICS OF HEART VALVE FUNCTION. *J. Biomech.* **42**, 1804–1824 (2009).
2. Anderson, R. H., Ho, S. Y. & Becker, A. E. Anatomy of the human atrioventricular junctions revisited. *Anat. Rec.* **260**, 81–91 (2000).
3. Anderson, R. Clinical anatomy of the aortic root. *Heart* **84**, 670–673 (2000).
4. Butcher, J. T. & Nerem, R. M. Valvular endothelial cells and the mechanoregulation of valvular pathology. *Philos. Trans. R. Soc. B Biol. Sci.* **362**, 1445–1457 (2007).
5. Manduteanu, I., Popov, D., Radu, A. & Simionescu, M. Calf cardiac valvular endothelial cells in culture: production of glycosaminoglycans, prostacyclin and fibronectin. *J. Mol. Cell. Cardiol.* **20**, 103–118 (1988).
6. Deck, J. D. Endothelial cell orientation on aortic valve leaflets. *Cardiovasc. Res.* **20**, 760–767 (1986).
7. Butcher, J. T. *et al.* Transcriptional profiles of valvular and vascular endothelial cells reveal phenotypic differences: influence of shear stress. *Arterioscler. Thromb. Vasc. Biol.* **26**, 69–77 (2006).
8. Bairati, A. & DeBiasi, S. Presence of a smooth muscle system in aortic valve leaflets. *Anat. Embryol. (Berl.)* **161**, 329–340 (1981).
9. Taylor, P. M., Allen, S. P. & Yacoub, M. H. Phenotypic and functional characterization of interstitial cells from human heart valves, pericardium and skin. *J. Heart Valve Dis.* **9**, 150–158 (2000).
10. Chester, A. H. & Taylor, P. M. Molecular and functional characteristics of heart-valve interstitial cells. *Philos. Trans. R. Soc. B Biol. Sci.* **362**, 1437–1443 (2007).
11. Rabkin-Aikawa, E., Farber, M., Aikawa, M. & Schoen, F. J. Dynamic and reversible changes of interstitial cell phenotype during remodeling of cardiac valves. *J. Heart Valve Dis.* **13**, 841–847 (2004).
12. Hortells, L., Sur, S. & St Hilaire, C. Cell Phenotype Transitions in Cardiovascular Calcification. *Front. Cardiovasc. Med.* **5**, 27 (2018).
13. Leopold Jane A. Cellular Mechanisms of Aortic Valve Calcification. *Circ. Cardiovasc. Interv.* **5**, 605–614 (2012).
14. Nkomo, V. T. *et al.* Burden of valvular heart diseases: a population-based study. *Lancet Lond. Engl.* **368**, 1005–1011 (2006).
15. d’Arcy, J. L. *et al.* Large-scale community echocardiographic screening reveals a major burden of undiagnosed valvular heart disease in older people: the OxVALVE Population Cohort Study. *Eur. Heart J.* **37**, 3515–3522 (2016).
16. Baumgartner, H. *et al.* 2017 ESC/EACTS Guidelines for the management of valvular heart disease. *Eur. Heart J.* **38**, 2739–2791 (2017).
17. Cuypers, J. A. A. E., Witsenburg, M., van der Linde, D. & Roos-Hesselink, J. W. Pulmonary stenosis: update on diagnosis and therapeutic options. *Heart Br. Card. Soc.* **99**, 339–347 (2013).
18. Otto, C. M., Lind, B. K., Kitzman, D. W., Gersh, B. J. & Siscovick, D. S. Association of aortic-valve sclerosis with cardiovascular mortality and morbidity in the elderly. *N. Engl. J. Med.* **341**, 142–147 (1999).
19. Otto, C. M. Calcific aortic valve disease: outflow obstruction is the end stage of a systemic disease process. *Eur. Heart J.* **30**, 1940–1942 (2009).
20. Stewart, B. F. *et al.* Clinical factors associated with calcific aortic valve disease. Cardiovascular Health Study. *J. Am. Coll. Cardiol.* **29**, 630–634 (1997).
21. Helseke, S., Kupari, M., Lindstedt, K. A. & Kovanen, P. T. Aortic valve stenosis: an active atheroinflammatory process. *Curr. Opin. Lipidol.* **18**, 483–491 (2007).
22. Simard Louis *et al.* Sex-Related Discordance Between Aortic Valve Calcification and Hemodynamic Severity of Aortic Stenosis. *Circ. Res.* **120**, 681–691 (2017).

23. Thaden, J. J. *et al.* Sex-related differences in calcific aortic stenosis: correlating clinical and echocardiographic characteristics and computed tomography aortic valve calcium score to excised aortic valve weight. *Eur. Heart J.* **37**, 693–699 (2016).
24. McCoy, C. M., Nicholas, D. Q. & Masters, K. S. Sex-related differences in gene expression by porcine aortic valvular interstitial cells. *PLoS One* **7**, e39980 (2012).
25. Masjedi, S., Lei, Y., Patel, J. & Ferdous, Z. Sex-related differences in matrix remodeling and early osteogenic markers in aortic valvular interstitial cells. *Heart Vessels* **32**, 217–228 (2017).
26. Porras, A. M., McCoy, C. M. & Masters, K. S. Calcific Aortic Valve Disease: A Battle of the Sexes. *Circ. Res.* **120**, 604–606 (2017).
27. Katz, R. *et al.* Features of the metabolic syndrome and diabetes mellitus as predictors of aortic valve calcification in the Multi-Ethnic Study of Atherosclerosis. *Circulation* **113**, 2113–2119 (2006).
28. Peltier, M. *et al.* Relation between cardiovascular risk factors and nonrheumatic severe calcific aortic stenosis among patients with a three-cuspid aortic valve. *Am. J. Cardiol.* **91**, 97–99 (2003).
29. Zentner, D. *et al.* Prospective evaluation of aortic stenosis in end-stage kidney disease: a more fulminant process? *Nephrol. Dial. Transplant. Off. Publ. Eur. Dial. Transpl. Assoc. - Eur. Ren. Assoc.* **26**, 1651–1655 (2011).
30. Cholesterol Treatment Trialists' (CTT) Collaborators *et al.* The effects of lowering LDL cholesterol with statin therapy in people at low risk of vascular disease: meta-analysis of individual data from 27 randomised trials. *Lancet Lond. Engl.* **380**, 581–590 (2012).
31. Cowell, S. J. *et al.* A randomized trial of intensive lipid-lowering therapy in calcific aortic stenosis. *N. Engl. J. Med.* **352**, 2389–2397 (2005).
32. Rossebø, A. B. *et al.* Intensive Lipid Lowering with Simvastatin and Ezetimibe in Aortic Stenosis. *N. Engl. J. Med.* **359**, 1343–1356 (2008).
33. Chan, K. L. *et al.* Effect of Lipid lowering with rosuvastatin on progression of aortic stenosis: results of the aortic stenosis progression observation: measuring effects of rosuvastatin (ASTRONOMER) trial. *Circulation* **121**, 306–314 (2010).
34. Gotoh, T. *et al.* Correlation between lipoprotein(a) and aortic valve sclerosis assessed by echocardiography (the JMS Cardiac Echo and Cohort Study). *Am. J. Cardiol.* **76**, 928–932 (1995).
35. Zheng, K. H. *et al.* Lipoprotein(a) and Oxidized Phospholipids Promote Valve Calcification in Patients With Aortic Stenosis. *J. Am. Coll. Cardiol.* **73**, 2150–2162 (2019).
36. Garg, V. *et al.* Mutations in NOTCH1 cause aortic valve disease. *Nature* **437**, 270 (2005).
37. Barker, A. J., Lanning, C. & Shandas, R. Quantification of Hemodynamic Wall Shear Stress in Patients with Bicuspid Aortic Valve Using Phase-Contrast MRI. *Ann. Biomed. Eng.* **38**, 788–800 (2010).
38. Faggiano, P. *et al.* Cardiac calcification as a marker of subclinical atherosclerosis and predictor of cardiovascular events: A review of the evidence. *Eur. J. Prev. Cardiol.* 2047487319830485 (2019). doi:10.1177/2047487319830485
39. Messika-Zeitoun, D. *et al.* Evaluation and clinical implications of aortic valve calcification measured by electron-beam computed tomography. *Circulation* **110**, 356–362 (2004).
40. Pawade, T. A. *et al.* Optimization and Reproducibility of Aortic Valve 18F-Fluoride Positron Emission Tomography in Patients With Aortic Stenosis. *Circ. Cardiovasc. Imaging* **9**, e005131 (2016).
41. Pawade, T. A., Newby, D. E. & Dweck, M. R. Calcification in Aortic Stenosis: The Skeleton Key. *J. Am. Coll. Cardiol.* **66**, 561–577 (2015).
42. Aikawa Elena & Otto Catherine M. Look More Closely at the Valve. *Circulation* **125**, 9–11 (2012).
43. Miller, J. D., Weiss, R. M. & Heistad, D. D. Calcific Aortic Valve Stenosis: Methods, Models, and Mechanisms. *Circ. Res.* **108**, 1392–1412 (2011).
44. Arjunon, S., Rathan, S., Jo, H. & Yoganathan, A. P. Aortic Valve: Mechanical Environment and Mechanobiology. *Ann. Biomed. Eng.* **41**, 1331–1346 (2013).
45. Chistiakov, D. A., Orekhov, A. N. & Bobryshev, Y. V. Effects of shear stress on endothelial cells: go with the flow. *Acta Physiol. Oxf. Engl.* **219**, 382–408 (2017).
46. Gomel, M. A., Lee, R. & Grande-Allen, K. J. Comparing the Role of Mechanical Forces in Vascular and Valvular Calcification Progression. *Front. Cardiovasc. Med.* **5**, (2019).

47. Pawade, T. A. *et al.* Optimization and Reproducibility of Aortic Valve 18F-Fluoride Positron Emission Tomography in Patients With Aortic Stenosis. *Circ. Cardiovasc. Imaging* **9**, e005131 (2016).
48. Poggianti, E. *et al.* Aortic valve sclerosis is associated with systemic endothelial dysfunction. *J. Am. Coll. Cardiol.* **41**, 136–141 (2003).
49. Miller, J. D. *et al.* Dysregulation of Antioxidant Mechanisms Contributes to Increased Oxidative Stress in Calcific Aortic Valvular Stenosis in Humans. *J. Am. Coll. Cardiol.* **52**, 843–850 (2008).
50. Farrar, E. J., Huntley, G. D. & Butcher, J. Endothelial-Derived Oxidative Stress Drives Myofibroblastic Activation and Calcification of the Aortic Valve. *PLoS ONE* **10**, (2015).
51. Simmons, C. A., Grant, G. R., Manduchi, E. & Davies, P. F. Spatial heterogeneity of endothelial phenotypes correlates with side-specific vulnerability to calcification in normal porcine aortic valves. *Circ. Res.* **96**, 792–799 (2005).
52. Mahler, G. J., Farrar, E. J. & Butcher, J. T. Inflammatory cytokines promote mesenchymal transformation in embryonic and adult valve endothelial cells. *Arterioscler. Thromb. Vasc. Biol.* **33**, 121–130 (2013).
53. Dahal, S., Huang, P., Murray, B. T. & Mahler, G. J. Endothelial to mesenchymal transformation is induced by altered extracellular matrix in aortic valve endothelial cells. *J. Biomed. Mater. Res. A* **105**, 2729–2741 (2017).
54. Demer, L. L. & Tintut, Y. Inflammatory, metabolic, and genetic mechanisms of vascular calcification. *Arterioscler. Thromb. Vasc. Biol.* **34**, 715–723 (2014).
55. O'Brien Kevin D. Pathogenesis of Calcific Aortic Valve Disease. *Arterioscler. Thromb. Vasc. Biol.* **26**, 1721–1728 (2006).
56. Mathieu, P., Bouchareb, R. & Boulanger, M.-C. Innate and Adaptive Immunity in Calcific Aortic Valve Disease. *J. Immunol. Res.* **2015**, 851945 (2015).
57. Coté, N. *et al.* Inflammation Is Associated with the Remodeling of Calcific Aortic Valve Disease. *Inflammation* **36**, 573–581 (2013).
58. Otto, C. M., Kuusisto, J., Reichenbach, D. D., Gown, A. M. & O'Brien, K. D. Characterization of the early lesion of 'degenerative' valvular aortic stenosis. Histological and immunohistochemical studies. *Circulation* **90**, 844–853 (1994).
59. El Hussein, D. *et al.* P2Y2 receptor represses IL-6 expression by valve interstitial cells through Akt: implication for calcific aortic valve disease. *J. Mol. Cell. Cardiol.* **72**, 146–156 (2014).
60. Nadlonek, N. *et al.* Interleukin-1 Beta Induces an Inflammatory Phenotype in Human Aortic Valve Interstitial Cells Through Nuclear Factor Kappa Beta. *Ann. Thorac. Surg.* **96**, (2013).
61. Kaden, J. J. *et al.* Interleukin-1 beta promotes matrix metalloproteinase expression and cell proliferation in calcific aortic valve stenosis. *Atherosclerosis* **170**, 205–211 (2003).
62. Jian, B., Narula, N., Li, Q., Mohler, E. R. & Levy, R. J. Progression of aortic valve stenosis: TGF-beta1 is present in calcified aortic valve cusps and promotes aortic valve interstitial cell calcification via apoptosis. *Ann. Thorac. Surg.* **75**, 457–465; discussion 465-466 (2003).
63. Mohty, D. *et al.* Association between plasma LDL particle size, valvular accumulation of oxidized LDL, and inflammation in patients with aortic stenosis. *Arterioscler. Thromb. Vasc. Biol.* **28**, 187–193 (2008).
64. Bouchareb, R. *et al.* Autotaxin Derived From Lipoprotein(a) and Valve Interstitial Cells Promotes Inflammation and Mineralization of the Aortic Valve. *Circulation* **132**, 677–690 (2015).
65. Yu, B. *et al.* Lipoprotein(a) Induces Human Aortic Valve Interstitial Cell Calcification. *JACC Basic Transl. Sci.* **2**, 358–371 (2017).
66. Nagy, E. *et al.* Upregulation of the 5-lipoxygenase pathway in human aortic valves correlates with severity of stenosis and leads to leukotriene-induced effects on valvular myofibroblasts. *Circulation* **123**, 1316–1325 (2011).
67. Wirrig, E. E., Gomez, M. V., Hinton, R. B. & Yutzey, K. E. COX2 inhibition reduces aortic valve calcification in vivo. *Arterioscler. Thromb. Vasc. Biol.* **35**, 938–947 (2015).
68. Skowasch, D. *et al.* Pathogen burden in degenerative aortic valves is associated with inflammatory and immune reactions. *J Heart Valve Dis* (2009).

69. Nakano, K. *et al.* Detection of cariogenic *Streptococcus mutans* in extirpated heart valve and atheromatous plaque specimens. *J. Clin. Microbiol.* **44**, 3313–3317 (2006).
70. Cohen, D. J. *et al.* Role of oral bacterial flora in calcific aortic stenosis: an animal model. *Ann. Thorac. Surg.* **77**, 537–543 (2004).
71. García-Rodríguez, C. *et al.* Toll-Like Receptors, Inflammation, and Calcific Aortic Valve Disease. *Front. Physiol.* **9**, (2018).
72. O’Brien, K. D. *et al.* Association of angiotensin-converting enzyme with low-density lipoprotein in aortic valvular lesions and in human plasma. *Circulation* **106**, 2224–2230 (2002).
73. Fujisaka, T. *et al.* Angiotensin II promotes aortic valve thickening independent of elevated blood pressure in apolipoprotein-E deficient mice. *Atherosclerosis* **226**, 82–87 (2013).
74. Torre, M., Hwang, D. H., Padera, R. F., Mitchell, R. N. & VanderLaan, P. A. Osseous and chondromatous metaplasia in calcific aortic valve stenosis. *Cardiovasc. Pathol.* **25**, 18–24 (2016).
75. Blaser, M. C. & Aikawa, E. Roles and Regulation of Extracellular Vesicles in Cardiovascular Mineral Metabolism. *Front. Cardiovasc. Med.* **5**, (2018).
76. Bertazzo, S. *et al.* Nano-analytical electron microscopy reveals fundamental insights into human cardiovascular tissue calcification. *Nat. Mater.* **12**, 576–583 (2013).
77. Mohler Emile R. *et al.* Bone Formation and Inflammation in Cardiac Valves. *Circulation* **103**, 1522–1528 (2001).
78. Aikawa, E. *et al.* Multimodality molecular imaging identifies proteolytic and osteogenic activities in early aortic valve disease. *Circulation* **115**, 377–386 (2007).
79. Rajamannan, N. M. *et al.* Human Aortic Valve Calcification Is Associated With an Osteoblast Phenotype. *Circulation* **107**, 2181–2184 (2003).
80. Liu, A. C., Joag, V. R. & Gotlieb, A. I. The Emerging Role of Valve Interstitial Cell Phenotypes in Regulating Heart Valve Pathobiology. *Am. J. Pathol.* **171**, 1407–1418 (2007).
81. Taylor, P. M., Batten, P., Brand, N. J., Thomas, P. S. & Yacoub, M. H. The cardiac valve interstitial cell. *Int. J. Biochem. Cell Biol.* **35**, 113–118 (2003).
82. New, S. E. P. & Aikawa, E. Molecular Imaging Insights into Early Inflammatory Stages of Arterial and Aortic Valve Calcification. *Circ. Res.* **108**, 1381–1391 (2011).
83. Edep, M. E., Shirani, J., Wolf, P. & Brown, D. L. Matrix metalloproteinase expression in nonrheumatic aortic stenosis. *Cardiovasc. Pathol. Off. J. Soc. Cardiovasc. Pathol.* **9**, 281–286 (2000).
84. Yip, C. Y. Y., Chen, J.-H., Zhao, R. & Simmons, C. A. Calcification by valve interstitial cells is regulated by the stiffness of the extracellular matrix. *Arterioscler. Thromb. Vasc. Biol.* **29**, 936–942 (2009).
85. Richards, J. M. *et al.* Crystallinity of hydroxyapatite drives myofibroblastic activation and calcification in aortic valves. *Acta Biomater.* **71**, 24–36 (2018).
86. van Engeland, N. C. A. *et al.* Aortic calcified particles modulate valvular endothelial and interstitial cells. *Cardiovasc. Pathol.* **28**, 36–45 (2017).
87. Bossé, Y. *et al.* Refining molecular pathways leading to calcific aortic valve stenosis by studying gene expression profile of normal and calcified stenotic human aortic valves. *Circ. Cardiovasc. Genet.* **2**, 489–498 (2009).
88. Komori, T. Regulation of osteoblast differentiation by Runx2. *Adv. Exp. Med. Biol.* **658**, 43–49 (2010).
89. Alexopoulos, A. *et al.* Bone regulatory factors NFATc1 and Osterix in human calcific aortic valves. *Int. J. Cardiol.* **139**, 142–149 (2010).
90. Boström, K. I., Rajamannan, N. M. & Towler, D. A. The regulation of valvular and vascular sclerosis by osteogenic morphogens. *Circ. Res.* **109**, 564–577 (2011).
91. Yang, X. *et al.* Bone morphogenic protein 2 induces Runx2 and osteopontin expression in human aortic valve interstitial cells: Role of Smad1 and extracellular signal-regulated kinase 1/2. *J. Thorac. Cardiovasc. Surg.* **138**, 1008-1015.e1 (2009).
92. Gomez-Stallons, M. V., Wirrig-Schwendeman, E. E., Hassel, K. R., Conway, S. J. & Yutzey, K. E. Bone Morphogenetic Protein Signaling Is Required for Aortic Valve Calcification. *Arterioscler. Thromb. Vasc. Biol.* **36**, 1398–1405 (2016).

93. Kaden, J. J. *et al.* Receptor activator of nuclear factor kappaB ligand and osteoprotegerin regulate aortic valve calcification. *J. Mol. Cell. Cardiol.* **36**, 57–66 (2004).
94. Hofbauer, L. C. *et al.* The roles of osteoprotegerin and osteoprotegerin ligand in the paracrine regulation of bone resorption. *J. Bone Miner. Res. Off. J. Am. Soc. Bone Miner. Res.* **15**, 2–12 (2000).
95. Hjortnaes, J. *et al.* Arterial and aortic valve calcification inversely correlates with osteoporotic bone remodelling: a role for inflammation. *Eur. Heart J.* **31**, 1975–1984 (2010).
96. Chen Jan-Hung, Chen Wen Li Kelly, Sider Krista L., Yip Cindy Ying Yin & Simmons Craig A.  $\beta$ -Catenin Mediates Mechanically Regulated, Transforming Growth Factor- $\beta$ 1-Induced Myofibroblast Differentiation of Aortic Valve Interstitial Cells. *Arterioscler. Thromb. Vasc. Biol.* **31**, 590–597 (2011).
97. Pohjolainen, V. *et al.* Noncollagenous bone matrix proteins as a part of calcific aortic valve disease regulation. *Hum. Pathol.* **39**, 1695–1701 (2008).
98. Mathieu, P. *et al.* Calcification of human valve interstitial cells is dependent on alkaline phosphatase activity. *J. Heart Valve Dis.* **14**, 353–357 (2005).
99. Linefsky, J. P. *et al.* Association of Serum Phosphate Levels with Aortic Valve Sclerosis and Annular Calcification: the Cardiovascular Health Study. *J. Am. Coll. Cardiol.* **58**, 291–297 (2011).
100. Hussein, D. E. *et al.* High Expression of the Pi-Transporter SLC20A1/Pit1 in Calcific Aortic Valve Disease Promotes Mineralization through Regulation of Akt-1. *PLOS ONE* **8**, e53393 (2013).
101. Rathan, S., Yoganathan, A. P. & O'Neill, W. C. The Role of Inorganic Pyrophosphate in Aortic Valve Calcification. *J. Heart Valve Dis.* **23**, 387–394 (2014).
102. Venardos, N. *et al.* Matrix Gla Protein Regulates Calcification of the Aortic Valve. *J. Surg. Res.* **199**, 1–6 (2015).
103. Nigam, V. & Srivastava, D. Notch1 represses osteogenic pathways in aortic valve cells. *J. Mol. Cell. Cardiol.* **47**, 828–834 (2009).
104. Soini, Y., Salo, T. & Satta, J. Angiogenesis is involved in the pathogenesis of nonrheumatic aortic valve stenosis. *Hum. Pathol.* **34**, 756–763 (2003).
105. Yoshioka, M. *et al.* Chondromodulin-I maintains cardiac valvular function by preventing angiogenesis. *Nat. Med.* **12**, 1151 (2006).
106. Hakuno, D., Kimura, N., Yoshioka, M. & Fukuda, K. Role of angiogenetic factors in cardiac valve homeostasis and disease. *J. Cardiovasc. Transl. Res.* **4**, 727–740 (2011).
107. Perrotta, I., Moraca, F. M., Sciangula, A., Aquila, S. & Mazzulla, S. HIF-1 $\alpha$  and VEGF: Immunohistochemical Profile and Possible Function in Human Aortic Valve Stenosis. *Ultrastruct. Pathol.* **39**, 198–206 (2015).
108. Akahori, H. *et al.* Nuclear factor- $\kappa$ B-hypoxia-inducible factor-2 pathway in aortic valve stenosis. *J. Heart Valve Dis.* **23**, 558–566 (2014).
109. Boshuizen Marieke C.S. & de Winther Menno P.J. Interferons as Essential Modulators of Atherosclerosis. *Arterioscler. Thromb. Vasc. Biol.* **35**, 1579–1588 (2015).
110. Isaacs, A. & Lindenmann, J. Virus interference. I. The interferon. *Proc. R. Soc. Lond. B Biol. Sci.* **147**, 258–267 (1957).
111. Ivashkiv, L. B. & Donlin, L. T. Regulation of type I interferon responses. *Nat. Rev. Immunol.* **14**, 36–49 (2014).
112. Ivashkiv, L. B. IFN $\gamma$ : signalling, epigenetics and roles in immunity, metabolism, disease and cancer immunotherapy. *Nat. Rev. Immunol.* **18**, 545–558 (2018).
113. de Weerd, N. A., Samarajiwa, S. A. & Hertzog, P. J. Type I interferon receptors: biochemistry and biological functions. *J. Biol. Chem.* **282**, 20053–20057 (2007).
114. Dunn, G. P., Koebel, C. M. & Schreiber, R. D. Interferons, immunity and cancer immunoediting. *Nat. Rev. Immunol.* **6**, 836–848 (2006).
115. Stark, G. R., Kerr, I. M., Williams, B. R., Silverman, R. H. & Schreiber, R. D. How cells respond to interferons. *Annu. Rev. Biochem.* **67**, 227–264 (1998).
116. Luu, K. *et al.* STAT1 plays a role in TLR signal transduction and inflammatory responses. *Immunol. Cell Biol.* **92**, 761–769 (2014).

117. Kotenko, S. V. & Durbin, J. E. Contribution of type III interferons to antiviral immunity: location, location, location. *J. Biol. Chem.* **292**, 7295–7303 (2017).
118. Lazear, H. M., Nice, T. J. & Diamond, M. S. Interferon-λ: Immune Functions at Barrier Surfaces and Beyond. *Immunity* **43**, 15–28 (2015).
119. Mogensen, T. H. IRF and STAT Transcription Factors - From Basic Biology to Roles in Infection, Protective Immunity, and Primary Immunodeficiencies. *Front. Immunol.* **9**, (2019).
120. Chen, Y.-J., Li, J., Lu, N. & Shen, X.-Z. Interferon regulatory factors: A key to tumour immunity. *Int. Immunopharmacol.* **49**, 1–5 (2017).
121. Subramaniam, P. S., Torres, B. A. & Johnson, H. M. So many ligands, so few transcription factors: a new paradigm for signaling through the STAT transcription factors. *Cytokine* **15**, 175–187 (2001).
122. Kiu, H. & Nicholson, S. E. Biology and significance of the JAK/STAT signalling pathways. *Growth Factors Chur Switz.* **30**, 88–106 (2012).
123. Aaronson, D. S. & Horvath, C. M. A road map for those who don't know JAK-STAT. *Science* **296**, 1653–1655 (2002).
124. Schindler, C., Levy, D. E. & Decker, T. JAK-STAT Signaling: From Interferons to Cytokines. *J. Biol. Chem.* **282**, 20059–20063 (2007).
125. Yamaoka, K. *et al.* The Janus kinases (Jaks). *Genome Biol.* **5**, 253 (2004).
126. Huynh, J., Etemadi, N., Hollande, F., Ernst, M. & Buchert, M. The JAK/STAT3 axis: A comprehensive drug target for solid malignancies. *Semin. Cancer Biol.* **45**, 13–22 (2017).
127. Hervas-Stubbs, S. *et al.* Direct Effects of Type I Interferons on Cells of the Immune System. *Clin. Cancer Res.* **17**, 2619–2627 (2011).
128. Shuai, K. & Liu, B. Regulation of JAK–STAT signalling in the immune system. *Nat. Rev. Immunol.* **3**, 900 (2003).
129. Tanaka, Y. Recent progress and perspective in JAK inhibitors for rheumatoid arthritis: from bench to bedside. *J. Biochem. (Tokyo)* **158**, 173–179 (2015).
130. McKeage, K. Ruxolitinib: A Review in Polycythaemia Vera. *Drugs* **75**, 1773–1781 (2015).
131. Plosker, G. L. Ruxolitinib: a review of its use in patients with myelofibrosis. *Drugs* **75**, 297–308 (2015).
132. Kishore, R. & Verma, S. K. Roles of STATs signaling in cardiovascular diseases. *JAK-STAT* **1**, 118 (2012).
133. Knight, R. A., Scarabelli, T. M. & Stephanou, A. STAT transcription in the ischemic heart. *JAK-STAT* **1**, 111–117 (2012).
134. Niessner, A. *et al.* Synergistic proinflammatory effects of the antiviral cytokine interferon-alpha and Toll-like receptor 4 ligands in the atherosclerotic plaque. *Circulation* **116**, 2043–2052 (2007).
135. Chmielewski, S. *et al.* STAT1-dependent signal integration between IFN $\gamma$  and TLR4 in vascular cells reflect pro-atherogenic responses in human atherosclerosis. *PLoS One* **9**, e113318 (2014).
136. Heinrich, P. C. *et al.* Principles of interleukin (IL)-6-type cytokine signalling and its regulation. *Biochem. J.* **374**, 1–20 (2003).
137. Anger, T. *et al.* VAP-1, Eotaxin3 and MIG as potential atherosclerotic triggers of severe calcified and stenotic human aortic valves: effects of statins. *Exp. Mol. Pathol.* **83**, 435–442 (2007).
138. Nagy, E. *et al.* Interferon- $\gamma$  Released by Activated CD8+ T Lymphocytes Impairs the Calcium Resorption Potential of Osteoclasts in Calcified Human Aortic Valves. *Am. J. Pathol.* **187**, 1413–1425 (2017).
139. Singleton, E. B. & Merten, D. F. An unusual syndrome of widened medullary cavities of the metacarpals and phalanges, aortic calcification and abnormal dentition. *Pediatr. Radiol.* **1**, 2–7 (1973).
140. Jang, M.-A. *et al.* Mutations in DDX58, which encodes RIG-I, cause atypical Singleton-Merten syndrome. *Am. J. Hum. Genet.* **96**, 266–274 (2015).
141. Rutsch, F. *et al.* A specific IFIH1 gain-of-function mutation causes Singleton-Merten syndrome. *Am. J. Hum. Genet.* **96**, 275–282 (2015).
142. Buers, I., Nitschke, Y. & Rutsch, F. Novel interferonopathies associated with mutations in RIG-I like receptors. *Cytokine Growth Factor Rev.* **29**, 101–107 (2016).
143. Lu, C. & MacDougall, M. RIG-I-Like Receptor Signaling in Singleton-Merten Syndrome. *Front. Genet.* **8**, 118 (2017).

144. Buers, I., Rice, G. I., Crow, Y. J. & Rutsch, F. MDA5-Associated Neuroinflammation and the Singleton-Merten Syndrome: Two Faces of the Same Type I Interferonopathy Spectrum. *J. Interferon Cytokine Res. Off. J. Int. Soc. Interferon Cytokine Res.* **37**, 214–219 (2017).
145. Takeuchi, O. & Akira, S. Pattern recognition receptors and inflammation. *Cell* **140**, 805–820 (2010).
146. Kawai, T. & Akira, S. The role of pattern-recognition receptors in innate immunity: update on Toll-like receptors. *Nat. Immunol.* **11**, 373–384 (2010).
147. Lemaitre, B., Nicolas, E., Michaut, L., Reichhart, J. M. & Hoffmann, J. A. The dorsoventral regulatory gene cassette *spätzle/Toll/cactus* controls the potent antifungal response in *Drosophila* adults. *Cell* **86**, 973–983 (1996).
148. Poltorak, A. *et al.* Defective LPS signaling in C3H/HeJ and C57BL/10ScCr mice: mutations in *Tlr4* gene. *Science* **282**, 2085–2088 (1998).
149. Takeda, K. & Akira, S. Toll-like receptors. *Curr. Protoc. Immunol.* **109**, 14.12.1–10 (2015).
150. Zähringer, U., Lindner, B., Inamura, S., Heine, H. & Alexander, C. TLR2 - promiscuous or specific? A critical re-evaluation of a receptor expressing apparent broad specificity. *Immunobiology* **213**, 205–224 (2008).
151. Alexopoulou, L., Holt, A. C., Medzhitov, R. & Flavell, R. A. Recognition of double-stranded RNA and activation of NF-kappaB by Toll-like receptor 3. *Nature* **413**, 732–738 (2001).
152. Carpenter, S. & O'Neill, L. A. J. Recent insights into the structure of Toll-like receptors and post-translational modifications of their associated signalling proteins. *Biochem. J.* **422**, 1–10 (2009).
153. Kawai, T. & Akira, S. Signaling to NF-kappaB by Toll-like receptors. *Trends Mol. Med.* **13**, 460–469 (2007).
154. Hayden, M. S. & Ghosh, S. NF-κB, the first quarter-century: remarkable progress and outstanding questions. *Genes Dev.* **26**, 203–234 (2012).
155. Roux, P. P. & Blenis, J. ERK and p38 MAPK-activated protein kinases: a family of protein kinases with diverse biological functions. *Microbiol. Mol. Biol. Rev. MMBR* **68**, 320–344 (2004).
156. Zhang, X., Jiang, D. & Li, H. The interferon regulatory factors as novel potential targets in the treatment of cardiovascular diseases. *Br. J. Pharmacol.* **172**, 5457–5476 (2015).
157. Ikushima, H., Negishi, H. & Taniguchi, T. The IRF Family Transcription Factors at the Interface of Innate and Adaptive Immune Responses. *Cold Spring Harb. Symp. Quant. Biol.* **78**, 105–116 (2013).
158. Drexler, S. K. & Foxwell, B. M. The role of toll-like receptors in chronic inflammation. *Int. J. Biochem. Cell Biol.* **42**, 506–518 (2010).
159. Mann, D. L. The emerging role of innate immunity in the heart and vascular system: for whom the cell tolls. *Circ. Res.* **108**, 1133–1145 (2011).
160. Schlotter, F. *et al.* Spatiotemporal Multi-Omics Mapping Generates a Molecular Atlas of the Aortic Valve and Reveals Networks Driving Disease. *Circulation* **138**, 377–393 (2018).
161. Zeng, Q. *et al.* Interleukin-37 suppresses the osteogenic responses of human aortic valve interstitial cells in vitro and alleviates valve lesions in mice. *Proc. Natl. Acad. Sci. U. S. A.* **114**, 1631–1636 (2017).
162. Babu, A. N. *et al.* Lipopolysaccharide stimulation of human aortic valve interstitial cells activates inflammation and osteogenesis. *Ann. Thorac. Surg.* **86**, 71–76 (2008).
163. Meng, X. *et al.* Expression of functional Toll-like receptors 2 and 4 in human aortic valve interstitial cells: potential roles in aortic valve inflammation and stenosis. *Am. J. Physiol.-Cell Physiol.* **294**, C29–C35 (2008).
164. López, J. *et al.* Viral and bacterial patterns induce TLR-mediated sustained inflammation and calcification in aortic valve interstitial cells. *Int. J. Cardiol.* **158**, 18–25 (2012).
165. Derbali, H. *et al.* Increased Biglycan in Aortic Valve Stenosis Leads to the Overexpression of Phospholipid Transfer Protein via Toll-Like Receptor 2. *Am. J. Pathol.* **176**, 2638–2645 (2010).
166. Song, R. *et al.* Biglycan induces the expression of osteogenic factors in human aortic valve interstitial cells via Toll-like receptor-2. *Arterioscler. Thromb. Vasc. Biol.* **32**, 2711–2720 (2012).
167. Li, F. *et al.* ADAMTS5 Deficiency in Calcified Aortic Valves Is Associated With Elevated Pro-Osteogenic Activity in Valvular Interstitial Cells. *Arterioscler. Thromb. Vasc. Biol.* **37**, 1339–1351 (2017).

168. Wang, B. *et al.* High-mobility group box-1 protein induces osteogenic phenotype changes in aortic valve interstitial cells. *J. Thorac. Cardiovasc. Surg.* **151**, 255–262 (2016).
169. Shen, W. *et al.* High mobility group box 1 induces calcification of aortic valve interstitial cells via toll-like receptor 4. *Mol. Med. Rep.* **15**, 2530–2536 (2017).
170. Zeng, Q. *et al.* Augmented osteogenic responses in human aortic valve cells exposed to oxLDL and TLR4 agonist: a mechanistic role of Notch1 and NF- $\kappa$ B interaction. *PLoS One* **9**, e95400 (2014).
171. Mazzone, A. *et al.* Neoangiogenesis, T-lymphocyte infiltration, and heat shock protein-60 are biological hallmarks of an immunomediated inflammatory process in end-stage calcified aortic valve stenosis. *J. Am. Coll. Cardiol.* **43**, 1670–1676 (2004).
172. Ghim, M., Pang, K. T., Arshad, M., Wang, X. & Weinberg, P. D. A novel method for segmenting growth of cells in sheared endothelial culture reveals the secretion of an anti-inflammatory mediator. *J. Biol. Eng.* **12**, (2018).
173. Laemmli, U. K. Cleavage of structural proteins during the assembly of the head of bacteriophage T4. *Nature* **227**, 680–685 (1970).
174. Fernández-Pisonero, I. *et al.* Lipopolysaccharide and Sphingosine-1-Phosphate Cooperate To Induce Inflammatory Molecules and Leukocyte Adhesion in Endothelial Cells. *J. Immunol.* **189**, 5402–5410 (2012).
175. Mosmann, T. Rapid colorimetric assay for cellular growth and survival: application to proliferation and cytotoxicity assays. *J. Immunol. Methods* **65**, 55–63 (1983).
176. Villa-Bellosta, R. & Hamczyk, M. R. Isolation and Culture of Aortic Smooth Muscle Cells and In Vitro Calcification Assay. *Methods Mol. Biol. Clifton NJ* **1339**, 119–129 (2015).
177. Gregory, C. A., Grady Gunn, W., Peister, A. & Prockop, D. J. An Alizarin red-based assay of mineralization by adherent cells in culture: comparison with cetylpyridinium chloride extraction. *Anal. Biochem.* **329**, 77–84 (2004).
178. Vermes, I., Haanen, C., Steffens-Nakken, H. & Reutelingsperger, C. A novel assay for apoptosis. Flow cytometric detection of phosphatidylserine expression on early apoptotic cells using fluorescein labelled Annexin V. *J. Immunol. Methods* **184**, 39–51 (1995).
179. Sancenon, V. *et al.* Development, validation and quantitative assessment of an enzymatic assay suitable for small molecule screening and profiling: A case-study. *Biomol. Detect. Quantif.* **4**, 1–9 (2015).
180. Kontzias, A., Kotlyar, A., Laurence, A., Changelian, P. & O’Shea, J. J. Jakinibs: A New Class of Kinase Inhibitors in Cancer and Autoimmune Disease. *Curr. Opin. Pharmacol.* **12**, 464–470 (2012).
181. O’Sullivan, K. E., Breen, E. P., Gallagher, H. C., Buggy, D. J. & Hurley, J. P. Understanding STAT3 signaling in cardiac ischemia. *Basic Res. Cardiol.* **111**, 27 (2016).
182. Cheng, H. *et al.* LysoPC activates the Akt pathway to up-regulate ECM protein production in human aortic valve cells. *J. Surg. Res.* **213**, 243–250 (2017).
183. Gu, X. & Masters, K. S. Role of the MAPK/ERK pathway in valvular interstitial cell calcification. *Am. J. Physiol. - Heart Circ. Physiol.* **296**, H1748–H1757 (2009).
184. Shahi, C. N. *et al.* Elevated Levels of Circulating Soluble Adhesion Molecules in Patients With Nonrheumatic Aortic Stenosis. *Am. J. Cardiol.* **79**, 980–982 (1997).
185. Kaden, J. J. *et al.* Expression of bone sialoprotein and bone morphogenetic protein-2 in calcific aortic stenosis. *J. Heart Valve Dis.* **13**, 560–566 (2004).
186. Jono, S. *et al.* Phosphate regulation of vascular smooth muscle cell calcification. *Circ. Res.* **87**, E10-17 (2000).
187. Reynolds, J. L. *et al.* Human Vascular Smooth Muscle Cells Undergo Vesicle-Mediated Calcification in Response to Changes in Extracellular Calcium and Phosphate Concentrations: A Potential Mechanism for Accelerated Vascular Calcification in ESRD. *J. Am. Soc. Nephrol.* **15**, 2857–2867 (2004).
188. Aggarwal Shivani R. *et al.* Sex Differences in Aortic Valve Calcification Measured by Multidetector Computed Tomography in Aortic Stenosis. *Circ. Cardiovasc. Imaging* **6**, 40–47 (2013).
189. Latif, N. *et al.* Modulation of human valve interstitial cell phenotype and function using a fibroblast growth factor 2 formulation. *PLoS One* **10**, e0127844 (2015).

190. Rajamannan, N. M. *et al.* Calcific Aortic Valve Disease: Not Simply a Degenerative Process A Review and Agenda for Research from the National Heart and Lung and Blood Institute Aortic Stenosis Working Group. *Circulation* **124**, 1783–1791 (2011).
191. Koos, R. *et al.* Sclerostin as a potential novel biomarker for aortic valve calcification: an in-vivo and ex-vivo study. *J. Heart Valve Dis.* **22**, 317–325 (2013).
192. Hu, X. *et al.* Role of TGF- $\beta$ 1 Signaling in Heart Valve Calcification Induced by Abnormal Mechanical Stimulation in a Tissue Engineering Model. *Curr. Med. Sci.* **38**, 765–775 (2018).
193. Poggio, P. *et al.* Noggin attenuates the osteogenic activation of human valve interstitial cells in aortic valve sclerosis. *Cardiovasc. Res.* **98**, 402–410 (2013).
194. Yu, Z. *et al.* Tumor necrosis factor- $\alpha$  accelerates the calcification of human aortic valve interstitial cells obtained from patients with calcific aortic valve stenosis via the BMP2-Dlx5 pathway. *J. Pharmacol. Exp. Ther.* **337**, 16–23 (2011).
195. Clark-Greuel, J. N. *et al.* Transforming growth factor-beta1 mechanisms in aortic valve calcification: increased alkaline phosphatase and related events. *Ann. Thorac. Surg.* **83**, 946–953 (2007).
196. Sévère, N., Dieudonné, F.-X. & Marie, P. J. E3 ubiquitin ligase-mediated regulation of bone formation and tumorigenesis. *Cell Death Dis.* **4**, e463 (2013).
197. Regitz-Zagrosek, V. & Kararigas, G. Mechanistic Pathways of Sex Differences in Cardiovascular Disease. *Physiol. Rev.* **97**, 1–37 (2017).
198. Zimna, A. & Kurpisz, M. Hypoxia-Inducible Factor-1 in Physiological and Pathophysiological Angiogenesis: Applications and Therapies. *BioMed Res. Int.* **2015**, 549412 (2015).
199. Koh, M. Y. *et al.* Molecular mechanisms for the activity of PX-478, an antitumor inhibitor of the hypoxia-inducible factor-1 $\alpha$ . *Mol. Cancer Ther.* **7**, 90–100 (2008).
200. Wu, D. & Yotnda, P. Induction and Testing of Hypoxia in Cell Culture. *J. Vis. Exp. JoVE* (2011). doi:10.3791/2899
201. Salhiyyah, K., Sarathchandra, P., Latif, N., Yacoub, M. H. & Chester, A. H. Hypoxia-mediated regulation of the secretory properties of mitral valve interstitial cells. *Am. J. Physiol. Heart Circ. Physiol.* **313**, H14–H23 (2017).
202. Cheon, H. & Stark, G. R. Unphosphorylated STAT1 prolongs the expression of interferon-induced immune regulatory genes. *Proc. Natl. Acad. Sci. U. S. A.* **106**, 9373–9378 (2009).
203. Asdonk, T. *et al.* MDA-5 activation by cytoplasmic double-stranded RNA impairs endothelial function and aggravates atherosclerosis. *J. Cell. Mol. Med.* **20**, 1696–1705 (2016).
204. Zhan, Q. *et al.* Activation of TLR3 Induces Osteogenic Responses in Human Aortic Valve Interstitial Cells through the NF- $\kappa$ B and ERK1/2 Pathways. *Int. J. Biol. Sci.* **11**, 482–493 (2015).
205. Zhan, Q. *et al.* Double-stranded RNA upregulates the expression of inflammatory mediators in human aortic valve cells through the TLR3-TRIF-noncanonical NF- $\kappa$ B pathway. *Am. J. Physiol. - Cell Physiol.* **312**, C407–C417 (2017).
206. Richards, J. *et al.* Side-Specific Endothelial-Dependent Regulation of Aortic Valve Calcification. *Am. J. Pathol.* **182**, 1922–1931 (2013).
207. Mongkoldhumrongkul, N., Latif, N., Yacoub, M. H. & Chester, A. H. Effect of Side-Specific Valvular Shear Stress on the Content of Extracellular Matrix in Aortic Valves. *Cardiovasc. Eng. Technol.* **9**, 151–157 (2018).
208. Miragoli, M. *et al.* Side-specific mechanical properties of valve endothelial cells. *Am. J. Physiol.-Heart Circ. Physiol.* **307**, H15–H24 (2014).
209. Aikawa, E. & Libby, P. A Rock and a Hard Place: Chiseling Away at the Multiple Mechanisms of Aortic Stenosis. *Circulation* **135**, 1951–1955 (2017).
210. Liang, C.-C., Park, A. Y. & Guan, J.-L. In vitro scratch assay: a convenient and inexpensive method for analysis of cell migration in vitro. *Nat. Protoc.* **2**, 329–333 (2007).
211. Lim, C. S., Kiriakidis, S., Sandison, A., Paleolog, E. M. & Davies, A. H. Hypoxia-inducible factor pathway and diseases of the vascular wall. *J. Vasc. Surg.* **58**, 219–230 (2013).
212. Volpi, S., Picco, P., Caorsi, R., Candotti, F. & Gattorno, M. Type I interferonopathies in pediatric rheumatology. *Pediatr. Rheumatol. Online J.* **14**, (2016).

213. Trinchieri, G. Type I interferon: friend or foe? *J. Exp. Med.* **207**, 2053–2063 (2010).
214. de Padilla, C. M. L. & Niewold, T. B. The Type I Interferons: Basic Concepts and Clinical Relevance in Immune-mediated Inflammatory Diseases. *Gene* **576**, 14–21 (2016).
215. Billiau, A. Anti-inflammatory properties of Type I interferons. *Antiviral Res.* **71**, 108–116 (2006).
216. Kovarik, P. *et al.* Stress-induced phosphorylation of STAT1 at Ser727 requires p38 mitogen-activated protein kinase whereas IFN-gamma uses a different signaling pathway. *Proc. Natl. Acad. Sci. U. S. A.* **96**, 13956–13961 (1999).
217. Ho, H. H. & Ivashkiv, L. B. Role of STAT3 in type I interferon responses. Negative regulation of STAT1-dependent inflammatory gene activation. *J. Biol. Chem.* **281**, 14111–14118 (2006).
218. Deng, X.-S., Meng, X., Song, R., Fullerton, D. & Jagers, J. Rapamycin Decreases the Osteogenic Response in Aortic Valve Interstitial Cells Through the Stat3 Pathway. *Ann. Thorac. Surg.* **102**, 1229–1238 (2016).
219. Kaur, S. *et al.* Role of the Akt pathway in mRNA translation of interferon-stimulated genes. *Proc. Natl. Acad. Sci. U. S. A.* **105**, 4808–4813 (2008).
220. Arthur, J. S. C. & Ley, S. C. Mitogen-activated protein kinases in innate immunity. *Nat. Rev. Immunol.* **13**, 679–692 (2013).
221. Song, R., Fullerton, D. A., Ao, L., Zhao, K.-S. & Meng, X. An epigenetic regulatory loop controls pro-osteogenic activation by TGF- $\beta$ 1 or bone morphogenetic protein 2 in human aortic valve interstitial cells. *J. Biol. Chem.* **292**, 8657–8666 (2017).
222. Bruderer, M., Richards, R. G., Alini, M. & Stoddart, M. J. Role and regulation of RUNX2 in osteogenesis. *Eur. Cell. Mater.* **28**, 269–286 (2014).
223. Nakashima, K. *et al.* The novel zinc finger-containing transcription factor osterix is required for osteoblast differentiation and bone formation. *Cell* **108**, 17–29 (2002).
224. Zheng, D. *et al.* MicroRNA-214 promotes the calcification of human aortic valve interstitial cells through the acceleration of inflammatory reactions with activated MyD88/NF- $\kappa$ B signaling. *Clin. Res. Cardiol.* **108**, 691–702 (2019).
225. Sikura, K. É. *et al.* Potential Role of H-Ferritin in Mitigating Valvular Mineralization. *Arterioscler. Thromb. Vasc. Biol.* **39**, 413–431 (2019).
226. Goto, S. *et al.* Standardization of Human Calcific Aortic Valve Disease in vitro Modeling Reveals Passage-Dependent Calcification. *Front. Cardiovasc. Med.* **6**, (2019).
227. Linefsky, J. P. *et al.* Serum Phosphate is Associated with Aortic Valve Calcification in the Multi-Ethnic Study of Atherosclerosis (MESA). *Atherosclerosis* **233**, 331–337 (2014).
228. Lau, W. L., Pai, A., Moe, S. M. & Giachelli, C. M. Direct effects of phosphate on vascular cell function. *Adv. Chronic Kidney Dis.* **18**, 105–112 (2011).
229. Mokas, S. *et al.* Hypoxia-inducible factor-1 plays a role in phosphate-induced vascular smooth muscle cell calcification. *Kidney Int.* **90**, 598–609 (2016).
230. Hortells, L., Sosa, C., Millán, Á. & Sorribas, V. Critical Parameters of the In Vitro Method of Vascular Smooth Muscle Cell Calcification. *PLOS ONE* **10**, e0141751 (2015).
231. Hodge, J. A. *et al.* The mechanism of action of tofacitinib - an oral Janus kinase inhibitor for the treatment of rheumatoid arthritis. *Clin. Exp. Rheumatol.* **34**, 318–328 (2016).
232. Huaman, M. A., Deepe, G. S. & Fichtenbaum, C. J. Elevated Circulating Concentrations of Interferon-Gamma in Latent Tuberculosis Infection. *Pathog. Immun.* **1**, 291–303 (2016).
233. Lauw, F. N. *et al.* Elevated Plasma Concentrations of Interferon (IFN)- $\gamma$  and the IFN- $\gamma$ -Inducing Cytokines Interleukin (IL)-18, IL-12, and IL-15 in Severe Melioidosis. *J. Infect. Dis.* **180**, 1878–1885 (1999).
234. Olsson, M. *et al.* Accumulation of T lymphocytes and expression of interleukin-2 receptors in nonrheumatic stenotic aortic valves. *J. Am. Coll. Cardiol.* **23**, 1162–1170 (1994).
235. Lees, J. R. Interferon gamma in autoimmunity: A complicated player on a complex stage. *Cytokine* **74**, 18–26 (2015).
236. Chang, Y.-P. *et al.* Autophagy facilitates IFN-gamma-induced Jak2-STAT1 activation and cellular inflammation. *J. Biol. Chem.* **285**, 28715–28722 (2010).

237. Fang, P., Hwa, V. & Rosenfeld, R. G. Interferon-gamma-induced dephosphorylation of STAT3 and apoptosis are dependent on the mTOR pathway. *Exp. Cell Res.* **312**, 1229–1239 (2006).
238. Rose, D. M., Winston, B. W., Chan, E. D., Riches, D. W. & Henson, P. M. Interferon-gamma and transforming growth factor-beta modulate the activation of mitogen-activated protein kinases and tumor necrosis factor-alpha production induced by Fc gamma-receptor stimulation in murine macrophages. *Biochem. Biophys. Res. Commun.* **238**, 256–260 (1997).
239. Sun, T. *et al.* Inhibition of tumor angiogenesis by interferon- $\gamma$  by suppression of tumor-associated macrophage differentiation. *Oncol. Res.* **21**, 227–235 (2014).
240. Liu, B., Faia, L., Hu, M. & Nussenblatt, R. B. Pro-angiogenic effect of IFN $\gamma$  is dependent on the PI3K/mTOR/translational pathway in human retinal pigmented epithelial cells. *Mol. Vis.* **16**, 184–193 (2010).
241. Lee, H. *et al.* A novel pro-angiogenic function for interferon- $\gamma$ -secreting natural killer cells. *Invest. Ophthalmol. Vis. Sci.* **55**, 2885–2892 (2014).
242. Chakrabarty, P. *et al.* Interferon- $\gamma$  induces progressive nigrostriatal degeneration and basal ganglia calcification. *Nat. Neurosci.* **14**, 694–696 (2011).
243. Yu, H. T. *et al.* Serum monokine induced by gamma interferon as a novel biomarker for coronary artery calcification in humans. *Coron. Artery Dis.* **26**, 317–321 (2015).
244. Teker, E. *et al.* Association Between the Interferon Gamma 874 T/A Polymorphism and the Severity of Valvular Damage in Patients with Rheumatic Heart Disease. *Biochem. Genet.* **56**, 225–234 (2018).
245. Mattyasovszky, S. G. *et al.* Cytokine Interferon- $\gamma$  suppresses the function of capsule myofibroblasts and induces cell apoptosis. *J. Orthop. Res. Off. Publ. Orthop. Res. Soc.* **35**, 2524–2533 (2017).
246. Shelton, G. D. *et al.* Necrotizing myopathy induced by overexpression of interferon-gamma in transgenic mice. *Muscle Nerve* **22**, 156–165 (1999).
247. Ibarra Urizar, A., Friberg, J., Christensen, D. P., Lund Christensen, G. & Billestrup, N. Inflammatory Cytokines Stimulate Bone Morphogenetic Protein-2 Expression and Release from Pancreatic Beta Cells. *J. Interferon Cytokine Res. Off. J. Int. Soc. Interferon Cytokine Res.* **36**, 20–29 (2016).
248. Ghaisas, N. K. *et al.* Adhesion molecules in nonrheumatic aortic valve disease: endothelial expression, serum levels and effects of valve replacement. *J. Am. Coll. Cardiol.* **36**, 2257–2262 (2000).
249. Linhartova, K. *et al.* Linking soluble vascular adhesion molecule-1 level to calcific aortic stenosis in patients with coronary artery disease. *Exp. Clin. Cardiol.* **14**, e80-83 (2009).
250. Fernández-Pisonero, I. *et al.* Synergy between Sphingosine 1-Phosphate and Lipopolysaccharide Signaling Promotes an Inflammatory, Angiogenic and Osteogenic Response in Human Aortic Valve Interstitial Cells. *PLoS ONE* **9**, (2014).
251. Rhee, S. H., Jones, B. W., Toshchakov, V., Vogel, S. N. & Fenton, M. J. Toll-like Receptors 2 and 4 Activate STAT1 Serine Phosphorylation by Distinct Mechanisms in Macrophages. *J. Biol. Chem.* **278**, 22506–22512 (2003).
252. Preissner, K. T. & Herwald, H. Extracellular nucleic acids in immunity and cardiovascular responses: between alert and disease. *Thromb. Haemost.* **117**, 1272–1282 (2017).
253. Raicevic, G. *et al.* Inflammation and Toll-like receptor ligation differentially affect the osteogenic potential of human mesenchymal stromal cells depending on their tissue origin. *Tissue Eng. Part A* **18**, 1410–1418 (2012).
254. Fan, L. *et al.* Toll-like receptor 3 acts as a suppressor gene in breast cancer initiation and progression: a two-stage association study and functional investigation. *Oncoimmunology* **8**, e1593801 (2019).
255. Teixeira, H., Zhao, J., Kinane, D. F. & Benakanakere, M. R. IFN- $\beta$  secretion is through TLR3 but not TLR4 in human gingival epithelial cells. *Mol. Immunol.* **111**, 27–31 (2019).
256. Yang, J. *et al.* Type I Interferons Triggered through the Toll-Like Receptor 3-TRIF Pathway Control Coxsackievirus A16 Infection in Young Mice. *J. Virol.* **89**, 10860–10867 (2015).
257. Lundberg, A. M. *et al.* Key differences in TLR3/poly I:C signaling and cytokine induction by human primary cells: a phenomenon absent from murine cell systems. *Blood* **110**, 3245–3252 (2007).

258. Huang, C. *et al.* TLR3 Ligand Poly(I:C) Prevents Acute Pancreatitis Through the Interferon- $\beta$ /Interferon- $\alpha/\beta$  Receptor Signaling Pathway in a Caerulein-Induced Pancreatitis Mouse Model. *Front. Immunol.* **10**, 980 (2019).
259. Orita, T., Kimura, K., Zhou, H.-Y. & Nishida, T. Poly(I:C)-induced adhesion molecule expression mediated by NF- $\kappa$ B and phosphoinositide 3-kinase-Akt signaling pathways in human corneal fibroblasts. *Invest. Ophthalmol. Vis. Sci.* **51**, 5556–5560 (2010).
260. Sirén, J., Pirhonen, J., Julkunen, I. & Matikainen, S. IFN-alpha regulates TLR-dependent gene expression of IFN-alpha, IFN-beta, IL-28, and IL-29. *J. Immunol. Baltim. Md 1950* **174**, 1932–1937 (2005).
261. King, K. R. *et al.* IRF3 and Type I Interferons Fuel a Fatal Response to Myocardial Infarction. *Nat. Med.* **23**, 1481–1487 (2017).
262. Hu, X. & Ivashkiv, L. B. Cross-regulation of signaling pathways by interferon-gamma: implications for immune responses and autoimmune diseases. *Immunity* **31**, 539–550 (2009).
263. Schroder, K., Sweet, M. J. & Hume, D. A. Signal integration between IFN $\gamma$  and TLR signalling pathways in macrophages. *Immunobiology* **211**, 511–524 (2006).
264. Chmielewski, S. *et al.* STAT1-Dependent Signal Integration between IFN $\gamma$  and TLR4 in Vascular Cells Reflect Pro-Atherogenic Responses in Human Atherosclerosis. *PLOS ONE* **9**, e113318 (2014).
265. Feng, S. *et al.* Mechanical Activation of Hypoxia-Inducible Factor 1 $\alpha$  Drives Endothelial Dysfunction at Atheroprone Sites. *Arterioscler. Thromb. Vasc. Biol.* **37**, 2087–2101 (2017).
266. Fernandez Esmerats, J. *et al.* Disturbed Flow Increases UBE2C (Ubiquitin E2 Ligase C) via Loss of miR-483-3p, Inducing Aortic Valve Calcification by the pVHL (von Hippel-Lindau Protein) and HIF-1 $\alpha$  (Hypoxia-Inducible Factor-1 $\alpha$ ) Pathway in Endothelial Cells. *Arterioscler. Thromb. Vasc. Biol.* **39**, 467–481 (2019).
267. Hiroi, M., Mori, K., Sakaeda, Y., Shimada, J. & Ohmori, Y. STAT1 represses hypoxia-inducible factor-1-mediated transcription. *Biochem. Biophys. Res. Commun.* **387**, 806–810 (2009).
268. Koyasu, S., Kobayashi, M., Goto, Y., Hiraoka, M. & Harada, H. Regulatory mechanisms of hypoxia-inducible factor 1 activity: Two decades of knowledge. *Cancer Sci.* **109**, 560–571 (2018).
269. Zhu, Y. *et al.* Inhibition of HIF-1 $\alpha$  by PX-478 suppresses tumor growth of esophageal squamous cell cancer in vitro and in vivo. *Am. J. Cancer Res.* **7**, 1198–1212 (2017).
270. Braverman, J., Sogi, K. M., Benjamin, D., Nomura, D. K. & Stanley, S. A. HIF-1 $\alpha$  Is an Essential Mediator of IFN- $\gamma$ -Dependent Immunity to Mycobacterium tuberculosis. *J. Immunol. Baltim. Md 1950* **197**, 1287–1297 (2016).
271. Rius, J. *et al.* NF- $\kappa$ B links innate immunity to the hypoxic response through transcriptional regulation of HIF-1 $\alpha$ . *Nature* **453**, 807–811 (2008).
272. Agarwal, S. *et al.* Inhibition of Hif1 $\alpha$  prevents both trauma-induced and genetic heterotopic ossification. *Proc. Natl. Acad. Sci. U. S. A.* **113**, E338–347 (2016).
273. Owens, D. S. *et al.* Incidence and progression of aortic valve calcium in the Multi-ethnic Study of Atherosclerosis (MESA). *Am. J. Cardiol.* **105**, 701–708 (2010).
274. Sritharen, Y., Enriquez-Sarano, M., Schaff, H. V., Casaclang-Verzosa, G. & Miller, J. D. Pathophysiology of Aortic Valve Stenosis: Is It Both Fibrocalcific and Sex Specific? *Physiology* **32**, 182–196 (2017).
275. Steiner, I., Kasparová, P., Kohout, A. & Dominik, J. Bone formation in cardiac valves: a histopathological study of 128 cases. *Virchows Arch. Int. J. Pathol.* **450**, 653–657 (2007).
276. Camper-Kirby Dreame *et al.* Myocardial Akt Activation and Gender. *Circ. Res.* **88**, 1020–1027 (2001).
277. Hervouet, E., Cartron, P.-F., Jouvenot, M. & Delage-Mourroux, R. Epigenetic regulation of estrogen signaling in breast cancer. *Epigenetics* **8**, 237–245 (2013).
278. Huang, C., Gu, H., Zhang, W., Herrmann, J. L. & Wang, M. Testosterone-down-regulated Akt pathway during cardiac ischemia/reperfusion: a mechanism involving BAD, Bcl-2 and FOXO3a. *J. Surg. Res.* **164**, e1–11 (2010).
279. Sharma, S. & Eghbali, M. Influence of sex differences on microRNA gene regulation in disease. *Biol. Sex Differ.* **5**, 3 (2014).
280. Gošev, I. *et al.* Epigenome alterations in aortic valve stenosis and its related left ventricular hypertrophy. *Clin. Epigenetics* **9**, (2017).

281. Wang, H. *et al.* MicroRNA Expression Signature in Human Calcific Aortic Valve Disease. *BioMed Res. Int.* **2017**, 4820275 (2017).
282. Kovats, S. Estrogen receptors regulate innate immune cells and signaling pathways. *Cell. Immunol.* **294**, 63–69 (2015).
283. Aomatsu, M., Kato, T., Kasahara, E. & Kitagawa, S. Gender difference in tumor necrosis factor- $\alpha$  production in human neutrophils stimulated by lipopolysaccharide and interferon- $\gamma$ . *Biochem. Biophys. Res. Commun.* **441**, 220–225 (2013).
284. Zhang, Y., Jiang, W., Wang, L. & Lingappan, K. Sex-specific differences in the modulation of Growth Differentiation Factor 15 (GDF15) by hyperoxia in vivo and in vitro: Role of Hif-1 $\alpha$ . *Toxicol. Appl. Pharmacol.* **332**, 8–14 (2017).
285. Hjortnaes, J. *et al.* Valvular Interstitial Cells Suppress Calcification of Valvular Endothelial Cells. *Atherosclerosis* **242**, 251–260 (2015).
286. Butcher, J. T. & Nerem, R. M. Valvular Endothelial Cells Regulate the Phenotype of Interstitial Cells in Co-culture: Effects of Steady Shear Stress. *Tissue Eng.* **12**, 905–915 (2006).
287. Huk, D. J. *et al.* Valve endothelial cell-derived Tgf $\beta$ 1 signaling promotes nuclear localization of Sox9 in interstitial cells associated with attenuated calcification. *Arterioscler. Thromb. Vasc. Biol.* **36**, 328–338 (2016).
288. El-Hamamsy, I. *et al.* Endothelium-dependent regulation of the mechanical properties of aortic valve cusps. *J. Am. Coll. Cardiol.* **53**, 1448–1455 (2009).
289. Mackay, F., Loetscher, H., Stueber, D., Gehr, G. & Lesslauer, W. Tumor necrosis factor alpha (TNF- $\alpha$ )-induced cell adhesion to human endothelial cells is under dominant control of one TNF receptor type, TNF-R55. *J. Exp. Med.* **177**, 1277–1286 (1993).
290. Brown, Z. *et al.* Chemokine gene expression and secretion by cytokine-activated human microvascular endothelial cells. Differential regulation of monocyte chemoattractant protein-1 and interleukin-8 in response to interferon-gamma. *Am. J. Pathol.* **145**, 913–921 (1994).
291. Heller Eric A. *et al.* Chemokine CXCL10 Promotes Atherogenesis by Modulating the Local Balance of Effector and Regulatory T Cells. *Circulation* **113**, 2301–2312 (2006).
292. Farrar, E. J. & Butcher, J. T. Heterogeneous susceptibility of valve endothelial cells to mesenchymal transformation in response to TNF $\alpha$ . *Ann. Biomed. Eng.* **42**, 149–161 (2014).
293. Lamas, S., Michel, T., Collins, T., Brenner, B. M. & Marsden, P. A. Effects of interferon-gamma on nitric oxide synthase activity and endothelin-1 production by vascular endothelial cells. *J. Clin. Invest.* **90**, 879–887 (1992).
294. Kuo, H.-P., Lee, D.-F., Xia, W., Wei, Y. & Hung, M.-C. TNF $\alpha$  induces HIF-1 $\alpha$  expression through activation of IKK $\beta$ . *Biochem. Biophys. Res. Commun.* **389**, 640–644 (2009).
295. Feng, S. *et al.* Mechanical Activation of Hypoxia-Inducible Factor 1 $\alpha$  Drives Endothelial Dysfunction at Atheroprone Sites. *Arterioscler. Thromb. Vasc. Biol.* **37**, 2087–2101 (2017).
296. Fernandez Esmerats, J. *et al.* Disturbed Flow Increases UBE2C (Ubiquitin E2 Ligase C) via Loss of miR-483-3p, Inducing Aortic Valve Calcification by the pVHL (von Hippel-Lindau Protein) and HIF-1 $\alpha$  (Hypoxia-Inducible Factor-1 $\alpha$ ) Pathway in Endothelial Cells. *Arterioscler. Thromb. Vasc. Biol.* **39**, 467–481 (2019).
297. McIntosh, C. T. & Warnock, J. N. Side-specific characterization of aortic valve endothelial cell adhesion molecules under cyclic strain. *J. Heart Valve Dis.* **22**, 631–639 (2013).
298. Nakajima, H. & Mochizuki, N. Flow pattern-dependent endothelial cell responses through transcriptional regulation. *Cell Cycle Georget. Tex* **16**, 1893–1901 (2017).
299. O’Shea, J. J. *et al.* The JAK-STAT pathway: impact on human disease and therapeutic intervention. *Annu. Rev. Med.* **66**, 311–328 (2015).
300. Boor, P. P. C. *et al.* JAK-inhibitor tofacitinib suppresses interferon alfa production by plasmacytoid dendritic cells and inhibits arthrogenic and antiviral effects of interferon alfa. *Transl. Res.* **188**, 67–79 (2017).
301. Charles-Schoeman, C. *et al.* Cardiovascular safety findings in patients with rheumatoid arthritis treated with tofacitinib, an oral Janus kinase inhibitor. *Semin. Arthritis Rheum.* **46**, 261–271 (2016).

302. Wu, J. J. *et al.* Effects of tofacitinib on cardiovascular risk factors and cardiovascular outcomes based on phase III and long-term extension data in patients with plaque psoriasis. *J. Am. Acad. Dermatol.* **75**, 897–905 (2016).
303. Nurmohamed, M. *et al.* The Impact of Biologics and Tofacitinib on Cardiovascular Risk Factors and Outcomes in Patients with Rheumatic Disease: A Systematic Literature Review. *Drug Saf.* **41**, 473–488 (2018).
304. Wendel, S. *et al.* Successful treatment of extensive calcifications and acute pulmonary involvement in dermatomyositis with the Janus-Kinase inhibitor tofacitinib – A report of two cases. *J. Autoimmun.* **100**, 131–136 (2019).
305. Cervantes, F. *et al.* Three-year efficacy, safety, and survival findings from COMFORT-II, a phase 3 study comparing ruxolitinib with best available therapy for myelofibrosis. *Blood* **122**, 4047–4053 (2013).
306. Kurozumi, A. *et al.* IL-6 and sIL-6R induces STAT3-dependent differentiation of human VSMCs into osteoblast-like cells through JMJD2B-mediated histone demethylation of RUNX2. *Bone* **124**, 53–61 (2019).
307. Hjortnaes, J. *et al.* Simulation of Early Calcific Aortic Valve Disease in a 3D platform: A Role for Myofibroblast Differentiation. *J. Mol. Cell. Cardiol.* **94**, 13–20 (2016).
308. Bogdanova, M. *et al.* Inflammation and Mechanical Stress Stimulate Osteogenic Differentiation of Human Aortic Valve Interstitial Cells. *Front. Physiol.* **9**, (2018).
309. Wang, X., Lee, J., Ali, M., Kim, J. & Lacerda, C. M. R. Phenotype Transformation of Aortic Valve Interstitial Cells Due to Applied Shear Stresses Within a Microfluidic Chip. *Ann. Biomed. Eng.* **45**, 2269–2280 (2017).
310. Lee, J. *et al.* A microfluidic cardiac flow profile generator for studying the effect of shear stress on valvular endothelial cells. *Lab. Chip* **18**, 2946–2954 (2018).
311. Sider, K. L., Blaser, M. C. & Simmons, C. A. Animal models of calcific aortic valve disease. *Int. J. Inflamm.* **2011**, 364310 (2011).

## **ANNEXS**



# ANNEXS

---

## ANNEX 1-MATERIALS

### **A.1.1-Chemical reagents**

- Ammonium hydroxide (NH<sub>4</sub>OH): Sigma-Aldrich, St. Louis, MO; Ref. 1336-21-6.
- Ammonium persulfate (APS): Sigma-Aldrich, St. Louis, MO; Ref. A-3670.
- Bromophenol blue: Sigma-Aldrich, St. Louis, MO; Ref. B8026.
- Calcium chloride (CaCl<sub>2</sub>): Merck, Darmstadt, Germany; Ref. 2382.
- Disodium hydrogen phosphate (Na<sub>2</sub>HPO<sub>4</sub>): Scharlab, Barcelona, Spain; Ref. SO0351000.
- EDTA: Sigma-Aldrich, St. Louis, MO; Ref. E5134.
- Glycerol: Sigma-Aldrich, St. Louis, MO; Ref. G5516.
- Glycine (C<sub>2</sub>H<sub>5</sub>NO<sub>2</sub>): Merck, Darmstadt, Germany; Ref. AC04061000.
- HEPES, 4-(2-hydroxyethyl)-1-piperazineethanesulfonic acid: Sigma-Aldrich, St. Louis, MO; Ref. H-3375.
- β-mercaptoethanol: Sigma-Aldrich, St. Louis, MO; Ref. M3148.
- Phenylmetilsulfonyl fluoride (PMSF): Roche Diagnostics, Barcelona, Spain; Ref. 10236608001.
- Potassium chloride (KCl): Merck, Darmstadt, Germany; Ref. 4936.
- Potassium dihydrogen phosphate (KH<sub>2</sub>PO<sub>4</sub>): Merck, Darmstadt, Germany; Ref. 4873.1000.
- Sodium azide: Merck, Darmstad, Germany; Ref. 6688.
- Sodium chloride (NaCl): Merck, Darmstadt, Germany; Ref. 4936.
- Sodium-dodecyl sulphate (SDS): Sigma-Aldrich, St. Louis, MO; Ref. 436143.
- Sodium fluoride (NaF): Sigma-Aldrich, St. Louis, MO; Ref. S-1504.
- Sodium di-hydrogen phosphate (Na<sub>2</sub>HPO<sub>4</sub>): Sigma-Aldrich, St. Louis, MO; Ref. 255793.
- Sodium hydroxide (NaOH): Sigma-Aldrich, St. Louis, MO; Ref. 211465.
- Sodium orthovanadate (Na<sub>3</sub>VO<sub>4</sub>): Sigma-Aldrich, St. Louis, MO; Ref. S6508.
- Tris Hydroxymethyl aminomethane (C<sub>4</sub>H<sub>11</sub>NO<sub>3</sub>): Merck, Darmstadt, Germany; Ref. TR0424000.

-Tris-Hydrochloride (Tris-HCl): Sigma-Aldrich, St. Louis, MO; Ref. RES3098T-B7.

-Tween-20: Scharlab, Barcelona, Spain; Ref. TW00220100.

### **A.1.2-Solvents**

-Chloroform (CHCl<sub>3</sub>): Merck, Darmstadt, Germany; Ref. 1.02445.1000.

-Ethanol (C<sub>2</sub>H<sub>5</sub>OH): Panreac, Barcelona, Spain; Ref. 141091.1214.

-Hydrochloric acid (HCl): Merck, Darmstadt, Germany; Ref. 100037.

-Isopropanol (2-Propanol; C<sub>3</sub>H<sub>8</sub>O): Thermo Scientific, Waltham, MA; Ref. A461-4.

-Methanol (CH<sub>3</sub>OH): Panreac, Barcelona, Spain; Ref. 141091.1224.

### **A.1.3- Cell culture solutions and material**

-Antibiotic-antimycotic solution (100 u penicillin, 100 µg/mL streptomycin, 0.25 µg/mL amphotericin B): Gibco Invitrogen, Carlsbad, CA; Ref. 15240-062.

-Cell culture flasks (75 cm<sup>2</sup>): Thermo Scientific, Waltham, MA; Ref. 156472.

-Cryotubes: DeltaLab, Okala, FL; Ref. 04180176.

-Dimethyl sulfoxide (DMSO): Sigma-Aldrich, St. Louis, MO; Ref. D2650.

-Earle's balanced salt solution (EBSS): Gibco Invitrogen, Carlsbad, CA; Ref. 14155.048.

-Endothelial Growth Medium-2: Lonza BioWhittaker, Basel, Switzerland; Ref. C-22011.

-EGM-2 supplement: Lonza BioWhittaker, Basel, Switzerland; Ref. C39216.

-Fetal bovine serum (FBS): Hyclone, Carlsbad, CA; Ref. SV30160.03.

-Gelatin: Sigma-Aldrich, St. Louis, MO; Ref. G1393.

-L-glutamine: Lonza BioWhittaker, Basel, Switzerland; Ref. BE17-605.

-M199 medium: Corning Life Sciences, Tewksbury, MA; Ref. 10-060-CVR.

-Phenol-red-free M199: Thermo Scientific, Carlsbad, MA; Ref. 11043023.

-Plates (6-, 12 and 96-well): Corning, Tewksbury, MA; Ref 3506 and 3512 respectively.

-RPMI-1640 medium: BioWhittaker, Walkersville, MD; Ref. BW09-774E.

-StemPro Accutase: Thermo Scientific, Carlsbad, CA; Ref. 11599686.

-Sterile pipettes (5, 10 and 25 mL): Thermo Scientific, Waltham, MA; Ref. 13-678-11D, 13-678-11E and 13-678-11 respectively.

- Trypsin EDTA: BioWhittaker®, Lonza Basel, Switzerland; Ref. BE17-161F.
- Type II collagenase: Gibco Invitrogen, Carlsbad, CA; Ref. 17101-015.
- Tubes (15- and 50-mL): Thermo Scientific, Waltham, MA, Ref. 05-539-5 and 352070 respectively.

### **A.1.4-Buffer composition**

- Annexin V binding buffer: 140 mmol/L NaCl, 2.5 mmol/L CaCl<sub>2</sub>, 10 mmol/L HEPES pH 7.4.
- Electrophoresis buffer: 25 mM Tris hydroxymethyl aminomethane, 192 mM glycine and 0.1% (w/v) SDS, pH 8.3.
- Laemli buffer 5X: 325 mM Tris-HCl pH 7.5, 50% glycerol, 10% (w/v) SDS, 10% β-mercaptoethanol, and 0,01 mg/mL bromophenol blue.
- Phosphate Buffered Saline (PBS): 137 mM NaCl, 2.68 mM KCl, 10 mM Na<sub>2</sub>HPO<sub>4</sub>, 1.8 mM KH<sub>2</sub>PO<sub>4</sub>, pH 7,4.
- TNE buffer: 20 mM Tris–HCl pH 7.4, 150 mM NaCl, 5 mM EDTA.
- Transfer buffer: 25 mM tris hydroxymethyl aminomethane, 192 mM glycine, 20% methanol (v/v) and 0.03% of SDS (w/v).
- TTBS (TBS-Tween): 10 mM Tris-HCl pH 7.6, 137 mM NaCl, 0.05% Tween-20 (v/v).

### **A.1.5-Cellular treatments (stimuli, inhibitors, and antagonists)**

#### **Treatments**

- Flagellin: Invivogen, San Diego, CA; Ref. tlr1-epstranscription factorla-5.
- Human recombinant IFN-α: Peptotech Inc, London, UK; Ref. 500-P32AG.
- Human recombinant IFN-γ: Peptotech Inc, -London, UK; Ref. 300-02.
- Human recombinant TGF-β1: Peptotech Inc, London, UK;Ref. 100-21.
- Human recombinant TNF-α: Cell Biolabs, Rocky Hill; Ref. CO 12105.
- Imiquimod: Invivogen, San Diego, CA; Ref. tlr1-imq.
- LPS from *Escherichia coli* O111B4: Sigma-Aldrich, St. Louis, MO; Ref. L2630.
- Pam<sub>2</sub>CSK<sub>4</sub>: Invivogen, San Diego, CA; Ref. tlr1-pm2s-1.
- Poly (I:C): Invivogen, San Diego, CA; Ref. tlr1-pic.

#### **Inhibitors**

- CAY10614: Cayman Chem, Ann Arbor, MI; Ref.13615.

- LY294002: Invitrogen, Carlsbad, CA; Ref. PHZ1144.
- NF- $\kappa$ B SN50: Calbiochem, Darmstad, Germany; Ref. 481480.
- Noggin: Invitrogen, Carlsbad, CA; Ref. PHC1506.
- PD98059: Tocris Bioscience, Bristol, UK; Ref. PD1213
- PX-478: MedChem Express, Monmouth Junction, NJ; Ref. HY-10231
- Ruxolitinib: InvivoGen, San Diego, CA; Ref. INCB018424.
- SB203580: Calbiochem, Darmstadt, Germany; Ref. 559389.
- SP600125: Sigma-Aldrich, St. Louis, MO; Ref. S5567.
- Tofacitinib: InvivoGen, San Diego, CA; Ref. CP-690550.

## **A.1.6-Antibodies**

### **Western Blot primary anti-human antibodies**

- Actin: Santa Cruz Biotech Inc, Santa Cruz, CA; Ref. sc-1615.
- eNOS: Cell Signalling, Danvers, MA; Ref. 9572.
- HIF-1 $\alpha$ : Novus Biologicals, Madrid, Spain; Ref. NB1000-449.
- Histone-H3: Abcam, Barcelona, Spain; Ref. ab1791.
- ICAM-1: Santa Cruz Biotech Inc, Santa Cruz, CA; Ref. sc-7891.
- NF- $\kappa$ B-p65: Cell Signalling, Danvers, MA; Ref. 3034.
- pAkt (Ser473): Cell Signalling Danvers, MA; Ref. 9271.
- pp44/42 MAPK (Erk1/2) (Thr202/Tyr204): Cell Signalling, Danvers, MA; Ref. 4376.
- pSAPK/JNK (Thr183/Tyr185): Cell Signalling, Danvers, MA; Ref 4668.
- pSTAT1 (Ser727): Cell Signalling, Danvers, MA; Ref. 9177.
- pSTAT1 (Tyr701): Cell Signalling, Danvers, MA; Ref. 9167.
- pSTAT3 (Tyr705): Cell Signalling, Danvers, MA; Ref. 9145.
- RUNX2: Santa Cruz Biotech Inc, Santa Cruz, CA; Ref. sc-32251.
- STAT1: Cell Signalling, Danvers, MA; Ref. 9172.
- STAT3: Cell Signalling, Danvers, MA; Ref. 9132.
- $\beta$ -tubulin: Sigma-Aldrich. St. Louis, MO; Ref. T7816.

-VCAM-1: Santa Cruz Biotech Inc, Santa Cruz, CA; Ref. sc-13160.

### Secondary antibodies

-Goat-anti-mouse IgG (Horseradish peroxidase-conjugated): Bio-Rad, Hercules, CA; Ref. 170-6516.

-Goat anti-rabbit IgG: Agilent Technologies, Santa Clara, CA; Ref. P0448.

### Immunofluorescence and cell sorting antibodies

-Alexa Fluor 488 goat anti-rabbit IgG antibody: Invitrogen, Carlsbad, CA; Ref. A11070.

-Alexa Fluor 488 goat anti-mouse IgG (H+L) antibody: Invitrogen, Carlsbad, MA; Ref. A-11001.

-Alexa Fluor 594 goat anti-rabbit IgG (H+L) antibody: Invitrogen, Carlsbad, CA; Ref. A-11012.

-Anti-human HIF-1 $\alpha$  antibody: Novus Biologicals, Centennial, CO; Ref. NB100-449.

-Anti-human  $\alpha$ -smooth muscle actin: Santa Cruz Biotech Inc, Santa Cruz, CA; Ref. sc3225.

-Anti-human CD31-FITC conjugated antibody (clone WM59): eBioscience, Waltham, MA; Ref. 11-0319-42.

-Mouse anti-human CD31: Agilent Technologies, Santa Clara, CA; Ref. M0823.

-Mouse IgG1 (isotype control): Sigma-Aldrich, St Louis, MO; Ref. M5409.

-Rabbit anti-human vWF: Agilent Technologies, Santa Clara, CA; Ref. A0082.

-Rat anti-mouse IgG (H+L) (FITC) antibody: eBioscience, Inc, San Diego, CA; Ref. 11-4011-85.

### Neutralising antibodies

-IFNAR monoclonal antibody: Millipore, Ontario, Canada; Ref. MAB1155.

## **A.1.7-RT-qPCR and knockdown experiments reagents**

-Dithiothreitol (0.1 M solution): Invitrogen, Carlsbad, CA; Ref. P/N Y00147.

-Dharmafect-1 reagent: Dharmacon, Lafayette, CO; Ref. T-2001-02.

-DEPC (Diethyl pyrocarbonate): Sigma-Aldrich, St. Louis, MO; Ref. D-5758.

-Deoxyribonucleotide tri-phosphate mix (dNTP): Amersham Biosciences, London, UK; Ref. 10297-018.

-M-MLV Reverse Transcriptase and buffer 5X First-Strand Buffer: Invitrogen, Carlsbad, CA; Ref. 28025-013, and P/N Y02321, respectively.

-Optimem medium: Gibco Invitrogen, Carlsbad, California; Ref. 31985-047.

-Random primers for RT reaction: Invitrogen, Carlsbad, CA; Ref. P/N 58875.

- Ribonucleases inhibitor RNAsin®: Promega, Madison, Wisconsin; Ref. N251B.
- siRNA duplexes: Thermo Scientific (Carlsbad, MA); HIF-1 $\alpha$  (ID s6539), STAT1 (ID s277), STAT3 (ID s743) or unspecific Silencer® target (negative control; Ref. 4390843).
- SYBRgreen master mix: Kapa Biosystems, Wilmington, MA; Ref. KK4610.
- TRI Reagent: Invitrogen, Carlsbad, CA; Ref. AM9738.

### **A.1.8-Commercial kits for ELISA, protein assay and calcium detection**

- BCA assay kit: Pierce™ BCA protein assay kit, Thermo Scientific, Carlsbad, CA; Ref. 23227.
- BMP-2 ELISA kit: RayBiotech Inc, Norcross, GA; Ref. ELH-BMP2.
- HRP blotting substrate (ECL): Thermo Scientific, Waltham, MA; Ref. 32106.
- IFN- $\beta$  ELISA kit: Elabscience, Houston, TX; Ref. E-EL-H0085.
- IL-6 ELISA kit: Diaclone, San Diego, CA; Ref. 950.030.048.
- IL-8 ELISA kit: Diaclone, San Diego, CA; Ref. 950.050.096.
- IP-10 ELISA kit: Diaclone, San Diego, CA; Ref. 850.950.096.
- MMP-1 ELISA kit: RayBiotech Inc, Norcross, Ref. GAELH-MMP1.
- Nuclear and cytoplasmic extract kit: Active Motif, Rixensart, Belgium; Ref. 40010.
- PGE<sub>2</sub> ELISA kit: Arbor assays; Ref. K051-H1.
- Quantichrom™ kit: Bioassay Systems, Hayward, CA; Ref. DICA500.
- TNF- $\alpha$  ELISA kit: Diaclone, San Diego, CA; Ref. 950.090.096.
- VEGF-A ELISA kit: ElabScience; Ref. E-EL-H0111.

### **A.1.9-Other reagents**

- Acrylamide 30%: Bio-Rad, Hercules, CA; Ref. 1610158.
- Alizarin red: Sigma-Aldrich, St. Louis, Mo; Ref. A5533.
- ApoScreen® propidium iodide: Southern Biotech, Birmingham, AL; Ref. 10040-01.
- Aprotinin: Sigma-Aldrich, St. Louis, MO; Ref. A4529.
- Autoradiography films: Fujifilm, Tokio; Japan; Ref. 4741019289.
- Calcein-AM: Thermo Scientific, Carlsbad, MA; Ref. 3099.
- Cell scraper: Corning, Tewksbury, MA; Ref. 3008.

- DABCO: Sigma-Aldrich, St. Louis, MO; Ref. 208-57-9.
- DAPI: Sigma-Aldrich, St. Louis, MO; Ref. D9564.
- Endotoxin-free water: Lonza BioWhittaker, Basel, Switzerland; Ref. W-50-100.
- FITC-ApoScreen® annexin V: Southern Biotech, Birmingham, AL; Ref. 10040-02.
- 4% formaldehyde solution: Sigma-Aldrich, St. Louis, MO; Ref 252549.
- Hybond polyvinylidene difluoride (PVDF) membranes: Amersham, Marlborough; MA; Ref. 1060023.
- Leupeptin: Sigma-Aldrich, St. Louis, MO; Ref. L2884.
- Molecular weight protein ladder: Thermo Scientific, Carlsbad, MA; Ref. 26634.
- MTT: Sigma-Aldrich, St. Louis, MO; Ref.M5655.
- p*-nitrophenyl phosphate: Sigma-Aldrich, St. Louis, MO; Ref. N4645.
- Nonidet P-40: Sigma-Aldrich, St. Louis, MO; Ref. 74385.
- Permafluor aqueous mounting fluid: Invitrogen, Carlsbad, MA; Ref. TA-006-FM.
- Polyvinyl alcohol: Sigma-Aldrich, St. Louis, MO; Ref. 363170.
- RIPA lysis buffer: Thermo Scientific, Carlsbad, CA, Ref. 89900.
- N, N, N', N'-Tetramethyl ethylenediamine (TEMED): Sigma-Aldrich, St. Louis, MO; Ref. T9281.
- Triton-x-100 (0.5%, v/v; Sigma Aldrich, St. Louis, MO; Ref. X100.

## **ANNEX 2-PEER-REVIEWED RESEARCH PAPERS**

Parra-Izquierdo, I., Castañeros-Mollor, I., López, J., Gómez, C., San Román, J.A., Sánchez Crespo, M., García-Rodríguez, C., 2019. **Lipopolysaccharide and interferon- $\gamma$  team up to activate HIF-1 $\alpha$  via STAT1 in normoxia and exhibit sex differences in human aortic valve interstitial cells.** *Biochim. Biophys. Acta Mol. Basis Dis.* <https://doi.org/10.1016/j.bbadis.2019.04.014>

Parra-Izquierdo, I., Castañeros-Mollor, I., López, J., Gómez, C., San Román, J.A., Sánchez Crespo, M., García-Rodríguez, C., 2018. **Calcification Induced by Type I Interferon in Human Aortic Valve Interstitial Cells Is Larger in Males and Blunted by a Janus Kinase Inhibitor.** *Arterioscler. Thromb. Vasc. Biol.* 38, 2148–2159. <https://doi.org/10.1161/ATVBAHA.118.311504>